KILOGRAM SCALE SYNTHESIS OF A TRIAZINE-BASED DENDRIMER AND THE DEVELOPMENT OF A GENERAL STRATEGY FOR THE INSTALLATION OF PHARMACOPHORES TO YIELD POTENTIAL DRUG DELIVERY AGENTS

A Dissertation

by

VINCENT JOSEPH VENDITTO

Submitted to the Office of Graduate Studies of
Texas A&M University
in partial fulfillment of the requirements for the degree of

DOCTOR OF PHILOSOPHY

December 2009

Major Subject: Chemistry

KILOGRAM SCALE SYNTHESIS OF A TRIAZINE-BASED DENDRIMER AND THE DEVELOPMENT OF A GENERAL STRATEGY FOR THE INSTALLATION OF PHARMACOPHORES TO YIELD POTENTIAL DRUG DELIVERY AGENTS

A Dissertation

by

VINCENT JOSEPH VENDITTO

Submitted to the Office of Graduate Studies of
Texas A&M University
in partial fulfillment of the requirements for the degree of

DOCTOR OF PHILOSOPHY

Approved by:

Chair of Committee,	Eric E. Simanek
Committee Members,	Brian T. Connell
	Marcetta Y. Darensbourg
	Gerard L. Coté
Head of Department,	David H. Russell

December 2009

Major Subject: Chemistry

ABSTRACT

Kilogram Scale Synthesis of a Triazine-Based Dendrimer and the Development of a General Strategy for the Installation of Pharmacophores to Yield Potential Drug Delivery Agents. (December 2009)

Vincent Joseph Venditto, B.S., Gettysburg College

Chair of Advisory Committee: Dr. Eric E. Simanek

Diverse dendrimer peripheries are often produced through convergent synthesis with multiple protection-deprotection steps. Achieving such diversity while maintaining monodispersity has previously proven problematic. Interception of an electrophilic poly(monochlorotriazine) dendrimer with a molecule of interest bearing a reactive, nucleophilic group presents an efficient method to achieve large quantities of dendrimers with biologically relevant peripheries.

Kilogram-scale synthesis of a triazine-based dendrimer relies on reaction of the dichlorotriazine monomer with the amine terminated dendrimer to afford a poly(monochlorotriazine) dendrimer. Normally, the dendrimer is then reacted with piperidine, an inexpensive "cap" due to its chemically inert nature after reaction. The dendrimer then undergoes a global deprotection to afford an amine-terminated dendrimer. Subsequent iterations with the dichlorotriazine monomer affords higher generation architectures. Intercepting the poly(monochlorotriazine) dendrimer with biologically relevant molecules containing reactive amines enables the development of a drug delivery vehicle. Desferrioxamine B, an iron chelate, and camptothecin, and anti-cancer drug, are two clinically approved drugs of interest investigated for macromolecular drug delivery. Upon acylation of each drug with BOC-isonipecotic acid, substitution on the dendrimer may occur with varying levels of success depending on the drug in question. Upon successful substitution to afford the desired product, biological studies may be performed. Each synthetic approach will be discussed along with alternative routes leading to this general strategy.

DEDICATION

I dedicate this dissertation to the loving memory of Lucy Venditto. It was through her fight with cancer that my struggles are put into perspective and this research finds relevance.

ACKNOWLEDGEMENTS

I would like to thank my committee chair, Dr. Eric E. Simanek, for being a most generous advisor. Your guidance over the past few years inside and outside of chemistry has had a great influence on my life and my future. I would also like to thank my committee members, Dr. Brian T. Connell, Dr. Marcetta Y. Darensbourg, Dr. Gerard L. Cote, for their guidance and support throughout the course of this research. I would also like to thank Dr. Clinton Allred and Mrs. Kimberly Allred for helping with the biological studies on the camptothecin constructs. Thanks also go to the Simanek Group, my friends and the entire Chemistry Department for making my time at Texas A&M University a great experience.

Finally, last but certainly not least, I would like to thank my mom and dad for putting up with me moving 1500 miles away and listening to me ramble on and on about dendrimers. And to my entire family for your encouragement and continued support throughout my education, which has made the journey a much more rewarding experience; one that I could not have done alone.

TABLE OF CONTENTS

		Page
ABSTRACT		iii
DEDICATION		iv
ACKNOWLEDGEMENTS		v
TABLE OF CONTENTS		vi
LIST OF FIGURES		viii
LIST OF SCHEMES		ix
LIST OF TABLES		x
CHAPTER		
I	INTRODUCTION	1
	1.1 The Evolution of Dendrimers	1
	1.2 Polymer Therapeutics	4
	1.3 Triazine-Based Dendrimer Synthesis	5
	1.4 Applications Using Triazine-Based Dendrimers	13
II	KILOGRAM SCALE SYNTHESIS OF A TRIAZINE-BASED DENDRIMER	17
	2.1 Introduction	17
	2.2 Results and Discussion	19
	2.3 Conclusions	23
	2.4 Experimental	24
III	THE USE OF TRIAZINE-BASED DENDRIMERS AS MACROMOLECULAR AGENTS FOR IRON-OVERLOAD THERAPY	35
	3.1 Introduction	35
	3.2 Results and Discussion	44
	3.3 Conclusions	48
	3.4 Experimental	49

CHAPTER Page

IV TRIAZINE-BASED DENDRIMERS CONTAINING CAMPTOTHECIN AS DRUG DELIVERY VEHICLES FOR CANCER THERAPY 51

4.1 Introduction 51
4.2 Results and Discussion 56
4.3 Conclusions 59
4.4 Experimental 60

V CONCLUSIONS 64

5.1 Summary 64
5.2 Recommendations 66

REFERENCES 68

APPENDIX A 99

APPENDIX B 131

APPENDIX C 134

VITA 155

LIST OF FIGURES

FIGURE		Page
1.1	Cartoon summary of the synthesis of: A) linear polymers, B) hyperbranched polymers and C) dendrimers.	2
1.2	Relative reactivity of a series of amines toward monochlorotriazines	7
1.3	The C_3-symmetric core containing three terminal amines and the bow-tie core with four peripheral amines	10
1.4	Examples of an AB_2 and AB_4 branching unit	11
1.5	Second-generation dendrimer with C_3-symmetric core and 12 terminal amines and a second-generation dendrimer with "bow-tie" core and 16 terminal amines.	11
1.6	Desferrioxamine B shown in the absence of iron and in the presence of iron as a hexadentate chelate	15
1.7	Camptothecin in the active lactone and inactive caboxylate forms	16
2.1	Structure of tris(piperazinyl) core and aminodipropylamino-dichlorotriazine monomer	20
3.1	DFOB, Exjade and Ferriprox with corresponding iron complexes	39
3.2	Correlation of log K_{MLH} values for DFOB against $K_{M(OH)}$ values for various metal ions	40
4.1	Quinoline modified camptothecins	54

LIST OF SCHEMES

SCHEME		Page
1.1	General reactivity of chlorotriazines with amine nucleophiles	7
1.2	Route used for kilogram-scale synthesis and functionalization of intermediates	13
2.1	Iterative synthesis of the second-generation dendrimer on kilogram scale.	21
3.1	Synthesis of the monochlorotriazine containing Fe-DFOB unable to add to the dendrimer due to poor reactivity, solubility and sterics	46
3.2	An unsuccessful click reaction with desferrioxamine B-azide and an alkyne-containing dendrimer	47
3.3	Synthesis of Inp-DFOB and subsequent unsuccessful reaction with the poly(monochloro triazine) dendrimer	48
4.1	Camptothecin in the lactone form and open carboxylate form	52
4.2	Installation of BOC-Inp on 20-(*S*)-camptothecin through a hydrolysable ester linkage.	56
4.3	Elaboration of the poly(monochlorotriazine) dendrimer to the amine and PEGylated targets	57

LIST OF TABLES

TABLE Page

1.1 Generalized reactivity trend of nucleophilic amines toward chlorotriazine derivatives..... 8

4.1 IC_{50} values of free drug and dendrimer-drug conjugates determined by MTT assay 58

CHAPTER I
INTRODUCTION

1.1 The Evolution of Dendrimers

During the early 1900's polymers became a major interest within the field of chemistry. Theoretical contributions from Staudinger[1] and experimental evidence of Carothers[2] paved the way for further advancements toward the development of polymerization catalysts by Ziegler[3] and Natta[4] and polymerization kinetics by Flory.[5] More recently, the development of "living" polymerization techniques have dcreased polydispersities toward the achievement of monodisperse architectures.[6, 7] However, improvements in linear polymerizations did not translate directly to branched polymers. The development of crosslinked and hyperbranched polymers showed many of the properties of linear polymers and improved structural properties but suffered from high polydispersity. The inability of simple branched olefins to undergo controlled reactions was due to the lack of differential reactivity between reactive centers. Such challenges opened the field to the development of dendrimer chemistry in the late 1970's.

Generally, polymerizations occur through addition of monomer and reagents to a single reaction vessel. The products obtained oftentimes have a wide range of molecular weights and structures. The inability to accurately characterize or purify the products leads to potential ambiguity in determining the mechanisms of action when used in biomedical applications. The ability to produce monodisperse polymers provides regulatory advantages, as well as advantages in deciphering complex mechanisms upon specific tailoring of molecules.

Typically, linear polymers grow in two directions with two terminal reactive units. Alternativelly, hyperbranched polymers achieved through the use of branched

---

This dissertation follows the style of *Molecular Pharmaceutics*.

monomer units generates a large number of terminal functionalities depending on the feed ratios of the monomer units. The development of dendrimers with exceptionally low polydispersity required monomer units with the ability to initiate and polymerize selectively. Such monomers were developed through the use of differential reactivity or protecting groups to achieve the desired products. **Figure 1.1** summarizes different polymerization techniques through the use of cartooned puzzle pieces for monomer units. Each terminal functional group (arrow) may react with its corresponding acceptor functionality (inverted arrow) to form polymers. Thus, as shown here, polymerization of linear polymers propagates when both monomers are present.

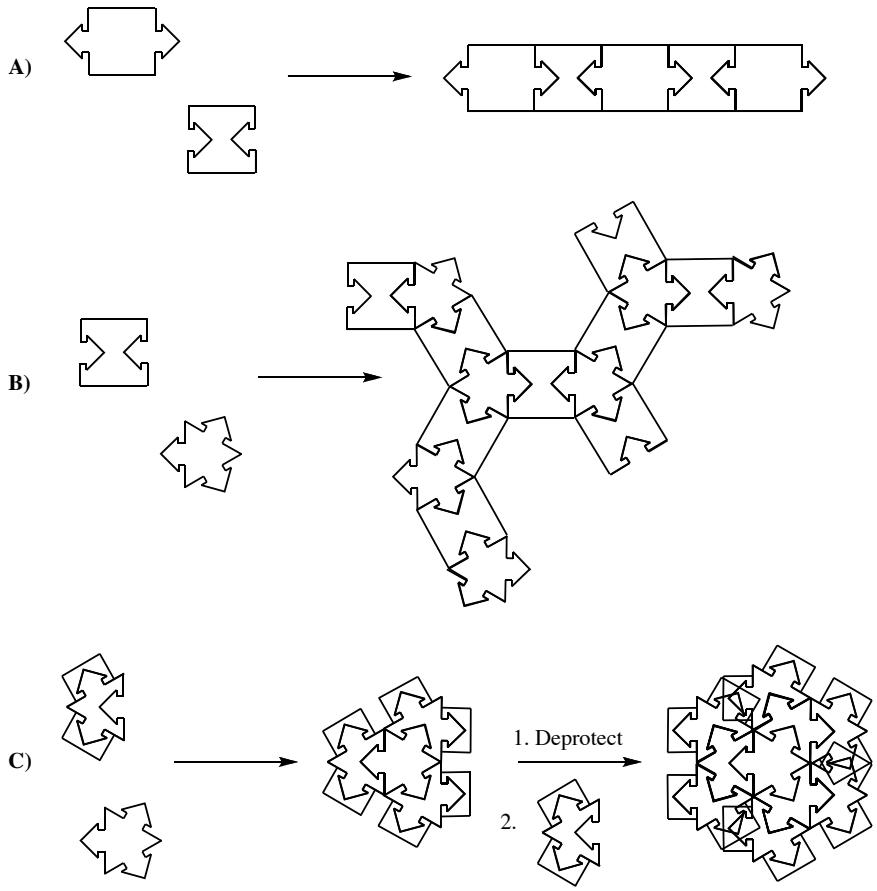

Figure 1.1: Cartoon summary of the synthesis of: A) linear polymers, B) hyperbranched polymers and C) dendrimers.

The dendrimer synthesis uses protecting groups as cartooned with caps on the arrows to prevent hyperbranching. Subsequent iterations of monomer addition and deprotection produce higher generations. The generation of a dendrimer is classified as the number of synthetic iterations performed. Therefore, when using a monomer that branches into two terminal groups, three "arrows" present on the core become six at the first generation. The second-generation dendrimer then has twelve "arrows" or terminal functional groups and so on.

While polymerization has been a flourishing field for over 100 years, the development of new monomer units spawned the area of dendrimer chemistry which continues to grow today.[8] Originally, these well-defined branched structures were known as cascade polymers,[9] but later adopted the names arborols[10] and dendrimers.[11] Vögtle first synthesized cascade polymers in 1978 as pseudo-cavities for ion binding.[9] The synthesis employed a core molecule with three reactive sites, which could undergo iterative synthetic steps to introduce the branches. This synthetic strategy became known as the divergent method of synthesis, which was later utilized by Denkewalter,[12] Newkome[10, 13-15] and Tomalia[11, 16-21] in the 1980's. The tree-like structure of the molecules suggested the name dendrimer, from the greek *dendros*, meaning tree. This new class of macromolecules quickly found utilization through functionalization of the multivalent periphery with "leaves" to generate macromolecular constructs for a variety of potential applications from medicine to materials science.

Poly(amidoamine) (PAMAM) dendrimers were the first constructs synthesized, which classified these new architectures as dendrimers.[11] The PAMAM dendrimers were synthesized through Michael addition with methyl acrylate and ethylene diamine from a core outward to form a water soluble polyamide architecture. The route of growth from the core outward is known as the divergent route. The scalablity of this dendrimer and ease of synthesis enabled commercialization and further exploitation. Initially, dendrimers showed copper sequestration ability[22] and were later exploited for radioimmunotherapy and imaging when decorated radionuclide or gadolinium complexes.[23, 24] However, shortly after the first report of PAMAM dendrimers, the

attempted synthesis of other architectures proved to be less successful due to significant challenges in purification arising from imperfections at higher generations. To overcome such drawbacks, a new synthetic technique was developed, which utilized the same concept, but built the dendrimer from the periphery inward.[25-27] This route was termed the convergent route. The two synthetic routes as well as the development of new monomer units and core molecules improved the synthetic efficiency and provided great potential toward macromolecules with interesting properties. Various other dendrimer architectures have been developed since the mid 1980's including new poly(amides),[28] phosphorous-based dendrimers[29, 30] and polyaryl dendrimers[31, 32] to name a few.

1.2 Polymer Therapeutics

Polymer therapeutics is a burgeoning field[33-36] that combines the therapeutic capabilities of small molecule drugs with the extended blood retention times of macromolecules. Namely, in cancer, polymers are designed to exploit tumor physiology[37, 38] and achieve improved efficacy. Small molecule drugs are chosen for incorporation into polymer therapeutics due to the various limitations of efficacy that would retard clinical application including: 1) poor solubility, 2) rapid clearance, 3) high systemic toxicity and 4) poor selectivity to the site of treatment.[39] Each of these limitations may be addressed through covalent or non-covalent attachment to polymer architectures. Accordingly, dendrimer based constructs present new possibilities to treat a variety of diseases.

Two notable features of polymers keep them at the forefront of therapeutic applications, namely their size and multivalency. Dendrimers have the additional benefit of monodispersity, which enables production of exact entities for biological evaluation. Dendrimers are on the scale of proteins and display a large number of peripheral groups for functionalization. Multivalency is useful in nature for a number of processes ranging from cell-cell interactions to viral infections.[40] Viruses, like dendrimers are large and have a multivalent periphery. Their size helps them to remain in the blood stream for

extended periods, while their multivalency aids in improving infection through enhanced ligand-receptor interactions. Previously, multivalency was exploited in dendrimers for HIV sequestration,[41] investigation of protein-cell interactions[42] and magnetic resonance imaging[24] among other areas. Dendrimers may also utilize their size for enhanced blood retention, and their multivalency for high drug loading capacity. Generally, small molecules are filtered quickly from the blood stream by the kidneys and are excreted rapidly within the urine or are converted to inactive metabolites. Through attachment of drugs to dendrimers, high drug loading is possible, with improved solubility and extended plasma half-life.

Polymeric therapies for cancer therapy have witnessed a significant amount of attention in recent years for the reasons mentioned above. More specifically, however, in cancer therapy one of the major challenges is tumor localization, causing damaging side effects to other organs. Through increased blood circulation and "leaky" vasculature at the site of the tumor, localized tumor therapy may be realized. The extended circulation and tumor accumulation has been termed the enhanced permeability and retention (EPR) effect.[37] The exploitation of physiology for improved therapy, however, may only be achieved after selection of the dendrimer platform best suited for the application. As we strive to develop dendrimers for biomedical applications, the proper selection of monomer and peripheral units enable us to achieve high molecular weights with improved pharmacokinetics.

1.3 Triazine-Based Dendrimer Synthesis

While dendrimers are more monodisperse than their original hyperbranched polymer counterparts, many of the constructs discussed have suffered from imperfections and complications during synthesis. The ability to synthesize new dendrimer architectures, which are easily synthesized with robust high yielding reactions for eventual scalable synthesis and commercialization are still desired, to more effectively produce a macromolecular architecture for affordable medicine. Our efforts

toward the scalable synthesis of monodisperse architectures, which are easily manipulated, began approximately ten years ago and continue today.

The commercial use of dendrimers for a variety of applications depends on the cost and scalability, which are determined by the synthetic ease of each reaction, the robust nature of the reactions and the cost of starting materials among other parameters. Each dendrimer mentioned above has been synthesized to address each of these aspects to varying levels of success, but maximum optimization derives from an educated selection of core, monomer and peripheral unit as well as the synthetic route employed. The possibility for infinite combinations makes the selection of each unit a cumbersome task. Herein, we aim to provide clarity toward our choice of synthetic route, core and branching units, which led to the kilogram-scale synthesis of a second-generation triazine-based dendrimer. En route to achieving this goal we synthesized a number of dendrimers, which enabled us to better understand the reactivity and continue to optimize our strategy. The reactivity and advantages of each unit and reaction sequence are summarized in the following section devoted to advancements in triazine-based dendrimer synthesis.

1.3.1 Triazine and Nucleophilic Amine Reactivities

A limited number of triazine-based polymeric architectures had previously been reported in the literature prior to 2000.[43-46] Of the published reports, however, many employ a nitrile cyclization to obtain the triazine ring. This method is applicable when synthesizing symmetric molecules, however, expanding this chemistry into the synthesis of complex asymmetric architectures containing a diverse periphery affords a mixture of products. To overcome such shortfalls of nitrile cyclization to obtain similar structures, the chemoselective reactivity of cyanuric chloride using nucleophilic aromatic substitution may be exploited. This enables one to synthesize such molecules with quite diverse peripheries and a limitless potential for eventual applications. Taking cues from the functionalization of cyanuric chloride in the late 1800's by Fries,[47, 48] we are able to

achieve macromolecular architectures with high monodispersity on large scale and in modest yield.

Cyanuric chloride is an attractive molecule for dendrimer synthesis due to the low cost and chemoselective reactivity.[49] The generally accepted reactivity trend, as shown in **Scheme 1.1**, proceeds at 0 °C for the first substitution while the second and third substitutions occur at 25 °C and 70 °C, respectively.[50]

Scheme 1.1: General reactivity of chlorotriazines with amine nucleophiles.

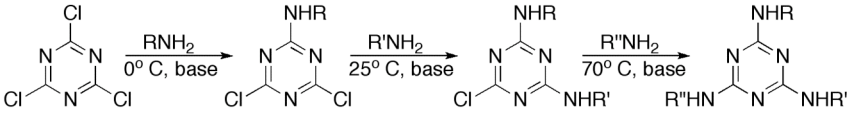

While this scheme explains the electrophilic differences between trichlorotriazines, dichlorotriazines and monochlorotriazines, abbreviating the nucleophile with an "R" group prevents the full comprehension of such reactions. The differences in amine reactivity enable further control over the generalized reactivity trend and allows for more efficient and robust dendrimer synthesis. To develop an understanding of the differential amine reactivity, monochlorotriazines were reacted with a variety of amines. The products were quantified over time using NMR to generate the following series and associated relative reactivity values (**Figure 1.2**).[50, 51]

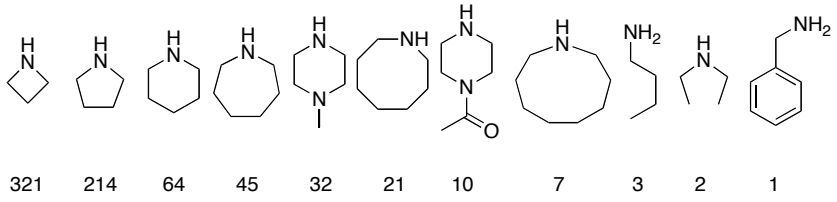

Figure 1.2: Relative reactivity of a series of amines toward monochlorotriazines.

The differential reactivity of amines has great impact in the synthesis of our dendrimers and enables us to perform reactions on the dendrimer, in some cases, without the use of protecting groups.[52] We have expanded on the general trend of chlorotriazine-based chemistry in **Table 1.1**. The trend follows a pattern of cyclic secondary amines > primary amines ≥ linear secondary amines > anilinic amines.

Table 1.1: Generalized reactivity trend of nucleophilic amines toward chlorotriazine derivatives.

	Aniline									Linear Secondary Amines									Primary Amines									Cyclic Secondary Amines								
Temp (°C)	0			25			70			0			25			70			0			25			70			0			25			70		
Time (h)	1	6	12	1	6	12	1	6	12	1	6	12	1	6	12	1	6	12	1	6	12	1	6	12	1	6	12	1	6	12	1	6	12	1	6	12
Trichlorotriazine																																				
Dichlorotriazine																																				
Monochlorotriazine																																				

This reactivity series can be explained using pKa, sterics and orbital characteristics. Firstly, the pKa of anilines are approximately 5.0, while most other amines used in this study range from 8.0 to 11.0 suggesting that pKa would have an effect, however, the differences in relative reactivity between pyrrolidine (214, pKa = 11.27) and piperidine (64, pKa = 11.22) would not be expected.[51] Additionally, sterics may decrease reaction rates as seen in the low reactivity of diethylamine (2, pKa = 10.64), which has comparable reactivity to that of butylamine (3, pKa = 10.59). While the numerical differences here are not significant, the difference in reactivity from the cyclic to linear form is apparent. Cyclic secondary amines are generally more reactive due to a combination of effects. As the ring size decreases, the ring strain and the s-orbital character increases, which is believed to cause an increase in orbital overlap with the electrophile and therefore increase the reaction rate. The extent of each effect on the relative reactivity and their participation in reactivity is unclear, however, each effect must be considered in combination with each other when attempting to fully exploit this chemistry. Our aim to exploit the differential reactivity of both amine nucleophiles and chlorotriazine electrophiles led us toward more efficient dendrimer syntheses.

1.3.2 Convergent vs. Divergent Synthesis

Triazine dendrimers may be synthesized using a convergent route, divergent route or a combination of both to afford desired structures for specific applications.[52] As explained previously, the convergent route involves synthesis of dendrons from the periphery inward, which are then joined to a core to afford the final dendrimer. The divergent route, however, begins with a core and grows each branch outward generation by generation. The convergent route benefits from a limited number of reactions occurring at each step, which generally remain the same throughout the synthesis, whereas the divergent route exponentially increases the number of reactions from generation to generation. The convergent route enables complex functionalities to be obtained on the periphery while the divergent route generally requires that each peripheral unit be the same. Due to the listed benefits, convergent syntheses are regarded as more efficient on the small scale, while divergent syntheses are used for kilogram-scale reactions. Triazine-based dendrimers have been synthesized using both convergent and divergent routes successfully. From our initial investigations in dendrimer synthesis, we aimed to expand our scope to implement a variety of core molecules, monomer units and peripheries to optimize the chemistry at each step, which eventually led us to our large-scale synthesis.

1.3.3 Selection of Core, Monomer Unit and Peripheral Group

Core molecules have been synthesized in our lab with functional groups numbering three or four, two examples are shown in **Figure 1.3**. When the core contains four functional groups we refer to this as a "bow-tie"[53] while three functional groups is a C_3-symmetric core, formed from a triazine at the center with three diamine linkers appended from it. A variety of diamines have been employed including primary diamines, cyclic secondary diamines as well as mixed primary/secondary diamines. From the reactivity series, the cyclic secondary amines are more reactive and facilitate tri-substitution to afford the core in high yields at room temperature. A core with three cyclic secondary amines exposed, also enables efficient addition of dichlorotriazine

monomer units at the first generation. The tris-piperazinyl triazine core is commonly utilized in our syntheses due to cost, ease of core formation and easy addition of monomer units. Amino-azetidine, however, was utilized as the core diamine molecule to form a tris-azetidine core with unique NMR signals, which was supplemented by aminopiperidine and aminopyrrolidine moieties at subsequent generations to better understand dendrimer motion and folding.[54] The bow-tie core uses a diamine through which two triazine molecules are linked. The synthesis of a bow-tie core involves additional synthetic steps to produce the monochlorotriazine, which is then coupled with a diamine. While chemoselectivity of the bow-tie forming reaction is exploited, additional steps on the kilogram scale are undesirable.

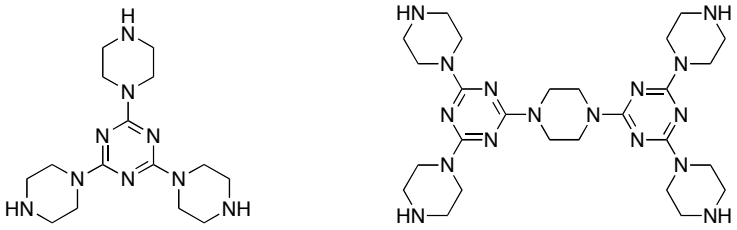

Figure 1.3: The C_3-symmetric core containing three terminal amines and the bow-tie core with four peripheral amines.

From the core we add branching units to increase the multivalency. Branching units are added iteratively to the core to produce successive dendrimer generations. Traditional polymer chemistry terminology classifies a linear symmetric bifunctional monomer unit as an AA monomer, which forms an -AAAAAA- polymer. An asymmetric unit, however, is classified as an AB monomer, which reacts with other monomer units to form an -ABABAB- polymer. Due to the branching character of dendritic monomer units a similar terminology is applied. In the case of triazine based branching units, a monochlorotriazine with two pendant amines is classified as an AB_2 monomer, while a monochlorotriazine with four pendant amines is classified as an AB_4 monomer as shown in **Figure 1.4**.

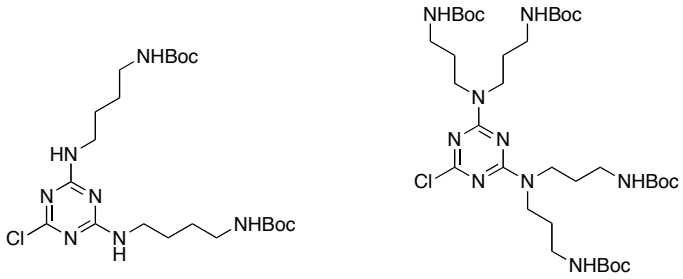

Figure 1.4: Examples of an AB_2 branching unit and an AB_4 branching unit.

Reaction of an AB_2 unit with a C_3-symmetric core affords a first generation with six terminal amines followed by twelve and 24 for the second and third generations as shown in **Figure 1.5**. Likewise, a "bow-tie" dendrimer contains eight, 16 and 32 terminal amines at the first, second and third generations, respectively. An AB_4 branching unit would then have twelve, 48 and 192 terminal groups at the first, second and third generations in the case of the C_3-symmetric core and 16, 64 and 256 terminal amines for the bow-tie core, respectively.

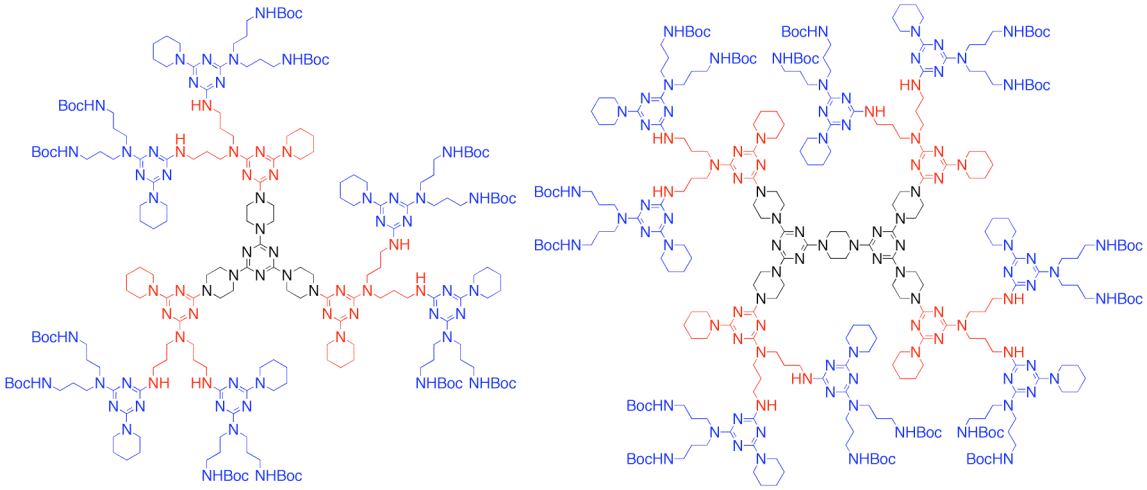

Figure 1.5: Second-generation dendrimer with C_3-symmetric core and 12 terminal amines and a second-generation dendrimer with "bow-tie" core and 16 terminal amines. The core of each dendrimer is shown in black with first and second generation in red and blue, respectively.

Triazine-based dendrimers are synthesized through nucleophilic aromatic substitution and therefore our monomer units require an aromatic electrophile and protected amine nucleophiles. The electrophile is the chlorotriazine moiety, which has remained consistent throughout our various dendrimers. Our selection of nucleophiles, however, has evolved over time. Initially, *p*-aminobenzylamine and piperazine were utilized, which enabled us to begin our investigations with dendrimer systems. The hydrophobicity and rigidity of these molecules allowed us to study non-covalent drug sequestration, however certain applications required a less rigid system, which led to diamines including aminomethyl piperidine[50] and diaminobutane,[55] which are more flexible, producing a less rigid dendrimer.

Recently, manipulation of the linker unit was exploited for the development of a library of dendrimers for gene transfection. In the original library, a variety of core structures were utilized. The cores included rigid structures containing piperazine linker groups; bowtie structures, which contain both piperazine and PEG-like diamine linkers and; flexible compounds, which contain a core having PEG-like diamine linkers. While generation and peripheral groups were also varied in this library, the results from the biological studies indicated that the dendrimer core has the most profound affect on transfection efficiency, with the highest gene transfer seen for the flexible structures.[56, 57]

The monomer unit for many of the dendrimers synthesized, including the family of transfection agents is a monochlorotriazine with two amines to form the AB_2 branching unit. Monochlorotriazines, however, are less reactive electrophiles than their dichlorotriazine counterparts and require a more reactive nucleophile for substitution. While the diamines and monomer units utilized were of great importance to the advancement of our research, the ability to synthesize dendrimers using these building blocks on the kilogram-scale was less than desirable. The need for more robust reactions was necessary, and thus a need for monomer units with increased reactivity.

To increase electrophilicity, an amine nucleophile was necessary that could be added to cyanuric chloride to produce a dichlorotriazine containing two peripheral amines. This was achieved successfully through use of a linear triamine with two

primary amines and a centrally located secondary amine. The implementation of this molecule greatly improved the synthesis of our dendrimers allowing for complex dendritic architectures and efficient synthesis, which has led to the synthesis of kilogram-scale quantities of dendrimer.[58, 59] **Scheme 1.2** summarizes our synthesis and post-synthetic dendrimer modifications to obtain functional dendrimers. The kilogram-scale synthesis is detailed in Chapter II.

Scheme 1.2: Route used for kilogram-scale synthesis and functionalization of intermediates.

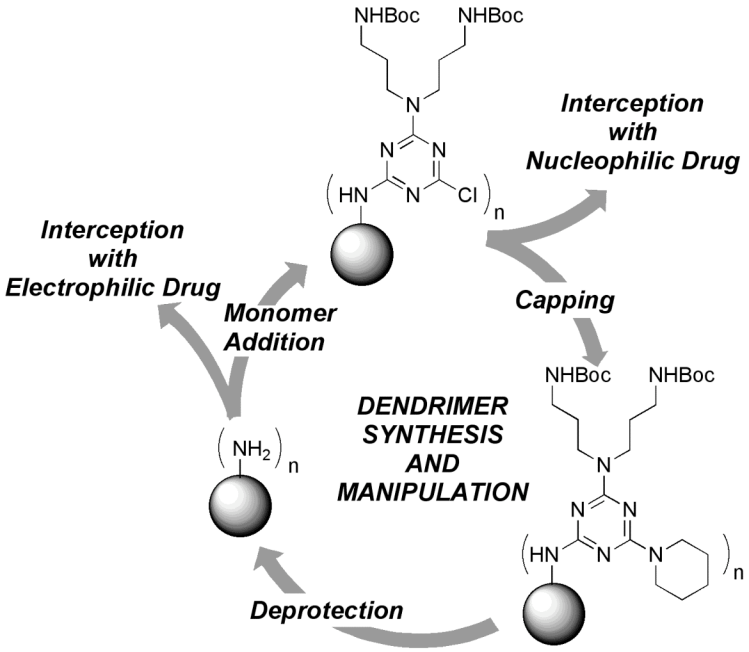

1.4 Applications Using Triazine-Based Dendrimers.

As shown in **Scheme 1.2**, there are two possible intermediates, which may be intercepted for further manipulation. The amine terminated dendrimer may undergo conjugation with an electrophilic linker while the poly(monochlorotriazine) dendrimer may undergo conjugation with a nucleophilic linker. Utilizing the amine-terminated dendrimer as a platform for manipulation, a library of dendrimers may be synthesized

for a variety of applications. Previous efforts in our lab successfully converted amine peripheries into carboxylate, sulfonate, phosphonate, guanidinylate and PEGylate peripheries.[60] This work proved to successfully modulate toxicity *in vitro*. Understanding of the relative toxicity of peripheral functional groups provides a basis for further manipulations when implementing biologically relevant molecules.

Through functionalization of the amine-terminated dendrimer with succinic anhydride, a polycarboxylate dendrimer is obtained which may be functionalized further with glucosamine moieties for potential suppression of immunologic function during inflammation caused during disease and injury as shown when using PAMAM constructs.[61] En route to the desired product new characterization methods using capillary electrophoresis were developed as a method to verify the purity obtained using mass spectrometry and NMR analysis.[62] While the triazine-based dendrimer platforms appeared to be more pure and more monodisperse than their PAMAM counterparts, the triazine dendrimers did not seem to have any effects on the immune system.

Alternatively, modifying the amine-terminated dendrimer with chlorotriazine-modified drugs has proven successful as a route toward drug delivery vehicles using paclitaxel.[63] Attempts to attach desferrioxamine B (DFOB) to the dendrimer in a similar manner were also visited. DFOB is a siderophore used in the treatment of iron overload due to the high affinity and high specificity for iron. Attachment of DFOB to a dendrimer would enable macromolecular iron chelation. The structure of DFOB (**Figure 1.6**) shows a linear chelate with three hydroxamic acids and one primary amine. Previous studies of the x-ray crystal structure provide solid-state evidence that the amine is outside of the coordination sphere of iron, offering a valid attachment point to the dendrimer.[64]

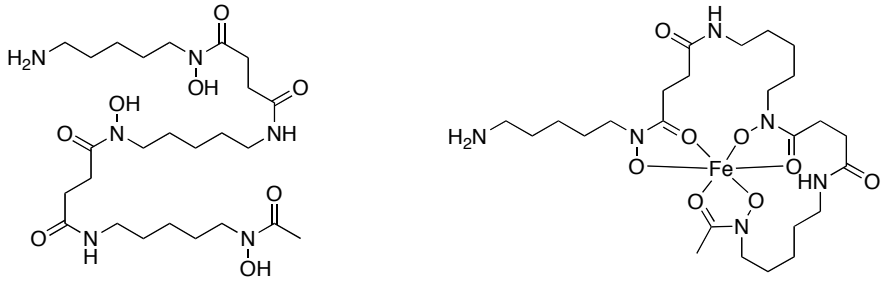

Figure 1.6: Desferrioxamine B shown in the absence of iron and in the presence of iron as a hexadentate chelate.

Through exploitation of the dichlorotriazine route for attachment, the primary amine may react with cyanuric chloride to afford a dichlorotriazine containing DFOB. This molecule may then be appended from the amine-terminated dendrimer. The similar pKa values between the primary amine and the three hydroxamic acids[65] led to new strategies for the installation o DFOB onto the dendrimer. Various routes will be discussed further in Chapter III.

While drug attachment to the dendrimer through a dichlorotriazine intermediate has proven successful, the additional steps for drug attachment led to the development of an alternative method, which takes advantage of the poly(monochlorotriazine) containing dendrimer obtained as an intermediate in the synthesis of dendrimers. To investigate this new route we chose 20-(*S*)-camptothecin as our drug of choice, shown in **Figure 1.7**. The camptothecins are DNA topoisomerase-I (TOP I) inhibitors.[66] When bound to the TOP I cleavage complex, DNA remains with a single-strand nick causing cell death. Functionalization of camptothecin with a secondary amine enables for efficient substitution of the poly(monochlorotriazine) dendrimer, which will be explained in more detail in Chapter IV.

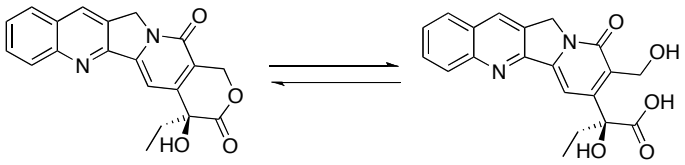

Figure 1.7: Camptothecin in the active lactone and inactive carboxylate forms.

Exploitation of a variety of synthetic routes for dendrimer synthesis has enabled us to obtain a dendrimer at kilogram-scale using routine laboratory equipment. Current methods to derivatize this dendrimer have given mixed results. While the success of this route has been largely dependent on molecule added to the dendrimer, the utility of such reactions will continue to be investigated by us toward the eventual goal of macromolecular-based therapeutics. Current efforts to attach drugs for cancer therapeutics and other biologically relevant molecules will prove to fuel the future of research in our lab as we move from synthesis to cellular toxicity and eventually in vivo therapeutics. Advances over the past ten years have proven promising to propel us into the next decade of applications using triazine dendrimers.

CHAPTER II

KILOGRAM-SCALE SYNTHESIS OF A TRIAZINE-BASED DENDRIMER

2.1 Introduction

Since the development and commercialization of PAMAM dendrimers, various other architectures have been developed, which address issues associated with the application for which the architecture is intended. Triazine-based dendrimers have had an impact on the field of dendrimer chemistry through the exquisite control over synthesis, which pushes the boundaries of design. Early in the synthesis of triazine-based dendrimers a third generation dendrimer was synthesized both convergently and divergently to afford a dendrimer with 16 terminal amines.[52] The convergent synthesis of this dendrimer was performed in the absence of protecting group or functional group manipulations. The divergent synthesis had poor yields upon addition of the monomer units at each generation and required multiple deprotection steps. The poor yields may be attributed to the poor relative reactivity between monochlorotriazines and benzyl amine. Furthermore, the reactions were carried out in organic solvents and required chromatography for purification.

Shortly thereafter, complex peripheries were attained through the introduction of orthogonally reactive protecting groups. The most complex dendrimer to date contains two hydroxyl groups, 16 BOC-protected amines, two t-butyl-diphenylsilyl (TBDPS)-protected alcohols, two thiopyridyl disulfides and two levulinic esters for a total of five different functional groups and 24 total peripheral groups.[67] This tailored complexity leads to the ability to attach specific molecules to each peripheral functional group for the development of multimodal theranostics containing imaging agents, drugs and biocompatibilizing agents. The complexity of this construct is a synthetic feat in dendrimer synthesis, but suffers from the inability to produce this architecture on large scale at high yields without the use of column chromatography. Since the successful completion of this complex triazine-based dendrimer, various other constructs were

developed in our lab, which come closer to development of a construct for achieving scalable synthesis.

After our initial success with dendrimer synthesis, various other architectures were synthesized by our group, which improved on past structures.[50, 51, 55, 59, 68-70] Finally, a triazine-based dendrimer was synthesized, which utilized dichlorotriazine monomer units containing two BOC-protected primary amines.[58] Synthesis from the commonly used tris(piperazinyl) core progressed divergently through monomer addition and subsequent reaction with piperidine, an inert capping group. The second-generation dendrimer had twelve terminal amines and was synthesized in great yield, but each reaction was run at a concentration of 0.1 M or less and some products required chromatography for purification. While the procedure originally performed to obtain the dendrimer was not ideal for kilogram-scale reactions, the structure and synthetic strategy led to further investigation and synthetic optimization for large-scale synthesis.

Although the synthetic route, core, monomer unit and peripheral functionality are among the most apparent parameters affecting synthesis, various other factors also play a major role in achieving dendrimer architectures at the kilogram scale. These parameters include solvent, concentration and other reagents. The majority of reactions to synthesize the dendrimers described above are performed in organic solvents at 0.1 M, which are commonplace in organic chemistry. At the kilogram-scale, the reactions would generate a significant amount of organic waste at these concentrations. To circumvent the issues of significant waste production, a number of efforts focused on optimizing reaction conditions to decrease the waste generation, to run more concentrated reactions and to use "green" solvents when possible. The kilogram-scale synthesis of a triazine-based dendrimer is described here with attention drawn to the approaches used to circumvent the production of large quantities of waste.

2.2 Results and Discussion

The dendrimer was synthesized through iterative reactions of monomer addition, capping and deprotection. Each of these steps was performed divergently from the core outward to obtain a second-generation dendrimer with twelve terminal amines.

Our initial selection of synthetic route stemmed from previous work in our lab and reports from other groups, which found that the divergent route is more advantageous for large-scale syntheses. While the convergent synthesis produces less moles of product than reactant used, the divergent route has the advantage of molar retention by increasing the molecular weight at each generation. The molecule central to this synthesis and most projects in our lab is cyanuric chloride, which undergoes chemoselective reactions with nucelophiles. The core is formed by reaction of cyanuric chloride with three diamines to form a symmetric core with three terminal amines. Our use of piperazine as the diamine affords a small molecule core with three cyclic secondary amines capable of reacting efficiently with mono and dichlorotriazines. This reactivity has proven useful in the past when making dendrimers with piperazine at each generation, however, the poor yields and rigid product precludes scalability and use in certain applications. Through the introduction of primary amines at the periphery of each generation, we are able to synthesize dendrimers with more versatile functionality. In an attempt to synthesize a dendrimer with primary amines on the periphery we lose reactivity seen with cyclic secondary amines. To circumvent this problem we must introduce dichlorotriazines as the monomer unit capable of high yielding reactions with primary amines. Therefore, increased yield and purity may be obtained through the use of a tris(piperazinyl) core and a dichlorotriazine with two primary amines. These structures are shown in **Figure 2.1**.

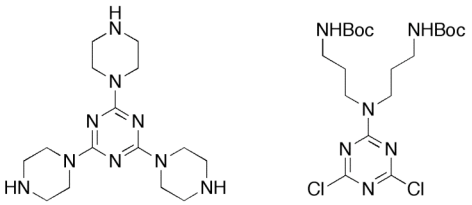

Figure 2.1: Structure of tris(piperazinyl) core and aminodipropylamino-dichlorotriazine monomer.

In the original procedure, the core molecule was synthesized through reaction of cyanuric chloride with excess 1-BOC-piperazine at a concentration of 0.04 M in tetrahydrofuran to yield 97% of the desired product. In the large-scale synthesis, the concentration was only slightly higher at 0.05 M with a 96% yield. Attempts to make this reaction "green" were unsuccessful as solubility was a problem in driving the reaction to completion. Furthermore, the concentration that the reaction was performed at was optimized, but showed little improvement over the previously reported method.

Protection of the triamine in "green" solvents also proved unsuccessful and was performed in tetrahydrofuran as originally reported. The advantage was evident with the increased concentration of the reaction. Originally, the reaction was carried out at concentration of 0.13 M in the presence of N,N-diisopropylethylamine resulting in 84% yield. The large-scale reaction proceeded in the same yield at a concentration of 0.33 M. These reaction conditions enabled the reaction to proceed in 0.6 L instead of the 1.5 L used in the previous procedure. Purification, in both cases, proceeded through crystallization. Reaction of the BOC-triamine with cyanuric chloride to form the monomer was then performed in THF at a concentration of 0.06 M in the presence of DIPEA and purified by crystallization to afford the product in 87% yield. In acetone and water the reaction proceeds at a concentration of 0.14 M using sodium bicarbonate as the base. The product was then obtained in 96% yield after purification through crystallization. The ability to synthesize the monomer unit in large scale at excellent yield with significantly less solvent is imperative due to the use of this monomer at each generation. Synthesis of the monomer proceeded with 362 g cyanuric chloride resulting in 810 g of monomer.

The next step to form the first generation poly(monochlorotriazine) dendrimer involved the reaction of a single core molecule with three monomer units. The iterative dendrimer synthesis to produce the second-generation dendrimer starting from the reaction of core and monomer is shown in **Scheme 2.1**. This reaction was achieved in organic solvents at a concentration of 0.018 M to yield 93% of the first generation poly(monochlorotriazine) dendrimer. Purification was then performed using a short silica gel chromatography column to by removing a majority of the impurities. The eluent was then concentrated and the product precipitated. Reaction of this product with piperidine, an inert capping group, at a concentration of 0.03 M yields 99% of BOC-protected first generation dendrimer. In acetone and water, the reaction of monomer and core proceeds at a concentration of 0.09 M. Due to the excess solvent necessary to perform chromatographic separation and the amount of silica gel necessary, the product

Scheme 2.1: Iterative synthesis of the second-generation dendrimer on kilogram scale.

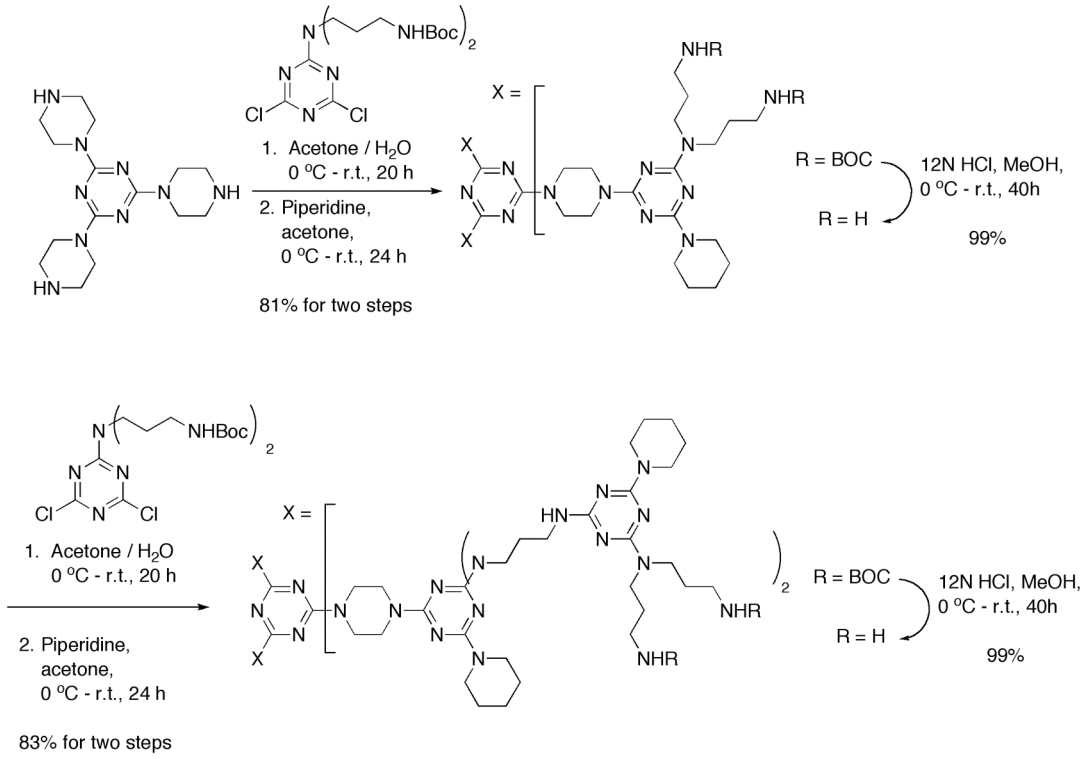

obtained in the large-scale synthesis was used in the next step without further purification. Slight excess in monomer unit is the only likely impurity, which is also capped upon reaction with piperidine. Addition of piperidine to this dendrimer in acetone proceeds at a concentration of 0.025 M to afford the product in 86% yield over both steps after purification. The unreacted monomer present at the beginning of this reaction was indeed present as the bis-piperidine capped monomer and was removed using a filtration rinse with acetone.

Deprotection of the BOC-protected amines in the next step occurs in methanol at a concentration of 0.01 M in both cases. Generally, a 6 M solution of hydrochloric acid in methanol is used to deprotect the dendrimer. Such harsh conditions are not necessary to achieve the desired product, but are utilized for synthetic and purification ease. Previously it has been shown that the dendrimer may be deprotected using trifluoroacetic acid, which proceeds in comparable yields but proceeds to completion slower than when utilizing HCl. The first generation dendrimer then has six terminal amines, which may then undergo reaction with monomer units to afford a second generation poly(monochlorotriazine) dendrimer with twelve BOC-protected amines and six monochlorotriazines.

The second-generation dendrimer was originally achieved at a concentration of 0.0035 M in 93% yield after purification through a short silica gel chromatography column and subsequent precipitation as was performed in the first generation. The pure dendrimer was then reacted with piperidine at a concentration of 0.016 M to yield 99% of the second-generation BOC-protected dendrimer. Alternatively, the reaction was performed in acetone and water at a concentration of 0.0056 M and used directly in the next step without further purification. Reaction with piperidine then proceeds at a concentration of 0.02 M. At this stage purification was attempted to remove the bis-piperidine capped monomer. The resulting solid proved to be more difficult to purify as the monomer was still apparent in the solid. The inability to remove the impurity led to the need for a single chromatographic purification step. Column chromatography was performed using ethyl acetate and hexanes as the eluting solvent for the piperidine-

capped monomer followed by a dichloromethane solution with 30% methanol to elute the desired product. A yield of 83% was determined for the collected product over both steps. Finally, deprotection of the dendrimer proceeded at concentration of 0.006 in the original report and 0.002 in the large-scale synthesis with a 99% yield in both cases.

2.3 Conclusions

This synthesis was performed in five steps in 70% yield with greater than 93% purity for under $10/g. While yield and purity are often parameters that measure the success of a synthesis, we found various other parameters that further enhance the utility of this construct. The synthetic ease, purification and use of water and acetone in a majority of the reactions also attest to the utility and potential commercial applicability of this triazine-based dendrimer. The original synthesis of this dendrimer on small scale was reported to the fifth generation. The purification and characterization became increasingly more difficult at each iteration and required significantly more effort with dramatically lower yields. Solubility and incomplete reactions also became problematic at the fifth generation. At the kilogram-scale the purification and characterization would prove to be too cumbersome to warrant investigation up to the fifth generation and thus our large scale synthesis was only carried out to the second generation.

Oftentimes, the use of specialized laboratory equipment is required for syntheses performed on this scale. Such equipment includes reactor vessels with multiple valves and attachments for handling ease and maximum collection efficiency of the products. In our hands, however, we completed the synthesis using routine laboratory equipment. Handling 22 L round bottom flasks and 4 L separatory funnels did pose certain safety precautions, however, the reactions were generally performed as would be routine with a 100 mL round bottom flask. Crystallization as the only purification method until the final chromatography column was also a major advantage to this route. The need to purify compounds using column chromatography is commonplace in many organic reactions, but oftentimes uses significant volumes of solvent to elute the product. Circumventing the use of chromatography decreases the amount of waste produced and

simplifies the collection of pure materials through filtration rather than evaporation of solvents. Finally, optimizing the reactions by increasing concentrations and using "green" solvents also generates less waste and less environmentally hazardous waste. The use of green solvents in industrial reactions is of much interest now and this reaction moves our chemistry one step closer toward triazine-based dendrimers with commercial applications.

The synthetic ease, modest yield and overall purity have propelled us to continue to investigate this dendrimer in a variety of applications. The low cost also suggests a potential for this construct in the development of affordable medicines for the third world. Our interest and success in using this platform as a drug-delivery vehicle is discussed later in Chapters III and IV.

2.4 Experimental

2.4.1 Materials and Methods

All solvents and reagents were purchased from commercial suppliers and used as received. Acetone (99.5%), 2-(*tert*butoxycarbonyloxyimino)-2-phenylacetonitrile (BOC-ON), chloroform (99.8%), 3,3'-diaminodipropylamine (98%), dichloromethane (99.6%), *N,N*-diisopropylethylamine (99%), methanol (99.8%), sodium chloride, sodium sulfate (anhydrous) and tetrahydrofuran (99.9%, anhydrous) were purchased from Sigma-Aldrich. Cyanuric chloride was purchased from Alfa Aesar. *N*-Boc-piperazine was purchased from AK Scientific. Hydrochloric acid andsodium bicarbonate were purchased from J. T. Baker. Sodium hydroxide was purchased from Fisher Scientific. Hexanes (98.5%) were purchased from Mallinckrodt. NMR spectra were recorded on a Varian Mercury 300 MHz spectrometer in $CDCl_3$, or DMSO-d6. All mass spectral analyses were carried out by the Laboratory for Biological Mass Spectrometry at Texas A&M University. HPLC analysis was performed using a Waters Delta 600 system and a Waters UV detector at 280 nm. Either a Zorbax C-8 column (4.6 x 50 mm) was used at 30 °C with a flow rate of 0.7 mL/min or a Halo C18 column (4.6 x 50 mm, 2.7 μm) was used at 50 °C with a flow rate of 1.5 mL/min. The mobile phase in both cases was a

95/5 (0.5% HClO4 in water/acetonitrile) with a gradient to 5/95 (0.5% HClO4 in water/acetonitrile) over 3 minutes, and an isocratic hold for 4 min followed by a gradient of 95/5 (0.5% HClO4 in water/acetonitrile) over 7 min.

2.4.2 Synthesis of 1,3,5-[Tris-piperazine]-triazine

A 1-L, three-necked, roundbottomed flask, fitted with a magnetic stirrer, condenser, nitrogen inlet, and 250 mL addition funnel was charged with 1,3,5-[*N*-(*tert*-butoxycarbonyl)-piperazine]-triazine (27.9 g, 44.1 mmol, 1.00 equiv) and 286 mL of methanol. The solution was left to stir at 0 °C for 30 min. A solution of 153 mL (0.918 mol, 21 equiv) of 6 N hydrochloric acid was then added over 70 min. keeping the temperature at ~ 1 °C and the resulting light yellow slurry was left to stir at 0 °C for 2 h. The reaction slurry then warmed to ambient temperature over 3 h and slowly heated to an internal temperature of 40 °C for 12 h (the slurry became homogeneous at 27 °C). Off-gassing was observed as the temperature increased. The volatile organic components were removed using a rotary evaporator 34–40 °C until only ca. 100 mL of water remained. The resulting aqueous solution was cooled to 0 °C and made alkaline (pH = 14) by addition of 237 mL (657 mmol, 15 equiv.) of a 10% NaOH solution. The resulting alkaline solution was then extracted with chloroform (3 x 250 mL), and the organic phases were combined and dried over sodium sulfate. The solvent was filtered and evaporated at 34 °C to afford the product as a white solid (14.1 g, 96 %), mp 200–208 °C.

The product has the following characteristics: TLC R*f* = 0.0 (silica gel 60 F_{254}, EMD Chemicals, Inc. in 10% methanol:dichloromethane); IR (neat) cm^{-1}: 3278, 2846, 1523, 1433, 1242, 1007, 806, 728; 1H NMR (400 MHz, $CDCl_3$) δ: 1.62 (s, 3 H), 2.81 (t, 12 H, *J* = 5.0), 3.68 (t, 12 H, *J* = 5.0); ^{13}C NMR (100 MHz, $CDCl_3$) δ: 44.3, 46.0, 165.2; MS (CI) *m/z* 334.4 Anal. Calcd. for $C_{15}H_{27}N_9$: C, 54.03; H, 8.16; N, 37.81. Found: C, 53.72; H, 8.32; N, 37.48.

2.4.3 Synthesis of 3,3'-Di-(tert-butoxycarbonyl)-aminodipropylamine

A 1 L, three-necked, round-bottomed flask equipped with a magnetic stirrer, a 500-mL addition funnel, a temperature probe and a static nitrogen inlet was charged with 3,3'-diaminodipropylamine (28.2 mL, 0.20 mol, 1.0 equiv), 300 mL of tetrahydrofuran, and *N,N*-diisopropylethylamine (100 mL, 0.57 mol, 2.8 equiv.). A separate 500-mL Erlenmeyer flask was charged with 2-(*tert*-butoxycarbonyloxyimino)-2-phenylacetonitrile (BOC-ON) (100 g, 0.41 mol, 2.0 equiv.) and 300 mL of tetrahydrofuran. The resulting solutions were separately stirred at 0 °C for 30 min. The BOC-ON solution was then transferred to the addition funnel and added dropwise to the solution of 3,3'-diaminodipropylamine over a 90-100 min period. After addition was complete, the solution was left to stir at 0 °C for 3 h, warmed to ambient temperature, and left to stir for an additional 20 h. The solvent was removed using a rotary evaporator at 39 °C and the residue was dissolved in 400 mL of dichloromethane. The organic solution was washed with 10% NaOH (3 x 200 mL), a saturated, aqueous solution of sodium chloride (1 x 300 mL), and dried over sodium sulfate. Following filtration, the solvent was removed using a rotary evaporator at 32–39°C to afford the product as an oily material which was then precipitated as an off-white solid by addition of hexane (500 mL) and traces of MeOH (3 mL). After standing in the freezer for 24 h, the solids were filtered, washed with hexane, and dried under vacuum overnight to provide the product as an off-white solid (54.2–55.9 g, 82–84 %), mp 68.1–70.0 °C.

The product has the following spectral characteristics: TLC R*f* = 0.0 (silica gel 60 F_{254}, EMD Chemicals, Inc. in 5:95 methanol:dichloromethane); IR (neat) cm^{-1}: 3342, 2975, 2931, 1686, 1518, 1365, 1273, 1250, 1168; ^{1}H NMR (400 MHz, $CDCl_3$) δ: 1.41 (s, 18 H), 1.60–1.66 (m, 4 H), 2.63 (t, 4 H, *J* = 6.6), 3.15–3.20 (br, 4 H), 5.2 (br, 2 H); ^{13}C NMR (100 MHz, $CDCl_3$) δ: 28.4(s), 29.7 (s), 38.9 (s), 47.4 (s), 78.9 (s), 156.1 (s); MS (CI), *m/z* 332.2 (M+H). Anal. Calcd. for $C_{16}H_{33}N_3O_4$: C, 57.98; H, 10.04; N, 12.68. Found: C, 57.86; H, 9.84; N, 12.51.

2.4.4 Synthesis of 2-[3,3'-Di-(tert-Butoxycarbonyl)-aminodipropylamine]-4,6-dichloro-1,3,5-triazine

A 3-L, three-necked, round-bottomed flask equipped with a mechanical stirrer, static nitrogen inlet and 1-L addition funnel was charged with cyanuric chloride (30.5 g, 0.165 mol, 1.00 equiv) and 300 mL of acetone. The resulting solution was left to stir at 0 ºC for 1 h. A cooled solution of 3,3'-di-(*tert*-butoxycarbonyl)-aminodipropylamine (54.9 g, 0.166 mol, 1.01 equivalent) in acetone (686 mL) was then added dropwise to the cyanuric chloride solution over a period of 3 h (the internal temperature remained at or below 2 ºC during this addition). A white suspension formed during the course of addition. Sodium bicarbonate (13.9 g, 0.166 mol, 1.00 equiv) in water (195 mL) was then added dropwise over a period of 1 h. A yellow mixture was obtained after complete addition. The resulting solution was left to stir at 0 ºC for 3 h, which resulted in the formation of a white suspension. The mixture was allowed to warm to ambient temperature and stirred for an additional 15 h. The reaction mixture was concentrated without filtration (to approximately 200 mL) on a rotary evaporator at 31–40 °C. The resulting aqueous suspension was filtered. The solids were dissolved in 600 mL of dichloromethane and washed with water (3 x 250 mL), and a saturated, aqueous solution of sodium chloride (300 mL). The organic layer was dried with sodium sulfate, filtered, and the solvent was concentrated using a rotary evaporator at 40 °C. The resulting solids were dried under vacuum to provide the product as an off-white solid (76.5 g, 0.160 mol, 96 %), mp 122.4-125.7 °C.

The product has the following characteristics: TLC R*f* = 0.3 (silica gel 60 F_{254}, EMD Chemicals, Inc. in 5% methanol:dichloromethane); IR (neat) cm^{-1}: 3349, 2976, 1691, 1573, 1475, 1233, 1160, 847, 733; 1H NMR (400 MHz, $CDCl_3$) δ: 1.41 (s, 18 H), 1.77 (tt, apparent quintet, 4 H, *J* = 6.6), 3.07-3.12 (br/quartet-depending on sample concentration, 4 H), 3.60 (t, 4 H, *J* = 7.1), 5.05 (br, 2H); ^{13}C NMR (100 MHz, $CDCl_3$) δ: 27.7 (s), 28.3 (s), 37.3 (s), 44.9 (s), 79.3 (s), 156.0 (s), 164.7 (s), 170.1 (s); MS (CI): *m/z* 479, 379. Anal. Calcd. for $C_{19}H_{32}Cl_2N_6O_4$: C, 47.60; H, 6.73; N, 17.54; Cl, 14.79. Found: C, 47.87; H, 6.82; N, 17.48; Cl, 14.47.

2.4.5 Synthesis of 1,3,5-[Tris-N-(tert-butoxycarbonyl)-piperazine]-triazine

A 2 L, three-necked, round-bottomed flask equipped with a magnetic stirrer**,** reflux condenser*,* temperature probe, glass stopper and static nitrogen inlet was charged with cyanuric chloride (10.0 g, 54.2 mmol, 1.00 equiv) and tetrahydrofuran (1 L). *N*-(*tert*-Butoxycarbonyl)-piperazine (34.0g, 183 mmol, 3.38 equiv) was added in ~10 g portions over 17 min (during the addition, the temperature rose from 20 to 28 °C; an ambient temperature water bath was used to moderate the exotherm). White solids formed in the reaction mixture during the addition of the piperazine. *N,N*-Diisopropylethylamine (96.2 mL, 552 mmol, 10.2 equiv) was then added, and the reaction mixture stirred at ambient temperature for 1 h, then heated to an internal temperature of 66 °C for 20 h at which point the reaction was judged to be complete by HPLC. Upon cooling to ambient temperature, a white precipitate forms. The solvent is removed using a rotary evaporator at 31 °C. The white residue was taken up in dichloromethane (300 mL) and washed with water (2 x 150 mL), 10% $NaHSO_4$ (2 x 150 mL) and a saturated, aqueous solution of sodium chloride (2 x 100 mL). The organic layer was dried over anhydrous sodium sulfate, filtered, and the solvent was removed using a rotary evaporator at 35–41 °C. The resulting white solids are granulated in EtOAc (35 mL, ca. 1 mL/g) to yield a white crystalline material (31.0–32.0 g, 90–93 %), mp 223.4–226.1 °C.

The product has the following characteristics: TLC, R*f* 0.35 (silica gel 60 F_{254}, EMD Chemicals, Inc. in 5% methanol:dichloromethane); IR (neat) cm^{-1}: 1679, 1535, 1419, 1227, 998, 725; ^{1}H NMR (400 MHz, $CDCl_3$) δ: 1.46 (s, 27 H), 3.42 (m, 12 H), 3.72 (m, 12 H); ^{13}C NMR (100 MHz, $CDCl_3$) δ: 28.4, 43.0, 79.9, 154.8, 165.2; MS (CI) *m/z* 634.3; Anal. Calcd. for $C_{30}H_{51}N_9O_6$: C, 56.85; H, 8.11; N, 19.89. Found: C, 56.69; H, 8.26; N, 19.82.

2.4.6 Synthesis of G1-[$N(CH_2CH_2CH_2NHBoc)_2]_3$-$Cl_3$

In a 4-L, 4-necked, jacketed reaction vessel equipped with a 250-mL addition funnel, temperature probe, static N_2 and mechanical stirrer, 2-[3,3'-di-(*tert*-butoxycarbonyl)-aminodipropylamine]-4,6-dichloro-1,3,5-triazine (73.0 g, 0.152 mol, 3.5 equiv.) was dissolved in acetone (1 L) and cooled to 0 °C. Separately, a chilled solution of 1,3,5-[*tris*-piperazine]-triazine (14.5 g, 43.5 mmol, 1.0 equiv) in H_2O (500 mL) was prepared and treated with a solution of sodium carbonate (46.1 g, 0.435 mol, 10 equiv.) in 250 mL of H_2O. This solution was left to stir at 0 °C for 30 min. The resulting aqueous solution was added in a dropwise fashion to the acetone solution at 0 °C over a period of 2 h. The white suspension obtained after complete addition was left to stir at 0 °C for 2.5 h before warming gradually to 21 °C, and then stirred for an additional 20 h. The white solid was collected by filtration on a 15 cm-diameter Büchner funnel. The reaction vessel was rinsed with 500 mL water, which was subsequently used to wash the filter cake. The wet solids were transferred back to the rinsed reaction vessel and dissolved in CH_2Cl_2 (1.5 L), washed with water (3 x 200 mL), a saturated, aqueous solution of sodium chloride (1 x 1.5 L), and then dried with 230 g of sodium sulfate. Following filtration, the solvent was removed using a rotary evaporator at 30 °C and dried under vacuum to yield an off-white crude material (76.1 g). This material was used in the next step without further purification.

A small amount of the product was purified for spectral characterization using column chromatography on silica gel eluting with 10% EtOAc:CH_2Cl_2 to give the unreacted starting material $C_3N_3[N(CH_2CH_2CH_2NHBoc)_2]Cl_2$ as a white solid followed by elution with (50:50) EtOAc:CH_2Cl_2 to give the product as a white solid.

The product has the following characteristics: TLC R*f* = 0.28 (Silica Gel 60 F_{254}, EMD Chemicals, Inc., 20:1 CH_2Cl_2:CH_3OH); IR (KBr pellet) cm^{-1}: 3375, 2976, 2931, 1713, 1571, 1539, 1493, 1437, 1390, 1367, 1248, 1167, 1081, 1041, 999, 983, 880, 801, 620, 465; ^1H NMR (400 MHz, $CDCl_3$) δ: 1.44 (s, 54 H, $C(C\mathbf{H}_3)_3$), 1.75 (m, 12 H, $NCH_2C\mathbf{H}_2$), 3.08 (m, 12 H, $C\mathbf{H}_2NHBoc$), 3.57 (m, 12 H, Boc-$NC\mathbf{H}_2$), 3.82 (m, 24 H, $C\mathbf{H}_2$, piperazine), 4.84 (br, 3 H, N**H**), 5.58 (br, 3 H, N**H**); ^{13}C NMR (100 MHz, $CDCl_3$)

δ: 28.0 (s, $NCH_2\mathbf{C}H_2$), 28.1 (s, $NCH_2\mathbf{C}H_2$), 28.6 (s, $C(\mathbf{C}H_3)_3$), 28.7 (s, $C(\mathbf{C}H_3)_3$), 37.0 (s, $\mathbf{C}H_2NHBoc$), 38.0 (s, $\mathbf{C}H_2NHBoc$), 42.9 (s, $\mathbf{C}H_2$), 43.1 (s, $\mathbf{C}H_2$), 43.6 (s, $\mathbf{C}H_2$, piperazine), 44.1 (s, $\mathbf{C}H_2$), 79.1 (s, $\mathbf{C}(CH_3)_3$), 79.5 (s, $\mathbf{C}(CH_3)_3$), 156.1 (s, $\mathbf{C}(O)$), 156.4 (s, $\mathbf{C}(O)$), 164.6 (s, C_3N_3), 165.2 (s, C_3N_3), 165.4 (s, C_3N_3), 169.6 (s, C_3N_3); HRMS (Thermo LTQ FT Ultra): Calcd. for (M+H): 1660.8746. Found: 1660.87555. Anal. Calcd. for $C_{72}H_{120}Cl_3N_{27}O_{12}$: C, 52.02; H, 7.28; N, 22.75; Cl, 6.40. Found: C, 52.14; H, 7.30; N, 22.63; Cl, 6.48.

2.4.7 Synthesis of G1-[$N(CH_2CH_2CH_2NHBoc)_2]_3$-piperidine$_3$

In a 4-L, 4-necked, jacketed reaction vessel equipped with a temperature probe, static N_2 inlet, glass stopper and mechanical stirrer, G1-[$N(CH_2CH_2CH_2NHBoc)_2]_3$-$Cl_3$ (74.8 g, 43.5 mmol, 1.0 equiv) was suspended in acetone (3 L) and left to stir at 0 °C for 1 h. Piperidine (79.3 mL, 68.4 g, 803 mmol, 18.5 equiv) was added in a single portion and the mixture stirred at 0 °C for 4 h. A white suspension formed after 30 min. The mixture warmed to 21 °C and stirred for an additional 20 h, at which time the reaction was judged to be complete by HPLC. The resulting suspension was filtered, washed with acetone (100 mL), and air-dried overnight to afford 97.3 g of a white solid. The white solid was dissolved in CH_2Cl_2 (1000 mL), transferred to a 2-L separatory funnel and washed with a 5% HCl solution (4 x 300 mL), 5% NaOH solution (1 x 300 mL), and a saturated, aqueous solution of sodium chloride (1 x 300 mL). The organic phase was dried over sodium sulfate (108 g) and the solvent was removed on a rotary evaporator at 30 °C to afford an off-white solid that was dried in a vacuum oven for 96 h to provide 67.4 g of the title product (86% yield over two steps).

The product has the following characteristics: TLC R*f* = 0.36 (Silica Gel 60 F_{254}, EMD Chemicals, Inc., 20:1 CH_2Cl_2:CH_3OH); IR (KBr pellet) cm^{-1}: 2975, 2931, 2853, 1717, 1530, 1487, 1434, 1366, 1293, 1249, 1173, 997; ^1H NMR (400 MHz, $CDCl_3$) δ: 1.42 (s, 54 H, $C(C\mathbf{H}_3)_3$), 1.56 (br, 12 H, $C_5\mathbf{H}_{10}N$, β-H), 1.62 (br, 6 H, $C_5\mathbf{H}_{10}N$, γ-H), 1.71 (br, 12 H, $NCH_2C\mathbf{H}_2$), 3.06 (br, 12 H, $C\mathbf{H}_2NHBoc$), 3.59 (br, 12 H, $C\mathbf{H}_2$, Boc-$NC\mathbf{H}_2$), 3.73 (br, 12 H, $C_5\mathbf{H}_{10}N$, α-H), 3.80 (br, 24 H, $C\mathbf{H}_2$, piperazine), 5.26 (br, 6 H, $N\mathbf{H}$); ^{13}C

NMR (100 MHz, $CDCl_3$) δ: 25.1 (**C**$_5$H$_{10}$N, γ-C), 26.0 (**C**$_5$H$_{10}$N, β-C), 27.8 (s, NCH$_2$**C**H$_2$), 28.7 (s, C(**C**H$_3$)$_3$), 37.4 (s, **C**H$_2$NHBoc), 41.9 (**C**$_5$H$_{10}$N, α-C), 43.2 (s, Boc-N**C**H$_2$), 43.4 (s, Boc-N**C**H$_2$), 44.4 (s, **C**H$_2$, piperazine), 79.1 (s, **C**(CH$_3$)$_3$), 156.2 (s, **C**(O)), 165.1 (s, C_3N_3), 165.5 (s, C_3N_3), 166.1 (s, C_3N_3); HRMS (Thermo LTQ FT Ultra) [M+H] calcd. for $C_{87}H_{150}N_{30}O_{12}$: 1808.2120. Found: 1808.20932. Anal. Calcd. for $C_{87}H_{150}N_{30}O_{12}$: C, 57.78; H, 8.36; N, 23.24. Found: C, 57.45; H, 8.10; N, 22.90.

2.4.8 Synthesis of G1-[N(CH$_2$CH$_2$CH$_2$NH$_2$)$_2$]$_3$

Prior to starting the reaction, methanol and concentrated HCl were cooled to 0 °C for 3 h. In a 22 L three neck roundbottomed flask fitted with a mechanical stirrer was dissolved G1-[N(CH$_2$CH$_2$CH$_2$NHBOC)$_2$]$_3$ (315 g, 0.17 mol) in CH_3OH (9 L) and the mixture was allowed to stir at 0 °C for 30 min. Concentrated HCl (12 N, 4.5 L) was added in 500 mL portions over a period of 2.5 h with a 15 min interval between each addition. The temperature slightly rose to 5 °C after addition. After complete addition, the resulting yellow solution was left to stir at 0 °C for 15 h and at 25 °C for 24 h. The volatile components were concentrated in vacuo until only about 800 mL of water remained. After cooling to 0 °C, the residue was made basic (pH = 14) with 1.5 L of a 5 M NaOH (aq.) solution. The resulting white suspension was filtered and attempt to dry this compound under vacuum and with low heating was unsuccessful. The solid was partially dissolved in $CHCl_3$ (4 L). The organic phase was separated by filtration. The remaining solid was dissolved in H_2O (3 L), and the resulting milky solution was extracted with $CHCl_3$ (1 L) using a 1 L size liquid-liquid extractor. The extraction was stopped when the aqueous solution turned clear (4-5 h). Fresh $CHCl_3$ was used after two successive extraction (500 mL each). The organic fractions were combined, dried with Na_2SO_4, and filtered, and the solvent was removed under reduced pressure. The desired material was isolated as a white solid by precipitation from the oily solution using hexane and upon standing for 48 h in the freezer (205 g, >99%). ^{1}H NMR (300 MHz, $CDCl_3$) δ: 3.74 (br, 24H), 3.66 (br, 12H), 3.58 (br t, $^3J_{H\text{-}H}$ = 7 Hz, 12H), 2.63 (br, 12H), 1.68 (br m, 12H), 1.57 (br, 6H), 1.49 (br, 12H), 1.38 (br, 12H). ^{13}C NMR (75.5 MHz,

$CDCl_3$) *δ*: 165.5, 165.2, 164.8, 44.0, 43.0, 42.4, 39.1, 39.0, 31.3, 25.7, 24.9. MS (MALDI): calcd. 1206.8904 (M)+, found 1207.9496 (M + H)+. Anal. Calcd. For $C_{57}H_{102}N_{30}•2H_2O$: C, 55.03; H, 8.52; N, 33.79. Found: C, 55.13; H, 8.16; N, 33.39.

2.4.9 Synthesis of G2-$[N(CH_2CH_2CH_2NHBOC)_2]_6$-$Cl_6$

A 22 L, three-neck roundbottomed flask equipped with a mechanical stirrer was charged with 130 g (0.11 mol) of G1-$[N(CH_2CH_2CH_2NH_2)_2]_3$ and 5 L of H_2O. A solution of Na_2CO_3 (205 g, 1.94 mol) in 1.5 L of H_2O was added, and the resulting slurry solution was stirred at 25 °C for 1 h. A solution of dichlorotriazine monomer(310 g, 0.65 mol) in acetone (13 L) was added, and the reaction mixture was stirred at 25 °C for 36 h. The reaction was monitored by MALDI-TOF MS and TLC (silica gel, 5% CH_3-OH/CH_2Cl_2, *Rf* = 0.2) and deemed to be complete as a result a yellow gummy precipitated at the bottom of the flask during this time. The solvent was removed on rotary evaporator (13 L), and the resulting aqueous suspension was dissolved in CH_2Cl_2 (4 L). The aqueous layer was removed, and the organic phase was washed with H_2O (3 x 500 mL) and brine (3 x 500 mL) and dried with Na_2SO_4. Following filtration, the solvent was removed on rotary evaporator to afford a white crude material (420 g, 99%). Both TLC and MALDI-TOF MS analysis of this material showed the presence of the desired product along a small amount of unreacted monomer. This material was suitable for use without further purification; however, a small amount was purified for spectral characterization using column chromatography on silica gel (40:1 CH_2Cl_2/CH_3OH; *Rf* = 0.19 using 20:1 CH_2Cl_2/CH_3OH as developing solvent) to afford the product as a white solid. The excess/unreacted monomer may also be recovered from this purification (*Rf* = 0.50 using 20:1 CH_2Cl_2/CH_3OH as the developing solvent). ^1H NMR (300 MHz, $CDCl_3$) δ: 6.60-4.80 (br, 18H), 3.80 (br, 24H), 3.72 (br, 12H), 3.56 (br, 36H), 3.36 (br, 12H), 3.05 (br, 24H), 1.83 (br, 12H), 1.70 (br, 30H), 1.60 (br, 12H), 1.42 (s, 54H), 1.39 (s, 54H). 13C NMR (75.5MHz, $CDCl_3$) δ: 169.2, 168.4, 165.4, 165.1, 164.9, 164.6, 156.0, 155.7, 78.9, 78.6, 44.0, 37.6, 36.6, 28.2, 27.7, 25.6, 24.8. MS (MALDI): calcd. 3860.1476 (M+), found 3860.5223. Anal. Calcd. for $C_{171}H_{288}Cl_6N_{66}O_{24}$: C, 53.14; H,

7.51; N, 23.92; Cl, 5.50. Found: C, 53.31; H, 7.52; N, 23.79; Cl, 5.41.

2.4.10 Synthesis of G2-[N($CH_2CH_2CH_2NHBOC)_2]_6$-piperidine$_6$

In a 22 L three-neck roundbottomed flask fitted with a mechanical stirrer, G2-[N($CH_2CH_2CH_2NHBOC)_2]_6Cl_6$ (1240 g, 0.32 mol) in acetone (16 L) was allowed to stir at 25 °C for 1 h. To the resulting solution was added piperidine (470 mL, 5.59 mol), and the mixture was allowed to stir at 25 °C for 48 h at which point the reaction was judged complete by MALDI-TOF MS and TLC (silica gel, *Rf*) 0.49 using 5% CH3OH/CH2Cl2). The resulting suspension was filtered, washed with acetone (2 L), and dried to afford 238 g of a lightweight white material. Analysis (NMR, MS, and TLC) of this material showed the presence of the pyridinum chloride salt and none of the desired product, and it was therefore discarded. The filtrate was evaporated to dryness under reduced pressure to yield a yellowish white solid. TLC analysis (SiO2, 5% MeOH-CH2Cl2) of the crude product showed two spots under UV lamp, one with an *Rf* value of 0.34 that corresponds to the desired product and the second with an *Rf* value of 0.48 and corresponds to piperidine capped monomer. Furthermore, a ninhydrin stain showed the presence of a third spot at the baseline which corresponds to the excess piperidine. The crude product was dissolved in CHCl3 (8 L) and was washed with 5% aqueous HCl solution (3 x 2 L), 5% aqueous NaOH solution (3 x 2 L), and then brine (3 x 1 L). TLC monitoring confirmed the disappearance of the excess piperidine. The organic phase was dried with Na_2-SO_4, and the solvent was removed in vacuo to afford a crude product which was passed through a chromatography column, eluting with EtOAc-hexane (1:1) to isolate the impurities, followed by a 30% CH_3OH-CH_2Cl_2 elution to isolate the product. The appropriate fractions were collected, and the solvent was removed under reduced pressure. The resulting yellowish white solid was dried under vaccum for 3 days. Yield: 1.105 kg, 83%. 1H NMR (300 MHz, $CDCl_3$) δ: 6.71-4.85 (br, 18H), 3.80 (br, 24H), 3.70 (br, 36H), 3.55 (br, 36H), 3.36 (br, 12H), 3.04 (br, 24H), 1.83 (br, 12H), 1.68 (br, 24H), 1.58 (br, 18H), 1.53 (br, 36H), 1.38 (s, 108H). 13C NMR (75.5 MHz, $CDCl_3$) δ: 165.7, 165.3, 164.9, 164.5, 156.0, 78.8, 44.0, 43.0, 41.9, 37.0, 28.4,

27.6, 25.7, 24.8. MS (MALDI): calcd 4154.8224 (M+), found 4155.2448 (M + H+). Anal. Calcd. for $C_{201}H_{348}N_{72}O_{24}$: C, 58.07; H, 8.44; N, 24.26. Found: C, 57.91; H, 8.33; N, 24.48. The piperidine capped monomer sideproduct was recovered during purification (92 g). ^{1}H NMR (300 MHz, $CDCl_3$) δ: 5.35 (br, 2H), 3.69 (t, $^{3}J_{H\text{-}H}$ = 5 Hz, 8H), 3.56 (t, $^{3}J_{H\text{-}H}$ = 6 Hz, 4H), 3.02 (t, $^{3}J_{H\text{-}H}$ = 6 Hz, 2H), 3.00 (t, $^{3}J_{H\text{-}H}$ = 6 Hz, 2H), 1.66 (m, 4H), 1.60 (br, 4H), 1.54 (br, 8H), 1.40 (s, 18H). ^{13}C NMR (75.5 MHz, $CDCl_3$) δ: 166.0, 164.9, 156.0, 78.8, 44.1, 41.0, 36.8, 28.4, 27.4, 25.7, 24.9. MS (ESI): calcd. 576.4112 (M+), found 577.3884 (M + H+). Anal. Calcd. for $C_{29}H_{52}N_8O_4$: C, 59.41; H, 8.96; N, 19.12. Found: C, 59.20; H, 8.96; N, 19.69.

2.4.11 Synthesis of G2-$[N(CH_2CH_2CH_2NH_2)_2]_6$

Concentrated aqueous HCl (50 mL) was added to a solution of G2-$[N(CH_2CH_2CH_2NHBOC)_2]_6$ (5.0 g, 0.32 mmol) in CH_3OH (100 mL), and the clear solution was stirred at 25 °C for 24 h. The volatile components were concentrated in vacuo until only ca. 40 mL of water remained. The residue was made basic (pH = 14) with 85 mL of 10% NaOH (aq) solution, and the resulting milky suspension was extracted with $CHCl_3$ (1 L) using a liquid-liquid extractor until the alkaline aqueous solution became clear. The organic phase was dried over Na_2SO_4, and then the solvent was removed in vacuo to afford the product as a white solid. Yield: 3.51 g, >99%. 1H NMR (300 MHz, CDCl3 with trace CD_3OD) δ: 5.22 (br, 6H), 3.68 (br, 24H), 3.60 (br, 12H), 3.52 (br, 36H), 3.45 (br, 24H), 3.19 (br, 12H), 2.48 (br, 24H), 1.69 (br, 12H), 1.57 (br, 24H), 1.48 (br, 18H), 1.39 (br, 36H). ^{13}C NMR (75.5 MHz, $CDCl_3$ with trace CD_3OD) δ: 165.8, 165.4, 165.2, 165.1, 165.0, 164.6, 164.3, 43.8, 42.8, 41.7, 38.1, 37.3, 30.3, 27.7, 25.5, 24.6. MS (MALDI): calcd 2954.1932 (M+); found 2955.0237 (M + H+). Anal. Calcd. for $C_{141}H_{252}N_{72}\bullet 1.5CHCl_3$: C, 54.54; H, 8.08; N, 32.15. Found: C, 54.80; H, 8.08; N, 32.48.

CHAPTER III
THE USE OF TRIAZINE-BASED DENDRIMERS AS MACROMOLECULAR AGENTS FOR IRON-OVERLOAD THERAPY

3.1 Introduction

3.1.1 Iron-Overload

Iron is a necessary metal for normal cellular metabolism and respiration, however, excess levels of iron are cytotoxic and fatal if left untreated.[71] Iron absorption from the gut into the body and subsequent transport to organs involves a complex pathway of proteins not yet fully understood.[72] The uptake of iron is known to be highly regulated through various factors including iron deficiency and hypoxia, both of which increase iron absorption.[71] Alternatively, iron-overload and inflammation decrease absorption.[71] Intestinal epithelial cells absorb about 1-2 mg of iron per day through the divalent metal transporter 1 (DMT1), which equates to about 10% of daily dietary uptake.[71] The body has no active mechanism for the release of iron. In cases of iron-overload, desquamation, menstruation and other blood loss maintains iron homeostasis.[73] The body is therefore considered a closed system, recycling the iron which is taken up and storing excess iron for emergency situations such as major blood loss and anemic conditions.[71] The acute and chronic uptake and storage of excess iron in the body represents a group of hereditary and acquired conditions referred to as iron-overload which cause severe problems in normal organ function.[74] Therapeutic methods to sequester iron must be employed to actively remove iron from the body in states of excess. Such techniques have been shown to be effective through improved kidney filtration in the urine and biliary drainage from hepatocytes into the fecal matter of chelated iron complexes.[74] Iron-overload is the most common, chronic metal toxicity condition worldwide with the highest morbidity and mortality rate.[75]

Iron overload has been found to be both a genetic disorder present in recessive and dominant forms and as an acquired disorder from dietary and transfusional uptake of iron.[71] The disorder was first described in diabetic patients with skin discolorations in

1865,[76] however, the connection with iron was not made until 1890.[77] Hereditary hemochromatosis was later described by Sheldon in 1935,[78] but a great deal was still unknown about the disease leaving it quite difficult to treat. Since that time, various genetic mutations have been observed and used to classify the disorder into five different types of hereditary hemochromatosis, however, discrepancies arise throughout the literature as some forms of the disorder are not understood.[71, 74, 79]

Type 1 hereditary hemochromatosis is the most common form of iron overload as it affects between 1:200 and 1:500 people in the world equaling about 1 million American cases.[80] The HFE gene responsible for Type 1 hemochromatosis was first cloned in 1996[81] and mutations of the gene were found to prevent dimerization of the encoded protein through missense mutations of cysteine for tyrosine at position 282.[82] The cysteine is believed to participate in protein-protein complex formation with the transferrin receptor, however, it is unclear how this disrupts the regulation of iron.[83] Other proteins and signaling pathways have been identified, including hepcidin,[84] tranferritin receptor 2[85] and hemojuvelin.[86] In states of excess iron, hepcidin has been found to decrease iron absorption from the gut and prevent loss of iron from macrophages.[84, 87] Hepcidin is upregulated by the proteins mentioned here among many others, which are expressed in the presence of excess iron. The role of each protein is still unclear, but dramatic effects are observed when mutations of these proteins are investigated.[71]

Secondary iron overload, or acquired iron overload is most often caused by multiple blood transfusions throughout one's lifetime due to other disorders. Thalassemia, for example, is a chronic disease marked by anemia due to insufficient production of one globulin chain that forms hemoglobin.[88, 89] This reduced production of one globin chain causes abnormal hemoglobin formation resulting in poor iron complexation and eventually anemia. Thalassemia remains one of the leading causes of iron overload due to the blood transfusion therapy required to treat patients suffering from this disorder.[90] Blood transfusions tend to cause elevated levels of free iron due to iron present in the blood from lysed blood cells, making iron-overload a major indirect

side effect of thalassemia.[91] There are an estimated 100 million asymptomatic heterozygous thalassemia carriers worldwide with more than three quarters of the thalassemia population living in the Middle East, South East Asia and the Mediterranean.[92]

Excess iron remains a problem for several reasons, but Fenton-like chemistry is the major concern of iron toxicity within the body, leading to oxidation of cellular organelles and cellular membranes.[93-95] The oxidative potential requires that iron be complexed in proteins such as transferrin, hemoglobin and ferritin. Transferrin consists of two iron binding regions and functions in iron transport throughout the blood. It is estimated that only about 1% of total body iron is located in transferrin, which is about 25-40% saturated at any given time.[96] The majority of iron is stored in cellular domains within the liver and heart among other organs.[96] With such small amounts of iron present in blood proteins and the variance of iron within the proteins, it is quite difficult to assess the actual levels of iron within the body. Furthermore, it is unclear what levels of iron constitute iron overload and what levels of iron are actually toxic.[97]

Free radical reactions associated with iron overload have been shown to cause lipid peroxidation of cells and cellular organelles causing membrane breakdown and cellular death and eventual tissue and organ dysfunction.[98-100] The heart, liver and endocrine system are the most common organs affected by iron-overload due to the propensity for iron to be taken up in these organs.[90] Excess iron stored in the heart tissue may cause congestive heart failure,[101] pulmonary hypertension[102] and myocarditis.[103] In the liver, portal fibrosis and cirrhosis remain major life-threatening side-effects of iron overload, which are shown to accelerate with viral infection and alcohol use.[88, 104-107]

The endocrine system is commonly affected by iron through hormonal deficiencies, which affect growth and reproduction while also affecting insulin production due to pancreatic iron uptake causing diabetes mellitus.[108-110] Treatment of patients with chelation therapy has shown dramatic results in reducing the side effects related with iron overload and a great decrease in the mortality rate when iron-overload is detected in a timely manner.[90] While heart and liver disease are the most common

causes of death in iron overload patients, the levels of blood flow necessary in the brain also causes damage to brain tissue. A great deal of research is currently focused on disorders such as Alzheimer's disease,[111, 112] Parkinson's disease,[113, 114] multiple sclerosis[115] and central pontine myelinolysis,[116] and their association with iron among other metals.[117-119] It has been found that transferrin deficient mice continue to receive high levels of iron in the brain ruling out the possibility that transferrin is the only vehicle which takes iron to the brain, however, intracellular trafficking is inhibited and produces iron pools causing subsequent tissue oxidation.[120-122]

Despite the high occurrence, many physicians inaccurately consider haemochromatosis to be a rare disease due to poor diagnosis.[123] Measurement of body iron levels has proven to be one of the major obstacles in diagnosis of iron-overload due to the inadequacies of detection. Indirect methods of measuring iron levels include measurement of serum ferritin concentrations,[124] serum transferrin saturation,[125] desferrioxamine-induced urinary iron excretion,[126] imaging of iron,[127] and evaluation of organ function.[128] Heart biopsy,[129] liver biopsy and superconducting susceptometry with a *S*uperconducting *QU*antum *I*nterference *D*evice (SQUID)[130] are the three methods of direct iron measurement. Direct tests are more ideal in the correlation of actual body iron levels; however, these tests are often invasive, painful and expensive. More commonly, indirect tests are performed, which tend to lack specificity and sensitivity with low correlation to actual iron levels. Indirect tests, however, are generally non-invasive and are inexpensive, but questionable results require further examination through direct methods and eventual therapy when a positive detection is achieved.

3.1.2 Desferrioxamine B as an Iron Sequestration Agent

Several iron specific chelation therapies have been proposed, however, the Food and Drug Administration has approved only three agents for preclinical or clinical use, to date, for iron overload therapy. Deferriprone (Ferriprox) as an investigational new drug, deferasirox (Exjade)[131] and desferrioxamine B (Desferal) are shown in **Figure 3.1**.

Desferrioxamine B (DFOB) is the most widespread therapy used, however, a significant amount of literature is available on the others.[92, 132-138]

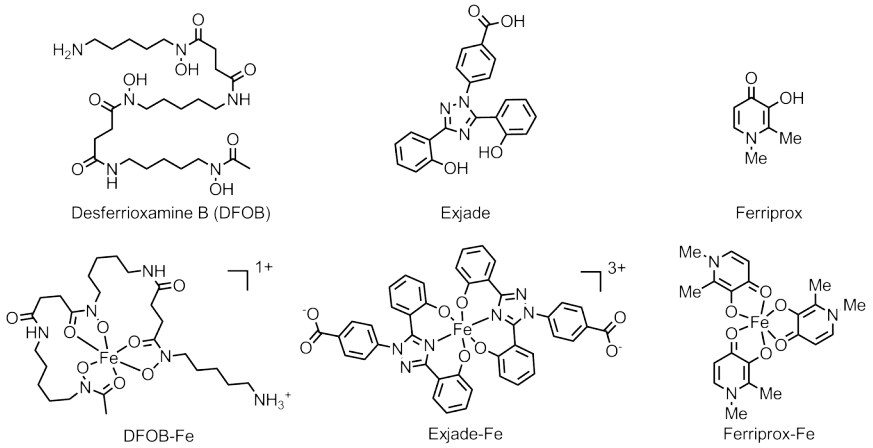

Figure 3.1: DFOB, Exjade and Ferriprox with corresponding iron complexes.

Desferrioxamine B (DFOB) is a siderophore produced by Actinomycetes (*Streptomyces pilosus)* and was first isolated and characterized in 1960.[139] Siderophores are microbial metabolites produced and released in oxic conditions to mobilize and allow for cellular trafficking of insoluble ferric ions for cellular function.[140] Many siderophores are known to chelate various metals, however, the hydroxamate functionality present in the ferrioxamine family of siderophores creates a highly specific iron chelate for cellular trafficking.[141] The ferrioxamines are a specific class of hydroxamate-based siderophores, which exist in linear and cyclic conformations.[142] DFOB is a linear ferrioxamine with a wide range of affinities for a variety of metals. Metal chelation for various applications with DFOB has been studied using Zr(IV);[143] V(IV) and V(V);[144] Cr(III);[145] Mn(III);[146] Fe(II) and Co(III);[147] Sr(II), Cu(II), Ni(II), Zn(II) and Mo(VI);[147-149] Ga(III), In(III) and Al(III);[150-153] Sn(II), Bi(III) and Hg(II);[154] Pb(II) and Eu(III);[155] Th(IV) and Pu(IV).[156] The metal binding affinity of DFOB for a variety of metals is shown in **Figure 3.2**, which is determined through correlation of the log K values of the DFOB with the log K values for hydroxide ions.[65] The linear relationship offers insight into the correlation

between acidity of the metal ion while the low y-intercept indicates the level of preorganization.[157] Ferric ions are hard and quite acidic requiring negatively charged, strongly basic oxygen donors for chelation as is present in the hydroxamic acid moieties of DFOB.[158] While the basicity favors more acidic metals, the low level of preorganization leads to slow metallation and demetallation kinetics providing a highly selective iron chelate.[157]

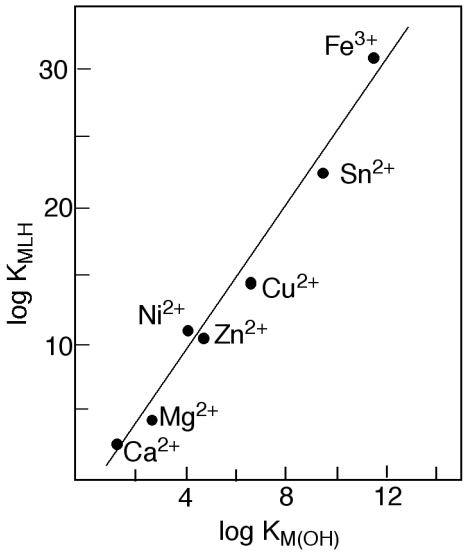

Figure 3.2: Correlation of log K_{MLH} values for DFOB against $K_{M(OH)}$ values for various metal ions.[65]

The three hydroxamic acids moieties present in DFOB form a hexadentate octahedral complex around iron (III) at physiological pH.[64] This complex creates a *cis* (facial) configuration forming two trigonal octahedral faces with the hydroxyls and carbonyl oxygens, of the three hydroxamates.[64] Furthermore, the solid state crystal structure shows that the primary amine present in the molecule does not contribute to the stability of the complex, but forms a dimer through electrostatic interaction with a perchlorate ion.[64] It has been proposed that the amine is used as a solubilizing group and as a recognition unit for cellular trafficking,[64] and thus it has also been the target of DFOB functionalization.[159-165]

While DFOB has an affinity for many metals, the high affinity for iron(III) presents the use of this siderophore as a therapy for iron-overload.[166-169] Initial studies with DFOB found that the drug was not orally available due to low lipophilicity, mainly due to the charged primary amine at physiological conditions, leading to only 15% bioavailability when orally administered.[167] Recommendations for the delivery of DFOB were shortly thereafter developed for the treatment of acute iron poising involving placement of 5-10g of DFOB in the stomach after gastric lavage, followed by *i.v.* administration of DFOB with regular urine monitoring.[170] The approval of the drug by the US Food and Drug Administration in 1968 opened the door to much more testing and development of an administration regimen. The effectiveness of 24 h i.v. infusions,[171, 172] 24 h subcutaneous administration[173, 174] and 12 h subcutaneous infusions[175] were reported. Currently, however, DFOB is most commonly administered through subcutaneous infusion over 6 or 7 hours, seven days a week as a person sleeps.[95] While the chronic regimen required has improved over the past few decades, the treatment of iron-overload using this method causes non-compliance with many patients due to high cost ($10,000-$30,000 annually), discomfort and minor side effects in a small number of patients.[138]

The side effects of Desferrioxamine B are rare, but include ocular and auditory abnormalities,[176-185] sensorimotor neurotoxicity,[186] changes in renal function,[187, 188] and pulmonary toxicity[189, 190] as well as evidence of failure to grow due to cartilaginous dysplasia in the spine and long bones.[191-196] Toxic side effects are generally observed over prolonged periods and during high-dose usage, as DFOB chelates metals and undergoes reduction to form oxidants[197] or as DFOB-Fe infiltrates the healthy cells and acts in the same manner.[198] Thus, the short half-life of DFOB poses problems due to the high rate of glomerular filtration by the kidneys[199] and plasma metabolism[200, 201] requiring high dose injections causing many of the undesired side-effects over time. Investigation of the major pathway for metabolism found that the plasma was responsible for the majority of inactivation of DFOB as compared to metabolism in the pancreas, small intestine, brain, liver, muscle, and spleen in various animals.[200]

Remarkably, human and dog plasma had significantly lower rates of DFOB metabolism as compared to rat, rabbit, guinea-pig, cat, bovine and pig, while mice had the fastest rate of metabolism.[200] Studies have proven that the major metabolites found in the urine involve conversion of the primary amine into a series of oxygenated species, which have decreased binding affinity.[202, 203] This data is in direct contradiction to the assertion that the primary amine does not contribute to the stability of the complex. With such high levels of renal filtration of both the free chelate and the iron complex, spectroscopic studies of patient urine after therapy may be performed to determine if free iron is present in the blood.[204] While DFOB is generally considered a chelate for non-transferrin bound iron in the blood, it has also been found to mobilize iron from ferritin storage within cells,[205] but poor lipophilicity of the chelate prevents cellular penetration. It is believed that DFOB must become internalized into the cell through endocytosis to have a direct effect on intracellular iron stores. This has been shown through in vitro cell studies that have undetectable decreases in intracellular iron stores treated with DFOB except in the case of Kupffer cells in the liver, which readily undergo endocytosis to easily allow DFOB to enter the cell.[206]

Although the majority of DFOB applications involve iron-overload, the chelation ability of DFOB may also be exploited in a variety of avenues including MR imaging, [207, 208] PET imaging,[143] antibacterials and antibiotics,[209] superoxide dismutase mimics,[146] hypoxia-mimetic agent[210, 211] and cancer therapy.[147, 151, 153, 165, 212]

3.1.3 The Development of Alternative Small Molecule Iron Chelates

Much research has now focused on the development of lipophilic iron chelates, which are then orally available and may easily traverse cell membranes and chelate non-transferrin bound iron stores within the cell. Two drugs, for example, which achieve these goals, are deferasirox and deferiprone. However, these orally active therapies suffer from side effects including nausea, abdominal discomfort, and high potential for renal failure among others.[138] Annual cost for deferasirox (Exjade®) has been estimated at $20,000-$60,000, thus, preventing widespread usage in the US as well as many

developing countries.[138] While delivery remains the major drawback of DFOB, the minimal side effects and low cost allows DFOB to remain as the desired chelation agent of choice.

Alternatively, small molecule bis-(hydroxylamino) triazine-based chelates have been developed by Melman and coworkers, which show high Fe(III) binding specificity in competition with other metals.[213, 214] Such structures have been synthesized in high yield and also show high binding affinity for Vanadium oxide for magnetic resonance imaging[215] and titanium for cancer therapy.[216-218] While limited studies are available on these chelates, the potential for further explotation of this ligand system which take advantage of synthetic ease and scalability are warranted.

3.1.4 Macromolecular Iron Chelation Agents

From the promising clinical data obtained with DFOB and the less than ideal pharmacokinetics of the therapy, the desire to find chelation therapies able to remain in the blood for significant lengths of time has attracted a great deal of focus. Prolonged blood plasma half-lives of macromolecular agents has shown great success due to the decreased glomerular filtration and hepatic cellular trafficking allowing for longer plasma circulation times.[24, 33, 37] Using increased size as an aid in developing chelating agents, DFOB was attached to dextran or hydroxyethyl-starch (HES) biocompatible polymers through reductive amination after oxidation of the polysaccharide.[159, 160, 219] DFOB loading on the polysaccharides varied according to the amount of periodate used in the oxidation of the starch and the amount of DFOB used in reductive amination, however, dextran had 20-30% incorporation by weight while HES had only 10-20% incorporation by weight.[159] Attempts to calculate the relative toxicity of the polymer-DFOB conjugates compared to DFOB alone and polymer-DFOB-Fe compared to DFOB-Fe failed due to the amount of dose necessary leading to lethal hypervolemic and hyperoncotic effects. The LD_{50} values for DFOB and DFOB-Fe through *i.v.* administration are 0.4 and 1.4 μmol/g, respectively, which are much below the range of the polymer conjugates.[219] During *in vivo* experiments with mice in which acute iron

poisoning was induced with iron sulfate injection or oral administration immediately followed by therapy, 100% survival was achieved with the conjugate compared to 22% for DFOB alone and 30% for polymer alone.[219] Efficacy of injection 1 hour after administration of iron resulted in 77% survival as compared to 0% survival in the other cases.[219] Furthermore, the long retention times in the vasculature of a mouse increased from 5.5 minutes for free DFOB to 67 minutes for the dextran conjugate and 84 minutes for the HES conjugate.[159] Iron excretion in the urine also proved to be comparable and better than DFOB alone,[159] leading the eventual pre-clinical studies in human subjects.[160] Plasma half-life of between 22 and 32 hours were reported for the HES-DFOB conjugates depending on the dosage, which ranged from 0.3 mL/kg to 9 mL/kg.[160] Generally 35-55% of initial dose of drug was recovered in the urine 48 hour along with up to 7 mg iron as compared to 0.06 mg in control patients.[160] The major drawback of this therapy was the 14,000 to 200,000 Da molecular weight range associated with the conjugates.[160] Development of monodisperse macromolecular iron sequestration agents such as chelate decorated dendrimers is of interest.

The first report of metal sequestration using dendrimer constructs appeared in 1999 for the sequestration of Cu(II) in unmodified PAMAM dendrimers.[220] This work opened the door to directed iron sequestration using salicylate-, catecholate- and hydroxypyridinonate-functionalized dendrimers for the sequestration of iron.[221-224] The advantage of using such monodisperse agents allows for more concrete characterization as compared to the dextran and starch therapeutics. The development of new dendrimer-chelate constructs remains a topic of interest. Our investigations toward the attachment of DFOB to triazine-based dendrimers are described.

3.2 Results and Discussion

3.2.1 Selective Reaction of the Primary Amine of DFOB

When devising a strategy to install DFOB on the dendrimer, both the nucleophilic and electrophilic linkage routes must be considered. The crystal structure of DFOB-Fe has shown that the primary amine is not involved in complexation, which

would suggest that selective functionalization of the amine would be the route of choice for attachment to the dendrimer. The amine alone is a nucleophile, however, primary amines such as this generally do not react easily with poly(monochlorotriazine) containing dendrimers. Therefore, we aimed to pursue the electrophilic route, where DFOB is reacted with cyanuric chloride to produce the dichlorotriazine. Initial attempts to obtain this molecule proved problematic due to the similar pKa values, and thus similar reactivities, between the primary amine and each of the hydroxamic acids.[65] The similar reactivity of each nucleophile in DFOB led to the formation of oligomers and polymers as determined by MALDI-TOF mass spectrometry. The poor selective reactivity toward cyanuric chloride led us to attempt various other amine selective chemistries, including reductive amination and acetate protection of the hydroxamic acids in the presence of 18-crown-6 as a transient amine protecting group. Each attempt at selective functionalization proved futile in our hands and a new method was needed.

To circumvent the nucleophilicity of the hydroxamic acids, iron was also utilized as a protecting group, which could be removed later through a number of potential routes. The lewis acidity of iron and the catalytic effect on chlorotriazine substitution is believed to catalyze the reaction to generate a mixture of mono- and di-substituted triazines. Understanding the reactivity of triazines and the results from this reaction, a dichlorotriazine containing propargylamine was then reacted with DFOB-Fe(III) to afford the desired monochlorotriazine as shown in **Scheme 3.1**. When reacted with the primary amine terminated second-generation dendrimer, however, complete reaction was unattainable. This result, although undesirable, was understood due to the poor nucleophilicity of primary amines, poor electrophilicity of monochlorotriazines, the steric hindrance and poor solubility of the product.

Scheme 3.1: Synthesis of the monochlorotriazine containing Fe-DFOB unable to add to the dendrimer due to poor reactivity, solubility and sterics.

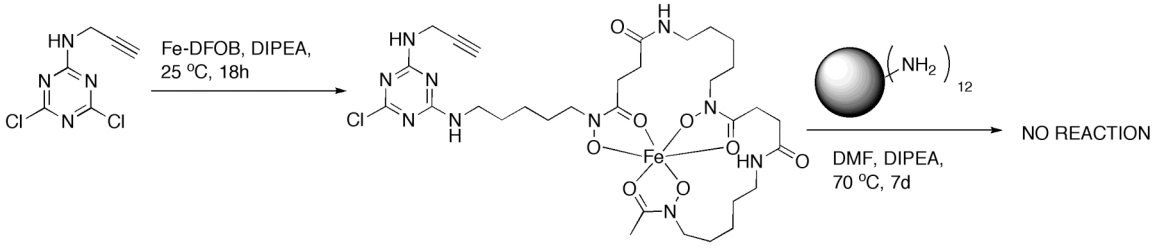

An alternative route for selective functionalization was then attempted using azide transfer chemistry. The Alper-Wong azide transfer reaction converts primary amines into azides through the use of triflic azide in the presence of a copper catalyst.[225] This reaction has been shown to proceed efficiently in the presence of a variety of functional groups and in high yield. Desferrioxamine B proved to be an ideal molecule for this reaction as the conversion of the primary amine to an azide proceeded in 62% yield. The obtained azide may then undergo the Huisgen-Sharpless "click" reaction.[226] Click reaction of the DFOB-azide with alkyne terminated dendrimers to afford the dendrimer-DFOB construct through a triazole linkage as shown in **Scheme 3.2**, proved problematic. While this reaction is robust and proceeds in a variety of conditions with a wide range of substrates, DFOB however, is unsuccessful as only a portion of DFOB-azide has been attached to the dendrimer. This incomplete reaction may be due to chelation of copper by desferrioxamine preventing catalysis to occur, however issues with solubility are more likely the ultimate limitation of this chemistry as amine functionalized DFOB has been shown to inhibit solubility.[163] Incomplete reactions may occur due to the hydrogen bond interactions present in the final product, which form insoluble aggregates. While poor solubility may be the culprit, methods to solubilize lipophilic drugs covalently and non-covalently linked to dendrimers have been addressed in the past. However, due to the extremely explosive triflyl azide intermediate used in the azide transfer reaction, this method has been abandoned.

Scheme 3.2: An unsuccessful click reaction with desferrioxamine B-azide and an alkyne-containing dendrimer.

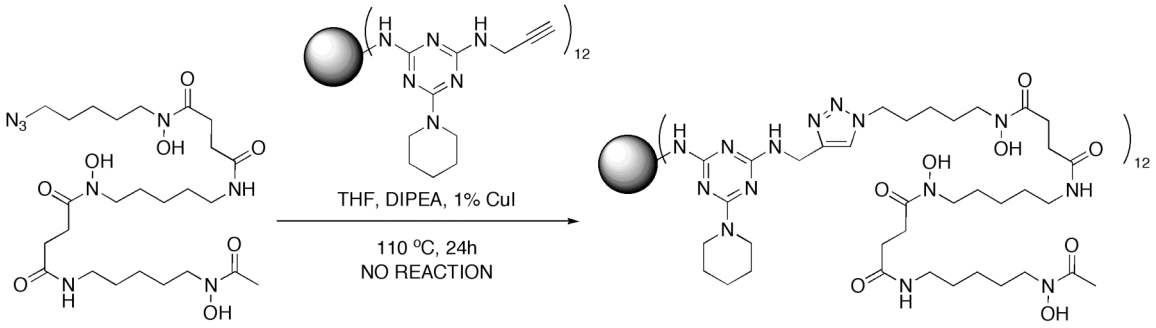

3.2.2 Increasing the Nucleophilicity of the Primary Amine

Another method to attach DFOB to the dendrimer is to increase the nucleophilicity of the primary amine with cyclic secondary amines, which will enable reaction with a poly(monochlorotriazine) dendrimer. Increasing the nucleophilicity of the primary amine through reaction with isonipecotic acid allows for reaction with chlorotriazines as the third substitution. This has been achieved through a one-pot reaction of DFOB with the NHS-ester of Fmoc-protected isonipecotic acid and deprotection to produce Inp-DFOB. Poor characterization data by mass spectrometry has led us to characterize the compounds using NMR alone. Purification is carried out through filtration with water to remove DBU, followed by toluene to remove 9-methylene fluorene produced in the deprotection. The secondary amine is then capable of reacting as the third substituent on the triazine ring using the poly(monochlorotriazine) dendrimer obtained in the kilogram-scale synthesis as shown in **Scheme 3.3**. During this reaction an insoluble mass forms, which is insoluble in all solvents for further characterization. Attempts to characterize the solid by NMR, mass spectrometry and infrared spectroscopy resulted in insufficient data to quantify the extent of the reaction or evidence of a reaction occurring at all. It is likely that the poor mass spectral data obtained with DFOB alone is likely compounded when multiple chelates are attached to the dendrimer. NMR was also unsuccessful at providing adequate data for a reaction taking place. The poor solubility of DFOB and the sterics

involved are likely to hinder reaction with the dendrimer. Various attempts to achieve the desired product using this construct resulted in solid masses, which were uncharacterizable. Other constructs also provided similar results with characterization showing greater potential than in the kilogram-scale dendrimer, but complete substitution was never achieved.

Scheme 3.3: Synthesis of Inp-DFOB and subsequent unsuccessful reaction with the poly(monochloro triazine) dendrimer.

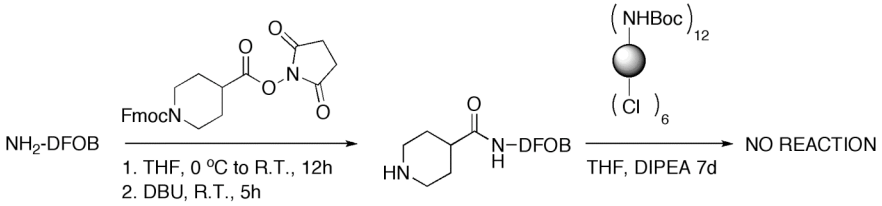

To overcome issues of solubility, PEG-mono-methylether was reacted in one pot with cyanuric chloride to form the first substitution followed by reaction with the dendrimer. Purification of the poly(monochlorotriazine) dendrimer was performed using ultrafiltration through regenerated cellulose membranes. The need for higher molecular weight PEG chains also led to a loss of monodispersity of the starting material inhibiting characterization of the product. This route was abandoned and further attempts to functionalize the dendrimer with DFOB was determined to be unwarranted.

3.3. Conclusions

Iron-overload is a serious condition, which is believed to affect a significant number of people around the world. The symptoms of this disease are oftentimes characterized as old age. Proper diagnosis requires invasive testing, which is still inaccurate due to the patient variability and the inability to accurately classify the limits of iron toxicity. However, when testing concludes that patients are suffering from the disease, therapy must be implemented to diminish the side effects. Current therapies include deferrioxamine B, deferiprone and deferasirox.

Desferrioxamine B is considered the gold standard in the treatment of iron-overload. While it has been used widely in patients with both hereditary hemochromatosis and secondary hemochromatosis, the poor bioavailabilty and inconvenient route of administration prevents the drug from achieving its full potential. New small molecule chelates such as deferiprone and deferasirox have improved bioavailability, but possess other issues such as toxicity and high cost. With poor drug pharmacokinetics and toxicity with the currently approved therapies, the utilization of polymer technologies provide additional benefits in treating this disease. From carbohydrate polymers containing DFOB to dendrimers with synthetic chelates, the field of polymer based iron chelation is burgeoning and continues to improve therapy.

In our hands, attachment of DFOB to a dendrimer has proven unsuccessful due to similar reactivities of the amine and hydroxamic acids. Furthermore, the solubility of the chelate and the inability to characterize insoluble products obtained through reaction with DFOB-Inp and the poly(monochlorotriazine) dendrimers were largely unsuccessful. While partial reaction was eventually achieved in one situation using a dendrimer containing propargylamine as one substituent on a poly(monochlorotriazine) dendrimer the ability to achieve monodisperse constructs for chelation therapy was never met. Attachment of DFOB to polydisperse polymers has been achieved in the past, but the utilizion of triazine-based dendrimers has proven to be problematic thus far and does not warrant further investigation with our current dendrimer system. Alternatively, the use of synthetic triazine-based small molecule chelates have shown great promise in iron chelation and shows greater promise toward inexpensive polymer therapeutics for the treatment of iron-overload.

3.4 Experimental

3.4.1 Materials and Instrumentation

All reagents were procured from Sigma-Aldrich (St. Louis, MO) and used as received without further purification. Fmoc-protected isonipecotic acid was purchased from NovaBiochem (San Diego, CA) and used without further purification. NMR

spectra were recorded on a Varian Mercury 300 MHz spectrometer in $CDCl_3$, or DMSO-d6. All mass spectral analyses were carried out by the Laboratory for Biological Mass Spectrometry at Texas A&M University.

3.4.2 Synthesis of Desferrixoamine B-Isonipecotic Amide

A round bottom flask containing 959.9 mg of desferrioxamine B mesylate (1.46 mmol) dissolved in 20 mL THF stirred on ice for 30 minutes. Then 655.0 mg Fmoc-Inp-NHS (1.46 mmol) was added and the reaction stirred warming to room temperature for 12 h. The reaction became cloudy white during this time. Then, 0.2 mL of 1,8-diazabicyclo[5.4.0]undec-7-ene (DBU) (1.34 mmol) was added to the solution and the solution immediately cleared and a precipitate formed. The solution stirred for 6 h and was concentrated in vacuo. The residue was then mixed with water to form a precipitate, which was filtered and collected. The resulting solid was then mixed with toluene to form 422 mg (0.63 mmol, 43%) of the off-white solid product collected by filtration. ^{1}H NMR (300MHz, $CDCl_3$): 1.21 (br m, 6H), 1.37 (br m, 6H), 1.49 (br m, 6H), 1.62 (br m, 4H), 1.89 (t, 1H), 1.96 (s, 3H), 2.26 (t, 3H), 2.30 (s, 1H), 2.45 (s, 1H), 2.50 (t, 2H), 2.52-2.67 (m, 8H), 2.90 (br m, 2H), 2.99 (q, 4H), 3.23 (t, 6H), 3.44 (t, 6H), 3.52 (br d, 1H), 7.81 (br s, 3H). ^{13}C NMR (75MHz, $CDCl_3$): 22.2, 25.8, 28.4, 29.6, 36.8, 43.6, 48.3, 52.8, 154.2, 161.9.

3.4.3 Synthesis of Desferrioxamine B-Containing Dendrimer

A round bottomed flask containing 12 mg of G2-$[N(CH_2CH_2CH_2NHBOC)_2]_6$ (0.004 mmol) stirred in 1 mL THF as 50 mg DFOB-Inp (0.074 mmol) was added to the solution. Then, 0.2 mL DIPEA was added and the solution continued to stir for 7d. A solid was obtained, which could not be characterized. The solution was concentrated and showed starting material by NMR and MS.

CHAPTER IV
TRIAZINE-BASED DENDRIMERS CONTAINING CAMPTOTHECIN AS DRUG DELIVERY VEHICLES FOR CANCER THERAPY*

4.1 Introduction

The camptothecins are cytotoxic, quinoline alkaloids characterized by a planar pentacyclic ring system.[227, 228] Isolated using an anticancer activity screen by Wall and Wani in 1966 from the bark of *Camptotheca acuminata*,[227] 20-(S)-camptothecin suffers from many limitions including poor solubility, rapid clearance, high systemic toxicity and/or poor selectivity toward cancer cells.[39] A year after the discovery of camptothecin, Wall and Wani discovered paclitaxel, another anticancer drug, which also showed great promise.[229] While both drugs showed powerful anticancer activity,[230] camptothecin's poor solubility and unpredictable adverse drug interactions favored the development of paclitaxel as a broad spectrum chemotherapeutic.[231]

The camptothecins gained much interest in the late 1980's when the molecular target was identified: DNA topoisomerase I (TOP I) is believed to be the single point of biological activity.[232-237] Crystal structures later confirmed the binding pocket for camptothecin as well as for a series of other compounds.[238-240] TOP I is an essential enzyme that relaxes supercoiled DNA prior to transcription through the formation of single strand breaks and religation. Upon irreversible binding to TOP I, camptothecin prevents religation and causes apoptosis. Pommier has reviewed the literature focusing on the genetic basis of TOP I inhibition.[66]

Various structure activity relationships have shown that while the A-D rings of camptothecin are necessary to maintain activity, modifications of these rings attenuate efficacy.[241] The E-ring lactone, however, is necessary for activity due to the binding site

---

* Reproduced by permission of The Royal Society of Chemistry: Venditto, V.J.; Allred, K.; Allred, C.; Simanek, E.E. *Chem. Commun.* **2009**, 5541-5542**.**

found in TOP I.[242] Upon removal of the lactone or hydrolysis to the carboxylate, all activity is lost. Camptothecin in the active lactone form and inactive carboxylate form are shown in **Scheme 4.1**. The equilibrium between the closed, active lactone and the open, inactive carboxylate form is further influenced by both the affinity of the carboxylate for human serum albumin and the local pH *in vivo*.[243] Originally, camptothecin was delivered as the sodium salt of the carboxylate to help overcome solubility issues, however, the poor efficacy created a need for new alternatives.[244] Two camptothecin derivatives, irinotecan and topotecan, were eventually approved for clinical use along with 10-hydroxycamptothecin, another naturally occurring derivative. Currently, the camptothecins — notably topotecan,[245-251] irinotecan,[252-257] 9-aminocamptothecin,[258, 259] 9-nitrocamptothecin[260, 261] and belotecan[262] — are commonly used as a late-stage therapy either alone or in combination therapies.

Scheme 4.1: Camptothecin in the lactone form and open carboxylate form.

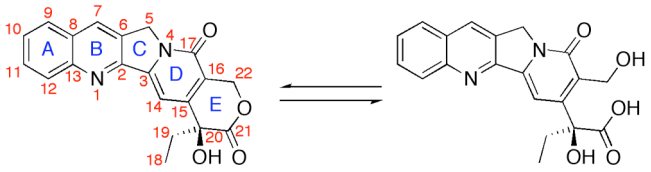

Even given the hydrolytic sensitivity, the drug remains highly active as an anticancer agent. When delivered in an intralipid formulation through i.m. administration, camptothecin showed nearly 100% growth inhibition and regression in colon, lung, breast, stomach, ovary and malignant melanoma xenografts.[263]

Pharmacokinetic studies of camptothecin in the lactone and carboxylate forms were performed in rats to better understand the focus of future work.[264] In various buffers at 37 °C the carboxylate was shown to be the predominant form. In PBS at pH 7.2, 7.4 and 8.0, the half-life of the lactone was 33 min, 22 min and 5.3 min, respectively. Furthermore, equilibrium was achieved between both forms 90 minutes after injection of either 1 mg/kg lactone or carboxylate in rats. The carboxylate was

cleared at a much faster rate through the urine and bile as compared to the lactone form. Clearance was also shown to be pH dependent, suggesting that decreasing pH of the urine may reduce bladder toxicity caused by the carboxylate form.[265] Additional studies in dogs, monkeys, rats and mice showed toxic effects, including emesis, diarrhea, dehydration, coma and death. Intravenous administration of 80 mg/kg or five doses of 0.625 mg/kg/day in dogs showed cumulative toxicity that was entirely reversible in survivors.[266] In human subjects, unpredictable toxicity associated with camptothecin halted clinical trials and opened the door for new antitumor agents.[267-271] The preparation and assessment of derivatives through classical structure activity relationships led to increased efficacy and better understanding of such activity.

Structure activity relationships (SAR) have been carried out, which have led to the development of new camptothecins with potent antitumor activity.[237, 241, 244, 272-278] Many efforts focused on stabilizing the lactone without compromising cytotoxicity. To summarize the SAR studies, the A and B rings are the most tolerant to modification with substitutions at positions 7, 9, 10 and 11 improving or retaining activity. Altering the C and D rings or substituting positions 12 and 14, however, inactivates the molecules. Interestingly, von Hoff has provided evidence that substitutions which increase hydrogen bonding at the 7-position improve binding to TOP I, thus increasing activity over camptothecin.[279] The E-ring, where binding to TOP I occurs, may undergo only minor modifications without dramatic negative effects. Additionally, modification of the C20 hydroxyl group through alkylation or acylation has been shown to stabilize the lactone by creating a prodrug form, which is the favored method to link camptothecin covalently to polymer constructs.

Quinoline ring modifications of camptothecin are the most common. These derivatives show increased solubility, lactone stability and antitumor activity. Derivatives include the FDA approved drugs, irinotecan[280] and topotecan[278] among many others. Quinoline modified camptothecins, which have been investigated *in vivo* are shown in **Figure 4.1**. Many quinoline modifications have aimed to improve solubility through introduction of protonable amines.[274, 278, 280-284] While other

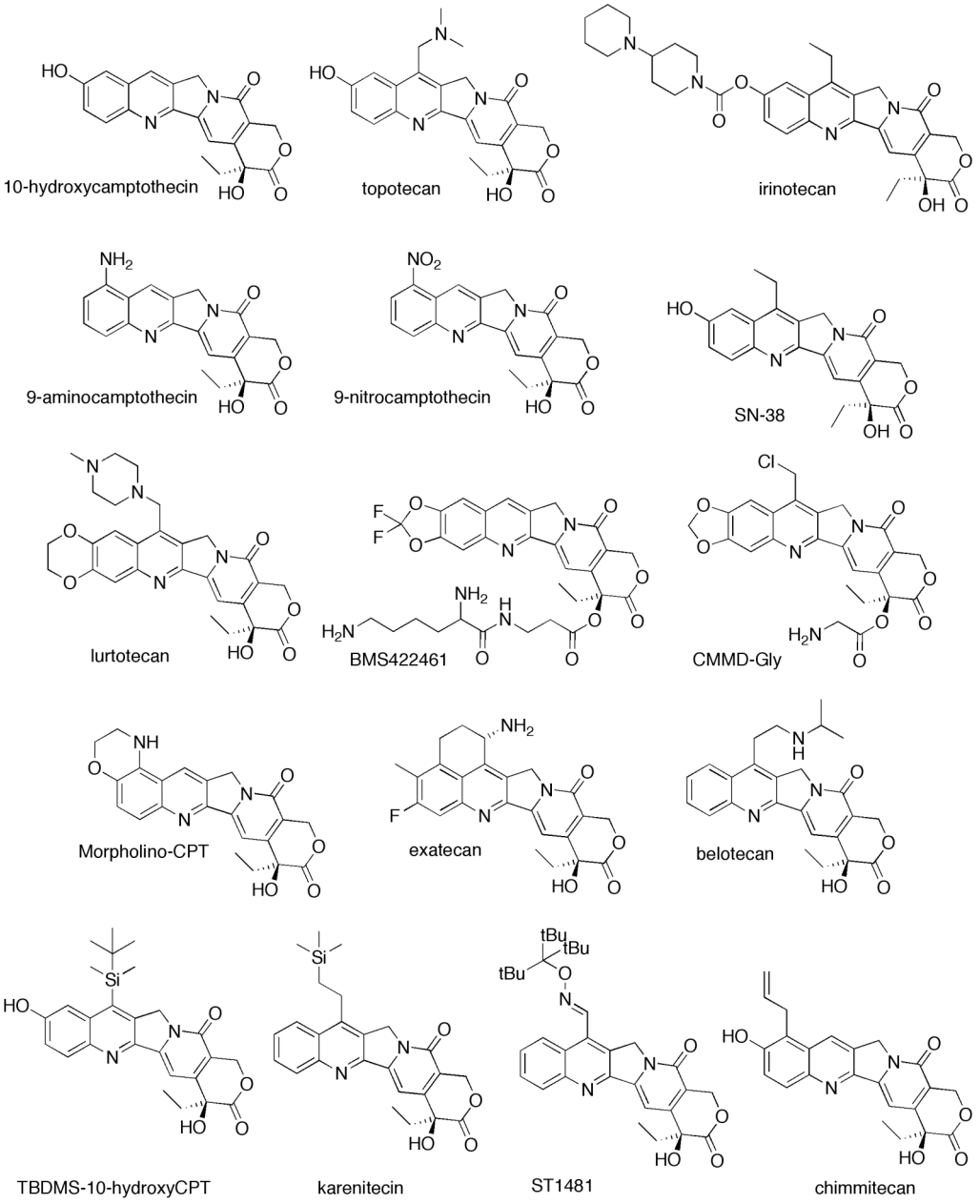

Figure 4.1: Quinoline modified camptothecins.

derivatives, including the siletecans,[285, 286] and chimmetican[287] have been synthesized to improve lipophilicity for improved blood brain barrier trafficking. Additional small molecule derivatives, which have not been investigated *in vivo* include Low's peptide folate conjugate,[288] Chen's 20-O-linked esters[289] and Battaglia's polyamine

conjugates.[290] Some modified lactone derivatives have been investigated *in vivo* including, the E-ring enlarged homocamptothecins characterized by a seven-membered beta-hydroxy lactone.[291, 292] While the homocamptothecins have shown improved lactone stability, irreversible inactivation of the drug through lactone hydrolysis is also observed.

Esterification or alkylation of the 20-hydroxyl group has also shown improved lactone stability in small molecules[293] and has become the favored method for covalent attachment in macromolecular drug delivery vehicles. A hypothesis proposed in 1992 implicates the hydroxyl group as a mediator of lactone hydrolysis by activation of water through a hydrogen bond interaction.[294]

The covalent conjugation of camptothecins to macromolecular architectures has shown great potential for improving pharmacokinetics and increasing tumor efficacy. Various covalent constructs have been tested *in vivo* including micelles,[295] linear polymers[296-302] and branched polymers.[303, 304] Most commonly, camptothecin is attached to the polymer through an ester bond with the 20-hydroxyl moiety. This linkage not only conveys solubility through conjugation with a water-soluble polymer, but also improves lactone stability. Some linkages are chosen as specific substrates for enzymatic cleavage, while others are used due to their pH sensitivity, but may also undergo hydrolysis. Covalent constructs offer advantages and disadvantages over non-covalent assemblies. Of the advantages, the opportunity to execute structure-activity studies in a very narrowly defined composition space is attractive. Disadvantages include, in addition to constituting a new drug entity, the burden of characterization. The characterization of covalent macromolecular constructs is oftentimes not trivial, and enthusiasm for biological results need to be tempered with the critical evaluation of the claims on composition. Noncovalent constructs have also been investigated *in vivo* including micelles,[305, 306] liposomes,[307-312] nanoparticles[313-315] and hydrogels.[316, 317] Various other covalent[318-327] and noncovalent[68, 328, 329] architectures have also been developed but still untested *in vivo*. Our approach to macromolecular covalent constructs for the delivery of camptothecin are discussed along with preliminary cytotoxicity data.

4.2 Results and Discussion

Upon completion of the kilogram-scale synthesis of a second generation dendrimer,[5] with attributes of a "universal" drug delivery vehicle we aimed to functionalize with camptothecin. Here, we describe the interception of the poly(monochlorotriazine) dendrimer with a camptothecin linked nucleophile. Our synthesis of the ester derivative of CPT (**Scheme 4.2**) utilizes 1-BOC-isonipecotic acid under standard coupling conditions to afforded **3** in 97% yield after methanol crystallization. Subsequent deprotection with trifluoroacetic acid gives the TFA salt of **4** in 82% after precipitation with methanol. Installation of the constrained secondary amine is a critical design element. These amines have been shown to be highly reactive towards monochlorotriazines.[20]

Scheme 4.2: Installation of BOC-Inp on 20-(*S*)-camptothecin through a hydrolysable ester linkage.

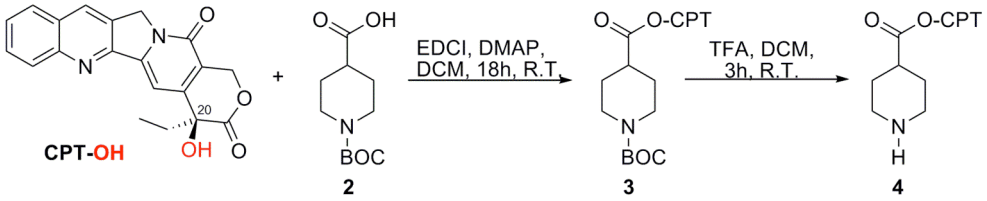

Scheme 4.3 shows the route for elaboration to the final products. Reaction of **4** with **1** was accomplished in *N,N*-dimethylformamide in the presence of *N,N*-diisopropylethylamine at 50 ^{o}C for 12 days to yield dendrimer **5**. While higher temperatures may accelerate this reaction; accelerated hydrolysis of the camptothecin ester led us to pursue this more conservative approach. Reaction progress could be followed with MALDI-TOF mass spectrometry with the desired species, **5**, appearing initially at day 4. While the spectra produced depend on matrix and ionization conditions, the reaction was continued until only lines corresponding to product, loss of BOC, and loss of a single CPT were observed. Purification was accomplished using Sephadex LH-20 size exclusion chromatography. While ^{1}H and ^{13}C NMR

corroborates the presence of six CPT groups on the dendrimer, NMR cannot be used to unambiguously quantify purities of these species due to the broad signals ineherent in these dendrimers.

Dendrimer **5** was deprotected using trifluoroacetic acid to afford **6** in nearly quantitative yield. PEGylation of the deprotected dendrimer was carried out using 2000 Da NHS-mPEG leading to dendrimer **7**. While both targets are water soluble, **7** was purified by ultrafiltration using a YM3 regenerated cellulose membrane in an Amicon stirred cell.

Scheme 4.3: Elaboration of the poly(monochlorotriazine) dendrimer to the amine and PEGylated targets.

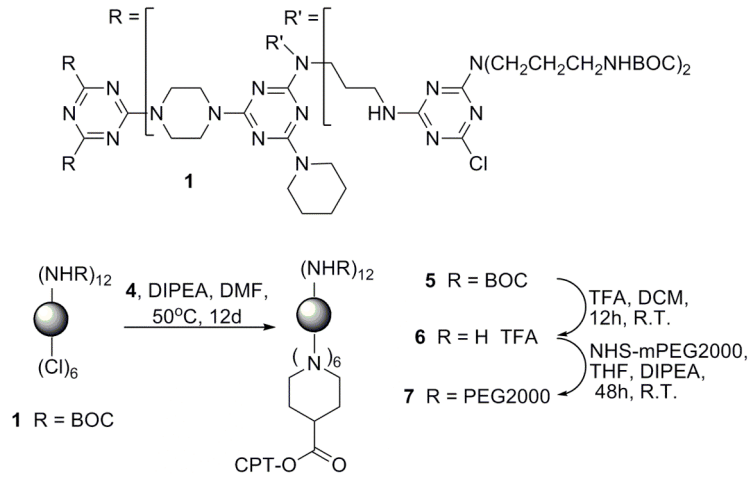

Cytotoxicity is measured using an assay that employs (3-(4,5-dimethylthiazol-2-yl)-2,5-diphenyltetrazolium bromide, or yellow MTT. The MTT assay quantitates the amount of living cells through the activity of mitochondria. In living cells, mitochondrial reductase converts the yellow tetrazole of MTT to a purple colored formazan. Therefore, the color of the media will not change when all the cells die from the cytotoxic agent investigated. Decreasing the dose from toxic to non-toxic generates a dose response curve. Evaluation of the dose-response curve at a

concentration where 50% of the cells die generates the IC_{50} value or the value where 50% of the cells are inhibited from proper function. Lower IC_{50} values therfore correspond to compounds with increased toxicity.

The cytotoxicity data for our compounds in comparison to the free drug is summarized in **Table 4.1** and is reported with respect to CPT concentration. Treatment of MCF7 and HT-29 cells provided dose dependent response curves for all analytes. The IC_{50} value for CPT was 0.2 μM regardless of cell line, while the IC_{50} value for irinotecan varied with line, 52 μM or 33 μM. Targets **6** and **7** showed intermediate values suggesting both an enhanced solubility of the construct over free CPT and similar behaviors of cationic and PEGylated vehicles. A drug-free dendrimer bearing piperidine groups instead of isonipecotic esters showed no toxicity up to 10 μM (60 μM in CPT equivalents) in MCF-7 cells, but an IC_{50} value of 2 μM in HT-29 cells. At this time it is unclear why there is a pronounced difference in toxicity between cell lines. Similar cell specific cytotoxicity has been observed using cyclic peptides.[21] Given the success of these constructs in vitro, further optimization of the synthetic strategy could offer routes to scales of material required for additional inquiry.

Table 4.1: IC_{50} values of free drug and dendrimer-drug conjugates determined by MTT assay.[a]

Cells	CPT	Irinotecan	G2-NH_2[b]	G2-CPT[d]	G2-CPT-PEG_{2000}[d]
MCF-7	0.2	52	14	9	13
HT-29	0.2	33	>60[c]	8	3

[a] IC_{50} values are reported in μM over three experiments in triplicate unless otherwise stated.
[b] Value is reported in terms of six potential CPT as compared to G2-CPT.
[c] No toxicity was observed up to the maximum dendrimer concentration of 10 μM determined by 9 experiments in triplicate.
[d] Values are reported in terms of six CPT present in each molecule.

4.3 Conclusions

Triazine-based dendrimers have shown promise as drug delivery vehicles, however further investigation must be completed to determine the full potential of such constructs. Through covalent attachment of camptothecin to the dendrimer through a hydrolysable linkage, we are able to improve the water solubility over the parent drug. The camptothecin containing PEGylated and cationic dendrimers both show improved water solubility over camptothecin alone and increased toxicity over the water soluble derivative, irinotecan. Our next step toward utilizing this triazine-based dendrimer containing camptothecin involves the efficacy of this construct in animals with human tumor xenografts.

As we move forward toward *in vivo* therapeutics, interpatient variability will likely play a significant role in success. Interpatient variability with both macromolecular constructs and free drug continues to hamper the widespread use of camptothecins. Some variability in pharmacokinetics has been shown to occur due to a mutation in ABCG2 transporter proteins when using diflomotecan.[330] This protein is believed to be responsible for natural detoxification and has been found to be overexpressed in the placenta, liver and intestine. Allele mutations have shown dramatically increased plasma AUC values for molecule substrates, which include 9-AC,[331] SN-38[332] and topotecan.[333] Although allele variants may provide insight into potential pharmacokinetic outcomes, it is likely that other physiological differences in tumors such as vascularization and expression of other proteins, may also cause variability. To overcome such challenges, our constructs are poised for codelivery of camptotehcin and DNA or RNA for transfection. Delivery of genetic information encoded for TOPI or ABCG2 protein expression will likely improve efficacy. Transfection enhanced toxicity with irinotecan has been observed through introduction of carboxylesterase enzymes,[334] which convert irinotecan to the active metabolized form in the cell rather than at the liver prior to tumor accumulation. Investigation with camptothecins using both transfection assisted therapy and macromolecular therapy is warranted.

4.4 Experimental

4.4.1 Materials and Instrumentation

All reagents were procured from Sigma-Aldrich (St. Louis, MO) and used as received without further purification. NHS-mPEG was purchased from NOF American Corporation. Amicon filters (YM-3: MWCO 3kDa) were purchased from Millipore. Size exclusion chromatography (SEC) was carried out using a Waters Delta 600 system and a Waters 2414 refractive index detector. A Suprema 10 micron GPC analytical column (1000 Å, 8 x 300mm) was used with 0.1 M $NaNO_3$ as the eluent and a flow rate of 1 mL/min. NMR spectra were recorded on a Varian Mercury 300 MHz spectrometer in $CDCl_3$, or DMSO-d6. All mass spectral analyses were carried out by the Laboratory for Biological Mass Spectrometry at Texas A&M University. MCF-7 (human breast cancer) cells were purchased from ATCC. Cells were maintained in phenol red free DMEM (Sigma) containing 10% fetal bovine serum (FBS) at 37°C in a 5% CO_2 atmosphere. HT-29 (human colon cancer) cells were purchased from ATCC. Cells were maintained in phenol red free DMEM F-12 (Sigma) containing 10 % FBS and 1% 1M HEPES.

4.4.2 Synthesis of BOC-Inp-CPT (3)

A solution of 1.40 g BOC-Inp (6.11 mmol) in 50 mL dichloromethane stirred as 3.55 g 1-ethyl-3-(3'-dimethylaminopropyl) carbodiimide (18.5 mmol) and 0.78 g N,N-dimethylaminopyridine (6.38 mmol)were added. After stirring for 30 minutes, 1.50 g camptothecin (4.31 mmol) was added and stirring continued for 18 h. The solution was concentrated *in vacuo* and the residue was precipitated with methanol to yield a yellow solid. Yield: 2.34 g, (4.18 mmol), 97%. ESI MS: calcd. mass for $(C_{31}H_{33}N_3O_7)^+$ 560.2398, found 560.2537. ^{1}H NMR (300MHz, $CDCl_3$): 0.98 (t, 3H), 1.43 (s, 9H), 1.71 (m, 3H), 1.97 (t, 2H), 2.15 (m, 1H), 2.27 (m,1H), 2.68 (m, 1H), 2.94 (m,2H), 3.98 (m,2H), 5.28 (s, 2H), 5.40 (d,1H), 5.68 (d, 1H), 7.21 (s, 1H), 7.68 (t,1H), 7.84 (t, 1H), 7.95 (d, 1H), 8.24 (d, 1H), 8.41 (s,1H). ^{13}C NMR (75MHz, $CDCl_3$): 8.3, 28.0, 28.2,

28.7, 30.9, 51.0, 67.0, 76.4, 79.4, 95.2, 119.5, 128.4, 128.7, 129.3, 129.6, 130.5, 131.1, 132.3, 146.1, 146.8, 148.5, 153.0, 154.5, 157.2, 167.8, 173.6.

4.4.3 Synthesis of Inp-CPT (4)

A solution of 1.01 g **3** (1.80 mmol) was stirred in 20 mL dichloromethane as 20 mL trifluoroacetic acid was added slowly. The reaction continued to stir for 3 h and was concentrated in vacuo to yield a yellow residue, which was precipitated with methanol to yield the TFA salt as a yellow solid. Yield: 0.82 g (1.47 mmol), 82%. ESI MS: calcd. mass for $(C_{26}H_{27}N_3O_5)^+$ 460.1873, found 460.1827. ^{1}H NMR (300MHz, DMSO-d_6): 0.95 (t, 3H), 1.79 (m, 2H), 2.17 (m, 4H), 3.05 (m, 3H), 3.28 (t, 2H), 5.30 (s, 2H), 5.52 (s, 2H), 7.06 (s, 1H), 7.72 (t, 1H), 7.87 (t, 1H), 8.14 (t, 2H), 8.70 (s, 1H). ^{13}C NMR (75MHz, DMSO-d_6): 8.3, 24.8, 25.2, 30.8, 37.7, 42.8, 51.0, 67.0, 76.8, 95.2, 119.4, 128.5, 128.7, 129.3, 129.6, 130.5, 131.1, 132.3, 146.0, 146.8, 148.5, 153.0, 157.2, 167.9, 172.9.

4.4.4 Synthesis of BOC-G2-CPT (5)

A solution of 54 mg of **4** (0.12 mmol) in 1 mL of N,N-dimethylformamide stirred as 22 mg second generation chlorotriazine dendrimer **8** (5.7 μmol) was added. The solution continued to stir as 40 μL of N,N-diisopropylethylamine was added to the reaction. The solution then heated to 50 ºC for 12 d and was cooled to rt. The reaction was then concentrated *in vacuo* and the residue was taken up in chloroform and passed through a Sephadex LH-20 size exclusion chromatography column. The purified material was dried *in vacuo*. MALDI-TOF MS: calcd. mass for $(C_{327}H_{444}N_{84}O_{54})^+$ 6399.36, found 6413.79. ^{1}H NMR (300MHz, DMSO-d_6): 0.99 (m, 18H), 1.10-2.50 (m, 245H), 2.75 (br m, 5H), 3.04 (br m, 30H), 3.34 (br m, 12H), 3.57 (br m, 30H), 3.76 (br m, 32H), 4.56 (br m, 12H), 5.27 (br m, 12H), 5.37 (br d, 6H), 5.71 (br d, 6H), 7.19 (br m, 6H), 7.66 (br m, 6H), 7.82 (br m, 6H), 7.92 (br m, 6H), 8.20, (br m, 6H), 8.38 (br m, 6H). ^{13}C NMR (75MHz, DMSO-d_6): 7.6, 25.0, 25.8, 27.8, 28.5, 31.8, 37.2, 42.4, 42.7,

43.1 44.1, 49.9 67.0, 79.0, 95.7, 120.1, 128.1, 128.4, 129.5, 130.6, 131.2, 145.9, 146.3, 148.8, 152.2, 156.0, 157.3, 164.9, 165.2, 167.4.

4.4.5 Synthesis of G2-CPT (6)

A solution of 25 mg of **5** (0.004 mmol) stirred in 2 mL dichloromethane as 1 mL trifluoroacetic acid was added. The solution stirred for 12 h and was concenctrated *in vacuo*. The residue was taken up in methanol and concentrated three times and used in the next step without further purification. MALDI-TOF MS: calcd. mass for $(C_{267}H_{336}N_{84}O_{30})^+$ 5202.07, found 5204.21. ^{1}H NMR (300MHz, $CDCl_3$): 0.95 (m, 18H), 1.10-2.50 (m, 245H), 2.88 (br m, 5H), 3.38 (br m, 12H), 3.61 (br m, 62H), 4.30 (br m, 12H), 5.24 (br m, 12H), 5.35 (br d, 6H), 5.57 (br d, 6H), 7.24 (br m, 6H), 7.64 (br m, 6H), 7.79 (br m, 6H), 7.93 (br m, 6H), 8.10, (br m, 6H), 8.43 (br m, 6H). ^{13}C NMR (75MHz, $CDCl_3$): 8.2, 26.0, 26.8, 28.0, 29.5, 30.8, 37.3, 42.4, 42.7, 43.0 44.1, 50.7 66.9, 76.5, 95.2, 119.4, 128.6, 129.3, 129.5, 131.0, 131.6, 132.7, 146.1, 146.7, 148.4, 152.8, 156.0, 157.3, 158.9, 159.3 165.3, 167.8, 173.6.

4.4.6 Synthesis of PEG2000-G2-CPT (7)

A solution of 7.2 mg of **6** (0.002 mmol) in 4 mL dimethylformamide stirred as 445 mg NHS-mPEG$_{2000}$ was added to the solution. Then, 20 μL of N,N-diisopropylethylamine was added to the solution and stirring continued for 48h and was concentrated in vacuo. The product was then purified with ultrafiltration using an Amicon stirred cell and YM3 regenerated cellulose membrane. Upon filtration of approximately 6 L of water, the retentate was collected and concentrated in vacuo to yield a yellow residue.

4.4.7 MTT Assay

Cells were plated at a density of 5,000 cells / well in 96 well plates. Plates were incubated for 24 hours at 37°C. Cells were treated with Control (DMSO), triton X-100 (all dead control), CPT, Irinotecan, G_2-CPT-PEG$_{2000}$, G_2-CPT, or G2NH$_2$ for 72 hours at 37°C. Treatment concentrations were as follows: 3% triton X-100 (all dead control), CPT (1µM-10mM), Irinotecan (1µM-50mM), G_2-CPT-PEG$_{2000}$ (1µM-1mM), G_2-CPT (1µM-1mM), or G2NH$_2$ (1µM-1mM). Cell toxicity was determined using an MTT (3-(4,5-Dimethylthiazol-2-yl)-2,5-diphenyltetrazolium bromide, a tetrazole) assay kit (Promega). For this analysis, 15 µl dye was added per well; plates were incubated for 4 hr at 37°C. Then a stop solution (100µl) was added and plates incubated for 1 hr at 37°C. Wells were mixed to create a uniform color and absorbance was read at 570 nm with a reference wavelength of 650 nm.

CHAPTER V
CONCLUSIONS

5.1 Summary

The use of polymeric architectures as drug delivery vehicles has been a burgeoning field of study in the past 20 years. Polymeric therapeutics have shown great potential at improving solubility, blood retention and diseased tissue accumulation of small molecule drugs. Better understanding of human physiology has enabled more efficient tailoring of polymer architectures to achieve desired pharmacokinetics for treatment of a variety of diseases. Furthermore, many tumor models show enhanced permeability and retention, which promotes accumulation of the polymer at the site of the tumor. Dendrimer architectures possess additional benefits of monodispersity and a well-defined multivalent periphery.

Triazine-based dendrimer architectures have also shown great potential as drug-delivery vehicles. The chemoselective reactivity of cyanuric chloride and use of amine nucleophiles results in efficient and inexpensive macromolecules. Various architectures have been developed, which improve the therapeutic index of small molecule drugs. The development of various architectures enabled us to optimize the synthesis to achieve a second-generation dendrimer at the kilogram-scale. Dichlorotriazine monomer units proved to be more reactive than the monochlorotriazine monomer units used in previous syntheses. Iterations of dichlorotriazine monomer addition to the amine terminated dendrimer and subsequent capping and deprotection afforded a second generation dendrimer with 12 terminal primary amines in greater that 70% yield with over 1 kg of product. This construct was synthesized for under $10/g and opens the door for inexpensive polymeric therapeutics.

Iterations en route to the kilogram-scale second-generation dendrimer affords amine terminated dendrimers and poly(monochlorotriazine) dendrimers. The amine terminated dendrimers have previously been utilized as a vehicle for paclitaxel with great success. Interception of the poly(monochlorotriazine) dendrimer with a drug

containing a nucleophilic linker offers a new route to functionalization. This route requires fewer steps and allows for a variety of molecules to be attached to the periphery. Our investigation of desferrioxamine B and camptothecin explores the utility of this route.

Desferrioxamine B, an iron chelate, used for the treatment of iron-overload suffers from poor pharmacokinetics. Attachment of DFOB to polymers has shown great potential toward improving the therapeutic index of the drug. In our hands, nucleophilic similarities between the amine and the hydroxamic acids create synthetic hurdles, which hinder attachment to the dendrimer. Acylation of the amine of DFOB with isonipecotic acid presents a more nucleophilic amine for reaction with the poly(monochlorotriazine) dendrimer. However, solubility precludes this route from being realized. Synthetic and characterization challenges with desferrioxamine B have forced us to abandon further attempts to attach DFOB to the dendrimer.

Camptothecin, however, has proven more successful. This antineoplastic agent has a lone hydroxyl group poised for reactivity with isonipecotic acid as was utilized in a similar manner to DFOB. Reaction of the modified camptothecin with the poly(monochlorotriazine) dendrimer affords a macromolecule with six camptothecins and twelve BOC-protected primary amines. Deprotection and subsequent PEGylation affords a dendrimer with an approximate molecular weight of 30 kDa. The PEGylated product proves to be more soluble in water than the free drug and wll presumably increase the therapeutic index *in vivo*. Investigation of each construct in an MTT assay provided dose-response curves in both breast and colon cancer cell lines.

Although the success of camptothecin was not observed with desferrioxamine B, this route offers great potential for functionalization with a variety of drugs or molecules of interest. While not all drugs will be successfully introduced on the dendrimer using this nucleophilic liners, the ability to investigate this route offers a new facet to the potential of triazine-based dendrimers for drug delivery.

5.2 Recommendations

While the kilogram-scale synthesis proved successful, further improvement of dendrimer synthesis must be sought. Great strides have been made from the initial synthesis of triazine-based dendrimer, but new routes and new architectures are necessary to optimize drug delivery. New architectures may also overcome the poor solubility issues observed with desferrioxamine B.

The attachment of desferrioxamine B to the dendrimer proved to be unsuccessful, but the development of small molecule triazine-based chelates with high-affinity for iron may prove to be an inexpensive alternative. Efficient synthesis of such chelates have proven promising as inexpensive alternatives to DFOB. Successful modification of the reported small molecules to allow attachment to triazine-based dendrimers will afford a macromolecular construct capable of iron sequestration. Upon successful synthesis, evaluation of the dendrimers for iron binding affinity and competition in the presence of other metals will offer insight into the potential use of this construct as a macromolecular iron sequestration agent. Further evaluation in animal models of iron-overload will then be required to determine the potential of this drug for further clinical investigation.

With success obtained with camptothecin in two cell lines, improved synthesis may potentially be met through the use of azetidinecarboxylic acid as the linker in place of isonipecotic acid. The improved synthesis on large scale will then provide significant amounts of construct for more rigorous characterization in a wide range of cell lines. Furthermore, the evaluation of this construct in animals bearing human tumor xenografts will generate relevant evidence of further clinical potential.

While the interests pursued here have focused on desferrioxamine B and camptothecin, a variety of other molecules with interesting biological and commercial applications may be investigated. For example, the introduction of fluorescent agents or radiolabels for imaging with primary amines available for PEGylation or drug loading will move our constructs toward theranostics and long-term biodistribution and chronic toxicity studies. Attachment of drugs to the poly(monochlorotriazine) dendrimer and

subsequent deprotection produces a cationic dendrimer capable of condensation of DNA or RNA. Successful delivery of genetic material and drug will potentially sensitize cells for more efficient drug activity.

REFERENCES

1. Staudinger, H.; Siegwart, J., Polymerization. *Ber. Dtsch. Chem. Ges.* **1920,** *53B*, 1073-1085.

2. Carothers, W. H., Polymerization and ring formation. I. Introduction to the general theory of condensation polymers. *J. Am. Chem. Soc.* **1929,** *51*, 2548-2559.

3. Ziegler, K., Metal-alkyls: their success and future prospects in industrial chemistry. *Chimie et Industrie* **1964,** *92* (6), 631-644.

4. Natta, G., Stereospecific polymerizations. *J. Poly. Sci* **1960,** *48*, 218-239.

5. Flory, P. J., *Principles of Polymer Chemistry*. Cornell University Press: Ithaca, NY, 1953.

6. Wang, J.-S.; Matyjaszewski, K., Controlled/"living" radical polymerization. atom transfer polymerization in the presence of transition-metal complexes. *J. Am. Chem. Soc.* **1995,** *117*, 5614-5615.

7. Chiefari, J.; Chong, Y.-K.; Ercole, F.; Krstina, J.; Jeffery, J.; Le, T. P. T.; Mayadunne, R. T. A.; Meijs, G. F.; Moad, C. L.; Moad, G.; Rizzardo, E.; Thang, S. H., Living free-radical polymerization by reversible addition-fragmentation chain transfer: the RAFT process. *Macromolecules* **1998,** *31*, 5559-5562.

8. Vogtle, F., *Dendrimers*. Springer-Verlag: Berlin, 1998.

9. Buhleier, E.; Wehner, W.; Vogtle, F., "Cascade"- and "nonskid-chain-like" synthesis of molecular cavity topologies. *Synthesis* **1978**, 155-158.

10. Newkome, G. R.; Yao, Z.-Q.; Baker, G. R.; Gupta, V. K., Cascade molecules: a new approach to micelles. A [27]-arborol. *J. Org. Chem.* **1985,** *50*, 2004-2006.

11. Tomalia, D. A.; Baker, H.; Dewald, J.; Hall, M.; Kallos, G.; Martin, S.; Roeck, J.; Ryder, J.; Smith, P., A new class of polymers: starburst-dendritic macromolecules. *Polym. J.* **1985,** *17*, 117-132.

12. Denkewalter, R. G.; Kolc, J. F.; Lukasavage, W. J. Macromolecular highly branched α,ω-diamino carboxylic acids. US Patent 4,289,872, April 6, 1979.

13. Newkome, G. R.; Baker, G. R.; Arai, S.; Saunders, M. J.; Russo, P. S.; Theriot, K. J.; Moorefield, C. N.; Rogers, L. E.; Miller, J. E., Cascade molecules. Part 6. Synthesis and characterization of two-directional cascade molecules and formation of aqueous gels. *J. Am. Chem. Soc.* **1990,** *112*, 8458-8465.

14. Newkome, G. R.; Baker, G. R.; Saunders, M. J.; Russo, P. S.; Gupta, V. K.; Yao, Z.; Miller, J. E.; Bouillion, K., Two-directional cascade molecules: synthesis and characterization of [9]-n-[9] arborols. *J. Chem. Soc. Chem. Commun.* **1986**, 752-753.

15. Newkome, G. R.; Yao, Z.; Baker, G. R.; Gupta, V. K.; Russo, P. S.; Saunders, M. J., Chemistry of micelles series. Part 2. Cascade molecules. Synthesis and characterization of a benzene [9]3-arborol. *J. Am. Chem. Soc.* **1986,** *108*, 849-850.

16. Naylor, A. M.; Goddard, W. A., III; Kiefer, G. E.; Tomalia, D. A., Starburst dendrimers. 5. Molecular shape control. *J. Am. Chem. Soc.* **1989,** *111*, 2339-2341.

17. Tomalia, D. A.; Baker, H.; Dewald, J., Dendritic macromolecules: synthesis of starburst dendrimers. *Macromolecules* **1986,** *19*, 2466-2468.

18. Tomalia, D. A.; Berry, V.; Hall, M.; Hedstrand, D. M., Starburst dendrimers. 4. Covalently fixed unimolecular assemblages reminiscent of spheroidal micelles. *Macromolecules* **1987,** *20*, 1164-1167.

19. Tomalia, D. A.; Dewald, J. R. Dense star polymers. US Patent 4,558,120, December 27, 1984.

20. Tomalia, D. A.; Hall, M.; Hedstrand, D. M., Starburst dendrimers.III. The importance of branch junction symmetry in the development of topological shell molecules. *J. Am. Chem. Soc.* **1987,** *109*, 1601-1603.

21. Tomalia, D. A.; Naylor, A. M.; Goddard, W. A., III, Starburst dendrimers: control of size shape, surface chemistry, topology and flexibiity in the conversion of atoms to macroscopic materials. *Angew. Chemie.* **1990,** *102*, 119-157.

22. Ottaviani, M. F.; Bossman, S.; Turro, N. J.; Tomalia, D. A., Characterization of starburst dendrimers by the EPR technique. 1. Copper complexes in water solution. *J. Am. Chem. Soc.* **1994,** *116*, 661-671.

23. Chuanchu, W.; Brechbiel, M. W.; Kozak, R. W.; Gansow, O. A., Metal-chelate-dendrimer-antibody constructs for use in radioimmunotherapy and imaging. *Bioorg. Med. Chem. Lett.* **1994,** *4*, 449-454.

24. Venditto, V. J.; Regino, C. A. S.; Brechbiel, M. W., PAMAM dendrimer based macromolecules as improved contrast agents. *Molec. Pharmaceut.* **2005,** *2*, 302-311.

25. Hawker, C. J.; Fréchet, J. M. J., A new convergent approach to monodisperse dendritic macromolecules. *J. Chem. Soc. Chem. Commun.* **1990**, 1010-1013.

26. Hawker, C. J.; Fréchet, J. M. J., Control of surface functionality in the synthesis of dendritic macromolecules using the convergent-growth approach. *Macromolecules* **1990,** *23*, 4726-4729.

27. Hawker, C. J.; Fréchet, J. M. J., Preparation of polymers with controlled molecular architecture. A new convergent approach to dendritic macromolecules. *J. Am. Chem. Soc.* **1990,** *112*, 7638-7647.

28. Newkome, G. R.; Kotta, K. K.; Moorefield, C. N., Design, synthesis and characterization of conifer-shaped dendritic architectures. *Chem. Eur. J.* **2006,** *21*, 3726-3734.

29. Launay, N.; Caminade, A.-M.; Lahana, R.; Majoral, J.-P., General synthetic strategy for neutral phosphorus-containing dendrimers. *Angew. Chemie.* **1994,** *106*, 1682-1684.

30. Launay, N.; Caminade, A.-M.; Majoral, J.-P., Synthesis and reactivity of unusual phosphorus dendrimers. A useful divergent growth approach up to the seventh generation. *J. Am. Chem. Soc.* **1995,** *117*, 3282-3283.

31. Xu, Z.; Moore, J. S., Stiff dendritic macromolecules. 2. Synthesis and characterization of a stiff dendrimer of high molecular weight. *Angew. Chemie. Int. Ed. Engl.* **1993,** *32*, 246-248.

32. Xu, Z.; Moore, J. S., Stiff dendritic macromolecules. 3. Rapid formation of large phenylacetylene dendrimers with molecular diameters up to 12.5 nanometers. *Angew. Chemie. Int. Ed. Engl.* **1993,** *32*, 1354-1357.

33. Duncan, R., The dawning era of polymer therapeutics. *Nat. Rev. Drug Discovery* **2003,** *2*, 347-360.

34. Kabanov, A. V., Polymer genomics: an insight into pharmacology and toxicology of nanomedicines. *Adv. Drug Delivery Rev.* **2006,** *58*, 1597-1621.

35. Duncan, R., Polymer conjugates as anticancer nanomedicines. *Nature Rev.* **2006,** *6*, 688-701.

36. Green, J. J.; Langer, R.; Anderson, D. G., A combinatorial polymer library approach yields insight into nonviral gene delivery. *Acc. Chem. Res.* **2008,** *41*, 749-759.

37. Matsumura, Y.; Maeda, H., A new concept for macromolecular therapeutics in cancer chemotherapy: mechanism of tumoritropic accumulation of proteins and the antitumor agent smancs. *Cancer Res.* **1985,** *46*, 6387-6392.

38. Greish, K.; Fang, J.; Inutsuka, T.; Nagamitsu, A.; Maeda, H., Macromolecular therapeutics: advantages and prospects with special emphasis on solid tumor targeting. *Clinical Pharmacokinetics* **2003,** *42*, 1089-1105.

39. Duncan, R., Polymer therapeutics for tumour specific delivery. *Chem. Ind.* **1997**, 262-263.

40. Mammen, M.; Choi, S.-K.; Whitesides, G. M., Polyvalent interactions in biological systems: implications for design and use of multivalent ligands and inhibitors. *Angew. Chem. Int. Ed.* **1998,** *37*, 2754-2794.

41. Kaminskas, L. M.; Boyd, B. J.; Karellas, P.; Krippner, G. Y.; Romina, L.; Kelly, B.; Porter, C. J. H., Impact of surface derivatization of poly(L-lysine) dendrimers with anionic arylsulfonate or succinate groups on intravenous pharmacokinetics and disposition *Molec. Pharmaceut.* **2007,** *4*, 949-961.

42. Kussrow, A.; Eiton, K.; Wolfenden, M. L.; Cloninger, M. J.; Finn, M. G.; Bornhop, D. J., Measurement of monovalent and polyvalent carbohydrate-lectin binding by back-scattering interferometry. *Anal. Chem.* **2006,** *81*, 4889-4897.

43. Hamerton, I., *Chemistry and technology of cyanate ester resins*. Blackie: London, 1994.

44. Meijer, E. W.; Bosman, H. J. M.; Vandenbooren, F. H. A. M.; De Branbander-van Den Berg, E.; Castelijns, A. M. C. F.; De Man, H. C. J.; Reintjens, R. W. E. G.; Stoelwinder, C. J. C.; Nijenhuis, A. J. Dendritic macromolecules and the preparation thereof. US Patent 5,610,268, March 11, 1996.

45. Maciejewski, M., Topology in the chemistry of polymers. *Polimery* **1995,** *40*, 404-409.

46. Maciejewski, M.; Janiszewski, J. Method of obtaining dendritic oligomers and polymers. Polish Patent 176,865, 1999.

47. Fries, H. H., Further contributions to the knowledge of cyanuric chloride and other cyanuric derivatives. *J. Chem. Soc.* **1886,** *49*, 739-743.

48. Fries, H. H., Contributions to a knowledge of cyanuric chloride. *J. Chem. Soc.* **1886,** *49*, 314-316.

49. Steffensen, M. B.; Hollink, E.; Kushel, F.; Bauer, M.; Simanek, E. E., Dendrimers based on [1,3,5]-triazines. *J. Polym. Sci. Part A: Polym. Chem* **2006,** *44*, 3411-3433.

50. Steffensen, M. B.; Simanek, E. E., Chemoselective building blocks for dendrimers from relaive reactivity data. *Organic Letters* **2003,** *5* (13), 2359-2361.

51. Moreno, K. X.; Simanek, E. E., Identification of diamine linkers with differing reactivity and their application in the synthesis of melamine dendrimers. *Tetrahedron Letters* **2008,** *49*, 1152-1154.

52. Zhang, W.; Simanek, E. E., Dendrimers based on melamine. Divergent and orthogonal, convergent syntheses of a G3 dendrimer. *Organic Letters* **2000,** *2* (6), 843-845.

53. Zhang, W.; Gonzalez, S. O.; Simanek, E. E., Structure-activity relationships in dendrimers based on triazines: Gelation depends on choice of linking and surface groups *Macromolecules* **2002,** *35*, 9015-9021.

54. Moreno, K. X.; SImanek, E. E., Conformational analysis of triazine dendrimers: Using NMR spectroscopy to probe the choreography of a dendrimer's dance. *Macromolecules* **2008,** *41*, 4108-4114.

55. Acosta, E. J.; Deng, Y.; White, G. N.; Dixon, J. B.; McInnes, K. J.; Senseman, S. A.; Frantzen, A. S.; Simanek, E. E., Dendritic surfactants show evidence for frustrated intercalation: a new organoclay morphology. *Chem. Mater.* **2003,** *15*, 2903-2909.

56. Merkel, O. M.; Mintzer, M. A.; Sitterberg, J.; Bakowsky, U.; Simanek, E. E.; Kissel, T., Triazine dendrimers as nonviral gene delivery systems: effect of molecular structure on biological activity. *Bioconjugate Chem.* **2009,** *20*, 1799-1806.

57. Mintzer, M. A.; Merkel, O. M.; Kissel, T.; Simanek, E. E., Polycationic triazine-based dendrimers: effect of peripheral groups on transfection efficiency. *New J. Chem.* **2009,** *33*, 1918-1925.

58. Crampton, H.; Hollink, E.; Perez, L. M.; Simanek, E. E., A divergent route towards single chemical entity triazine dendrimers with opportunities for sturctural diversity. *New Journal of Chemistry* **2007,** *31*, 1283-1290.

59. Hollink, E.; Simanek, E. E., A divergent route to diversity in macromolecules. *Organic Letters* **2006,** *8* (11), 2293-2295.

60. Chen, H. T.; Neerman, M. F.; Parrish, A. R.; Simanek, E. E., Cytotoxicity, hemolysis, and acute in vivo toxicity of dendrimer based on melamine, candidate vehicles for drug delivery. *J. Am. Chem. Soc.* **2004,** *126*, 10044-10048.

61. Shaunak, S.; Thomas, S.; Giamasi, E.; Godwin, A.; Jones, E.; Teo, I.; Mireskandari, K.; Luthert, P.; Duncan, R.; Patterson, S.; Khaw, P.; Brocchini, S., Polyvalent dendrimer glucosamine conjugates prevent scar tissue formation. *Nature Biotech.* **2004,** *22*, 977-984.

62. Lalwani, S.; Venditto, V. J.; Chouai, A.; Rivera, G. E.; Shaunak, S.; Simanek, E. E., Electrophoretic behavior of anionic triazine and PAMAM dendrimers: methods for improving resolution and assessing purity using capillary electrophoresis. *Macromolecules* **2009,** *42*, 3152-3161.

63. Lim, J.; Simanek, E. E., Synthesis of water soluble dendrimers based on melamine bearing sixteen paclitaxel groups. *Org. Lett.* **2008,** *10*, 201-204.

64. Dhungana, S.; White, P. S.; Crumbliss, A. L., Crystal structure of ferrioxamine B: a comparative analysis and implications for molecular recognition. *J. Biol. Inorg. Chem.* **2001,** *6*, 810-818.

65. Kiss, T.; Farkas, E., Metal-binding ability of desferrioxamine B. *J. Inclus. Phenom. Mol.* **1998,** *32*, 385-403.

66. Pommier, Y., Topoisomerase I inhibitors: camptothecins and beyond. *Nature Rev.* **2006,** *6*, 789-802.

67. Steffensen, M. B.; Simanek, E. E., Synthesis and manipulation of orthogonally protected dendrimers: building blocks for library synthesis. *Angew. Chem. Int. Ed.* **2004,** *43*, 5178-5180.

68. Zhang, W.; Jiang, J.; Qin, C.; Perez, L. M.; Parrish, A. R.; Safe, S. H.; Simanek, E. E., Triazine dendrimers for drug delivery: evaluation of solubilization properties, activity in cell culture, and in vivo toxicity of a candidate vehicle. *Supramol. Chem.* **2003,** *15*, 607-616.

69. Acosta, E. J.; Carr, C. S.; Simanek, E. E.; Shantz, D. F., Engineering nanospaces: iterative synthesis of melamin-based dendrimers on amine-functionalized SBA-15 leading to complex hybrids with controllable chemistry and porosity. *Adv. Mater.* **2004,** *16*, 985-989.

70. Lim, J.; Simanek, E. E., Toward the next-generation drug delivery vehicle: synthesis of a dendrimer with four orthogonally reactive groups. *Molec. Pharmaceut.* **2005,** *2*, 273-277.

71. Beutler, E., Iron storage disease: facts, fiction and progress. *Blood Cells Mol. Dis.* **2007,** *39*, 140-147.

72. Wessling-Resnick, M., Iron transport. *Annu. Rev. Physiol.* **2000,** *20*, 129-150.

73. McCance, R. A.; Widdowson, E. M., Absorption and excretion of iron. *Lancet* **1937,** *2* (680-684), 680.

74. Siah, C. W.; Trinder, D.; Olynyk, J. K., Iron overload. *Clinica Chimica Acta* **2005,** *358*, 24-36.

75. Kontoghiorghes, G. J., New oral-iron-chelating drugs for th treatment of transfusional iron overload and other diseases. *Drugs of the Future* **2005,** *30*, 1241-1251.

76. Trousseau, A., Glycosurie, diabète sucré. *Clinique médicale de l'Hotel-Dieu de Paris* **1865,** *2*, 663-698.

77. Recklinghausen, F. D. v., Hämochromatosis. *Tageblatt der Naturforscheden Versammiung* **1890**, 324.

78. Ramage, H.; Sheldon, J. H., Haemochroatosis: 1. The content of the tissues in iron and sulphur 2. The results of spectrographc examination with special reference to copper and calcium. *QJM: An International Journal of Medicine* **1935,** *4*, 121-129.

79. Pietrangelo, A., Hereditary hemochormatosis - A new look at an old disease. *New Engl. J. Med.* **2004,** *350*, 2383-2397.

80. Jeffrey, G.; Adams, P. C., Blood from patients with hereditary hemochromatosis--a wasted resource. *Transfusion* **1999,** *39*, 549-550.

81. Feder, J. N.; Gnirke, A.; Thomas, W.; Tsuchihashi, Z.; Ruddy, D. A.; Basava, A.; Dormishian, F.; Jr., R. D.; Ellis, M. C.; Fullan, A.; Hinton, L. M.; N.L.Jones; Kimmel, B. E.; Kronmal, G. S.; Lauer, P.; Lee, V. K.; Loeb, D. B.; Mapa, F. A.; McClelland, E.; Meyer, N. C.; Mintier, G. A.; Moeller, N.; Moore, T.; Morikang, E.; Prass, C. E.; QUintana, L.; Starnes, S. M.; Schatzman, R. C.; Bunke, K. J.; Drayna, D. T.; Risch, N. J.; Bacon, B. R.; Wolff, R. K., A novel MHC class 1-like gene is mutated in patients with hereditary haemochromatosis. *Nat. Genet.* **1996,** *13*, 399-408.

82. Andrews, N. C., Disorders of iron metabolism. *New Engl. J. Med.* **1999,** *341*, 1986-1999.

83. Andrews, N. C.; Schmidt, P. J., Iron homeostasis. *Annu. Rev. Physiol.* **2007,** *69*, 69-85.

84. Nicolas, G.; Bennoun, M.; Devaux, I.; Beaumont, C.; Grandchamp, B.; Kahn, A.; Vaulont, S., Lack of hepcidin gene expression and severe tissue iron overload in upstream stimulatory factor 2 (USF2) knockout mice. *Proc. Natl. Acad. Sci. USA* **2001,** *98*, 8780-8785.

85. Kawabata, H.; Yang, R.; Hirama, T.; Vuong, P. T.; Kawano, S.; Gombart, A. F.; Koeffler, H. P., Molecular cloning of transferrin receptor 2. A new member of the transferrin receptr-like family. *J. of Biol. Chem.* **1999,** *274*, 20826-20832.

86. Rodriguez, M. A.; Onni, N.; Parkkila, S., Heptaic and extrahepatic expression of the new iron regulatory protein hemojuvelin. *Haematologica* **2004,** *89*, 1441-1445.

87. Pigeon, C.; Ilyin, G.; Courseland, B.; Leroyer, P.; Turlin, B.; Brissot, P.; Loreal, O., A new mouse liver-specific gene, encoding a protein homologous to human antimicrobial peptide hepcidin, is overexpressed during iron overload. *J. Biol. Chem.* **2001,** *276*, 7811-7819.

88. Zurlo, M. F.; De Stefano, P.; Borgna-Pagnatti, C.; Di Palma, A.; Piga, A.; Melevendi, C.; Di Gregorio, F.; Burattini, M. G.; Terzoli, S., Survival and causes of death in thalassemia major. *Lancet* **1989**, 27.

89. Rund, D.; Rachmilewitz, F. A., β-Thalassemia. *New Engl. J. Med.* **2005,** *353*, 1135-1146.

90. Olivieri, N. F.; Brittenham, G. M., Iron-chelating therapy and the treatment of thalassemia. *Blood* **1997,** *89*, 739-761.

91. Andrews, N. C., A genetic view of haemochromatosis. *Semin. Hematol.* **2002,** *39*, 227-234.

92. Kontoghiorghes, G. J., Future chelation monotherapy and combination therapy strategies in thalassemia and other conditions. Comparison of deferiprone, deferoxamine, ICL670, GT56-252, L1NA11, and starch deferoxamine polymers. *Hemoglobin* **2006,** *30*, 329-347.

93. Halliwell, B.; Gutteridge, J. M. C., Oxygen toxicity, oxygen radicals, transition metals and disease. *Biochem. J.* **1984,** *219*, 1-14.

94. Slater, T. F., Free radical mechanisms in tissue therapy. *Biochem. J.* **1984,** *222*, 1-15.

95. Hershko, C.; Weatherall, D.; Finch, C., Iron-chelation therapy. *CRC Crit. Rev. Clin. Lab Sco.* **1988,** *26*, 303-345.

96. Ramsay, W. N. M., The determination of the total iron-binding capacity of serum. *Clin Chim. Acta* **1957,** *2*, 221-226.

97. Blanc, B.; Vannotti, A., Transferrin behaviour in haemochromatosis. *Nature* **1966,** *212*, 480-481.

98. Jiang, C.; Hansen, R. M.; Gee, B. E.; Kurth, S. S.; Fulton, A. B., Rod and rod mediated function in patients with β-thalassemia major. *Doc Opthamol.* **1999,** *96*, 333-345.

99. Whitten, C. F.; Gibson, G. W.; Good, M. S.; Goodwin, J. F.; Brough, A. J., Studies in acute iron poisoning. I. Desferrioxamine in the treatment of acute iron poisoning: clinical observations, experimental studies and theoretical considerations. *Pediatrics* **1965,** *36*, 322-335.

100. Whitten, C. F.; Brough, A. J., The pathophysiology of acute iron poisoning. *Clin. Toxicol.* **1971,** *4*, 585-595.

101. Engle, M. A.; Erlandson, M.; Smith, C. H., Late cardiac complications of chronic, severe, refractory anemia with hemochromatosis. *Circulation* **1964,** *30*, 698-705.

102. Gisaru, D.; Rachmilewitz, F. A.; Mosseri, M., Cardiopulmonary assessment in β-thalassemia major. *Chest* **1990,** *98*, 1138.

103. Kremastinos, D. T.; Tiniakos, G.; Theodorakis, G. N.; Katritsis, D. G.; Toutouzas, P. K., Myocarditis in β-thalassemia major: A cause of heart failure. *Circulation* **1995,** *91*, 66-71.

104. Li, C. K.; Chik, K. W.; Lam, C. W. K.; To, K. F.; Yu, S. C. H.; Lee, V. K.; Shing, M. M. K.; Cheung, A. Y. K.; Yuen, P. M. P., Liver disease in transfusion dependent thalassemia major. *Arch. Dis. Child* **2002,** *86*, 344-347.

105. Tsukamoto, H.; Horne, W.; Kamimura, S.; Niemela, O.; Parkkola, S.; Yla-Herttuala, S.; Brittenham, G. M., Experimental liver cirrhosis induced by alcohol and iron. *J. Clin. Invest.* **1995,** *96*, 620-630.

106. Sher, G. D.; Milone, S. D.; Cameron, R.; Jamieson, F. B.; Krajden, M.; Collins, A. F.; Matsui, D.; Entsuah, B.; Berkovitch, M.; Hackman, R.; Francombe, W. H.;

Oliveri, N. F., Hepatitis C virus infection in transfused patients with β hemoglobinopathies accelerates iron-induced hepatic damage. *Blood* **1993,** *82*, 360a.

107. Piperno, A.; Fargion, S.; D'Alba, R.; Roffi, L.; Fracanzani, A. L.; Vecchi, L.; Failla, M.; Fiorelli, G., Liver damage in Italian patients with hereditary hemochromatosis in highly influenced by hepatitis B and C virus infection. *J. Hepatol.* **1992,** *16*, 364-368.

108. Kwan, E. Y. W.; A.C.W., L.; A.M.C., L.; Tam, S. C.; Chan, C. F.; Lau, Y. L.; Low, L. C., A cross-sectional study of growth, puberty and endocrine function in patients with thalassemia major in Hong Kong. *J. Paed. Child Health* **1995,** *31*, 83-87.

109. Grundy, R. G.; Woods, R. A.; Savage, M. O.; Evans, J. P. M., Relationship of endocriopathy to iron chelation status in young patients with thalassemia major. *Arch. Dis. Child.* **1994,** *71*, 128-132.

110. Lee, D. H.; Liu, D. Y.; Jacobs, D. R.; Shin, H. R.; Song, K.; Lee, I. K.; Kim, B.; Hider, R. C., Common presence of non-transerrin-bound iron among patients with type 2 diabetes. *Diabetes care* **2006,** *29*, 1090-1095.

111. Connor, J. R.; Menzies, S. L.; St Martin, S. M.; Mufson, E. J., A histochemical study of iron, transferrin and ferritin in Alzheimer's diseased brains. *J. Neurosci. Res.* **1992,** *31*, 75-83.

112. Lehman, D. J.; Worwood, M.; Ellis, R.; Wimhurst, V. L.; Merryweather-Clarke, A. T.; Warden, D. R.; Smith, A. D.; Robson, K. J., Iron genes, iron load and risk of Alzheimer's disease. *J. Med. Genet.* **2006,** *43*, 52-55.

113. Floor, E., Iron as a vulnerability factor in nigrostriatal degeneration in aging and Parkinson's disease. *Cell Mol Biol.* **2000,** *46*, 709-720.

114. Costello, D. J.; Walsh, S. L.; H.J., H.; Walsh, C. H., Concurrent hereditary hemochromatosis and idiopathic Parkinson's disease: a case report series. *J. Neurol. Neurosurg. Psychiatry* **2004,** *75*, 631-633.

115. Esiri, M. M.; Taylor, C. R.; Mason, D. Y., Applications of an immunoperoxidase method to a study of human formalin-fixed material. *Neuropathol. Appl. Neurobiol.* **1976,** *2*, 233-246.

116. Goscht, A.; Lohler, J., Changes in glial cell markers in recent and old demyelinated lesions in central pontine myelinolysis. *Acta. Neuropathol.* **1990,** *80*, 46-58.

117. Thompson, K. J.; Shoham, S.; Connor, J. R., Iron and neurodegenerative disorders. *Brain Research Bulletin* **2001,** *55*, 155-164.

118. Bush, A. I., Metals and neuroscience. *Curr. Opin. Chem. Biol.* **2000,** *4*, 184-191.

119. Campbell, A.; Smith, M. A.; Sayre, L. M.; Bondy, S. C.; Perry, G., Mechanisms by which metals promote events connected to neurodegenerative diseases. *Brain Res. Bull.* **2001,** *55*, 125-132.

120. Dickinson, T. K.; Devenyi, A. G.; Connor, J. R., Distribution of injected iron 59 and manganese 54 in hypotransferrinemic mice. *J. Lab. Clin. Med.* **1996,** *128*, 270-278.

121. Ueda, F.; Raja, K.; Simpson, R. J.; Trowbridge, I. S.; Bradbury, M. W., Rate of 59Fe uptake into brain and cerebrospinal fluid and the influence in alterations in brain iron homeostasis. *J. Neurochem.* **1993,** *60*, 106-113.

122. Malecki, E. A.; Devenyi, A. G.; Beard, J. L.; Connor, J. R., Transferrin is required for normal distribution of 59Fe and 54Mn in mouse brain *J. Neurol. Sci.* **1999,** *170*, 112-118.

123. Adams, P. C., The modern diagnosis and management of haemochromatosis. *Aliment. Pharm. Ther.* **2006,** *23*, 1681-1691.

124. Brittenham, G. M.; Cohen, A. R.; McLaren, C.; Martin, M.; Griffith, P. M.; Niehuis, A. W.; Young, N. S.; Allen, C. J.; Farrell, D. E.; Harris, J. W., Hepatic iron stores and plasma ferritin concentration in patients with sickle cell anemia and thalassemia major. *Am. J. Hematol.* **1993,** *42*, 81-85.

125. Borgna-Pagnatti, C.; Castriota-Scanderberg, A., Methods of evaluating iron stores and efficacy of chelation in transfusional hemosiderosis. *Haematologica* **1991,** *76*, 409-413.

126. Pippard, M. J.; Callender, S. T.; Finch, C. A., Ferrioxamine excretion in iron loaded man. *Blood* **1982,** *60*, 288-294.

127. Olivieri, N. F.; Koren, G.; Matsui, D.; Liu, P. P.; Blendis, L.; Cameron, R.; McClelland, R. A.; Templeton, D. M., Reduction of tissue iron stores and normalization of serum ferritin during treatment with oral iron chelator L1 in thalassemia intermedia. *Blood* **1992,** *79*, 2741-2748.

128. Liu, P.; Olivieri, N. F., Iron overload cardiomyopathies: new insights into an old disease. *Cardiovasc. Drugs Ther.* **1994,** *8*, 101-110.

129. Olson, L. J.; Edwards, W. D.; McCall, J. Y.; Ilstrup, D. M.; Gersh, B. J., Cardiac iron deposition in idiopathic hemochromatosis: histologic and analytic assessment of 14 hearts from autopsy. *J. Am. Coll. Cardiol.* **1987,** *10*, 1239-1243.

130. Nielsen, P.; Fischer, R.; Engelhardt, R.; Tondury, P.; Gabbe, E. E.; Janka, G. E., Liver iron stores in patients with secondary haemosiderosis under iron chelation therapy with deferoxamine or deferiprone. *Brit. J Haemotol.* **1995,** *91*, 827-833.

131. Alvey, L., FDA approves first oral drug for chronic iron overload. *FDA News* **2005**.

132. Liu, Z. D.; Hider, R., Design of iron chelators with therapeutic application. *Coordin. Chem. Rev.* **2002,** *232*, 151-171.

133. Hershko, C.; Konijn, A. M.; Nick, H. P.; Breuer, W.; Cabantchik, Z. I.; Link, G., ICL670A: a new synthetic ral chelator: evaluation in hypertransfused rats with selective radioiron probes of hepatocellular and reticuloendothelial iron stores and in iron-loaded rat heart cells in culture. *Blood* **2001,** *97*, 1115-1122.

134. Barman-Balfour, J. A.; Foster, R. H., Deferiprone: A review of its clinical potential in iron overload in β-thalassemia major and other transfusion-dependent diseases. *Drugs* **1999,** *58*, 553-578.

135. Liu, D. Y.; Liu, Z. D.; Hider, R., Oral iron chelators - development and application. *Best Pract. Res. Cl. Ha.* **2002,** *15*, 369-384.

136. Capellini, M. D., Iron-chelating therapy with the new oral agent ICL670 (exjade). *Best Pract. Res. Cl. Ha.* **2005,** *18*, 289-298.

137. Franchini, M.; Veneri, D., Iron-chelation therapy: an update. *Haemotology* **2004,** *5*, 287-294.

138. Neufeld, E. J., Oral chelators deferasirox and deferiprone for transfusional iron overload in thalassemia major: new data, new questions. *Blood* **2006,** *107*, 3436-3441.

139. Bickel, H.; Hall, G. E.; W., K.-S.; Prelog, V.; Vischer, E.; Wettstein, A., Stoffwechselproduckte von actinomyceten. Üer die konstitution von ferrioxamin B. *Helv. Chim. Acta* **1960,** *43*, 2129-2138.

140. Neilands, J. B., Hydroxamic acids in nature. *Science* **1967,** *156*, 1443-1447.

141. Muller, G.; Raymond, K. N., Specificity and mechanism of ferrioxamine-mediated

iro transport in *streptomyces pilosus*. *J. Bacteriol.* **1984,** *160*, 304-312.

142. Bickel, H.; Bosshardt, R.; Gäumann, E.; Reusser, P.; Vischer, E.; Voser, W.; Wettstein, A.; Zahner, H., Stoffwechselproduckte von actinomyceten. Über die isolierung und charkterisierung der ferrioxamine A-F, neuer wuchsstoffe der sideramin-gruppe. *Helv. Chim. Acta* **1960,** *43*, 2118-2128.

143. Verel, I.; Visser, G. W. M.; Boellard, R.; Stigter-van Walsum, M.; Snow, G. B.; van Dongen, G. A. M. S., 89Zr Immuno-PET: comprehensive procedures for the production of 89Zr-labeled monoclonal antibodies. *J. Nucl. Med.* **2003,** *44*, 1271-1281.

144. Buglyó, P.; Culeddu, N.; Kiss, T.; Micera, G.; Sanna, D., Vanadium (IV) and vanadium (V) complexes of deferoxamine B in aaqueous solution. *J. Inorg. Biochem.* **1995,** *60*, 45-59.

145. Leong, J.; Raymond, K. N., Coordination isomers of bilogical iron transport compounds. IV. Geometrical isomers of chromic desferrioxamine B. *J. Am. Chem. Soc.* **1975,** *97*, 293-296.

146. Faulkner, K.; Stevens, R. D.; Fridovich, I., Characterization of Mn(III) complexes of linear and cyclic desferrixoamines as mimics of superoxide dismutase activity. *Arch. of Biochem. Biophys.* **1994,** *3*, 341-346.

147. Joshi, R. R.; Ganesh, K. N., Duplex and triplex directed DNA cleavage by oligonucleotide-Cu(II/Co(III) metallodesferal conjugates. *Biochim Biophys Acta* **1994,** *1201*, 454-460.

148. Anderegg, G.; L'Eplattenier, F.; Schwerzenbach, G., Hydroxamatkomplexe II. Die anwendung per pH-methode. *Helv. Chim. Acta* **1963,** *46*, 1400-1408.

149. Farkas, E.; Csoka, H.; Micera, G.; Dessi, A., Copper(II), nickel(II), zinc(II) and molybdenum(VI) complexes of desferrioxamine B in aqueous solution. *J. Inorg. Biochem.* **1997,** *65*, 281-286.

150. Evers, A.; Hancock, R. D.; Martell, A. E.; Motekaitis, R. J., Metal ion recognition in ligands with negatively charged oxygen donor groups. *Inorg. Chem.* **1989,** *28*, 2189-2195.

151. Pochon, S.; Buchegger, F.; Pélegrin, A.; Mach, J. P.; Offord, R. E.; Ryser, J. E.; Rose, K., A novel derivative of the chelon desferrioxamine for site-specific conjugation to antibodies. *Int. J. Cancer* **1989,** *43*, 1188-1194.

152. Borgias, B.; Hugi, A. D.; Raymond, K. N., Isomerization and solution structures

of desferrioxamine B complexes of Al3+ and Ga3+. *Inorg. Chem.* **1989,** *28*, 3538-3545.

153. Smith-Jones, P. M.; Stolz, B.; Bruns, C.; Albert, R.; Reist, H. W.; Fridrich, R.; Macke, H. R., Gallium-67/gallium-68-[DFO]-octreotide - A potential radiopharmaceutical for PET imaging of somatostatin receptor-positive tumors: synthesis and radiolabeling in vitro and preliminary in vivo studies. *Inorg. Chim. Acta.* **1994,** *244*, 179-184.

154. Hernlem, B. L.; Vane, L. M.; Sayles, G. D., Stability constants for complexes of siderophore desferrioxamine B with selected heavy metal cations. *Inorg. Chim. Acta.* **1996,** *244*, 179-184.

155. Kraemer, S.; Xu, J.; Raymond, K. N.; Sposito, G., Adsorption of Pb(II) and Eu(III) by oxide minerals in the presence of natural and synthetic hydroxamate siderophores. *Environ. Sci. Technol.* **2002,** *36*, 1287-1291.

156. Whistenhunt, D. W.; Neu, M. P.; Hou, Z.; Xu, J.; Hoffman, D. C.; Raymond, K. N., Specific sequestering agents for the actinides. 29. Stability of the thorium(IV) complexes of desferrioxamine B (DFO) and three actadentate catecholate or hydroxypyridinonate DFO derivatives: DFOMTA, DFOCAMC, and DFO-1,2-HOPO. Comparative stability of the plutonium (IV) DFOMTA complex. *Inorg. Chem.* **1996,** *35*, 4128-4136.

157. Martell, A. E.; Hancock, R. D., *The selectivity of ligands of biological interest for metal ions in aqueous solution. Some implications for biology*. Plenum Press: New York, 1996.

158. Martell, A. E.; Hancock, R. D., *Medical Applications of Metal Complexes*. Plenum Press: New York, 1996.

159. Hallaway, P. E.; Eaton, J. W.; Panter, S. S.; Hedlund, B. E., Modulation of deferoxamine toxicity and clearance by covalent attachment of biocompatible polymers. *Proc. Natl. Acad. Sci. USA* **1989,** *86*, 10108-10112.

160. Dragsten, P. R.; Hallaway, P. E.; Hanson, G. J.; Bergeb, A. E.; Bernard, B.; Hedlund, B. E., First human studies with a high-molecular-weight iron chelator. *J. Lab. Clin. Med.* **2000,** *135*, 57-65.

161. Yehuda, Z.; Hadar, Y.; Chen, Y., Immobilized EDDHA and DFOB as iron carriers to cucumber plants. *J. Plant Nutrition* **2003,** *26*, 2043-2056.

162. Rodgers, S. J.; Raymond, K. N., Ferric ion sequestrting agents. 11. Synthesis and

kinetics of iron removal from transferrin of catechol derivatives of desferrioxamine B. *J. Med. Chem.* **1983,** *26*, 439-442.

163. Ihnat, P. M.; Vennerstrom, J. L.; Robinson, D. H., Synthesis and solution properties of deferoxamine amides. *J. Pharm. Sci.* **2000,** *89*, 1525-1536.

164. Moggia, F.; Brisset, H.; Fages, F.; Chaix, C.; Mandrand, B.; Dias, M.; Levillain, E., Design, synthesis and redox properties of two ferrocene-containing iron chelators. *Tet. Lett.* **2006,** *47*, 3371-3374.

165. Mathias, C. J.; Wang, S.; Lee, R. J.; Waters, D. J.; Low, P. S.; Green, M. A., Tumor-selective radiopharmaceutical targeting via receptor-mediated endocytosis of gallium-67 deferoxamine-folate. *J. Nucl. Med.* **1996,** *37*, 1003-1008.

166. Desferrioxamine and iron. *Lancet* **1964**, 708-709.

167. Hwang, Y.-F.; Brown, E. B., Effect of desferrioxamine on iron absorption. *Lancet* **1965**, 135-137.

168. Westlin, W. F., Deferoxamine as a chelating agent. *Clin. Toxicol.* **1971,** *4*, 597-602.

169. Moeshlin, S.; Schnider, U., Treatment of primary and secondary hemochromatosis and acute iron poisoning with a new, potent, iron-eliminating agent (Desferrixamine B). *New Engl. J. Med.* **1963,** *269*, 1648-1653.

170. McEnery, J. T.; Greengard, J., Treatment of acute iron ingestion with deferoxamine in 20 children. *J. Pediatr.* **1966,** *68*, 773-779.

171. Modell, C. B.; Beck, J., Long-term desferrioxamine therapy in thalassemia. *Ann. NY Acad. Sci.* **1974,** *232*, 201-210.

172. Propper, R. D.; Shurin, S. B.; Nathan, D. G., Reassessment of the use of desferrioxamine B in iron overload. *New Engl. J. Med.* **1976,** *294*, 1421-1423.

173. Hussain, M. A. M.; Flynn, D. M.; Green, N.; Hussein, S.; Hoffbrand, A. V., Subcutaneous infusion and intramuscular injection of desferrioxamine in patients with transfusional iron overload. *Lancet* **1976,** *2*, 1278-1280.

174. Propper, R. D.; Cooper, B.; Rufo, R. R.; Niehuis, A. W.; Anderson, W. F.; Bunn, H. F.; Rosenthal, A.; Nathan, D. G., Continuous subcutaneous administration of deferoxamine in patients with iron overload. *New Engl. J. Med.* **1977,** *297*, 418-423.

175. Pippard, M. J.; Callender, S. T.; Weatherall, D. J., Intensive iron-chelation therapy with desferrioxamine in iron-loading anemias. *Clin. Sci. Mol. Med.* **1982,** *54*, 99-106.

176. Olivieri, N. F.; Buncic, R.; Chew, E.; Gallant, T.; Harrison, R. V.; Keenan, N.; Logan, W.; Mitchell, D.; Ricci, G.; Skarf, B., Visual and auditory neurotoxicity in patients receiving subcutaneous deferoxamine infusions. *New Engl. J. Med.* **1986,** *314*, 869-873.

177. Bloomfield, S. E.; Markeson, A. I.; Miller, D. R.; Peterson, C. M., Lens opacities in thalassemia. *J. Pediatr. Optholmol Strab.* **1978,** *15*, 154-156.

178. Porter, J. B.; Huehns, E., The toxic effects of desferrioxamine. *Bailliere's Clin. Haematol.* **1989,** *2*, 459-474.

179. Davies, S. C.; Marcus, R. E.; Hungerford, J. L.; Miller, M. H.; G.B., A.; Huehns, E., Ocular toxcity of high-dose intravenous desferrioxamine. *Lancet* **1983,** *2*, 181-184.

180. Borgna-Pagnatti, C.; De Stefano, P.; Broglia, A. M., Visual loss in a patient on high-dose subcutaneous deferoxamine therapy. *Lancet* **1984,** *1*, 681.

181. Orton, R.; de Veber, L.; Sulh, I., Ocular and auditory toxicity of high dose subcutaneous deferoxamine. *Can. J. Opthalmol.* **1985,** *20*, 153-156.

182. Rahi, A. H. S.; Hungerford, J. L.; Ahmed, A., Ocular and auditory toxicity of desferrioxamine: light microscopic, histochemical and ultrastructural findings. *Br. J. Opthalmol.* **1986,** *70*, 373-381.

183. Dickerhoff, R., Acute aphasia and loss f vision with desferrioxamine overdose. *Am. J. Ped. Hematol. Oncol.* **1987,** *9*, 287-288.

184. De Virgilis, S.; Turco, M. P.; Frau, F.; Dessi, C.; Argiolu, F.; Sorcinelli, R.; Sitzia, A.; Cao, A., Depletion of trace elements and acute ocular toxicity induced by desferrioxamine in patients with thalassemia. *Arch. Dis. Child* **1988,** *63*, 250-255.

185. Pall, H.; Blake, D.; Winyard, P.; Lunec, J.; Williams, A.; Good, P. A.; Kritzinger, E. E.; Cornish, A.; Hider, R., Ocular toxicity of desferrioxamine: an example of copper promoted auto-oxidative damage. *Br. J. Opthalmol.* **1989,** *73*, 42-47.

186. Levine, J. E.; Cohen, A. R.; MacQueen, M.; Martin, M.; Giardina, P. J.,

Sensorimotor neurotoxicity associated with high-dose deferoxamine treatment. *J. Ped. Hemat. Onc.* **1997,** *19*, 139-141.

187. Koren, G.; Bentur, Y.; Strong, D.; Harvey, E.; Klein, J.; Baumal, R.; Spielberg, S. P.; Freedman, M. H., Acute changes in renal function associated with deferoxamine therapy. *Am. J. Dis. Child.* **1989,** *143*, 1077-1080.

188. Koren, G.; Kochavi-Atiya, Y.; Bentur, Y.; Oliveri, N. F., The effects of subcutaneous deferoxamine administration on renal function in thalassemia major. *Int. J. Haematol.* **1992,** *54*, 371-375.

189. Freedman, M. H.; Oliveri, N. F.; Gisaru, D.; McCluskey, I.; Thorner, P., Pulmonary syndrome in patients receiving intravenous deferoxamine infusions. *Am. J. Dis. Child.* **1990,** *144*, 565-569.

190. Tenebein, M.; Kowalski, S.; Sienko, A.; Bowden, D. H.; Adamson, I. Y. R., Pulmonary toxic effects of continuous desferrioxamine administration in acute iron poisoning. *Lancet* **1992,** *339*, 699-701.

191. De Sanctis, V.; Pinamonti, A.; Di Palma, A.; Sprocati, M.; Atti, G.; Gamberini, M. R.; Vullo, C., Growth and development in thalassemia major patients with severe bone lesions due to desferrioxamine. *Eur. J. Pediatr.* **1996,** *155*, 368-372.

192. Hatori, M.; Sparkman, J.; Teixeira, C. C.; Grynpas, M.; Nervina, J.; Oliveri, N. F.; Shapiro, I. M., Effects of deferoxamine on chondrocyte alkaline phosphate activity: pro-oxidant role of deferoxamine in thalassemia. *Calcif. Tissue Int.* **1995,** *57*, 229-236.

193. Orzincolo, C.; Scutellaru, P. N.; Castaldi, G., Growth plate injury of the long bones in treated β-thalassemia. *Skeletal Radiol.* **1992,** *21*, 39-44.

194. Brill, P. W.; Winchester, P.; Giardina, P. J.; Cunningham-Rundles, S., Desferrioxamine-induced bone dysplasia in patients with thalassemia major. *Am. J. Roentgenol.* **1991,** *156*, 561-565.

195. Piga, A.; Luzzatto, L.; Capalbo, P.; Gambotto, S.; Tricta, F.; Gabutti, V., High-dose desferrioxamine as a cause of growth failure in thalassemic patients. *Eur. J. Haematol.* **1988,** *40*, 380-381.

196. Rodda, C. P.; Reid, E. D.; Johnson, S.; Doery, J.; Matthews, R.; Bowden, D. H., Short stature in homozygous β-thalassemiais due to disproportionate truncal shortening. *Clin. Endocrinol.* **1995,** *42*, 587-592.

197. Arcasoy, A., Zinc status and zinc therapy in beta thalassemia. *Am. J. Ped.*

Hematol. Oncol. **1989,** *11*, 245-246.

198. Borg, D. C.; Schaich, K. M., Prooxidant action of desferrioxamine: fenton-like productaion of hydroxyl radicals by reduced ferrioxamine. *J. Free Red. Biol. Med.* **1986,** *2*, 237-243.

199. Peters, G.; Keberle, H.; Schmid, K.; Brunner, H., Distribution and renal excretion of desferrioxamine B and ferrioxamine B. *Helv. Phys. Pharm. Acta* **1963,** *31*, C42-C45.

200. Meyer-Brunot, H. G.; Keberle, H., The metabolism of desferrioxamine B and ferrioxamine B. *Helv. Phys. Pharm. Acta* **1967,** *16*, 527-535.

201. Roggo, B. E.; Peter, H. H., Synthesis of the metabolite N-hydroxy-desferrioxamine B. *J. Antibiot.* **1993,** *46*, 294-299.

202. Singh, S.; Hider, R. C.; Porter, J. B., Seperation and identification of desferrioxamine and its iron chelating metabolites by high-performance liquid chromatography and fast atom bombardment spectrometry: choice of complexing agent and application to biological fluids. *Anal. Biochem.* **1990,** *187*, 212-219.

203. Keberle, H., The biochemistry of desferrioxamine and its relation to iron metabolism. *Ann. NY Acad. Sci.* **1964,** *119*, 758-768.

204. De Wael, J.; Ploem, J. E., Determination of desferrioxamine-B methane sulphonate in urine. *Clin. Chim. Acta* **1965,** *11*, 135-138.

205. Klassen, C. D., *Goodman and Gilman's the Pharmacological Basis of Therapeutics*. McGraw-Hill: New York, 1996.

206. Glickstein, H.; Ben El, R.; Shvartsman, M.; Cabantchik, Z. I., Intracellular labile iron pools as direct targets of iron chelators: a fluorescence study of chelator action in living cells. *Blood* **2005,** *1*, 3242-3250.

207. Hedlund, B. E.; Hallaway, P. E. Polymer-deferoxamine-ferric iron adducts for use in magnetic resonance imaging. US Patent 5,268,165, December 7, 1993.

208. Duewell, S.; Wüthrich, R.; von Schulthess, G. K.; Jenny, H. B.; Muller, R. N.; Moerker, T.; Fuchs, W. A., Nonionic polyethylene glycol-ferrioxamine as a renal magnetic resonance contrats agent. *Invest. Radiol.* **1991,** *26*, 50-57.

209. Lowy, F. D.; Pollack, S.; Fadl-Allah, N.; Steigbigel, N. H., Susceptibilities of bacterial and fungal urinary tract isolates to desferrioxamine. *Antimicrob. Agents Ch.* **1984,** *25*, 375-376.

210. Guo, M.; Song, L.-P.; Liu, W.; Yu, Y.; Chen, G.-Q., Hypoxia-mimetic agents desferrioxamine and cobalt chloride induce leukemic cell apoptosis through different hypoxia-inducible factor-1α independent mechanisms. *Apoptosis* **2006,** *11*, 67-77.

211. Clavijo, C.; Chem, J. L.; Kim, K.-J.; Reyland, M. E.; Ann, D. K., Protein kinase Cδ-dependant and -independent signaling in genotoxic response to treatment of desferrioxamine, a hypoxia-mimetic agent. *Am. J. Physiol. Cell Physiol.* **2007,** *292*, C2150-C2160.

212. Richardson, D.; Ponka, P.; Baker, E., The effect of the iron(III) chelator, desferrioxamine on iron and transferrin uptake by the human malignant melanoma cell. *Cancer Res.* **1994,** *54*, 685-689.

213. Gun, J.; Ekeltchik, I.; Lev, O.; Shelkov, R.; Melman, A., Bis-(hydroxyamino)triazines: highly stable hydroxylamine-based ligands for iron(III) cations. *Chem. Commun.* **2005**, 5319-5321.

214. Ekeltchik, I.; Gun, J.; Lev, O.; Shelkov, R.; Melman, A., Bis(hydroxyamino)triazines: versatile and high-affinity tridentate hydroxylamine ligands for selective iron(III) chelation. *Dalton Trans.* **2006**, 1285-1293.

215. Nikolakis, V. A.; Tsalavoutis, J. T.; Stylianou, M.; Evgeniou, E.; Jakusch, T.; Melman, A.; Sigalas, M. P.; Kiss, T.; Keramidas, A. D.; Kabanos, T. A., Vanadium(V) compounds with the bis(hydroxylamino)-1,3,5-triazine ligand, H2bihyat: synthetic, structural and physical studies of [V2vO3(bihyat)2] and of the enhanced hydrolytic stability species cis-[VvO2(bihyat)]-. *Inorg. Chem.* **2008,** *47*, 11698-11710.

216. Hermon, T.; Tshuva, E. Y., Synthesis and conformational analysis of constrained ethylene-bridged bis(hydroxylamino-1,3,5-triazine) compounds as tetradentate ligands; structure of rigid dinulcear Ti(V) complex. *J. Org. Chem.* **2008,** *73*, 5953-5938.

217. Peri, D.; Alexander, J. S.; Tshuva, E. Y.; Melman, A., Distinctive structural features of hydroxyamino-1,3,5-triazine ligands leading to enhanced hydrolytic stability of their titanium complexes. *Dalton Trans.* **2006**, 4169-4172.

218. Shavit, M.; Peri, D.; Melman, A.; Tshuva, E. Y., Antitumor reactivity of non-metallocene titanium complexes of oxygen-based ligands: is ligand lability essential? *J. Biol. Inorg. Chem.* **2007,** *12*, 825-830.

219. Mahoney, J. R.; Hallaway, P. E.; Hedlund, B. E.; Eaton, J. W., Acute iron

poisoning: rescue with macromolecular chelators. *J. Clin. Invest.* **1989,** *84*, 1362-1366.

220. Diallo, M. S.; Balough, L.; Shafagati, A.; Johnson, J. H.; Goddard, W. A.; Tomalia, D. A., Poly(amidoamine) dendrimers: a new class of high capapcity chelating agents for Cu(II) ions. *Environ. Sci. Technol.* **1999,** *33*, 820-824.

221. Cohen, S. M.; Petoud, S.; Raymond, K. N., Synthesis of metal binding properties of salicylate-,catecholate-, and hydroxypyridinonate-functionalised dendrimers. *Chem. Eur. J.* **2001,** *7*, 272-279.

222. Zhou, T.; Hider, R. C.; Liu, Z. D.; Neubert, H., Iron(III)-selective dendritic chelators. *Tet. Lett.* **2004,** *45*, 9393-9396.

223. Berndt, U. E. C.; Zhou, T.; Hider, R. C.; Liu, Z. D.; Neubert, H., Structural characterization of chelator-terminated dendrimers and their synthetic intermediates by mass spectrometry. *J. Mass Spectrom.* **2005,** *40*, 1203-1214.

224. Zhou, T.; Liu, Z. D.; Neubert, H.; Xiao, L. K.; Yong, M. M.; Hider, R., High affinity iron(III) scavanging by a novel hexadentate 3-hydroxypyridin-4-one-based dendrimer: synthesis and characterization. *Bioorg. Med. Chem. Lett* **2005,** *15*, 5007-5011.

225. Alper, P. B.; Hung, S.-C.; Wong, C. H., Metal catalyzed diazo transfer for the synthesis of azides from amines. *Tet. Lett.* **1996,** *37*, 6029-6032.

226. Huisgen, R.; Szeimies, G.; Moebius, L., 1,3-Dipolar cycloadditions. XXXII. Kinetics of the addition of organic azides to carbon-carbon multiple bonds. *Chem. Ber.* **1967,** *100*, 2494-2507.

227. Wall, M. E.; Wani, M. C.; Cooke, C. E.; Palmer, K. H.; McPhail, A. T.; Sim, G. A., Plant antitumor agents. I. The isolation and structure of camptothecin, a novel alkaloidal leukemia and tumor inhibitor from *Camptotheca acuminata*. *J. Am. Chem. Soc.* **1966,** *88*, 3888-3890.

228. Gallo, R. C.; Whang-Peng, J.; Adamson, R. H., Studies on the antitumor activity, mechanism of action and cell cylce effects of camptothecin. *J. Nat. Cancer Inst.* **1971,** *46*, 789-795.

229. Wani, M. C.; Taylor, H. L.; Wall, M. E.; Coggon, P.; McPhail, A. T., Plant antitumor agents. VI. The isolation and structure of taxol, a novel antileukemic and antitumor agent from *taxus brevifolia*. *J. Am. Chem. Soc.* **1971,** *93*, 2325-2327.

230. Slichenmyer, W. J.; Von Hoff, D. D., New natural products in cancer chemotherapy. *J. Clin. Pharmacol.* **1990,** *30*, 770-788.

231. Wall, M. E., Camptothecin and taxol: discovery to clinic. *Med. Res. Rev.* **1998,** *18*, 299-314.

232. Hsiang, Y.-H.; Hertzberg, R.; Hecht, S.; Liu, L. F., Camptothecin induces protein-linked DNA breaks via mammalian DNA topoisomerase I. *J. Biol. Chem.* **1985,** *260*, 14873-14878.

233. Thomsen, B.; Mollerup, S.; Bonven, B. J.; Frank, R.; Blocker, H.; Nielsen, O. F.; Westergaard, O., Sequence specificity of DNA topoisomerase I in the presence and absence of camptothecin. *EMBO J.* **1987,** *6*, 1817-1823.

234. Pommier, Y.; Covey, J. M.; Kerrigan, D.; Markovits, J.; Pham, R., DNA unwinding and inhibition of mouse leukemia L1210 DNA topoisomerase I by intercalators. *Nucl. Acids Res.* **1987,** *15*, 6713-6731.

235. Jaxel, C.; Kohn, K. W.; Pommier, Y., Topoisomerase I interactions with SV40 DNA in the presence and absence of camptothecin. *Nucl. Acids Res.* **1988,** *16*, 11157-11170.

236. Kjeldsen, E.; Mollerup, S.; Thomsen, B.; Bonven, B. J.; Bolund, L.; Westergaard, O., Sequence-dependent effect of camptothecin on human topoisomerase I DNA cleavage. *J. Mol. Biol.* **1988,** *202*, 333-342.

237. Jaxel, C.; Kohn, K. W.; Wani, M. C.; Wall, M. E.; Pommier, Y., Structure-activity study of the actions of camptothecin derivatives on mammalian topoisomerase I: evidence for site specific receptor site and a relation to antitumor activity. *Cancer Res.* **1989,** *49*, 1465-1469.

238. Redinbo, M. R.; Stewart, L.; Kuhn, P.; Champoux, J. J.; Hol, W. G. J., Crystal structure of human topoisomerase I in covalent and noncovalent complexes with DNA. *Science* **1998,** *279*, 1504-1513.

239. Staker, B. L.; Hjerrild, K.; Feese, M. D.; Behnke, C. A.; Burgin Jr., A. B.; Stewart, L., The mechanism of topoisomerase I poisoning by a camptothecin analog. *Proc. Natl. Acad. Sci. USA* **2002,** *99*, 15387-15392.

240. Staker, B. L.; Feese, M. D.; Cushman, M.; Pommier, Y.; Zembower, D.; Stewart, L.; Burgin Jr., A. B., Structures of three classes of anticancer agents bound to the human topoisomerase I-DNA covalent complex. *J. Med. Chem.* **2005,** *48*, 2336-2345.

241. Wani, M. C.; Ronman, P. E.; Lindley, J. T.; Wall, M. E., Plant antitumor agents. 18. Synthesis and biological activity of camptothecin analogues. *J. Med. Chem.* **1980,** *23*, 554-560.

242. Adamovics, J. A.; Hutchinson, C. R., Prodrug analogs of the antitumor alkaloid camptothecin. *J. Med. Chem.* **1979,** *22*, 310-314.

243. Gabr, A.; Kuin, A.; Aalders, M.; El-Gawly, H.; Smets, L. A., Cellular pharmacokinetics and cytotoxicity of camptothecin and topotecan at normal and acidic pH. *Cancer Res.* **1997,** *57*, 4811-4816.

244. Hsiang, Y.-H.; Liu, L. F.; Wall, M. E.; Wani, M. C.; Nicholas, A. W.; Manikumar, G.; Kirshenbaum, S.; Silber, R.; Potmesil, M., DNA topoisomerase I-mediated DNA cleavage and cytotoxicity of camptothecin analogues. *Cancer Res.* **1989,** *49*, 4385-4389.

245. Hotte, S. J.; Oza, A.; Winquist, E. W.; Moore, M.; Chen, E. X.; Brown, S.; Pond, G. R.; Dancey, J. E.; Hirte, H. W., Phase I trial of UCN-01 in combination with topotecan in patients with advanced solid cancers: a Princess Margaret Hospital phase II consortium study. *Ann. Oncol.* **2006,** *17*, 334-340.

246. Anzai, H.; Frost, P.; Abbruzzese, J. L., Synergistic cytotoxicity with 2'-deoxy-5-azacytidine and topotecan in vitro and in vivo. *Cancer Res.* **1992,** *52*, 2180-2185.

247. Romanelli, S.; Perego, P.; Graziella, P.; Cerenini, N.; Tortoreto, M.; Zunino, F., In vitro and in vivo interaction between cisplatin and topotecan in ovarian carcinoma systems. *Cancer Chemother. Pharmacol.* **1998,** *41*, 385-390.

248. Crump, M.; Lipton, J.; Hedley, D.; Sutton, D.; Shepherd, F.; Minden, M.; Stewart, K.; Beare, S.; Eisenhauer, E., Phase I trial of sequential topotecan followed by etoposide in adults with myeloid leukemia: a National Cancer Institute of Canada Clinical Trials Group Study. *Leukemia* **1999,** *13*, 343-347.

249. Schmidt, F.; Schuster, M.; Strefer, J.; Schabet, M.; Weller, M., Topotecan-based combination chemotherapy for human malignant glioma. *Anticancer Res.* **1999,** *19*, 1217-1221.

250. Raymond, E.; Burris, H. A.; Rowinsky, E. K.; Eckardt, J. R.; Rodriguez, G.; Smith, L.; Weiss, G.; von Hoff, D. D., Phase I study of daily times five topotecan and single injection of cisplatin in patients with previously untreated non-small-cell lung carcinoma. *Ann. Oncol.* **1997,** *8*, 1003-1008.

251. Hammond, L. A.; Eckardt, J. R.; Ganapathi, R.; Burris, H. A.; Rodriguez, G. A.; Eckhardt, S. G.; Rothenberg, M. L.; Weiss, G. R.; Kuhn, J. G.; Hodges, S.; von

Hoff, D. D.; Rowinsky, E. K., A phase I and traslational study of sequential administration of the topoisomerase I and II inhibitors topotecan and etoposide. *Clin. Cancer Res.* **1998,** *4*, 1459-1467.

252. Britten, C. D.; Hilsenbeck, S. G.; Eckhardt, S. G.; Marty, J.; Mangold, G.; MacDonald, J. R.; Rowinsky, E. K.; von Hoff, D. D.; Weitman, S. D., Enhanced antitumor activity of 6-hydroxymethylacylfulvene in combination with irinotecan and 5-fluorouracil in the HT29 human colon tumor xenograft model. *Cancer Res.* **1999,** *59*, 1049-1053.

253. Cao, S.; Rustum, Y. M., Synergistic antitumor activity of irinotecan in combination with 5-fluorouracil in rats bearing advanced colorectal cancer: role of drug sequence and dose. *Cancer Res.* **2000,** *60*, 3717-3721.

254. Wasserman, E.; Sutherland, W.; Esteban, C., Irinotecan plus oxaliplatin: a promising combination for advanced colorectal cancer. *Clin. Colorectal Cancer* **2001,** *1*, 149-153.

255. Mayer, L. D.; Janoff, A. S., Optimizing combination chemotherapy by controlling drug ratios. *Mol. Interv.* **2007,** *7*, 216-223.

256. Guichard, S.; Arnould, S.; Hennebelle, I.; Bugat, R.; Canal, P., Combination of oxaliplatin and irinotecan on human colon cancer cell lines: activity *in vitro* and *in vivo*. *Anti-Cancer Drugs* **2001,** *12*, 741-751.

257. Harasym, T. O.; Tardi, P. G.; Harasym, N. L.; Harvie, P.; Johnstone, S. A.; Mayer, L. D., Increased preclinical efficacy of irinotecan and floxuridine coencapsulated inside liposomes is associated with tumor delivery of synergistic drug ratios. *Oncol. Res.* **2007,** *16*, 361-374.

258. Kirichenko, A. V.; Rich, T. A.; Newman, R. A.; Travis, E. L., Potentiation of murine MCa-4 carcinoma radioreponse by 9-amino-20-(S)-camptothecin. *Cancer Res.* **1997,** *57*, 1929-1933.

259. Lamond, J. P.; Mehta, M. P.; Boothman, D. A., The potential of topoisomerase I inhibitors in the treatment of CNS malignancies: report of a synergistic effect between topotecan and radiation. *J. Neuro.-Oncol.* **1996,** *30*, 1-6.

260. Karaberis, E.; Mourelatos, D., Enhanced cytogenetic and antitumor effects by 9-nitrocamptothecin and antineoplastics. *Teratogen. Carcin. Mut.* **2000,** *20*, 141-146.

261. Lawson, K. A.; Anderson, K.; Snyder, R. M.; Simmons-Menchaca, M.; Atkinson,

J.; Sun, L.-Z.; Bandyopadhyay, A.; Knight, V.; Gilbert, B. E.; Sanders, B. G.; Kline, K., Novel vitamine E analogue and 9-nitro-camptothecin administered as liposome aerosols decrease syngeneic mouse mammary tumor burden and inhibit metastasis. *Cancer Chemother. Pharmacol.* **2004,** *54*, 421-431.

262. Lee, D. H.; Kim, S.-W.; Bae, K.-S.; Hong, J.-S.; Suh, C.; Kang, Y.-K.; Lee, J.-S., A phase I and pharmacologic study of belotecan in combination with cisplatin in patients with previously untreated extensive-stage disease small cell lung cancer. *Clin. Cancer Res.* **2007,** *13*, 6182-6186.

263. Giovanella, B. C.; Hinz, H. R.; Kozielski, A. J.; Stehlin, J. S.; Silber, R.; Potmesil, M., Complete growth inhibition of human cancer xenografts in nude mice by treatment with 20-(S)-camptothecin. *Cancer Res.* **1991,** *51*, 3052-3055.

264. Scott, D. O.; Bindra, D. S.; Stella, V. J., Plasma pharmacokinetics of the lactone and carboxylate forms of 20(S)-camptothecin in anesthetized rats. *Pharm. Res.* **1993,** *10*, 1451-1457.

265. Scott, D. O.; Bindra, D. S.; Sutton, S. C.; Stella, V. J., Urinary and biliary disposition of the lactone and carboxylate forms of 20(S)-camptothecin in rats. *Drug Metabolism and Disposition* **1994,** *22*, 438-442.

266. Schaeppi, U.; Fleischman, R. W.; Cooney, D. A., Toxicity of camptothecin (NSC-100880). *Cancer Chemother. Rep.* **1974,** *5*, 25-35.

267. Gottlieb, J. A.; Guarino, A. M.; Call, J. B.; Oliverio, V. T.; Block, J. B., Preliminary pharmacological and clinical evaluation of camptothecin sodium (NSC 100880). *Cancer Chemother. Rep.* **1970,** *54*, 461-470.

268. Creaven, P. J.; Allen, L. M.; Muggia, F. M., Plasma camptothecin (NSC-100880) levels during a 5-day course of treatment: relation to dose and toxicity. *Cancer Chemother. Rep.* **1972,** *56*, 573-578.

269. Muggia, F. M.; Creaven, P. J.; Hansen, H. H.; Cohen, M. N.; Selawry, D. S., Phase I clinical trials of weekly and daily treatment with camptothecin (NSC100880). Correlation with clincial studies. *Cancer Chemother. Rep.* **1972,** *56*, 515-521.

270. Gottlieb, J. A.; Luce, J. K., Treatment of malignant melanoma with camptothecin (NSC 100880). *Cancer Chemother. Rep.* **1972,** *56*, 103-105.

271. Moertel, C. G.; Schutt, A. J.; Reitmeier, R. J.; Hahn, R. G., Phase II study of camptothecin (NSC 100880) in the treatment of advanced gastrointestinal cancer. *Cancer Chemother. Rep.* **1972,** *56*, 95-101.

272. Wall, M. E.; Wani, M. C.; Cook, C. E.; Palmer, K. H.; McPhail, A. T.; Sim, G. A., Plant antitumor agents. I. Isolation and structure of camptothecin, a novel alkaloidal leukemia and tumor inhibitor from *Camptotheca acuminata*. *J. Am. Chem. Soc.* **1966,** *88*, 3888-3890.

273. Wall, M. E.; Wani, M. C.; Natschke, S. M.; Nicholas, A. W., Plant antitumor agents. 22. Isolation of 11-hydroxycamptothecin from camptotheca acuminata decne: total synthesis and biological activity. *J. Med. Chem.* **1986,** *29*, 1553-1555.

274. Wani, M. C.; Nicholas, A. W.; Wall, M. E., Plant antitumor agents. 23. Synthesis and antileukemic activity of camptothecin analogs. *J. Med. Chem.* **1986,** *29*, 2358-2363.

275. Wani, M. C.; Nicholas, A. W.; Manikumar, G.; Wall, M. E., Plant antitumor agents. 25. Total synthesis and antileukemic activity of ring A substituted camptothecin analogs. Structure-activity correlations. *J. Med. Chem.* **1987,** *30*, 1774-1779.

276. Wani, M. C.; Nicholas, A. W.; Wall, M. E., Plant antitumor agents. 28. Resolution of a key tricyclic synthon, 5'(RS)-1,5-dioxo-5'-hydroxy-2'H,5'H,6'H-6'-oxopyrano[3',4'-f]-6,8-tetrahydroindolizine: total synthesis and antitumor activity of 20(S)- and 20(R)-camptothecin. *J. Med. Chem.* **1987,** *30*, 2317-2319.

277. Nicholas, A. W.; Wani, M. C.; Manikumar, G.; Wall, M. E.; Kohn, K. W.; Pommier, Y., Plant antitumor agents. 29. Synthesis and biological activity of ring D and ring E modified analogs of camptothecin. *J. Med. Chem.* **1990,** *33*, 972-978.

278. Sawada, S.; Matsuoka, S.; Nokata, K.; Nagata, H.; Furuta, T.; Yokokura, T.; Miyasaka, T., Synthesis and antitumor activity of 20(S)-camptothecin derivatives: a-ring modified and 7,10-disubstituted camptothecins. *Chem. Pharm. Bull.* **1991,** *39*, 3183-3188.

279. Wadkins, R. M.; Bearss, D.; Manikumar, G.; Wani, M. C.; Wall, M. E.; von Hoff, D. D., Hydrophilic camptothecin analogs that form extremely stable cleavable complexes with DNA and topoisomerase I. *Cancer Res.* **2004,** *64*, 6679-6683.

280. Kingsbury, W. D.; Boehm, J. C.; Jakas, D. R.; Holden, K. G.; Hecht, S. M.; Gallagher, G.; Caranfa, M. J.; McCabe, F. L.; Faucette, L. F.; Johnson, R. K., Synthesis of water soluble (aminoalkyl) camptothecin analogues: inhibition of topoisomerase I and antitumor activity. *J. Med. Chem.* **1991,** *34*, 98-107.

281. Luzzio, M. J.; Besterman, J. M.; Emerson, D. L.; Evans, M. G.; Lackey, K.; Leitner, P. L.; McIntyre, G.; Morton, B.; Myers, P. L.; Peel, M.; Sisco, J. M.; Sternbach, D. D.; Tong, W.-Q.; Truesdale, A.; Uehling, D. E.; Vuong, A.; Yates, J., Synthesis and antitumor activity of novel water soluble derivatives of camptothecin as specific inhibitors of topoisomerase I. *J. Med. Chem.* **1995,** *38*, 395-401.

282. Kim, D.-K.; Ryu, D. H.; Lee, J. Y.; Lee, N.; Kim, Y.-K.; Kim, J.-S.; Chang, K.; Im, G.-J.; Kim, T.-K.; Choi, W.-S., Synthesis and biological evaluation of novel A-ring modified hexacyclic camptothecin analogues. *J. Med. Chem.* **2001,** *44*, 1594-1602.

283. Sun, F.-X.; Tohgo, A.; Bouvet, M.; Yagi, S.; Nassirpour, R.; Moossa, A. R.; Hoffman, R. M., Efficacy of camptothecin analog DX-8951f (exatecan mesylate) on human pancreatic cancer in an orthotopic metastatic model. *Cancer Res.* **2003,** *63*, 80-85.

284. Lee, J.-H.; Lee, J.-M.; Kim, J.-K.; Ahn, S.-K.; Lee, S.-J.; Kim, M.-Y.; Jew, S.-S.; Park, J.-G.; Hong, C. I., Antitumor activity of 7-[2-(N-Isopropylamino)ethyl]-(20S)-camptothecin, CKD602, as a potent DNA topoisomerase I inhibitor. *Arch. Pharm. Res.* **1998,** *21*, 581-590.

285. Pollack, I. F.; Erff, M.; Bom, D.; Burke, T.; Strode, J. T.; Curran, D. P., Potent topoisomerase I inhibition by novel silatecans eliminates glioma proliferation *in vitro* and *in vivo*. *Cancer Res.* **1999,** *59*, 4898-4905.

286. Van Hattum, A. H.; Pinedo, H. M.; Schluper, H. M. M.; Hausheer, F. H.; Boven, E., New highly lipophilic camptothecin BNP1350 is an effective drug in experimental human cancer. *Int. J. Cancer* **2000,** *88*, 260-266.

287. Huang, M.; Gao, H.; Chen, Y.; Zhu, H.; Cai, Y.; Zhang, X.; Miao, Z.; Jiang, H.; Zhang, J.; Shen, H.; Lin, L.; Wei, L.; Ding, J., Chimmitecan, a novel 9-substituted camptothecin, with improved anticancer pharmacologic profiles in vitro and in vivo. *Clin. Cancer Res.* **2007,** *13* (4), 1298-1307.

288. Henne, W. A.; Doorneweerd, D. D.; Hilgebrink, A. R.; Kularatne, S. A.; Low, P. S., Synthesis and of a folate peptide camptothecin prodrug. *Bioorg. Med. Chem. Lett.* **2006,** *16*, 5350-5355.

289. Lu, H.; Lin, H.; Jiang, Y.; Zhou, X.; Wu, B.; Chen, J., Synthesis and antitumor activity of 20-O-linked succinate-based camptothecin ester derivatives. *Lett. Drug Design Disc.* **2006,** *3*, 83-86.

290. Samor, C.; Guerrini, A.; Varchi, G.; Beretta, G. L.; Fontana, G.; Bombardelli, E.;

Carenini, N.; Zunino, F.; Bertucci, C.; Fiori, J.; Battaglia, A., The role of polyamine architecture on the pharmacological activity of open lactone camptothecin-polyamine conjugates. *Bioconjugate Chem.* **2008,** *19*, 2270-2279.

291. Lesueur-Ginot, L.; Demarquay, D.; Kiss, R.; Kasprzyk, P. G.; Dassonneville, L.; Bailly, C.; Camara, J.; Lavergne, O.; Bigg, D. C. H., Homocamptothecin, an E-ring modified camptothecin with enhanced lactone stability, retains topoisomerase I-targeted activity and antitumor properties. *Cancer Res.* **1999,** *59*, 2939-2943.

292. Demarquay, D.; Huchet, M.; Coulomb, H.; Lesueur-Ginot, L.; Lavergne, O.; Camara, J.; Kasprzyk, P. G.; Prevost, G.; Bigg, D. C. H., BN89027: a novel homocamptothecin that inhibits proliferation of human tumor cells in vitro and in vivo. *Cancer Res.* **2004,** *64*, 4942-4949.

293. Lerchen, H.-G.; Baumgarten, J.; von dem Bruch, K.; Lehmann, T. E.; Sperzel, M.; Kempka, G.; Fiebig, H.-H., Design and optimization of 20-O-linked camptothecin glycoconjugates as anticancer agents. *J. Med. Chem.* **2001,** *44*, 4186-4195.

294. Fassberg, J.; Stella, J. V., A kinetic and mechanistic study of the hydrolysis of camptothecin and some analogues. *J. Pharm. Sci.* **1992,** *81*, 676-684.

295. Koizumi, F.; Kitagawa, M.; Negishi, T.; Onda, T.; Matsumoto, S.-I.; Hamaguchi, T.; Matsumura, Y., Novel SN-38-incorporating polymeric micelles, NK012, eradicate vascular endothelial growth factor-secreting bulky tumors. *Cancer Res.* **2006,** *66*, 10048-10056.

296. Greenwald, R.; Pendri, A.; Conover, C.; Gilbert, C.; Yang, R.; Xia, J., Drug delivery systems. 2.Camptothecin-20-O-poly(ethylene glycol) ester transport forms. *J. Med. Chem.* **1996,** *39*, 1938-1940.

297. Cheng, J.; Khin, K. T.; Davis, M. E., Antitumor activity of β-cyclodextrin polymer-camptothecin conjugates. *Molec. Pharmaceut.* **2004,** *1*, 183-193.

298. Zou, Y.; Wu, Q.-P.; Tansey, W.; Chow, D.; Hung, M.-C.; Charnsangavej, C.; Wallace, S.; Li, C., Effectiveness of water soluble poly(L-glutamic acid)-camptothecin conjugate against resistant human lung cancer xenografted in nude mice. *Int. J. Oncol.* **2001,** *18*, 331-336.

299. Caiolfa, V. R.; Zamai, M.; Fiorino, A.; Frigerio, E.; Pellizzoni, C.; d'Argy, R.; Ghigleri, A.; Castelli, M. G.; Farao, M.; Pesenti, E.; Gigli, M.; Angelucci, F.; Suarato, A., Polymer-bound camptothecin: initial biodistribution and antitumour activity studies. *J. Control. Release* **2000,** *65*, 105-119.

300. Harada, M.; Sakakibara, H.; Yano, T.; Suzuki, T.; Okuno, S., Determinants for the drug release from T-0128, camptothecin analogue-carboxymethyl dextran conjugate. *J. Control. Release* **2000,** *69*, 399-412.

301. Inoue, K.; Kumazawa, E.; Kuga, H.; Susaki, H.; Masubuchi, N.; Kajimura, T., CM-dextran-polyalcohol-camptothecin conjugate. In *Polymer Drugs in the Clinical Stage*, Maeda, H., Ed. Kluwer Academic/Plenum Publishers: New York, 2003.

302. Lee, N.-J.; Ju, S.-S.; Cho, W.-J.; Kim, S.-H.; Kang, K.-T.; Brady, T.; Theodorakis, E. A., Synthesis and biological activity of medium molecular weight polymers of camptothecin. *Eur. Poly. J.* **2003,** *39*, 367-374.

303. Sapra, P.; Zhao, H.; Mehling, M.; Malaby, J.; Kraft, P.; Longley, C.; Greenberger, L. M.; Horak, I. D., Novel delivery of SN38 markedly inhibits tumor growth in xenografts, including a camptothecin-11- refractory model. *Clin. Cancer Res.* **2008,** *14*, 1888-1896.

304. Fox, M. E.; Guillaudeu, S.; Fréchet, J. M. J.; Jerger, K.; Macaraeg, N.; Szoka, F. C., Synthesis and *in vivo* antitumor efficacy of PEGylated poly(L-lysine) dendrimer-camptothecin conjugates. *Molec. Pharmaceut.* **2009** *published online.*

305. Watanabe, M.; Kawano, K.; Yokoyama, M.; Opanasopit, P.; Okano, T.; Maitani, Y., Preparation of camptothecin-loaded polymeric micelles and evaluation of their incorporation and circulation stability. *Int. J. Pharm.* **2006,** *308*, 183-189.

306. Ding, X.-Q.; Chen, D.; Wang, A.-X.; Li, S.; Chen, Y.; Wang, J., Antitumor effects of hydroxycamptothecin-loaded poly[ethylene glycol]-poly[γ-benzyl-L-glutamate] micelles against oral squamous cell carcinoma. *Oncol. Res.* **2007,** *16*, 313-323.

307. Sugarman, S. M.; Zou, Y.; Wasan, K.; Poirot, K.; Kumi, R.; Reddy, S.; Perez-Soler, R., Lipid-complexed camptothecin: formulation and initial biodistribution and antitumor activity studies. *Cancer Chemother. Pharmacol.* **1996,** *37*, 531-538.

308. Tardi, P.; Choice, E.; Masin, D.; Redelmeier, T.; Bally, M. B.; Madden, T. D., Liposomal encapsulation of topotecan enhances anticancer efficacy in murine and human xenograft models. *Cancer Res.* **2000,** *60*, 3389-3393.

309. Messerer, C. L.; Ramsay, E. C.; Waterhouse, D.; Ng, R.; Simms, E. M.; Harasym,

N.; Tardi, P.; Mayer, L. D.; Bally, M. B., Liposomal irinotecan: formulation deelopment and therapeutic assessment in murine xenograft models of colorectal cancer. *Clin. Cancer Res.* **2004,** *10*, 6638-6649.

310. Zhang, J. A.; Xuan, T.; Parmar, M.; Ma, L.; Ugwu, S.; Ali, S.; Ahmad, I., Development and characterization of a novel liposome-based formulation of SN-38. *Int. J. Pharm.* **2004,** *270*, 93-107.

311. Colbern, G. T.; Dykes, D. J.; Engbers, C.; Musterer, R.; Hiller, A.; Pegg, E.; Saville, R.; Weng, S.; Luzzio, M. J.; Uster, P.; Amantea, M.; Working, P. K., Encapsulation of the topoisomerase I inhibitor GL147211C in PEGylated (STEALTH) liposomes: pharmacokinetics and antitumor activity in HT29 colon tumor xenografts. *Clin. Cancer Res.* **1998,** *4*, 3077-3082.

312. Yu, N. Y.; Conway, C.; Pena, R. L. S.; Chen, J. Y., STEALTH Liposomal CKD-602, a topoisomerase I inhibitor, improves teh therapeutic index in human tumor xenograft models. *Anticancer Res.* **2007,** *27*, 2541-2546.

313. Min, K. H.; Park, K.; Kim, Y.-S.; Bae, S. M.; Lee, S.; Jo, H. G.; Park, R. W.; Kim, I.-S.; Jeong, S. Y.; Kim, K.; Kwon, I. C., Hydrophobically modified glycol chitosan nanoparticles-encapsulated camptothecin enhance the drug stability and tumor targeting in cancer therapy. *J. Control. Release* **2008,** *127*, 208-218.

314. Williams, J.; Lansdown, R.; Sweitzer, R.; Romanowski, M.; LaBell, R.; Ramaswami, R.; Unger, E., Nanoparticle drug delivery system for intravenous delivery of topoisomerase inhibitors. *J. Control. Release* **2003,** *91*, 167-172.

315. Dadashzadeh, S.; Derakhshandeh, K.; Shirazi, F. H., 9-Nitrocamptothecin polymeric nanoparticles: cytotoxicity and pharmacokinetic studies of lactone and total forms of drug in rats. *Anti-Cancer Drugs* **2008,** *19*, 805-811.

316. Chenite, A.; Chaput, C.; Wang, D.; Combes, C.; Buschmann, M.; Hoemann, C. D.; Leroux, J. C.; Atkinson, B. L.; Binette, F.; Selmani, A., Novel injectable neutral solutions of chitosan form biodegradable gels in situ. *Biomaterials* **2000,** *21*, 2155-2161.

317. Lalloo, A.; Chao, P.; Hu, P.; Stein, S.; Sinko, P. J., Pharmacokinetic and pharmacodynamic evaluation of a novel in situ forming poly(ethylene glycol)-based hydrogel for the controlled delivery of the camptothecins. *J. Control. Release* **2006,** *112*, 333-342.

318. Gopin, A.; Rader, C.; Shabat, D., New chemical adaptor unit designed to release a drug from a tumor targeting davice by enzymetic triggering. *Bioorg. Med. Chem.* **2004,** *12*, 1853-1858.

319. Pessah, N.; Reznik, M.; Shamis, M.; Yantiri, F.; Xin, H.; Bowdish, K.; Shomron, N.; Ast, G.; Shabat, D., Bioactivation of carbamate-based 20(*S*)-camptothecin prodrugs. *Bioorg. Med. Chem.* **2004,** *12*, 1859-1866.

320. Shamis, M.; Lode, H. N.; Shabat, D., Bioactivation of self-immolative dendritic prodrugs by catalytic antibody 38C2. *J. Am. Chem. Soc.* **2004,** *126*, 1726-1731.

321. Gopin, A.; Ebner, S.; Attali, B.; Shabat, D., Enzymatic activation of second-generation denritic prodrugs: canjugation of self-immolative dendrimers with poly(ethylene glycol) via click chemistry. *Bioconjugate Chem.* **2006,** *17*, 1432-1440.

322. Erez, R.; Ebner, S.; Attali, B.; Shabat, D., Chemotherapeutic bone-targeted bisphophonate prodrugs with hydrolytic mode of activation. *Bioorg. Med. Chem. Lett.* **2008,** *18*, 816-820.

323. Venditto, V. J.; Allred, K.; Allred, C. D.; Simanek, E. E., Intercepting the synthesis of triazine dendrimers with nucleophilic pharmacophores: a general strategy toward drug delivery vehicles. *Chem. Commun.* **2009,** *DOI: 10.1039/b911353c*.

324. Parrish, B.; Emrick, T., Soluble camptothecin derivatives prepared by click cycloaddition chemistry on functional aliphatic polyesters. *Bioconjugate Chem.* **2007,** *18*, 263-267.

325. Mu, L.; Chrastina, A.; Levchenko, T.; Torchilin, V. P., Micelles from Poly(ethylene glycol)-phosphatidyl ethanolamine conjugates (PEG-PE) as pharmaceutical nanocarriers for poorly soluble drug camptothecin. *J. Biomed. Nanotechnol.* **2005,** *1*, 190-195.

326. Cabral, H.; Nakanishi, M.; Kumagai, M.; Jang, W.-D.; Nishiyama, N.; Kataoka, K., A photo-activated targeting chemotherapy using glutathione sensitive camptothecin-loaded polymeric micelles. *Pharm. Res.* **2009,** *26*, 82-92.

327. Liu, Z.; Robinson, J. T.; Sun, X.; Dai, H., PEGylated nanographene oxide for delivery of water-insoluble cancer drugs. *J. Am. Chem. Soc.* **2008,** *130*, 10876-10877.

328. Kolhatkar, R. B.; Swaan, P.; Ghandehari, H., Potential oral delivery of 7-ethyl-10-hydroxy-camptothecin (SN-38) using poly(amidoamine) dendrimers. *Pharmaceutical Res.* **2008,** *25*, 1723-1729.

329. Morgan, M. T.; Nakanishi, Y.; Kroll, D. J.; Griset, A. P.; Carnahan, M. A.;

Wathier, M.; Oberlies, N. H.; Manikumar, G.; Wani, M. C.; Grinstaff, M. W., Dendrimer-encapsulated camptothecins: increased solubility, cellular uptake, and cellular retention affords enhanced anticancer activity *in vitro*. *Cancer Res.* **2006,** *66*, 11913-11921.

330. Sparrenboom, A.; Gelderbolm, H.; Marsh, S.; Ahluwalia, R.; Obach, R.; Principe, P.; Twelves, C.; Verweij, J.; McLeod, H. L., Diflomotecan pharmacokinetics in relation to ABCG2 421>CA genotype. *Clin. Pharmacol. Ther.* **2004,** *76*, 38-44.

331. Rajendra, R.; Grounder, M. K.; Saleem, A.; Schellens, J. H.; Ross, D. D.; Bates, S. E.; Sinko, P. J.; Rubin, E. H., Differential effects of the breat cancer resistance protein on the cellular accumulation and cytotoxicity of 9-aminocamptothecin and 9-nitrocamptothecin. *Cancer Res.* **2003,** *63*, 3228-3233.

332. Nakatomi, K.; Yoshikawa, M.; Oka, M.; Y., I.; Hayasaka, S.; Sano, K.; Shiozawa, K.; Kawabata, S.; Soda, H.; Ishikawa, T.; Tanabe, S.; Kohno, S., Transport of 7-ethyl-10-hydroxycamptothecin (SN-38) by breast cancer resistance protein ABCG2 in human lung cancer cells. *Biochem. Biophys. Res. Commmun.* **2001,** *288*, 827-832.

333. Maliepaard, M.; van Gastelen, M. A.; de Jong, L. A.; Pluim, D.; van Waardenburg, R. C.; Ruevekamp-Helmers, M. C.; Floot, B. G.; Schellens, J. H., Overexpression of the BCRP/MXR/ABCP gene in a topotecan-selected ovarian tumor cell line. *Cancer Res.* **1999,** *59*, 4559-4563.

334. Dong, Y. B.; Yang, H. L.; McMasters, K. M., E2F-1 overexpression sensitizes colorectal cancer cells to camptothecin. *Cancer Gene Ther.* **2003,** *10*, 168-178.

APPENDIX A

SPECTRA FOR CHAPTER II

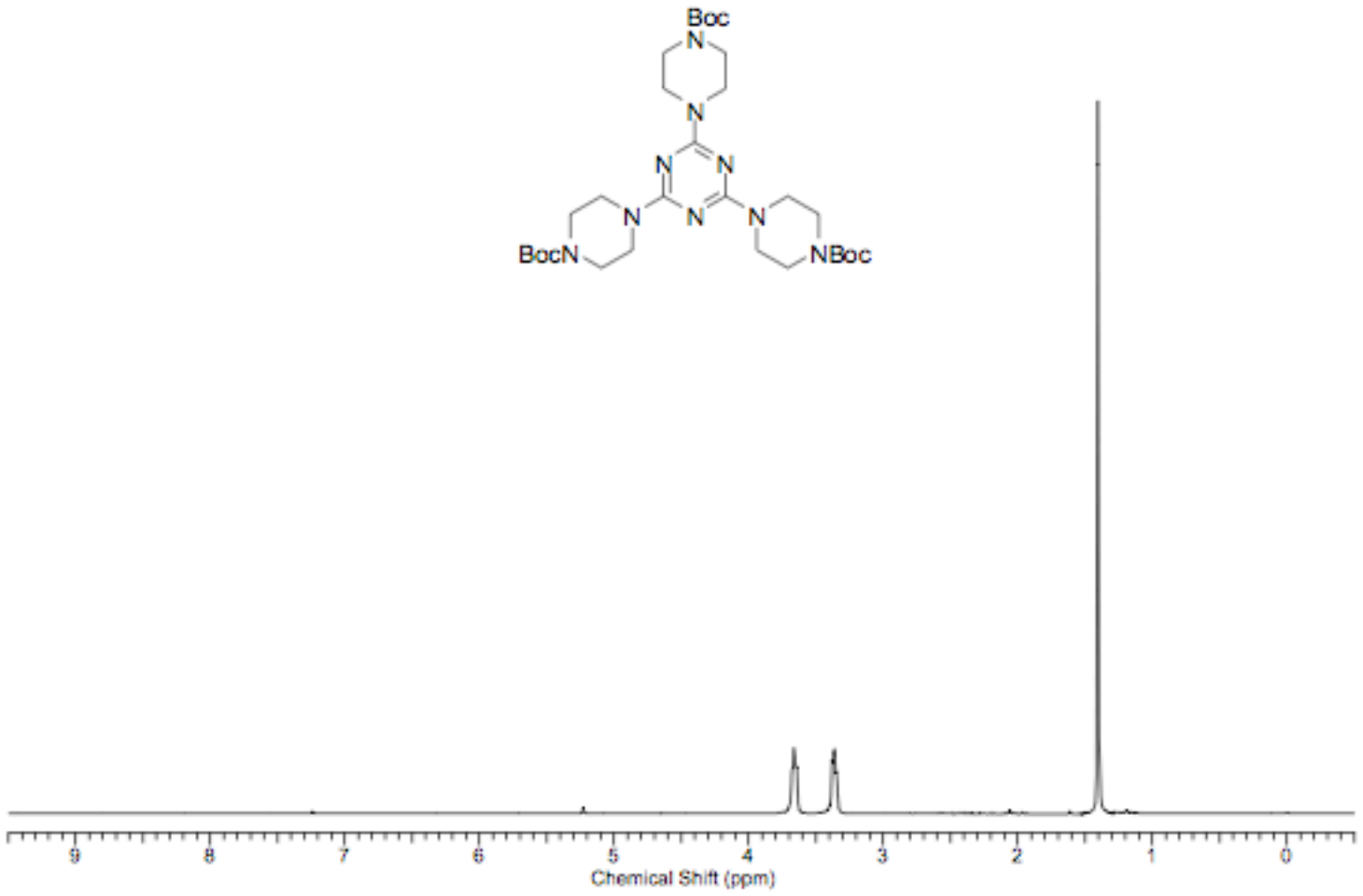
Boc
N
N
N
N
N
N
N
BocN
NBoc
9
8
7
6
5
4
3
2
1
0
Chemical Shift (ppm)

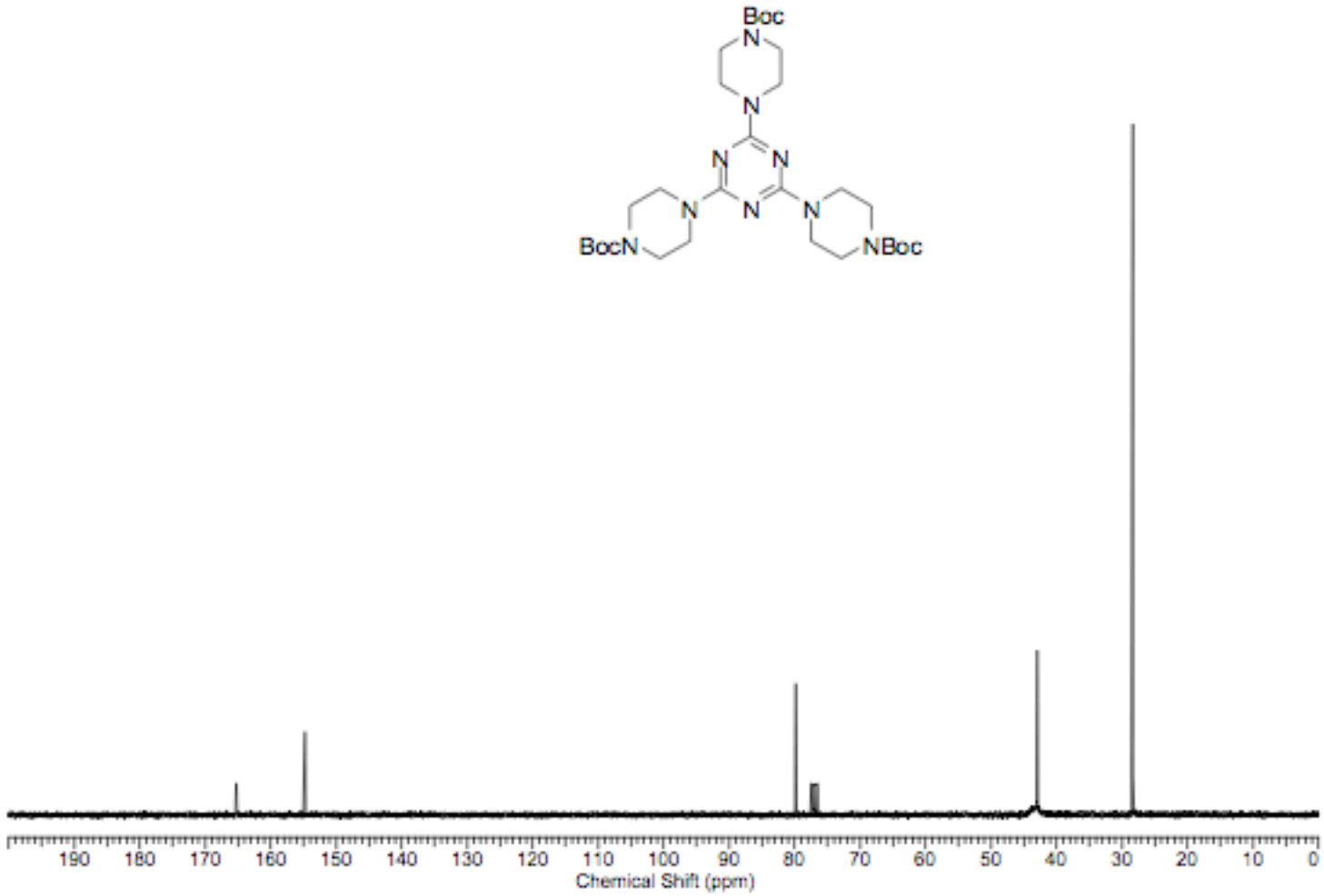
Boc
N
N
N
N
N
N
N
BocN
NBoc
190
180
170
160
150
140
130
120
110
100
90
80
70
60
50
40
30
20
10
0
Chemical Shift (ppm)


634.3913
Boc
N
N
N
N
N
N
N
BocN
NBoc
m/z, amu

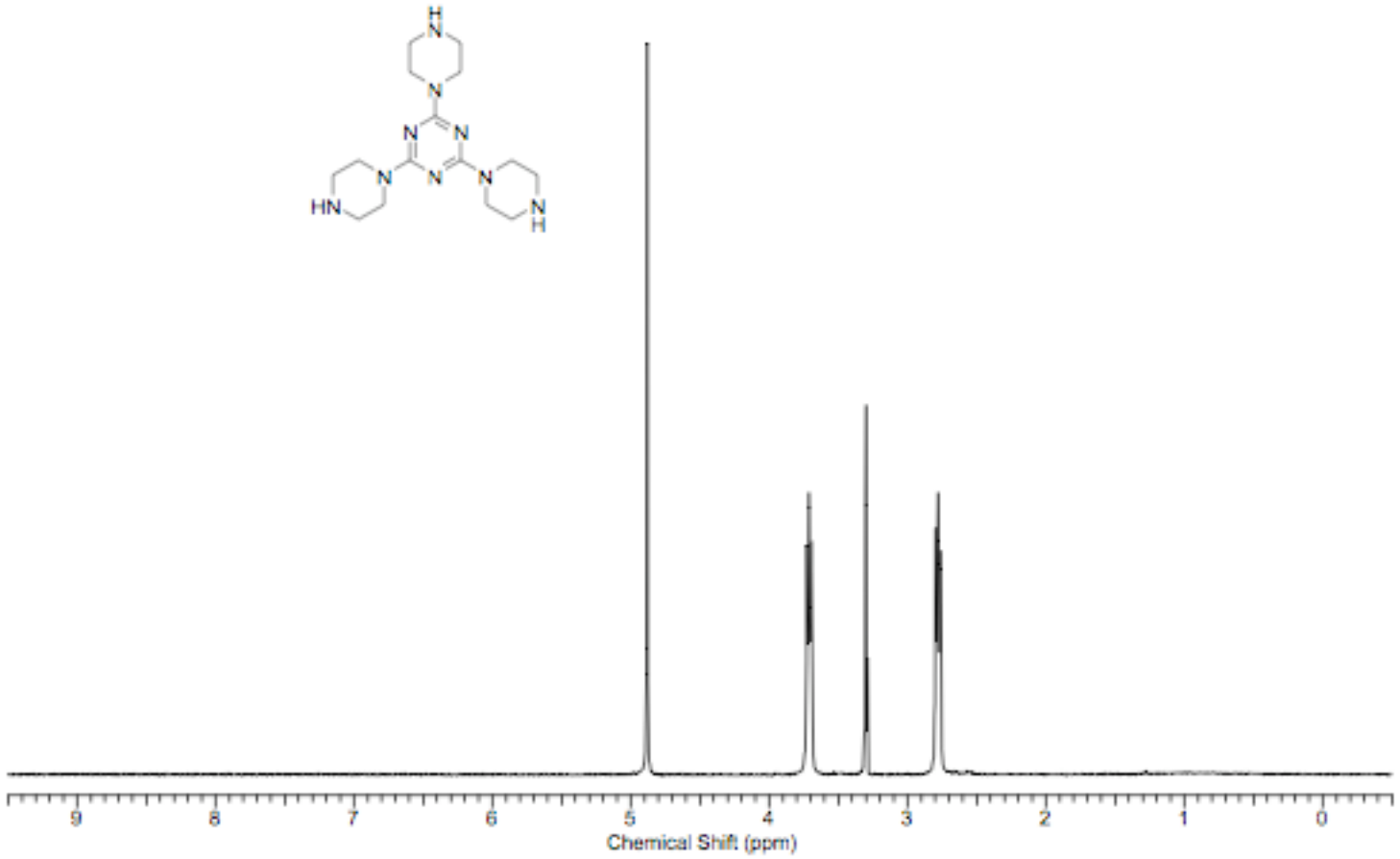
H
N
N
N
N
N
N
HN
N
H
9
8
7
6
5
4
3
2
1
0
Chemical Shift (ppm)

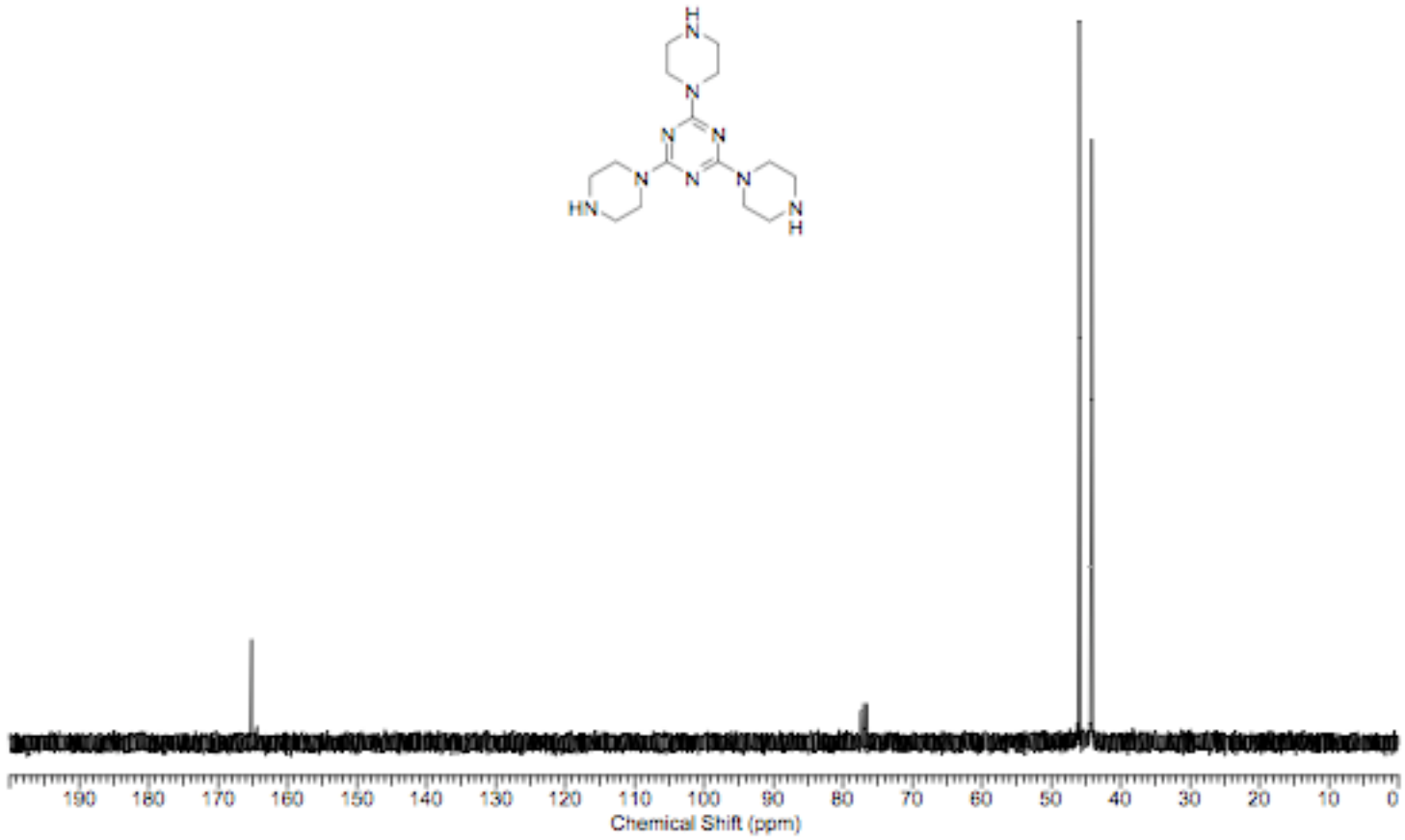
HN
N
N
N
N
N
N
N
N
H
N
H
190
180
170
160
150
140
130
120
110
100
90
80
70
60
50
40
30
20
10
0
Chemical Shift (ppm)

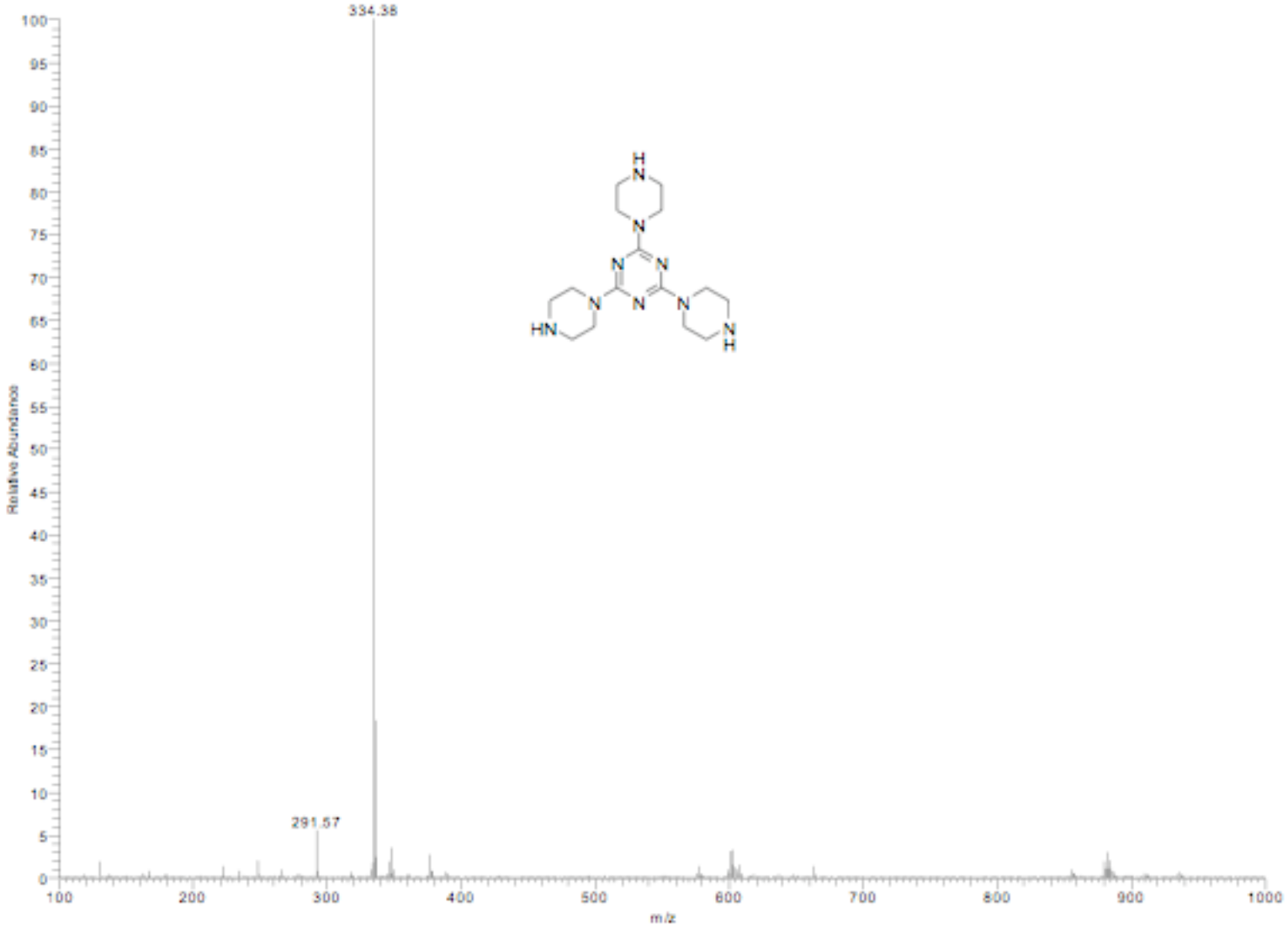
334.38
291.57
Relative Abundance
m/z
100
95
90
85
80
75
70
65
60
55
50
45
40
35
30
25
20
15
10
5
0
100
200
300
400
500
600
700
800
900
1000
H
N
N
N
N
N
N
N
HN
N
H

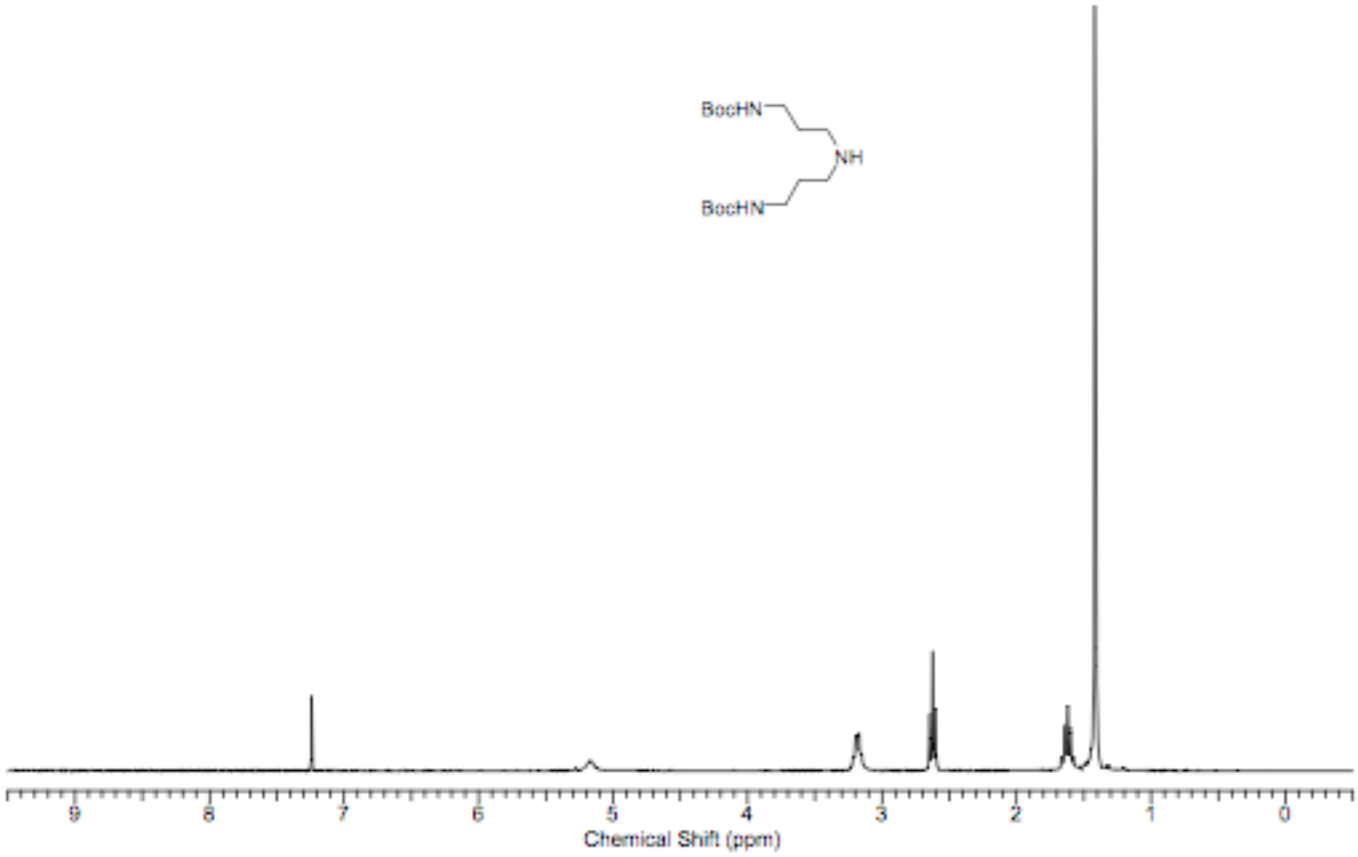
BocHN
NH
BocHN
9
8
7
6
5
4
3
2
1
0
Chemical Shift (ppm)

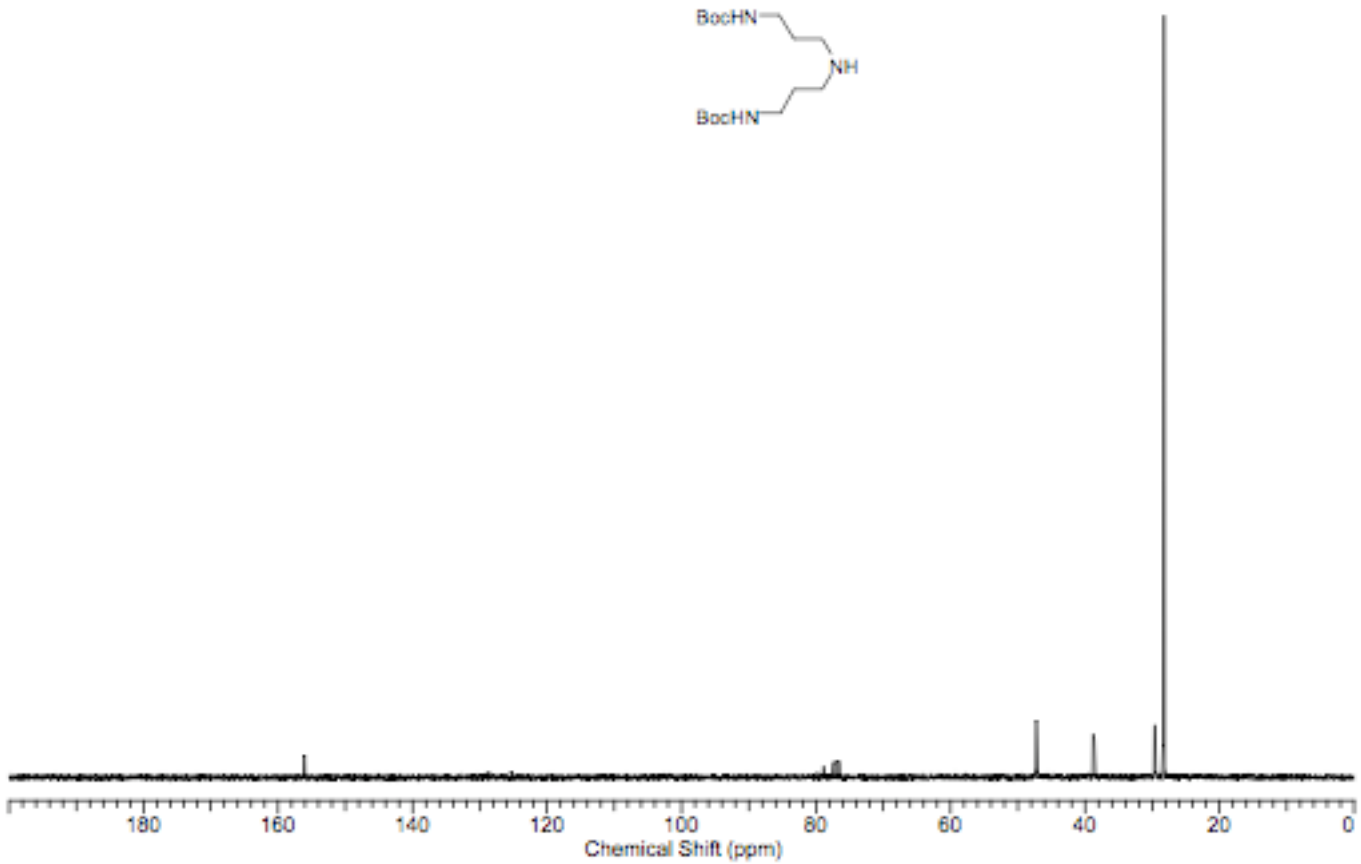
BocHN
NH
BocHN
180
160
140
120
100
80
60
40
20
0
Chemical Shift (ppm)

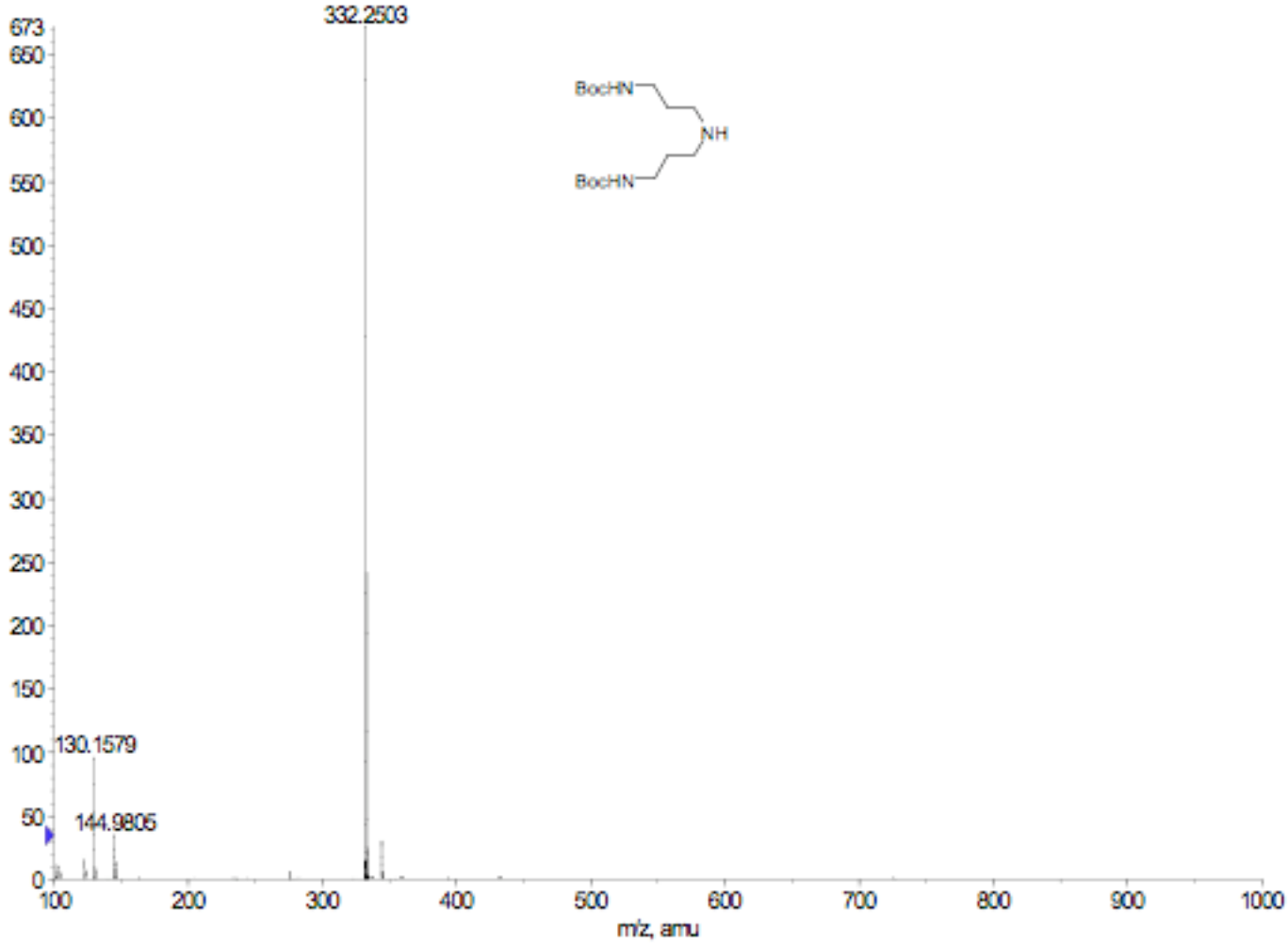
332.2503
130.1579
144.9805
BocHN
NH
BocHN
673
650
600
550
500
450
400
350
300
250
200
150
100
50
0
100
200
300
400
500
600
700
800
900
1000
m/z, amu

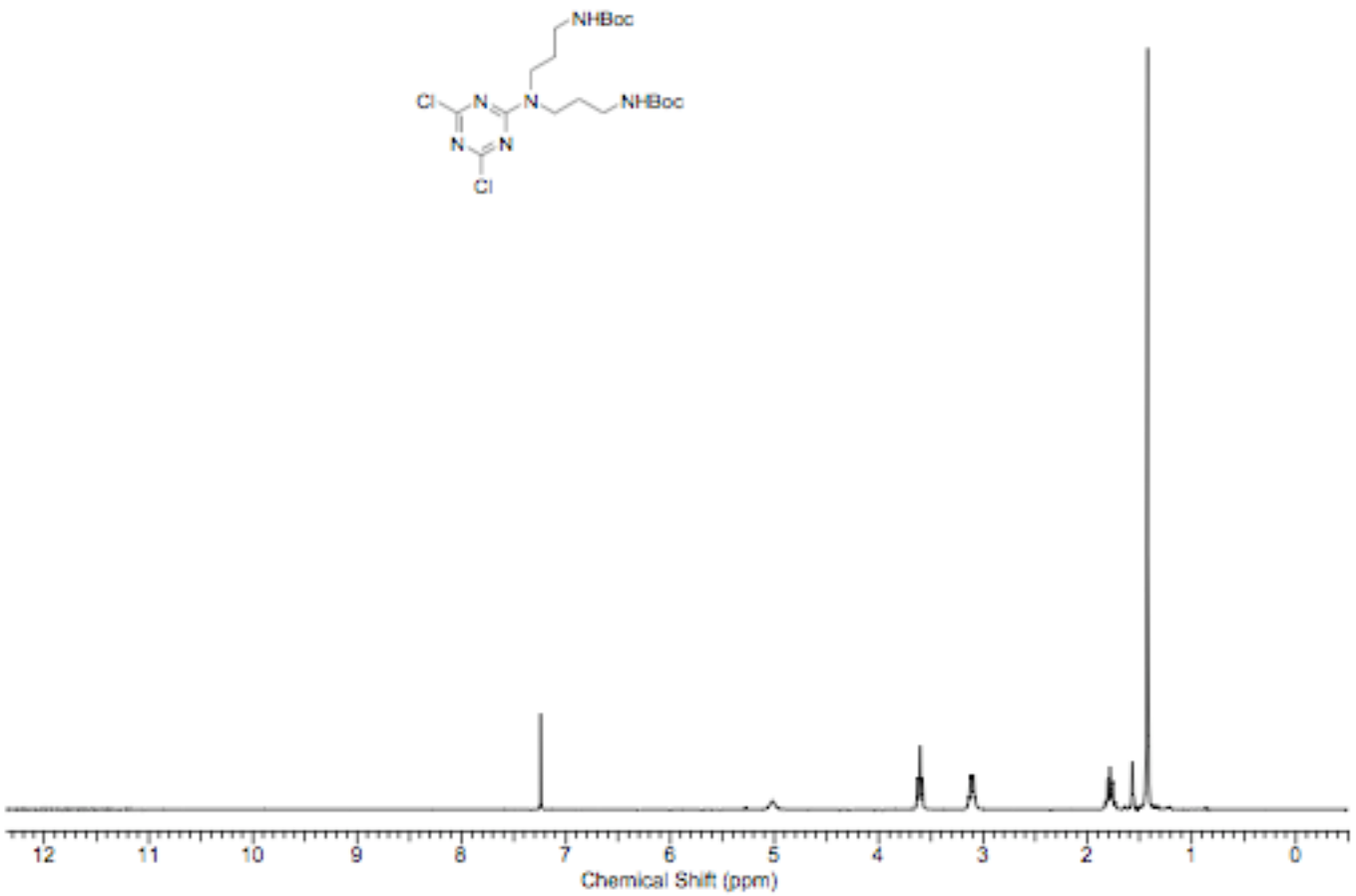
NHBoc
Cl
N
N
NHBoc
N
N
Cl
12
11
10
9
8
7
6
5
4
3
2
1
0
Chemical Shift (ppm)

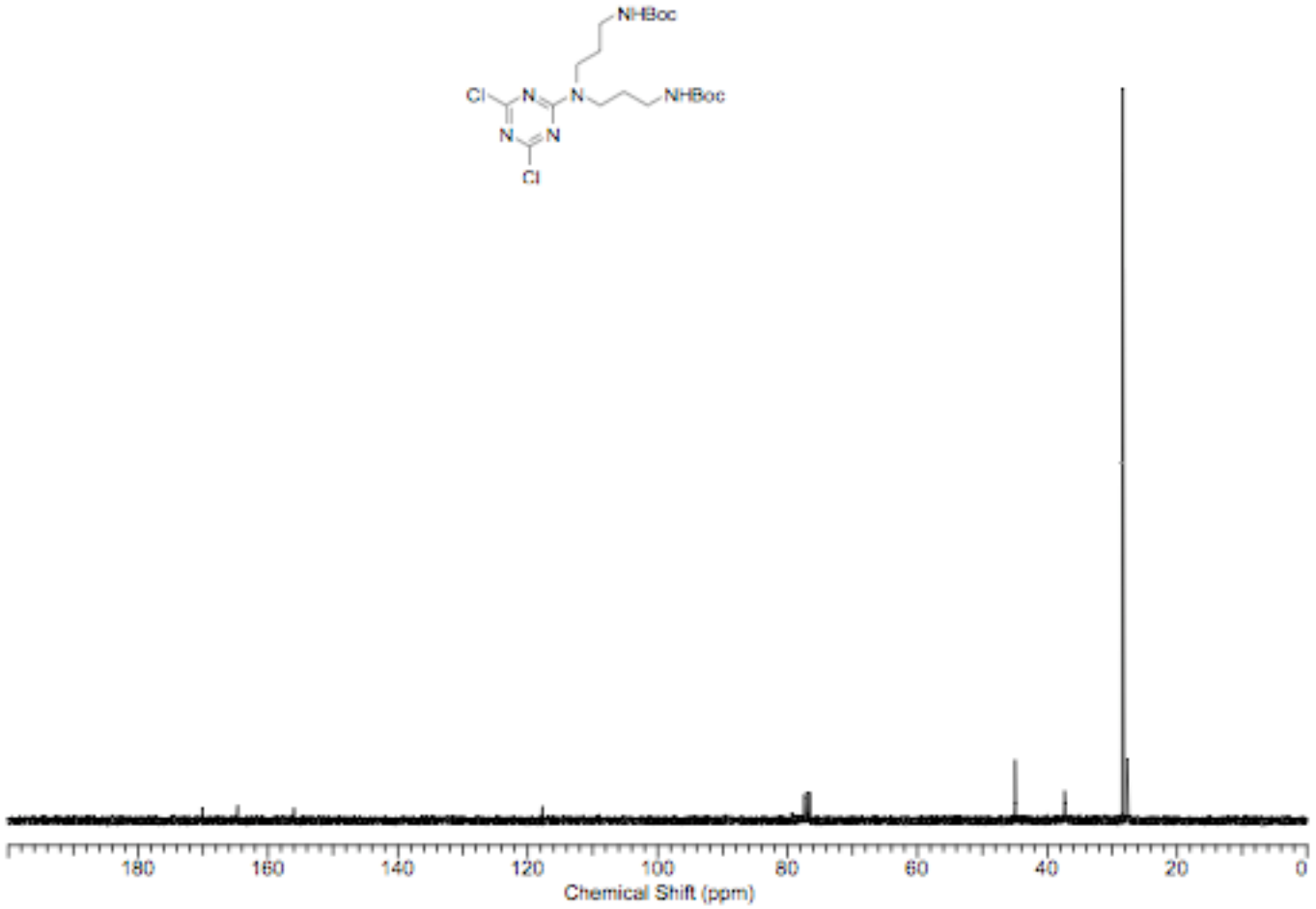
NHBoc
Cl
N
N
N
N
NHBoc
Cl
180
160
140
120
100
80
60
40
20
0
Chemical Shift (ppm)

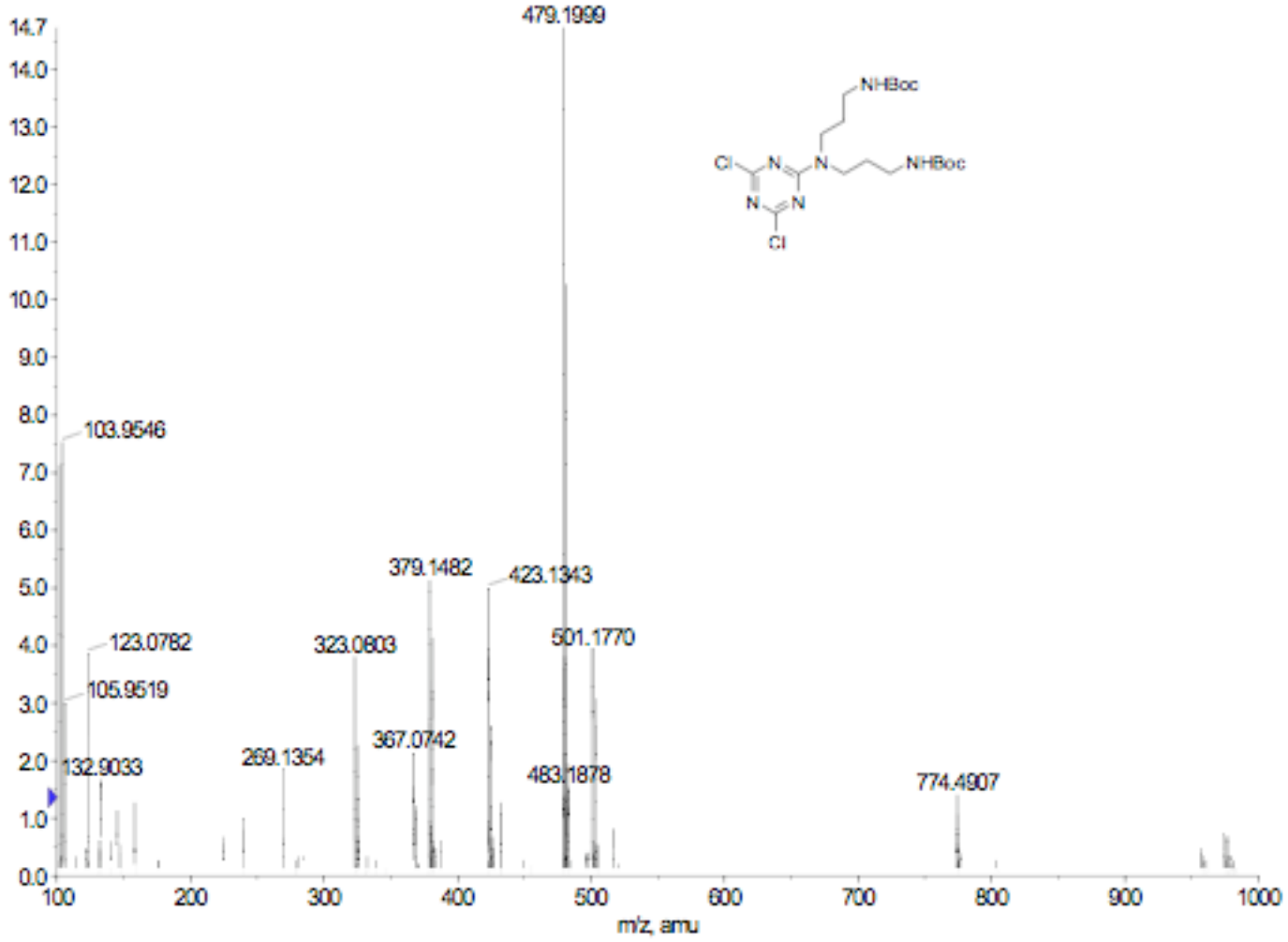
479.1999
103.9546
379.1482
423.1343
123.0782
323.0803
501.1770
105.9519
367.0742
269.1354
132.9033
483.1878
774.4907
m/z, amu
NHBoc
NHBoc
Cl
Cl

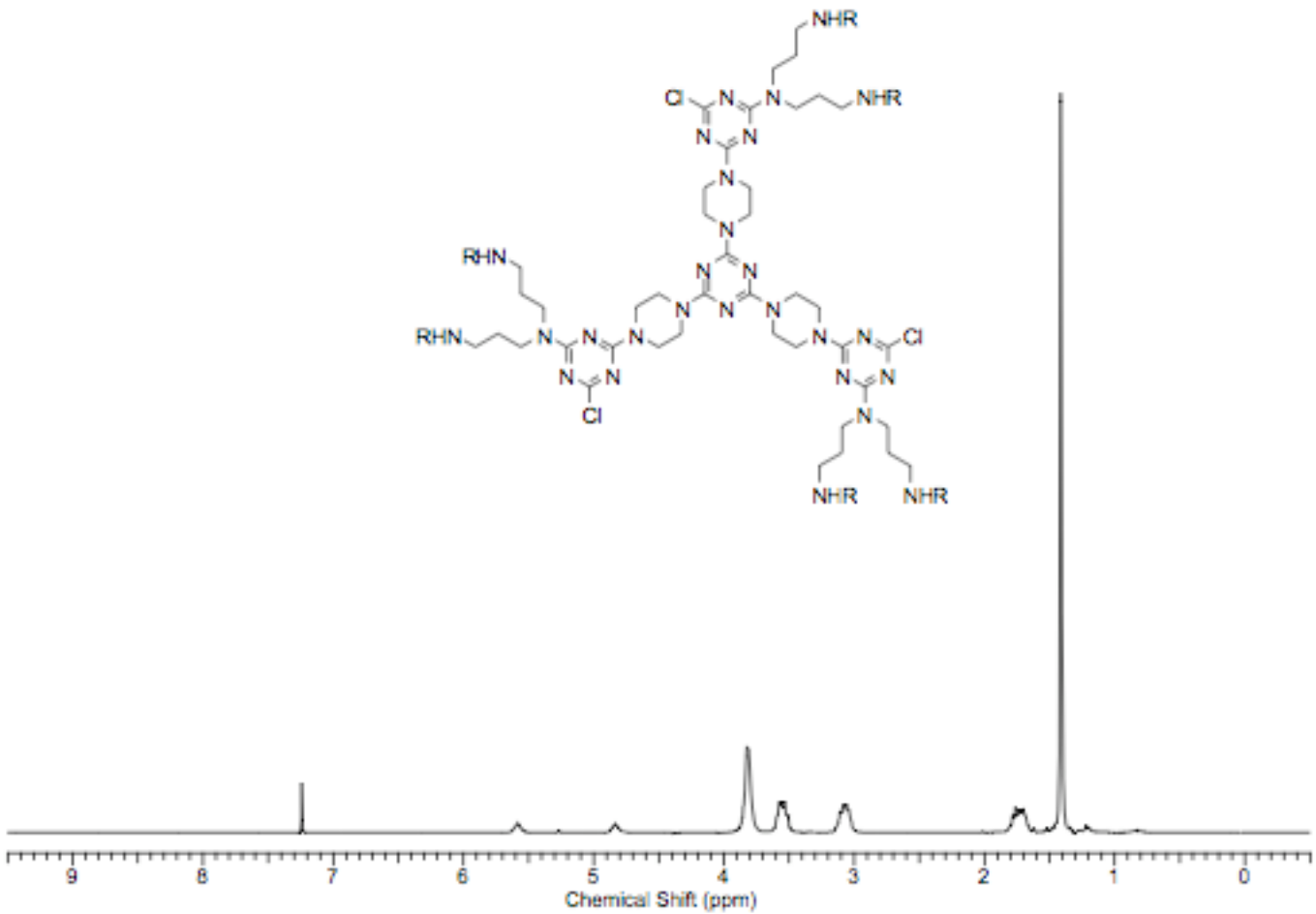
NHR
Cl
N
N
N
N
NHR
N
N
N
N
N
N
N
N
N
N
N
N
N
N
RHN
RHN
N
N
N
N
N
N
N
N
Cl
Cl
N
N
N
NHR
NHR
9
8
7
6
5
4
3
2
1
0
Chemical Shift (ppm)

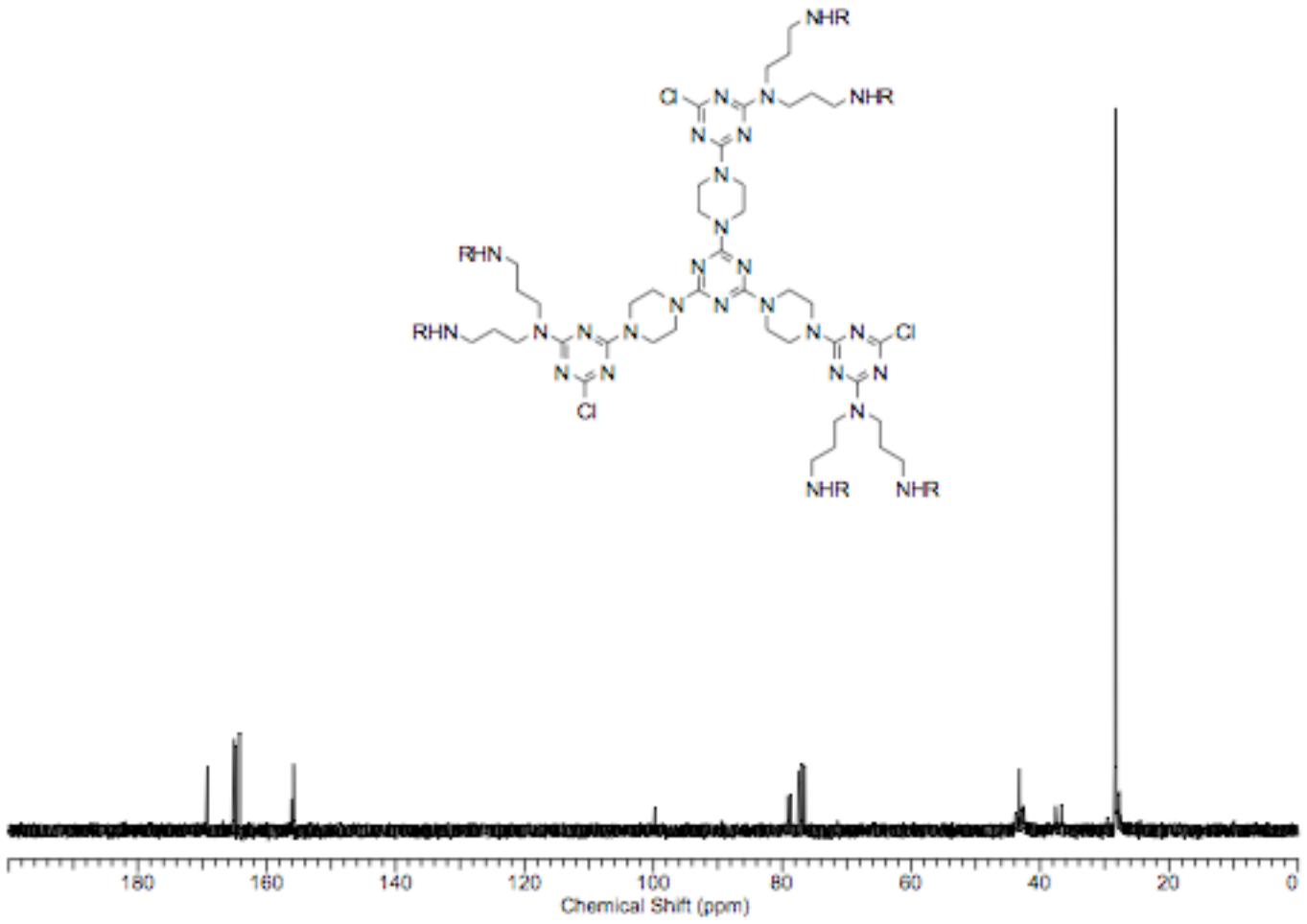
NHR
Cl
N
NHR
RHN
RHN
Cl
Cl
NHR
NHR
180
160
140
120
100
80
60
40
20
0
Chemical Shift (ppm)

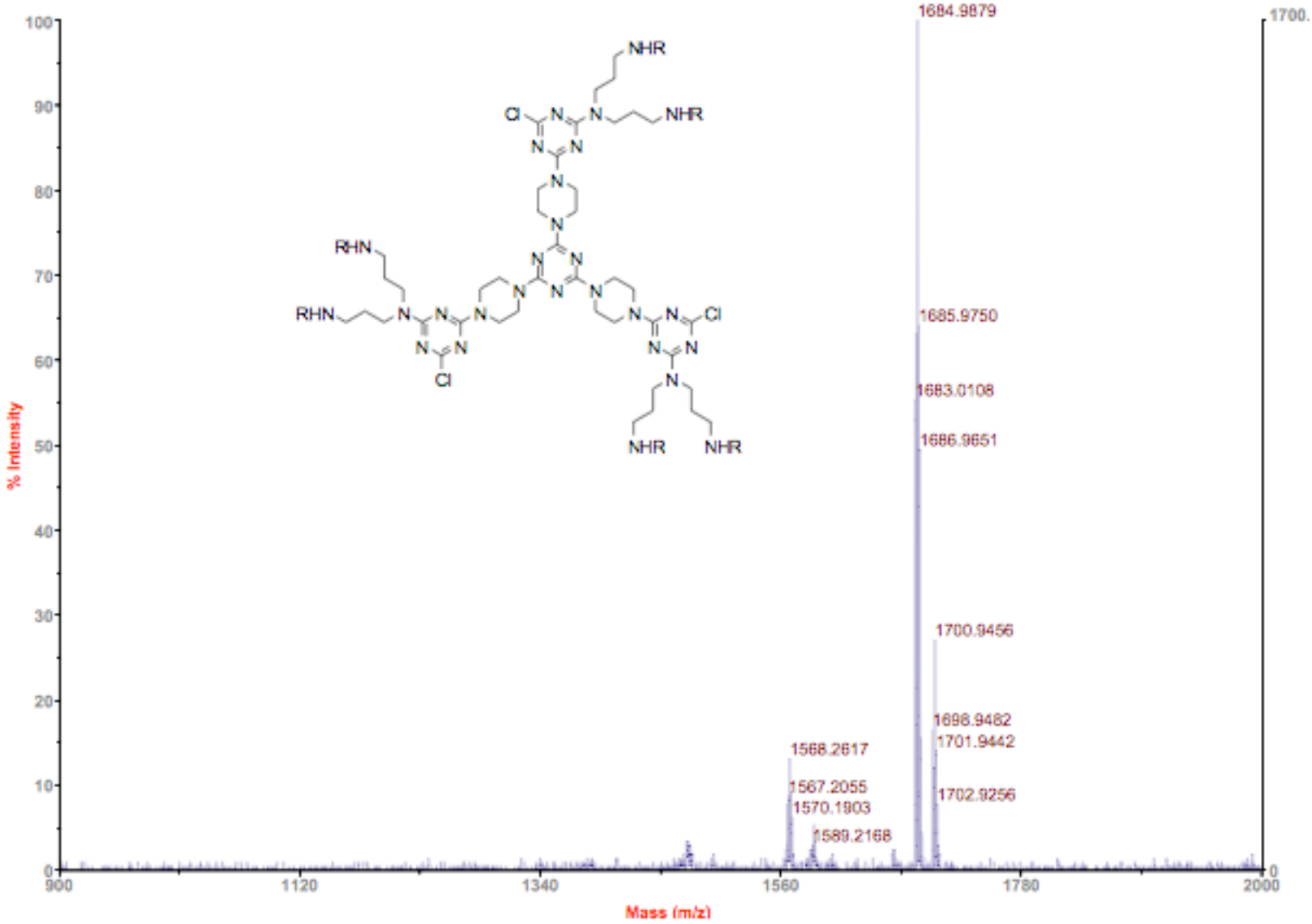
1684.9879
1700.
1685.9750
1683.0108
1686.9651
1700.9456
1698.9482
1701.9442
1568.2617
1567.2055
1570.1903
1702.9256
1589.2168
% Intensity
Mass (m/z)
100
90
80
70
60
50
40
30
20
10
0
900
1120
1340
1560
1780
2000
NHR
Cl
RHN
NHR
RHN
Cl
NHR
NHR

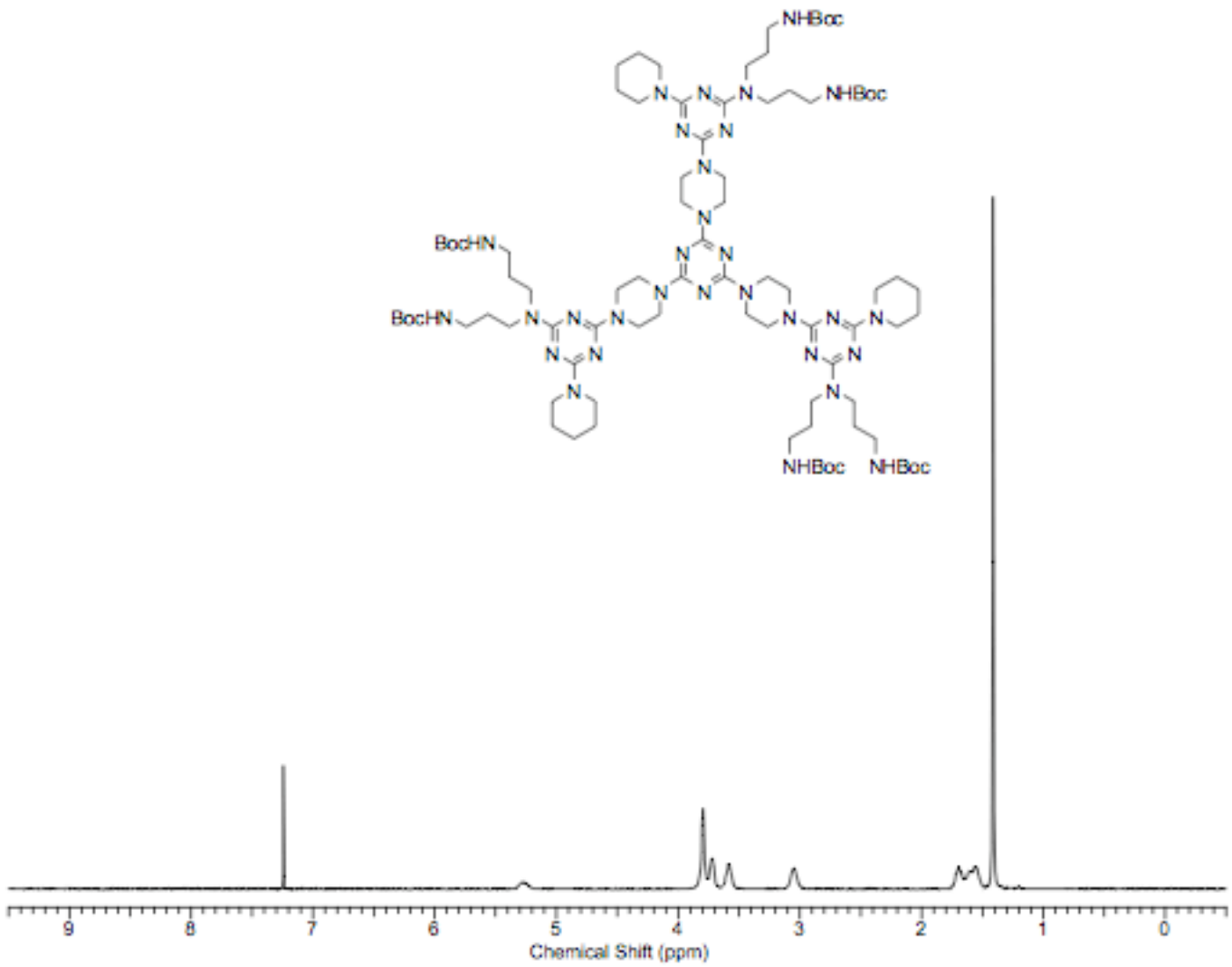
NHBoc
NHBoc
BocHN
BocHN
NHBoc
NHBoc
9
8
7
6
5
4
3
2
1
0
Chemical Shift (ppm)

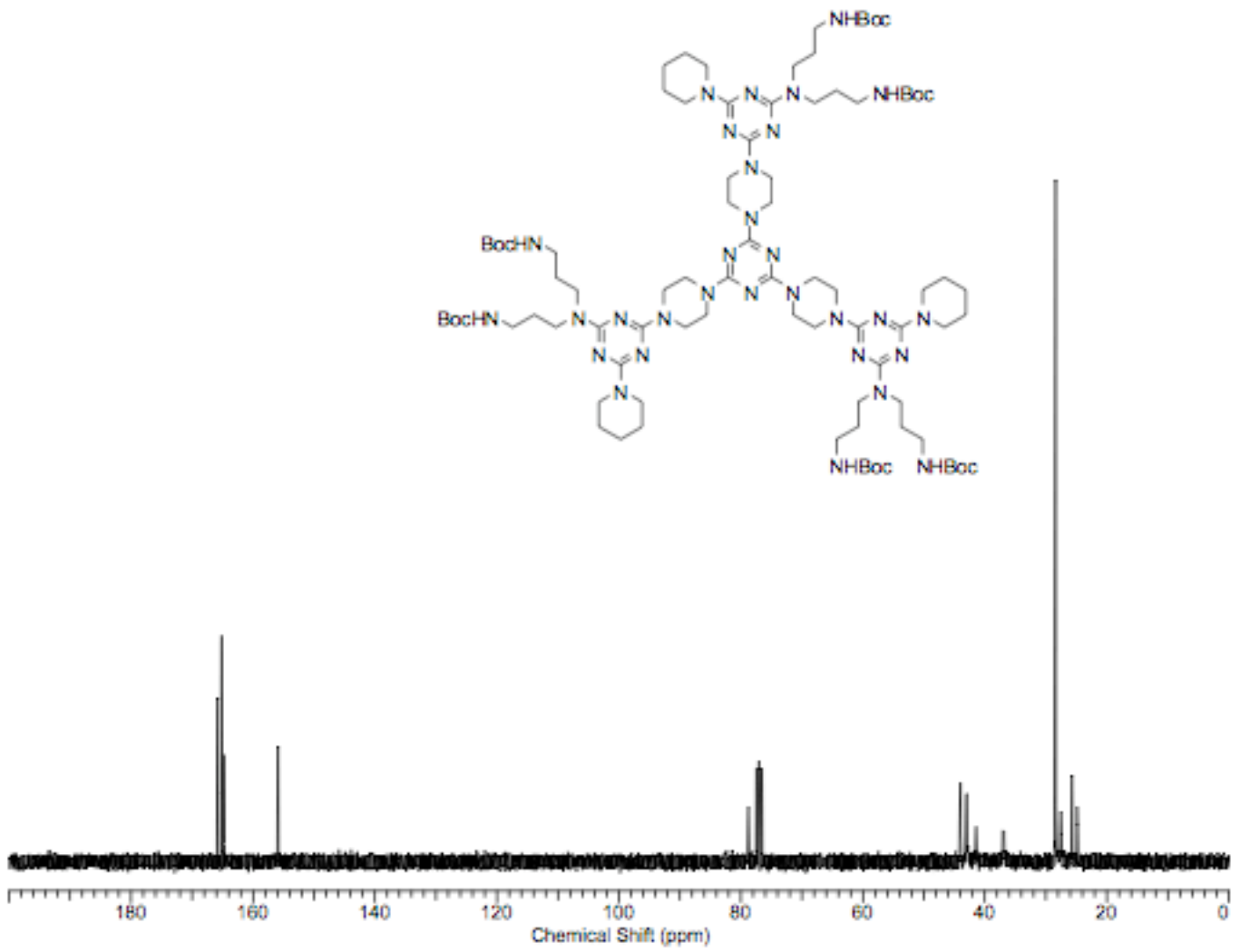
NHBoc
NHBoc
BocHN
BocHN
NHBoc
NHBoc
180
160
140
120
100
80
60
40
20
0
Chemical Shift (ppm)

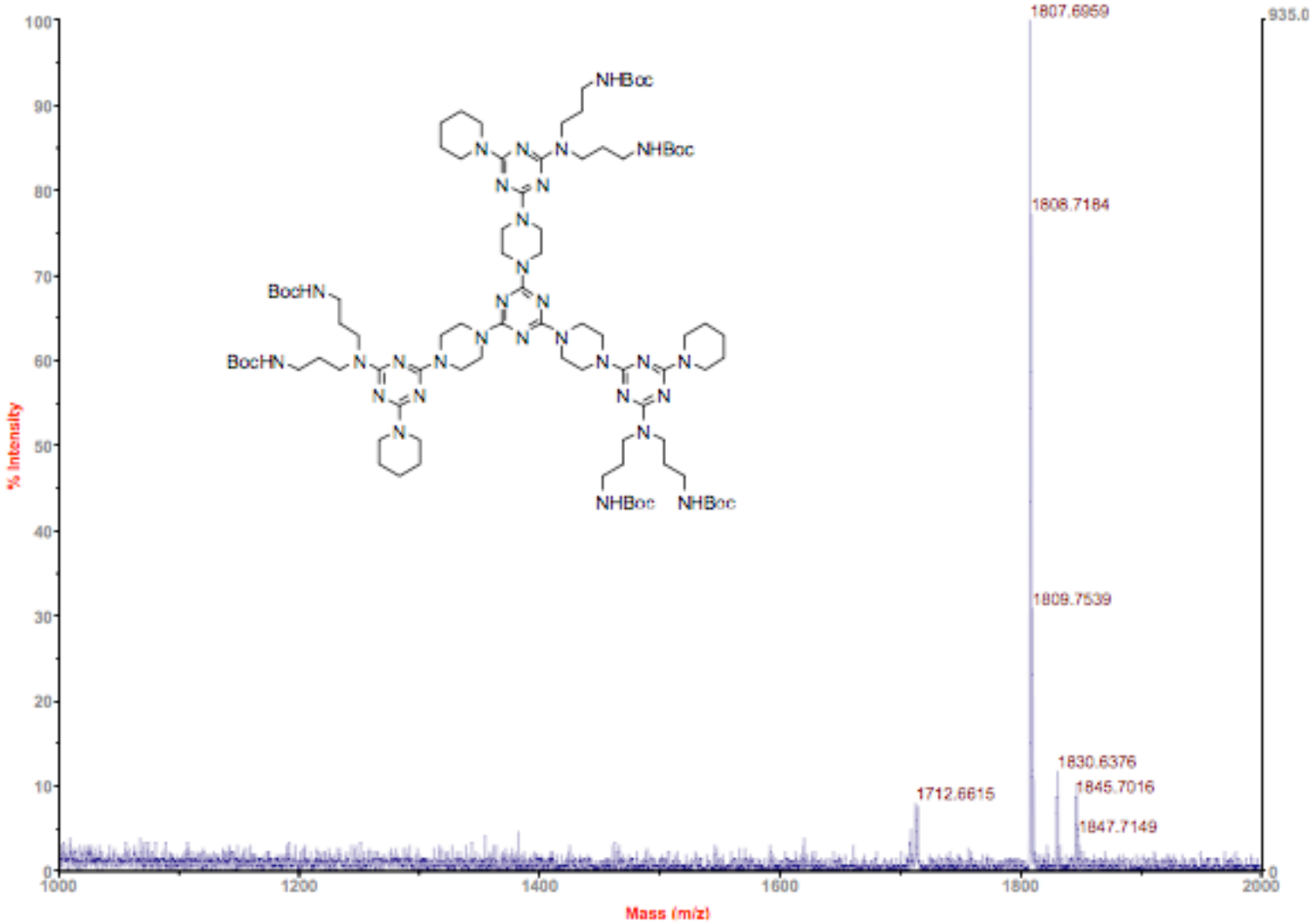
1807.6959
935.0
1808.7184
1809.7539
1830.6376
1845.7016
1847.7149
1712.6615
% Intensity
Mass (m/z)
100
90
80
70
60
50
40
30
20
10
0
1000
1200
1400
1600
1800
2000
NHBoc
NHBoc
BocHN
BocHN
NHBoc
NHBoc

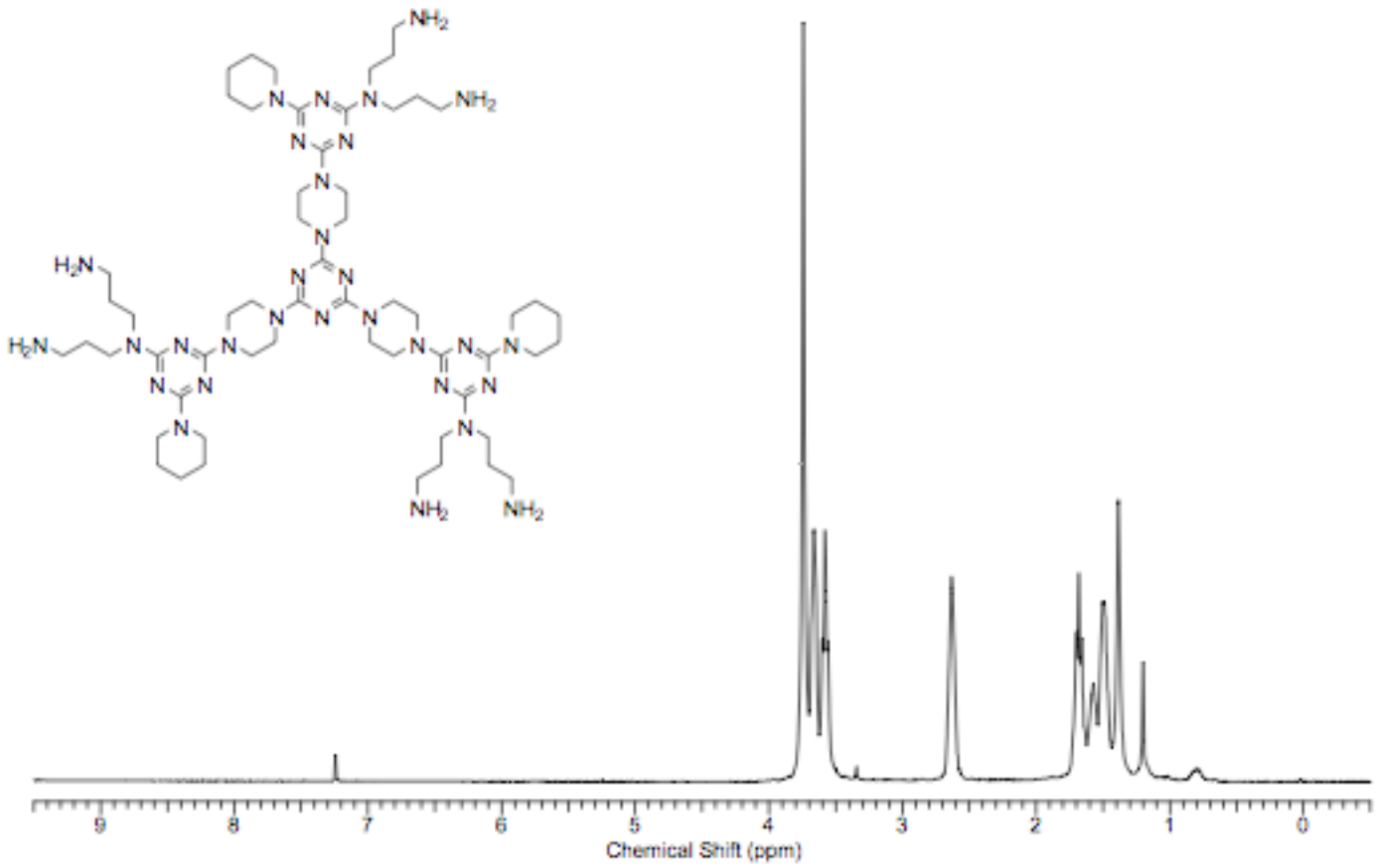
NH2
NH2
H2N
H2N
NH2
NH2
9
8
7
6
5
4
3
2
1
0
Chemical Shift (ppm)

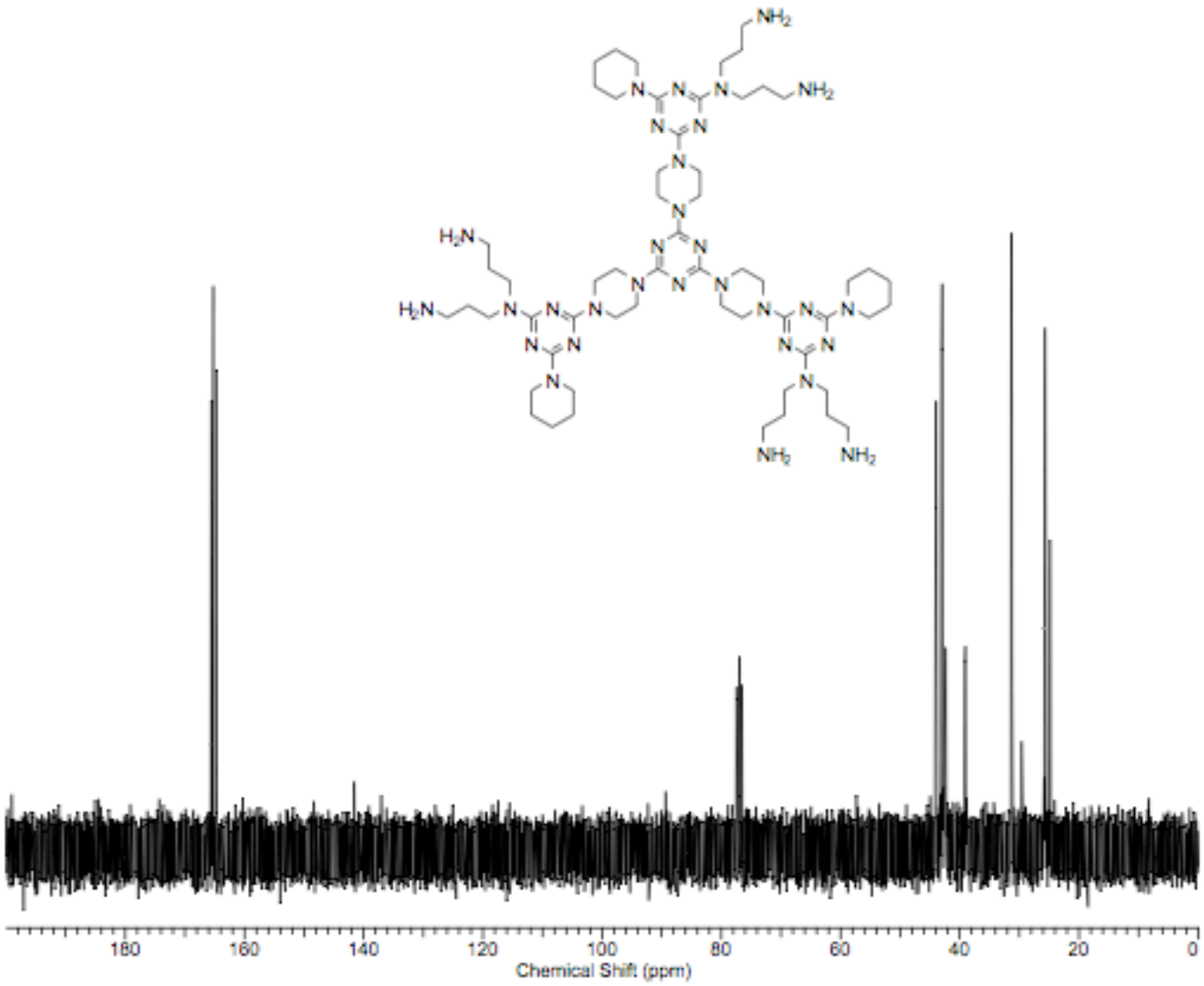
NH2
NH2
H2N
H2N
NH2
NH2
180
160
140
120
100
80
60
40
20
0
Chemical Shift (ppm)

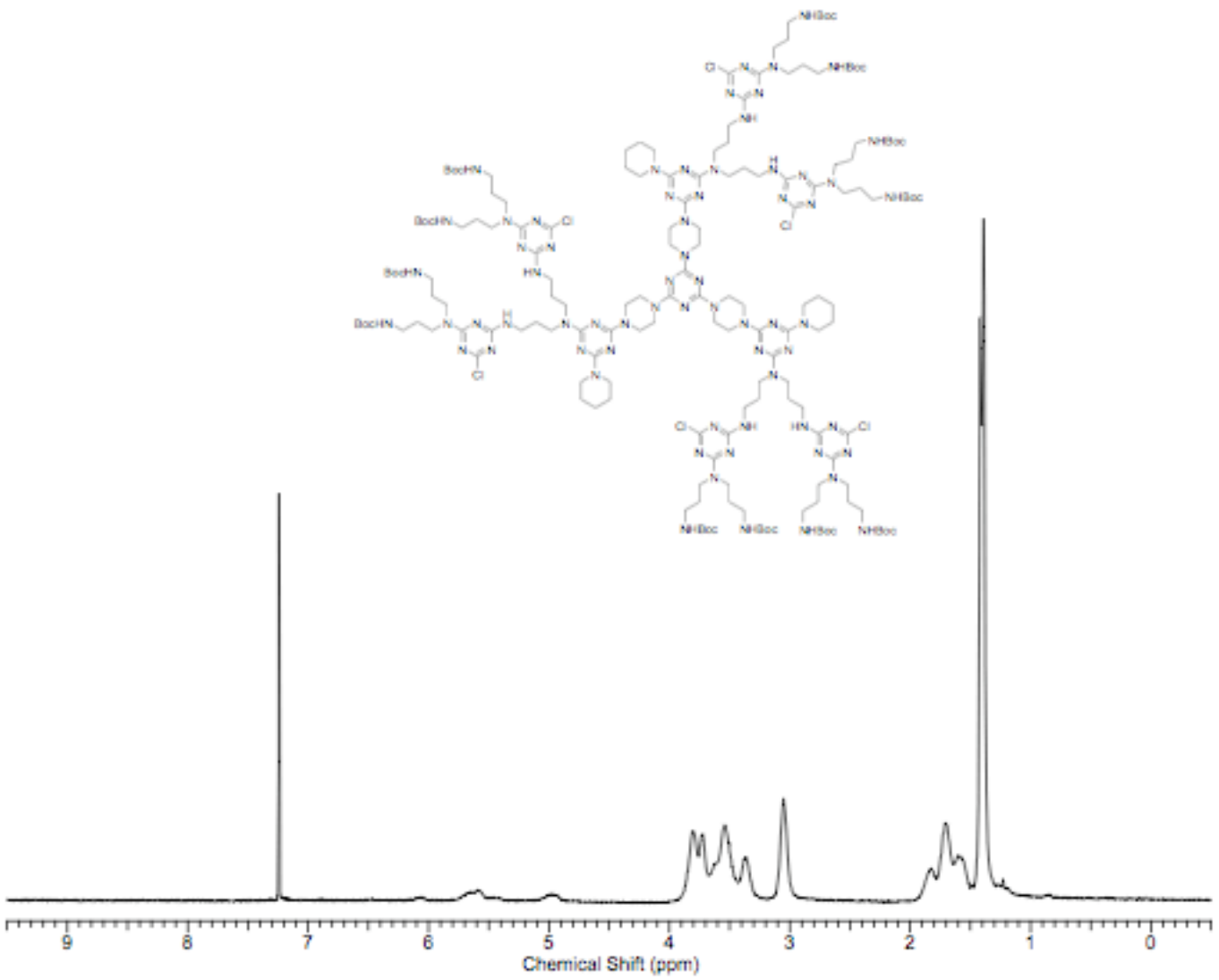
9
8
7
6
5
4
3
2
1
0
Chemical Shift (ppm)

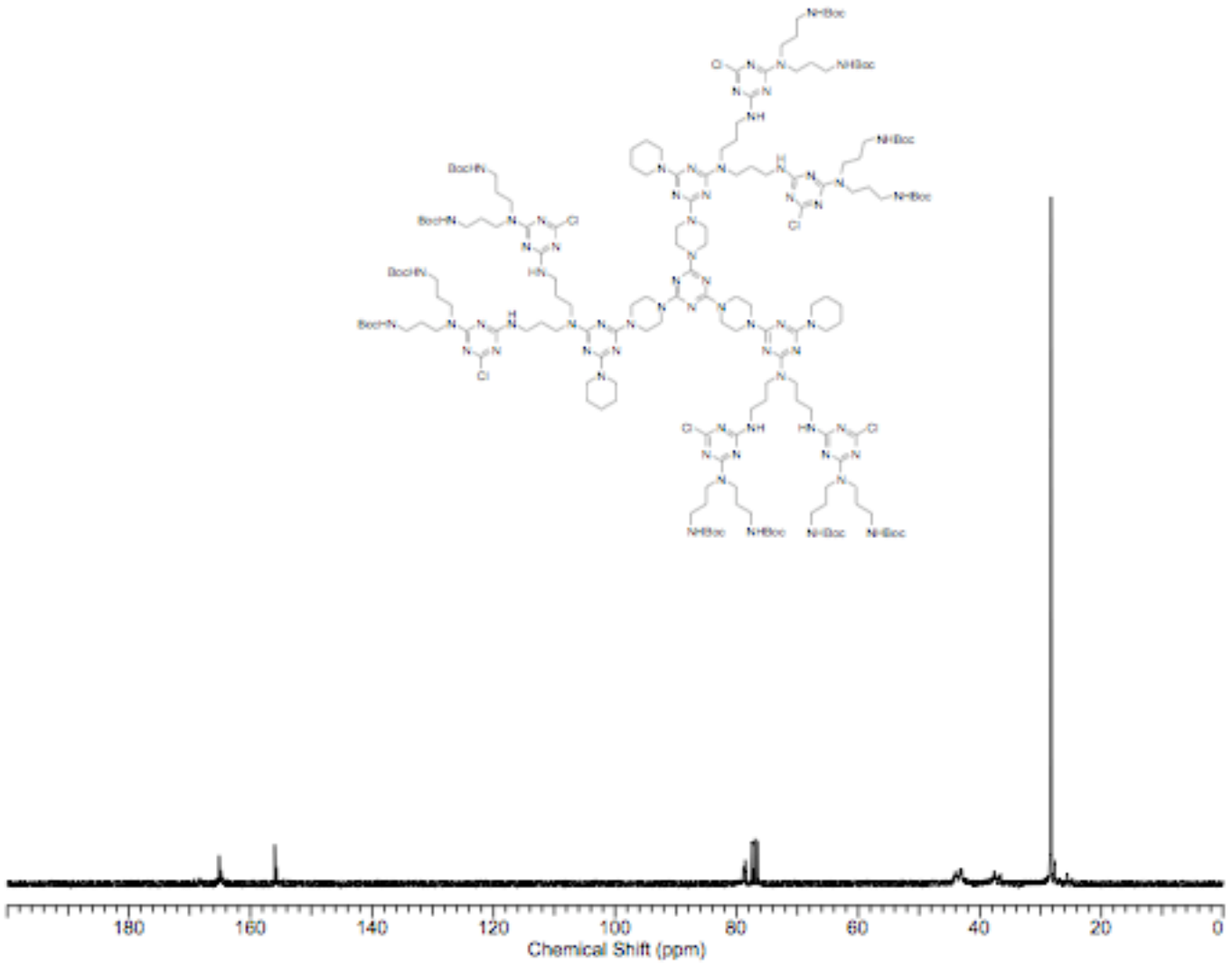
180
160
140
120
100
80
60
40
20
0
Chemical Shift (ppm)

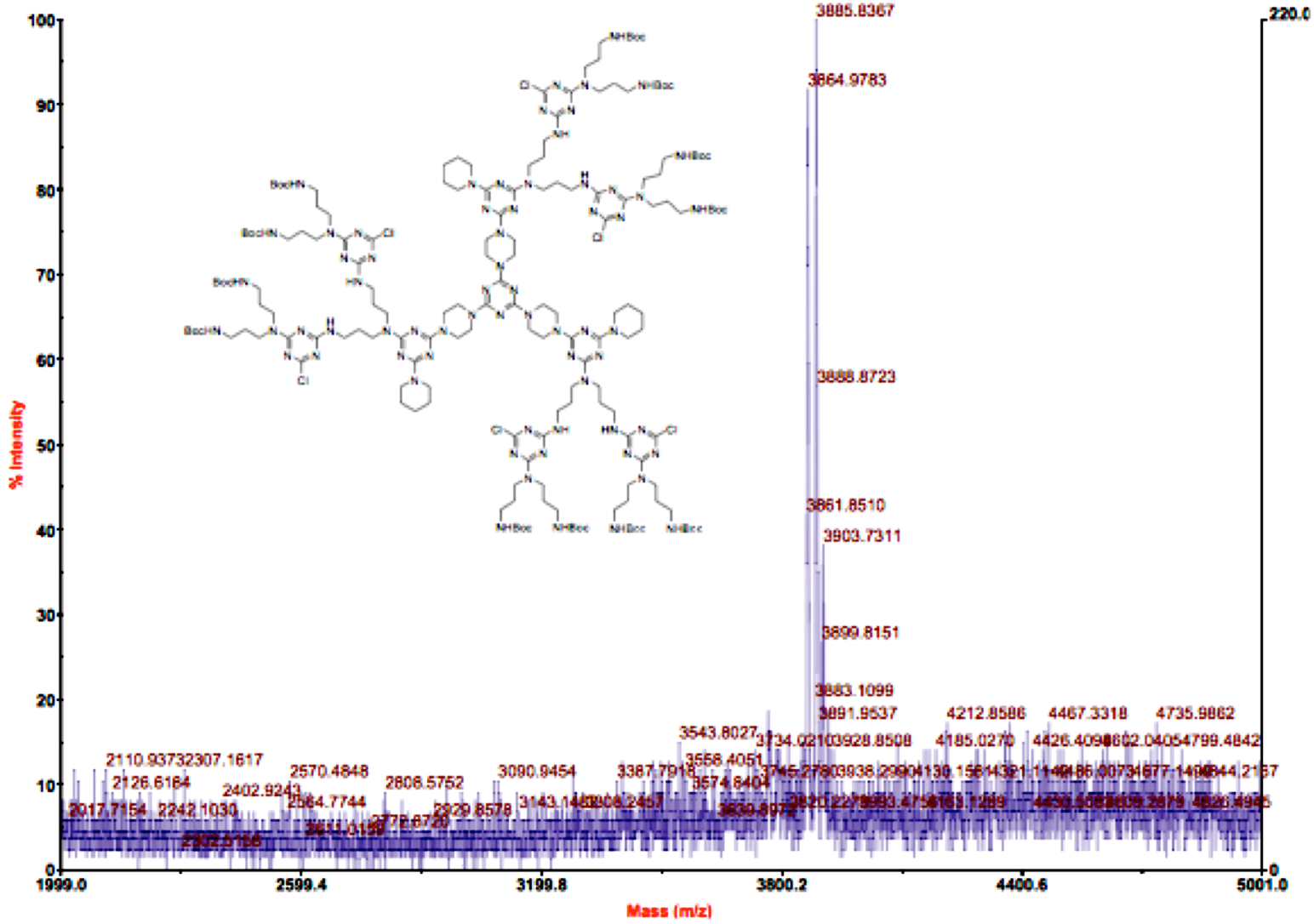
% Intensity
Mass (m/z)
100
90
80
70
60
50
40
30
20
10
0
1999.0
2599.4
3199.8
3800.2
4400.6
5001.0
220.0
3885.8367
3864.9783
3888.8723
3861.8510
3903.7311
3899.8151
3883.1099
3891.9537
4212.8586
4467.3318
4735.9862
3543.8027
4185.0270
2110.93732307.1617
2126.6164
2570.4848
2808.5752
3090.9454
3387.7918
3558.4051
3574.6404
2017.7154
2242.1030
2402.9243
2584.7744
2929.8578
2779.8720
2902.2156

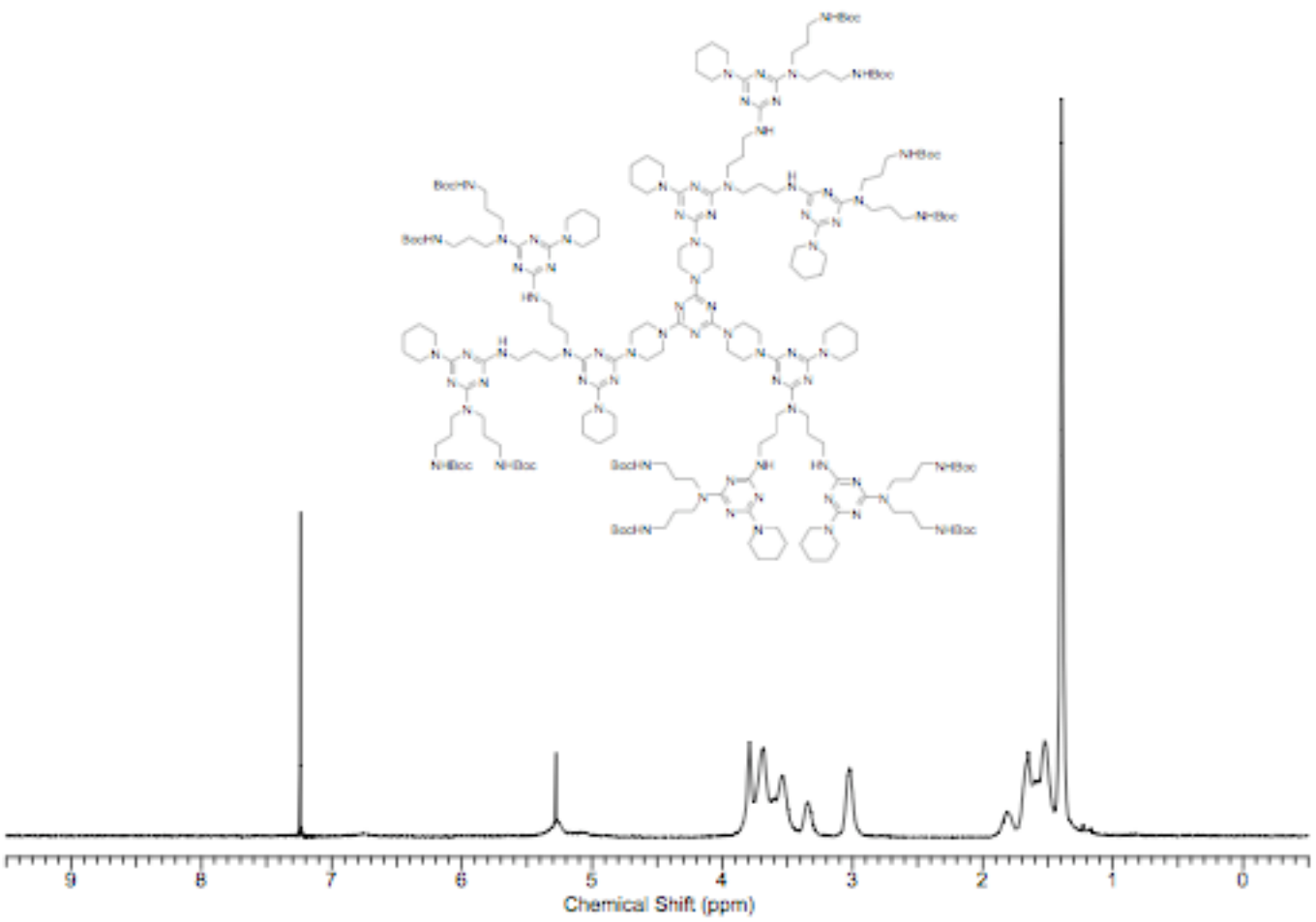
NHBoc
NHBoc
NH
NHBoc
NHBoc
BocHN
BocHN
HN
NHBoc
NHBoc
BocHN
NH
HN
NHBoc
BocHN
NHBoc
9
8
7
6
5
4
3
2
1
0
Chemical Shift (ppm)

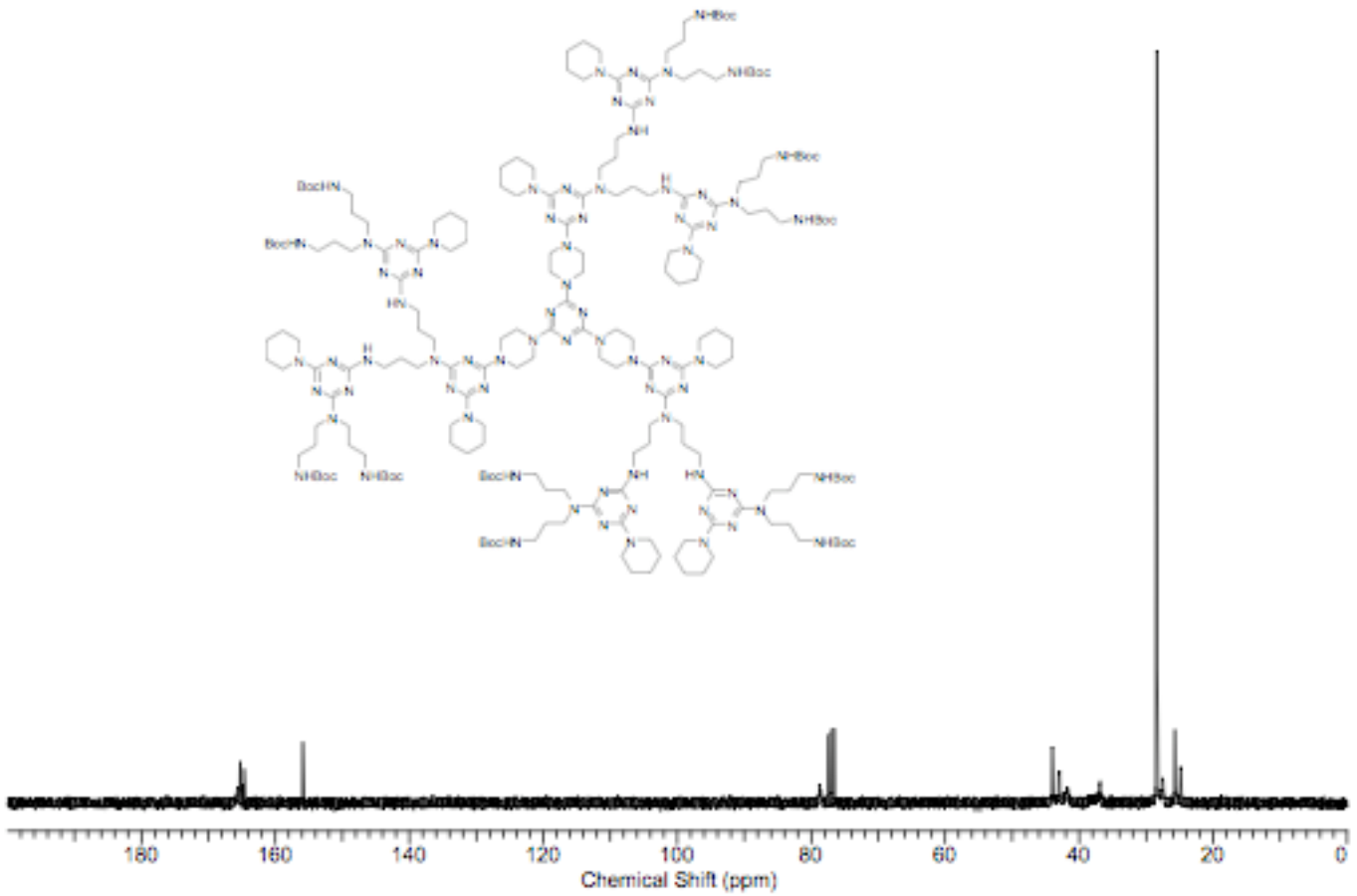
NHBoc
NHBoc
NH
NHBoc
NHBoc
BocHN
BocHN
HN
NHBoc
NHBoc
BocHN
NH
HN
NHBoc
BocHN
NHBoc
180
160
140
120
100
80
60
40
20
0
Chemical Shift (ppm)

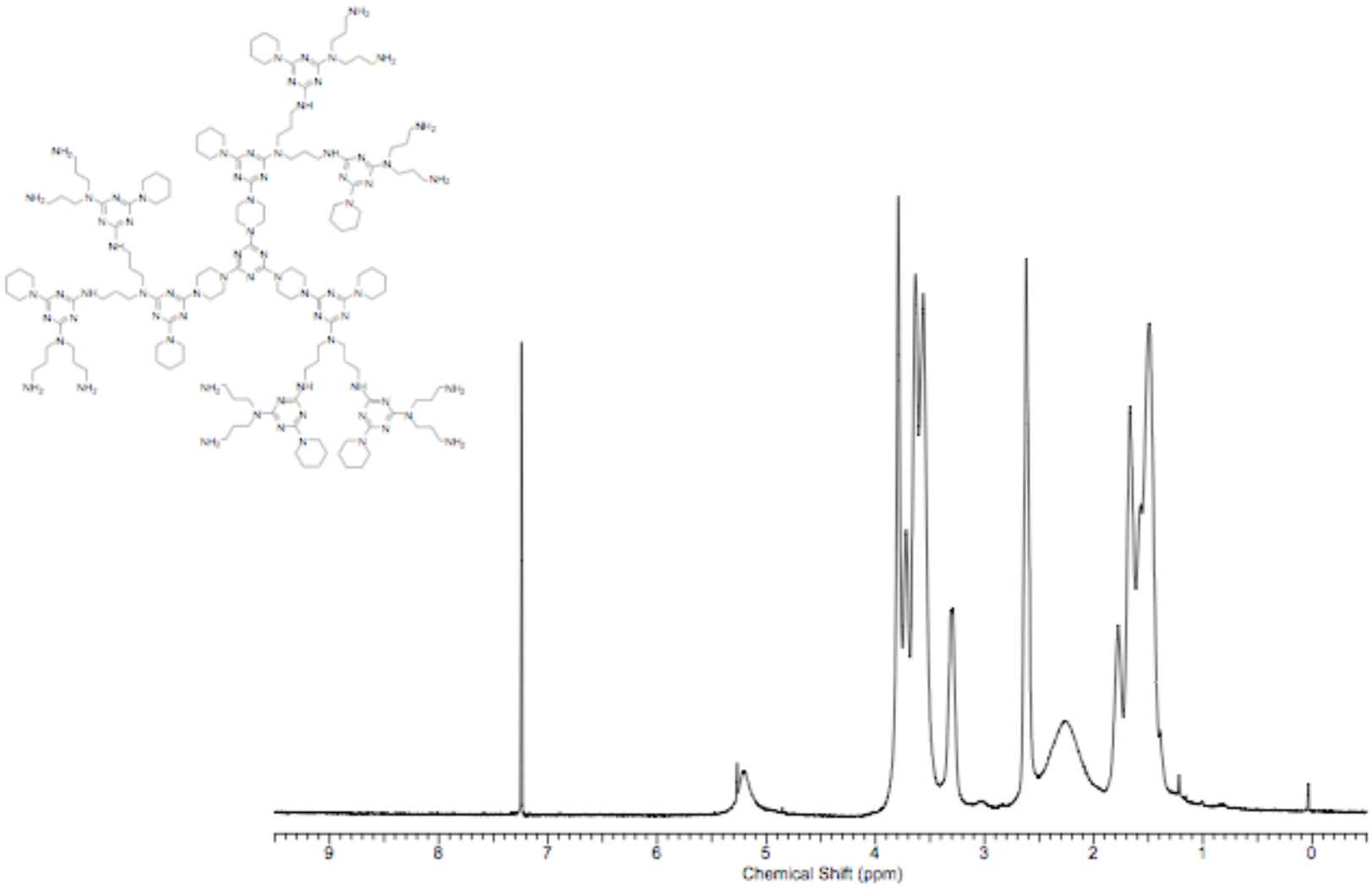
9
8
7
6
5
4
3
2
1
0
Chemical Shift (ppm)

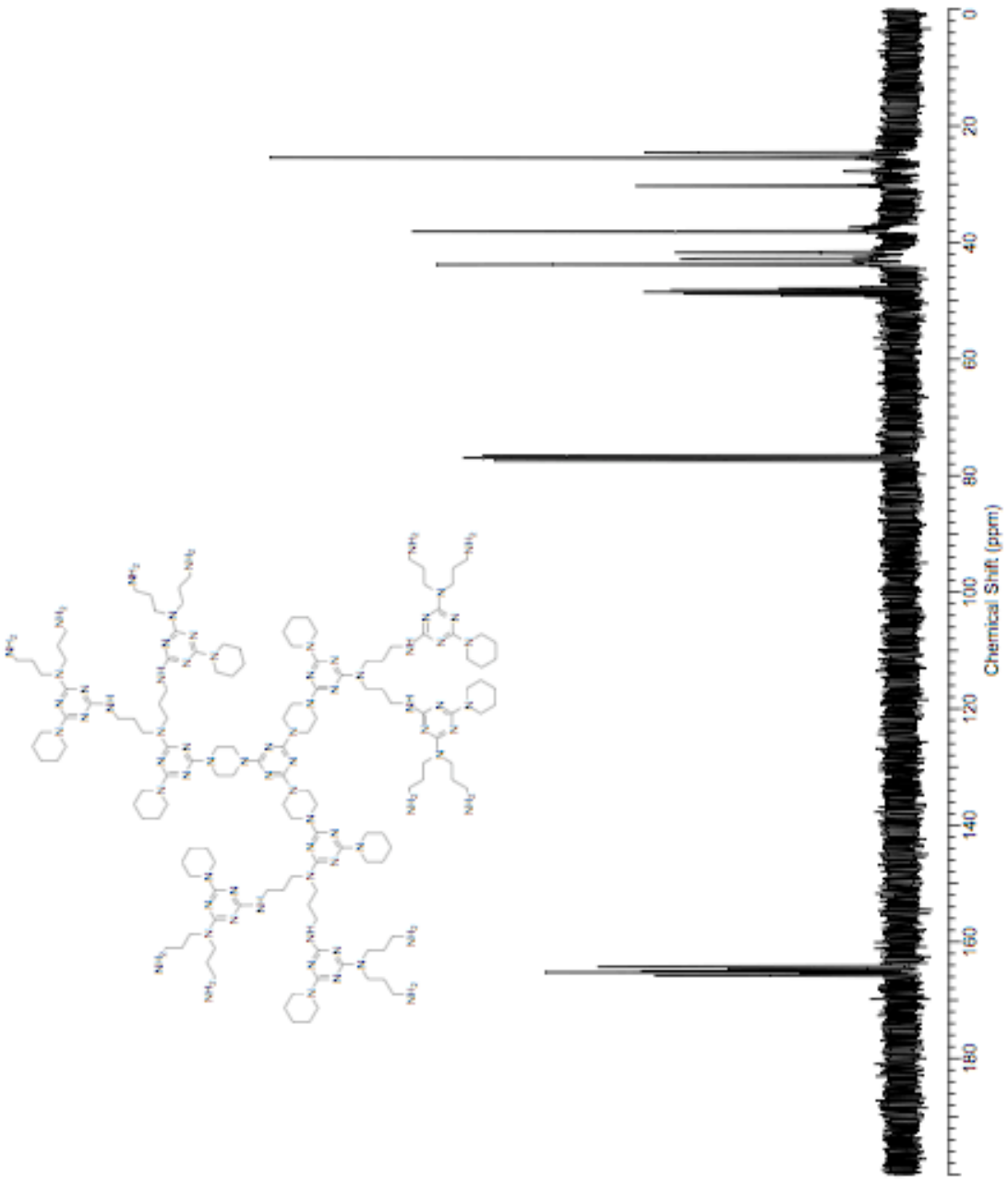
0
20
40
60
80
100
120
140
160
180
Chemical Shift (ppm)

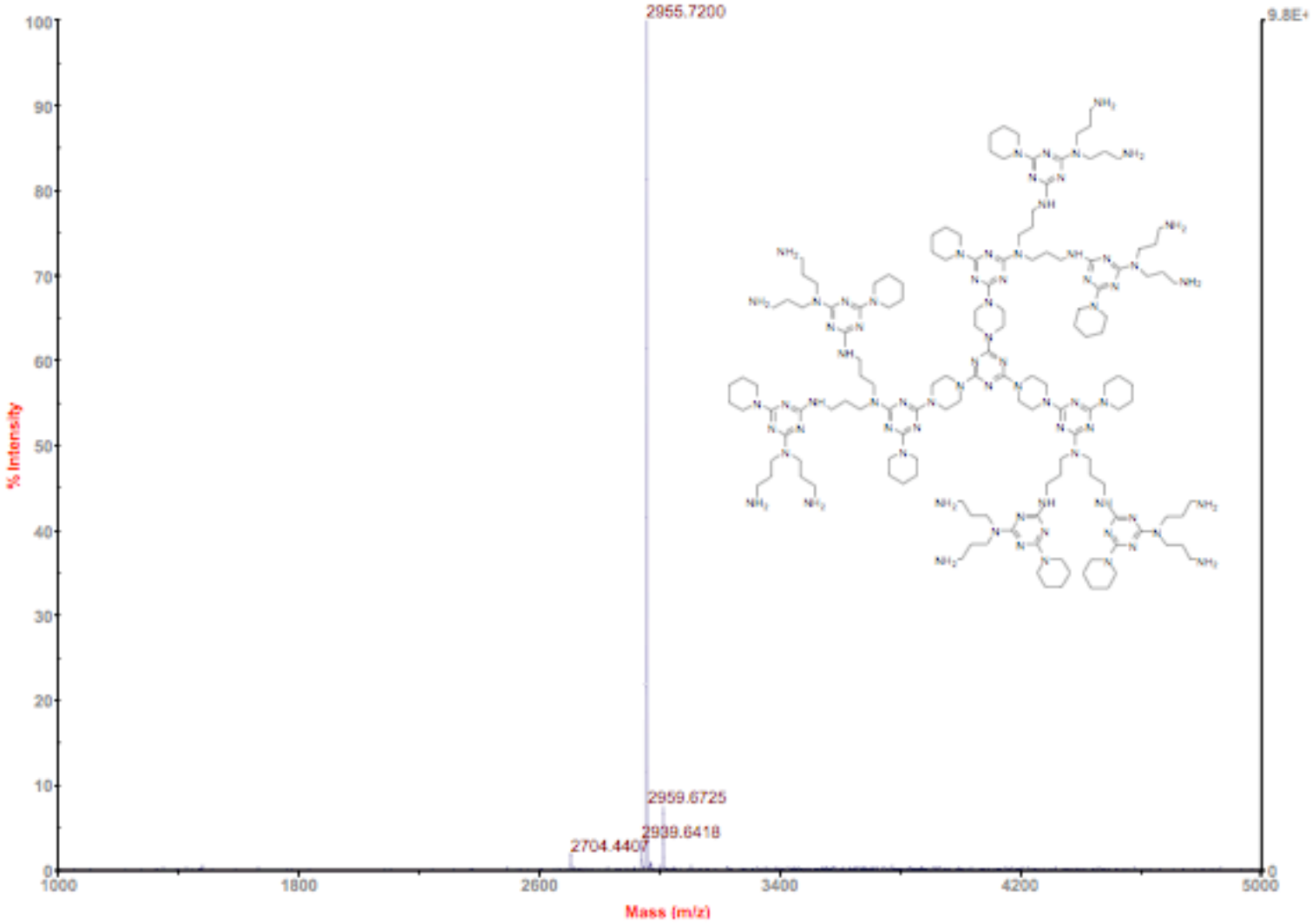
2955.7200
9.8E+
100
90
80
70
60
50
40
30
20
10
0
% Intensity
2959.6725
2939.6418
2704.4407
1000
1800
2600
3400
4200
5000
Mass (m/z)

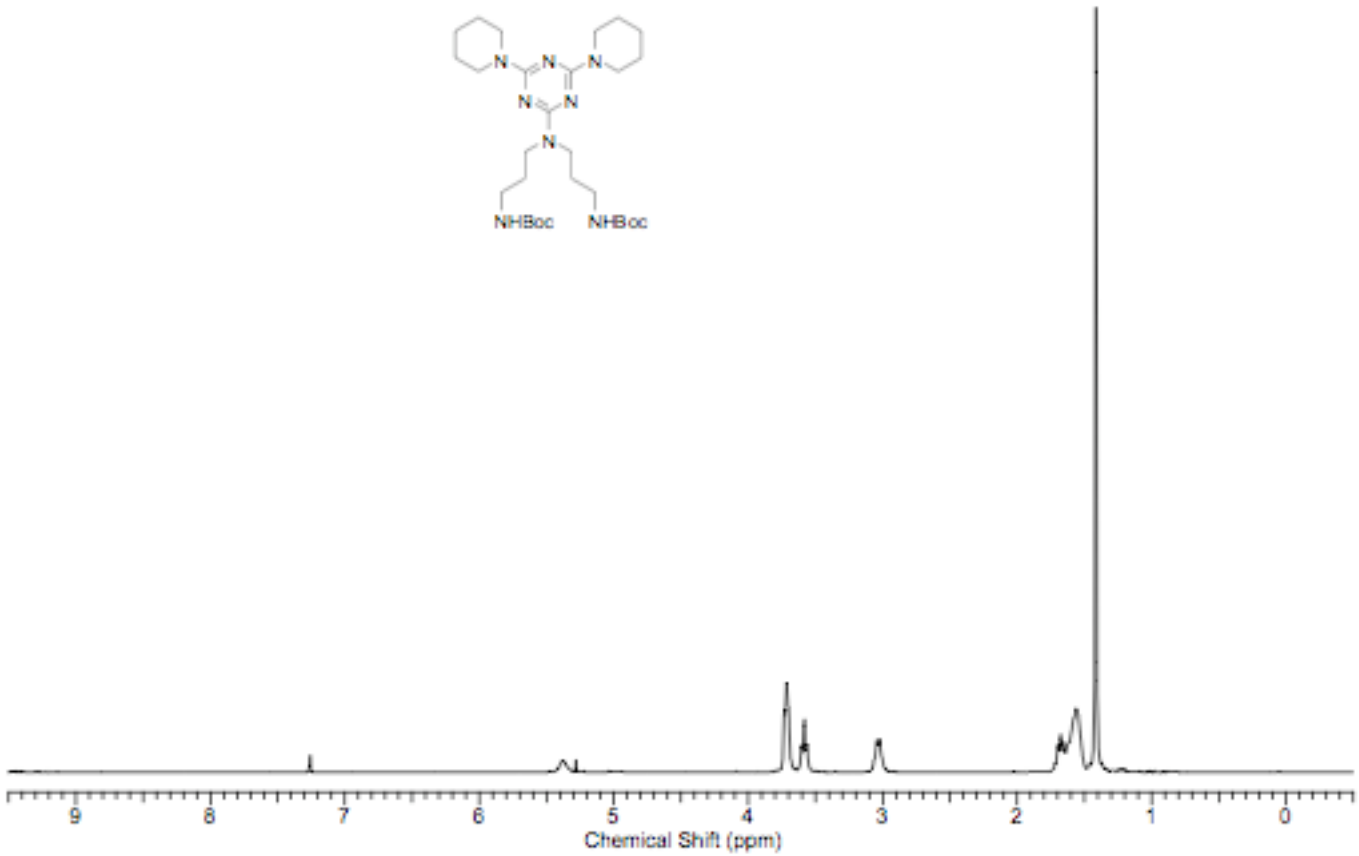
NHBoc
NHBoc
9
8
7
6
5
4
3
2
1
0
Chemical Shift (ppm)

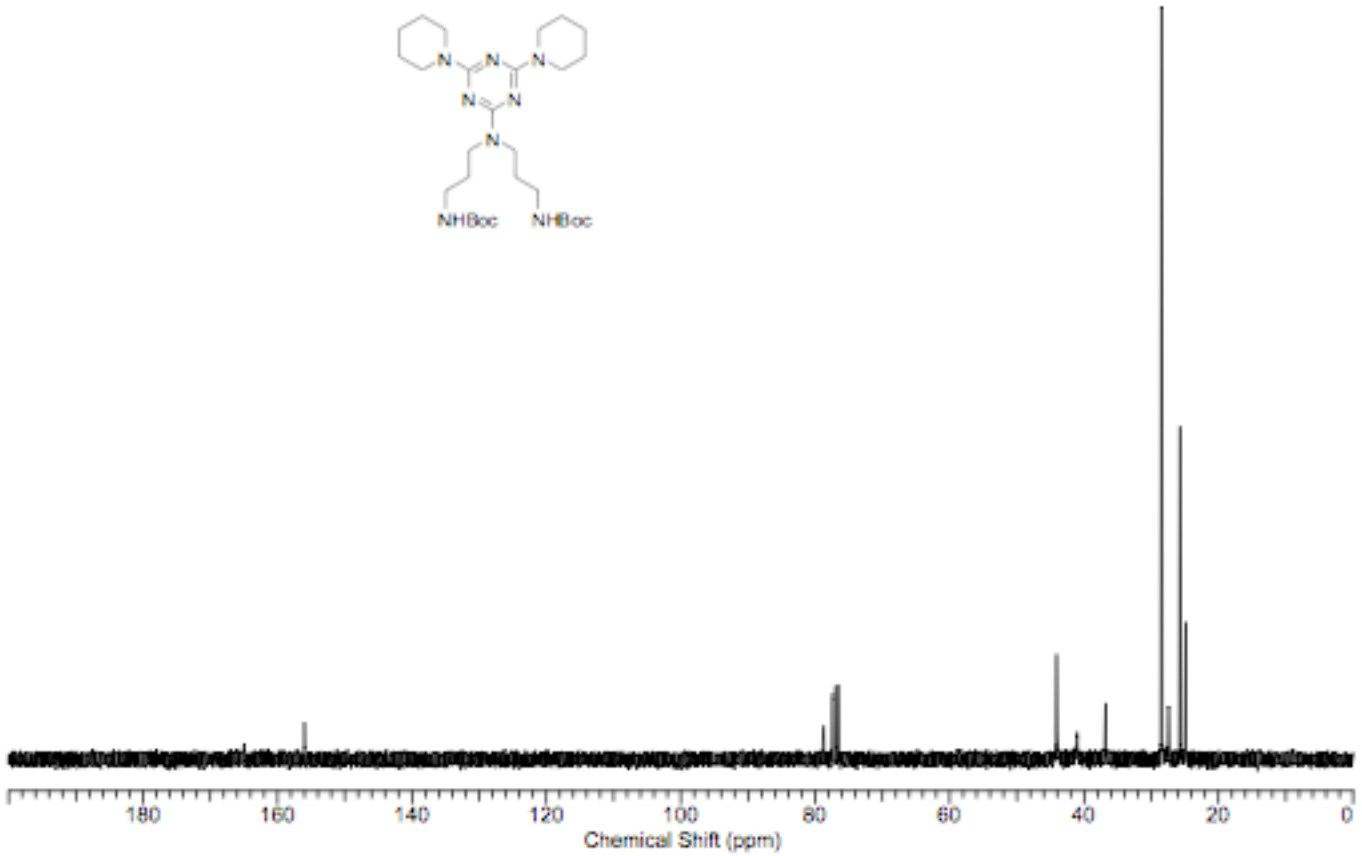
N
N
N
N
N
N
N
NHBoc
NHBoc
180
160
140
120
100
80
60
40
20
0
Chemical Shift (ppm)

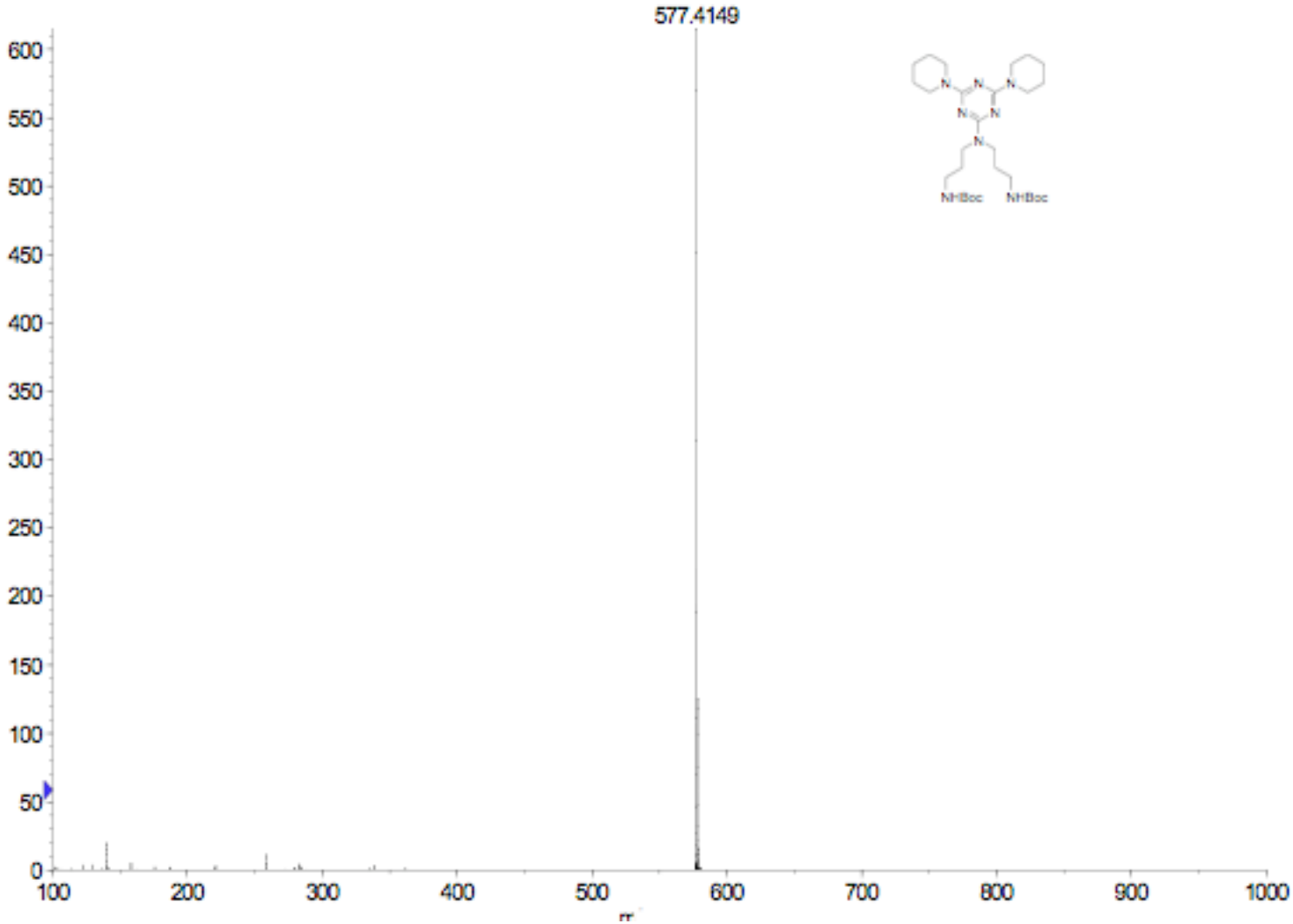
577.4149
600
550
500
450
400
350
300
250
200
150
100
50
0
100
200
300
400
500
600
700
800
900
1000
m/z
NHBoc
NHBoc

APPENDIX B

SPECTRA FOR CHAPTER III

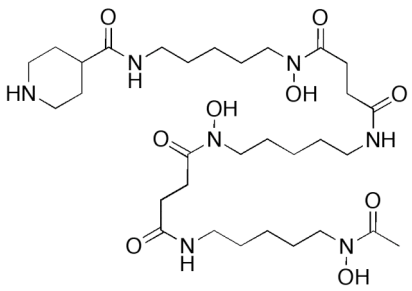
O
N
H
HN
O
N
OH
O
OH
O
N
NH
O
O
N
H
O
N
OH

9
8
7
6
5
4
3
2
1
Chemical Shift (ppm)

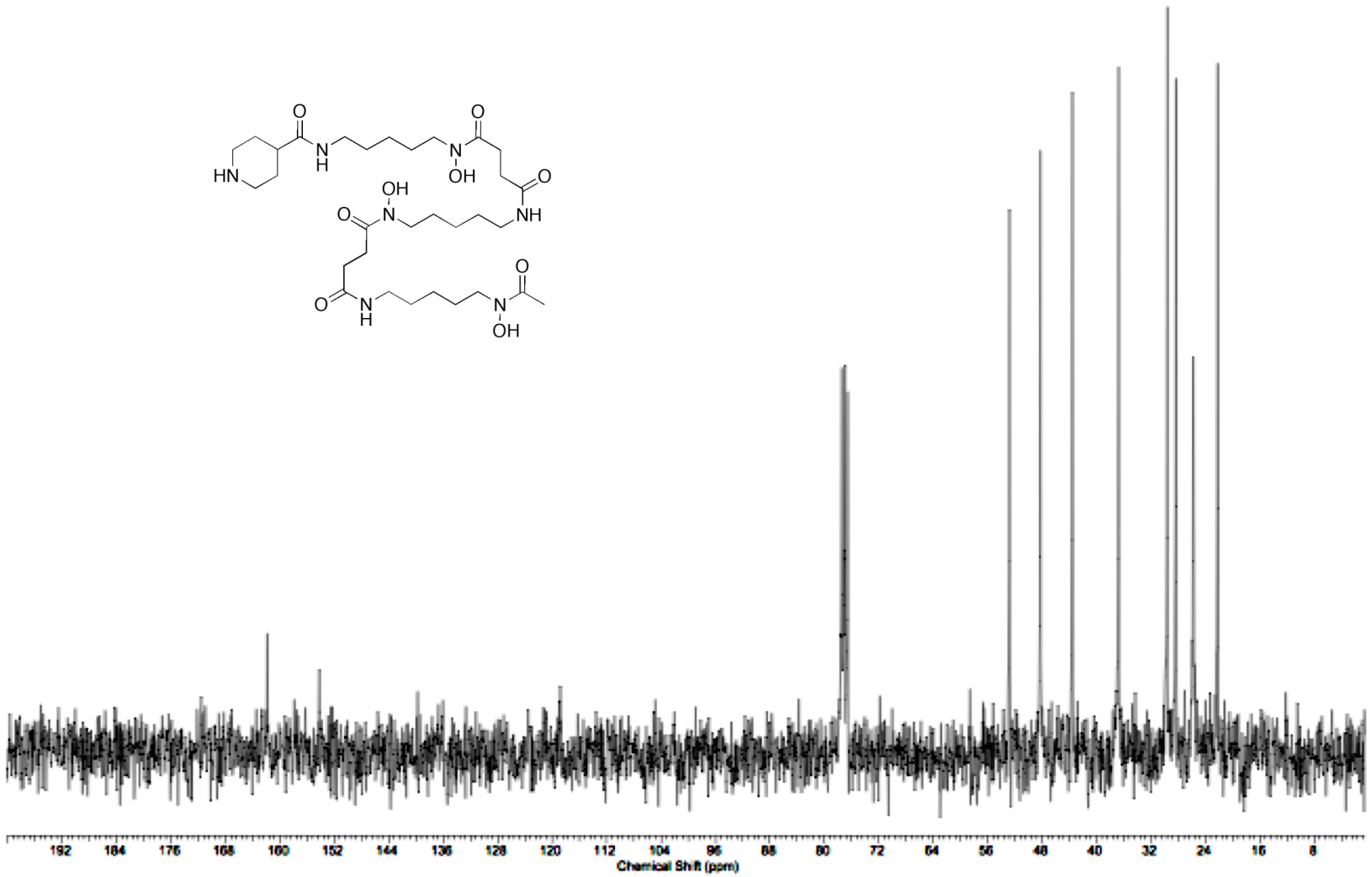
HN
O
N
H
O
N
OH
O
OH
N
O
NH
O
N
H
O
N
OH
192
184
176
168
160
152
144
136
128
120
112
104
96
88
80
72
64
56
48
40
32
24
16
8
Chemical Shift (ppm)

APPENDIX C

SPECTRA FOR CHAPTER IV

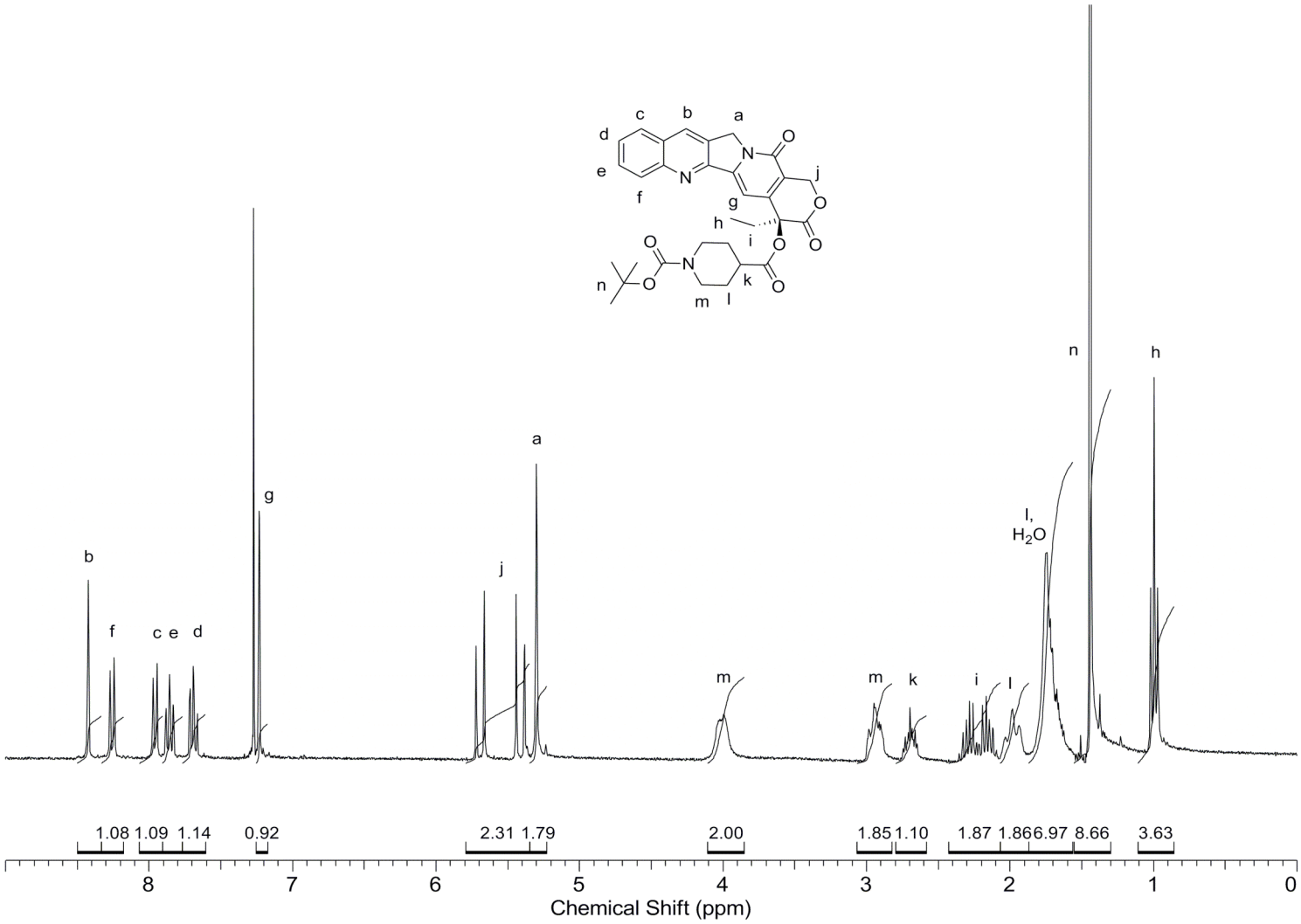
c b a
d
e
f
g
h
i
j
k
l
m
n
O
N
O
O
O
O
O
O
N
O
O
b
f
c e d
g
j
a
m
m
k
i
l
l,
H2O
n
h
1.08 1.09 1.14
0.92
2.31 1.79
2.00
1.85 1.10
1.87 1.86 6.97 8.66
3.63
8
7
6
5
4
3
2
1
0
Chemical Shift (ppm)

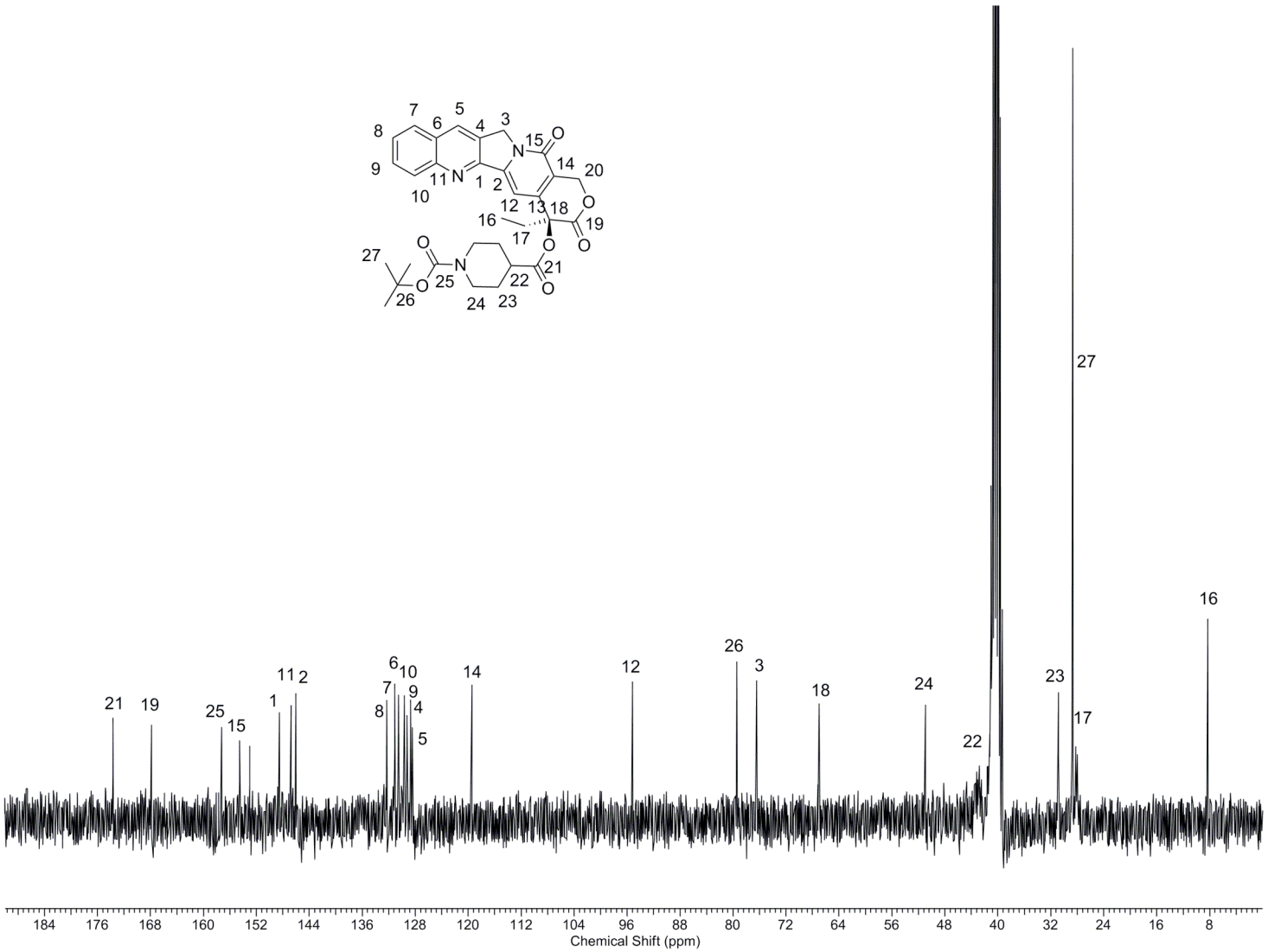
Chemical Shift (ppm)

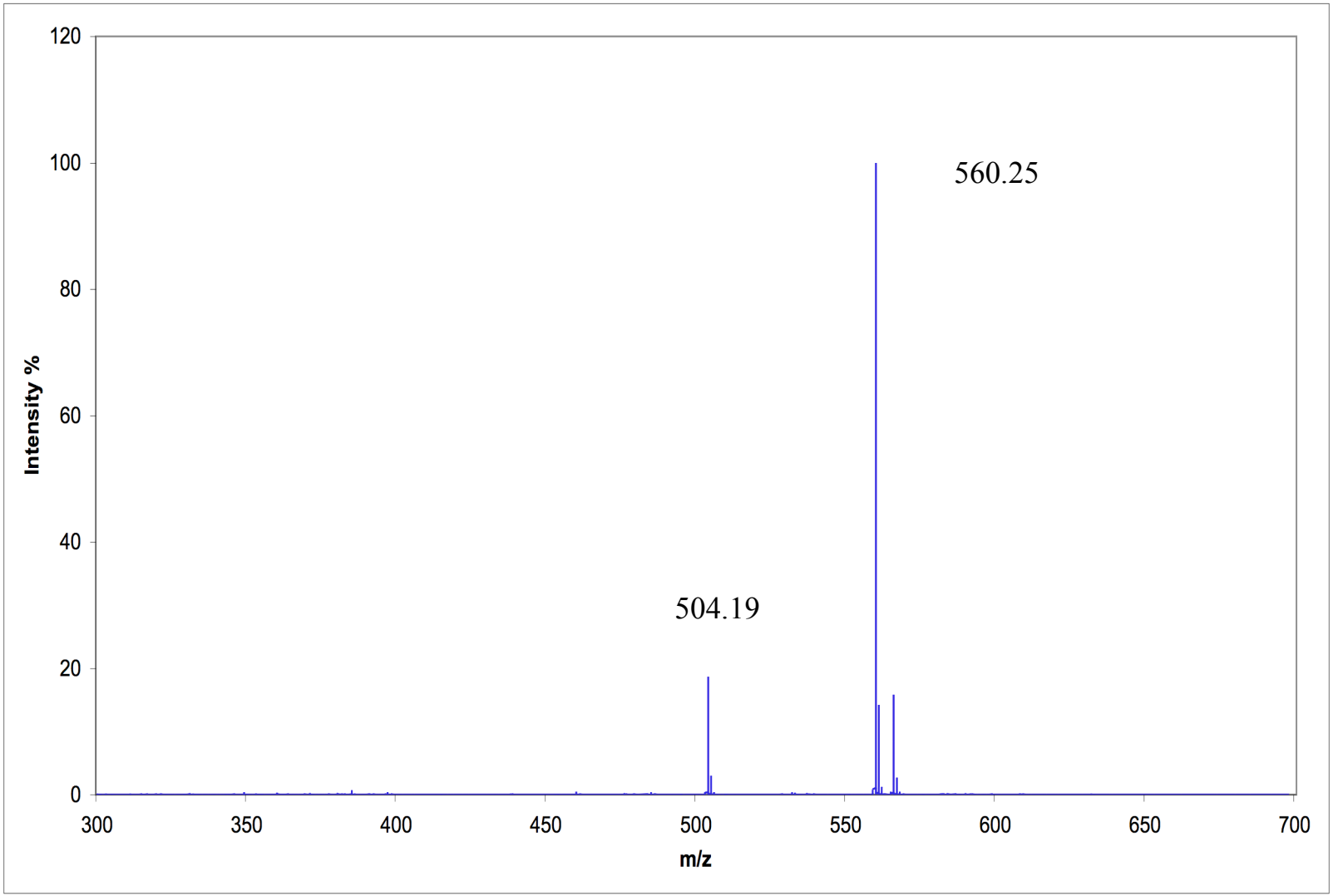
120
100
80
60
40
20
0
Intensity %
560.25
504.19
300
350
400
450
500
550
600
650
700
m/z

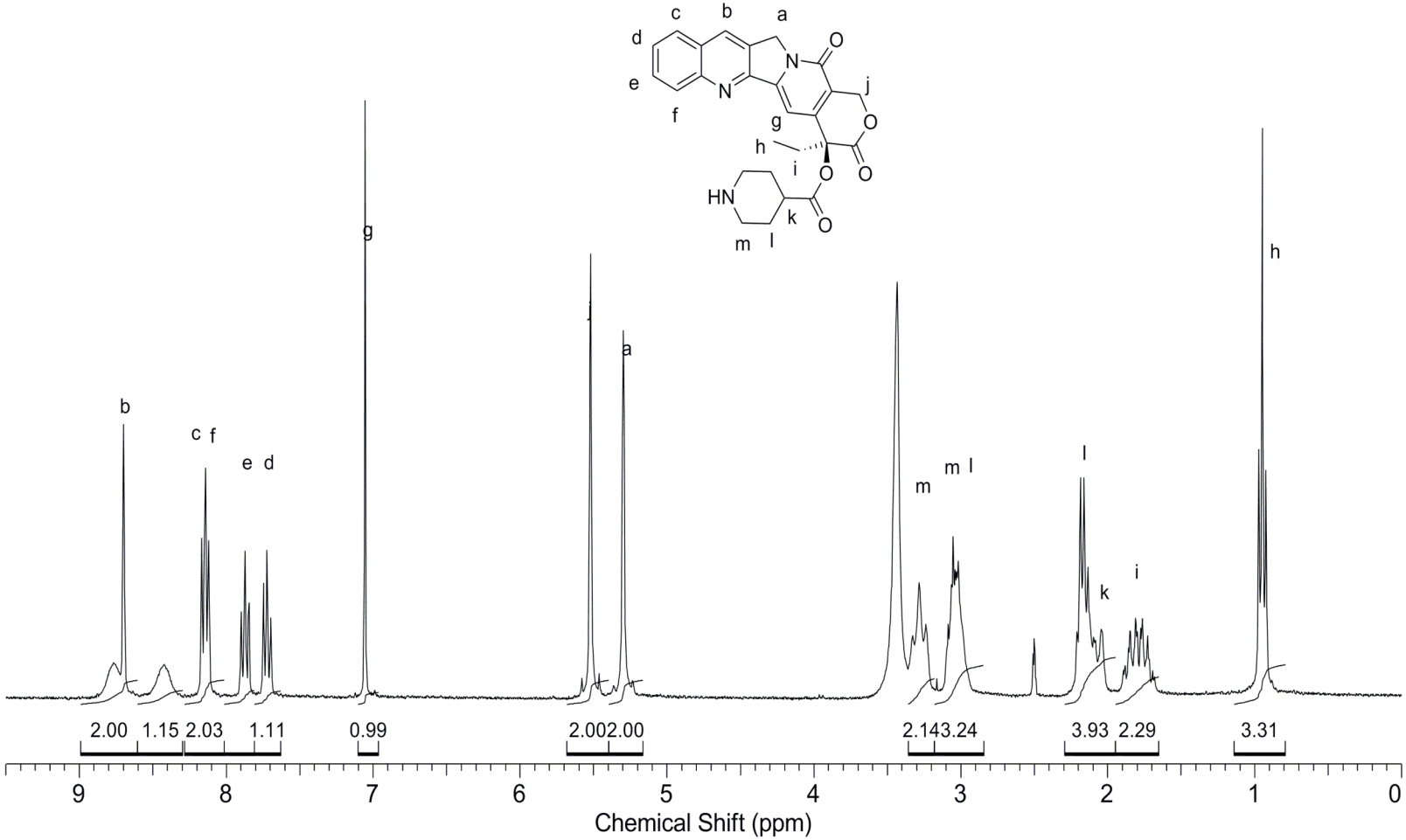
c b a
d
e
f
g
h
i
j
k
l
m
N
O
HN
b
c f
e d
g
a
m
m l
l
k
i
h
2.00 1.15 2.03 1.11
0.99
2.002.00
2.143.24
3.93 2.29
3.31
9 8 7 6 5 4 3 2 1 0
Chemical Shift (ppm)

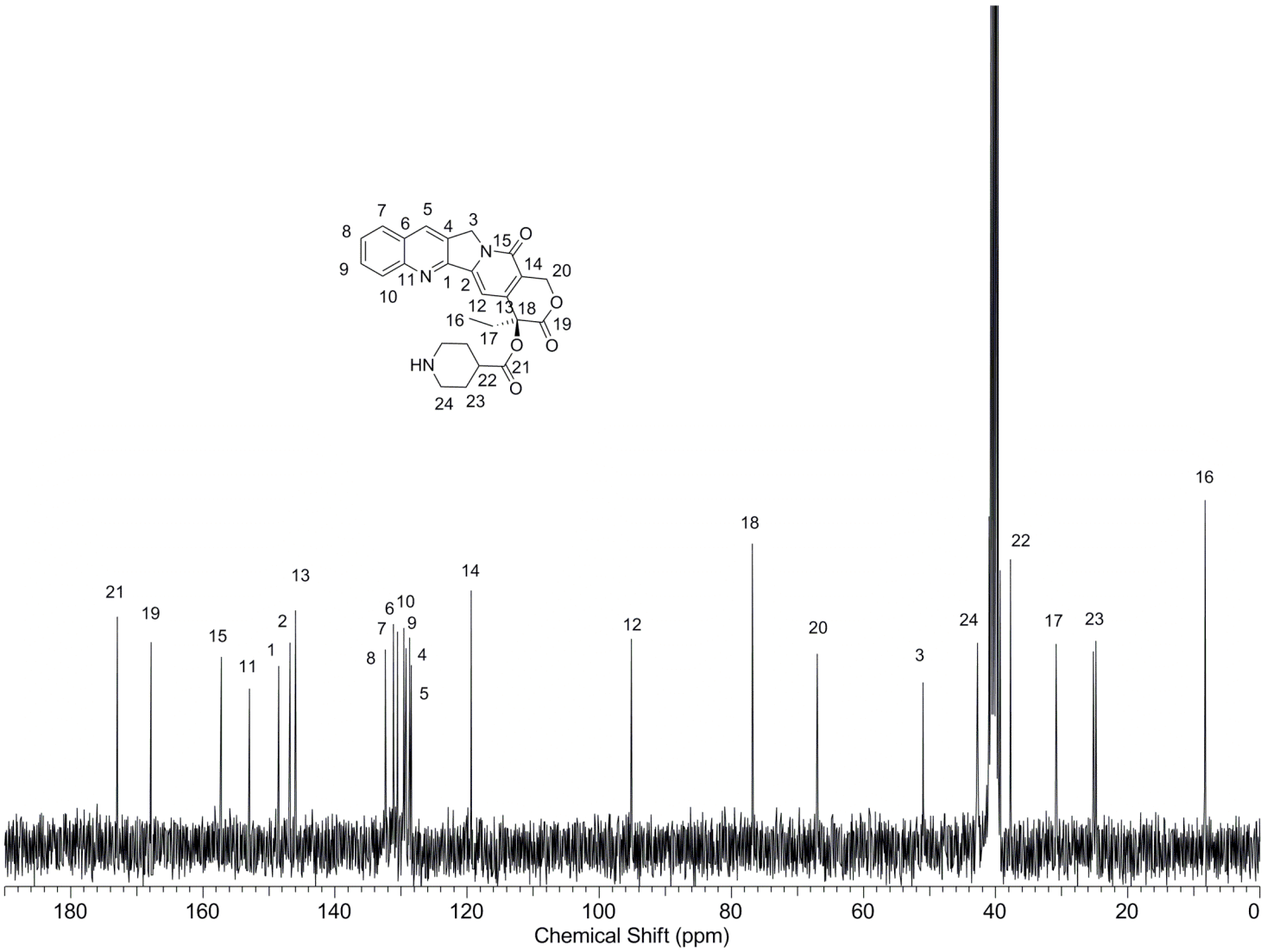
Chemical Shift (ppm)
180
160
140
120
100
80
60
40
20
0

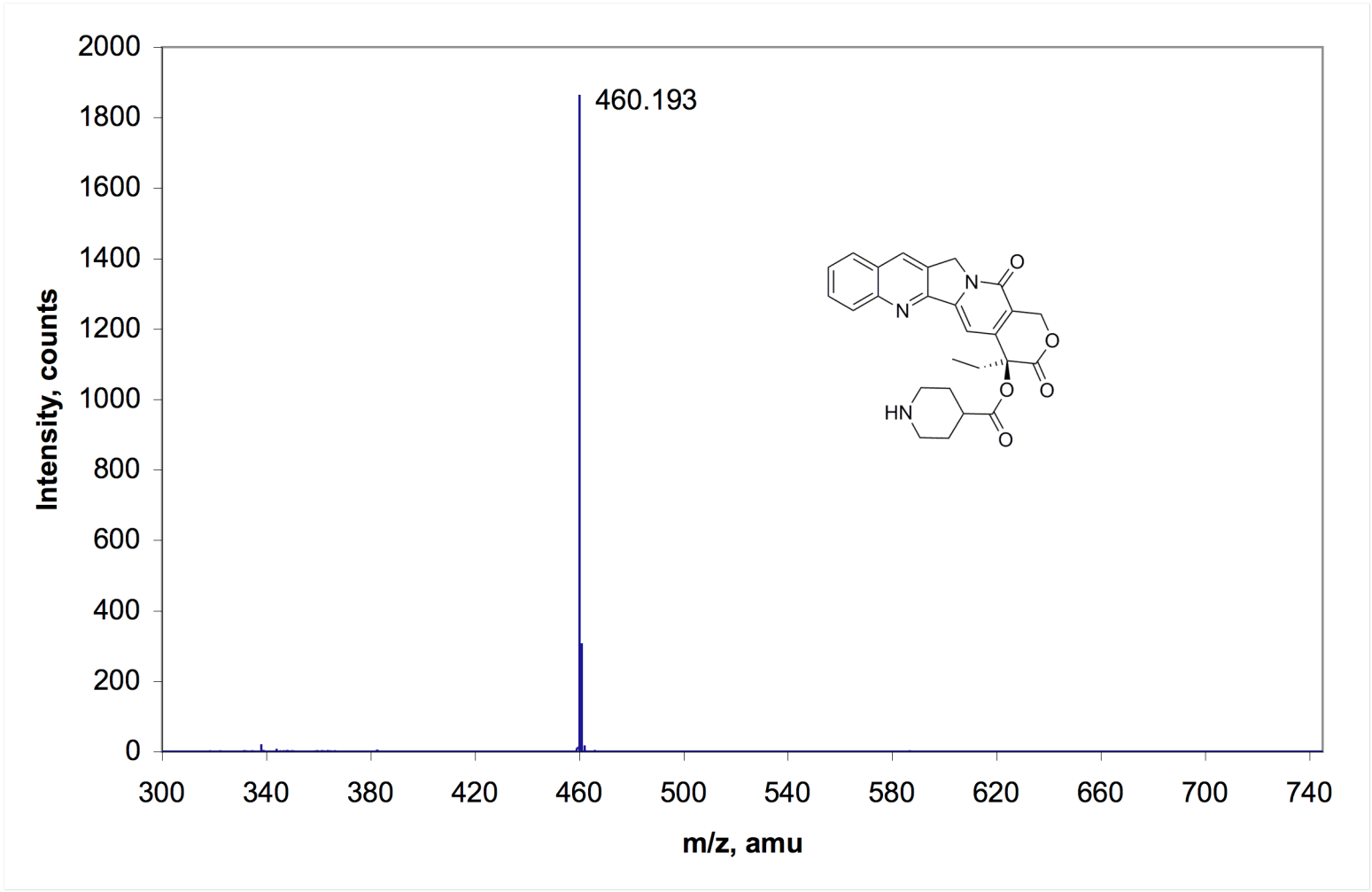
2000
1800
1600
1400
1200
1000
800
600
400
200
0
Intensity, counts
460.193
300
340
380
420
460
500
540
580
620
660
700
740
m/z, amu
N
N
O
O
O
O
HN
O

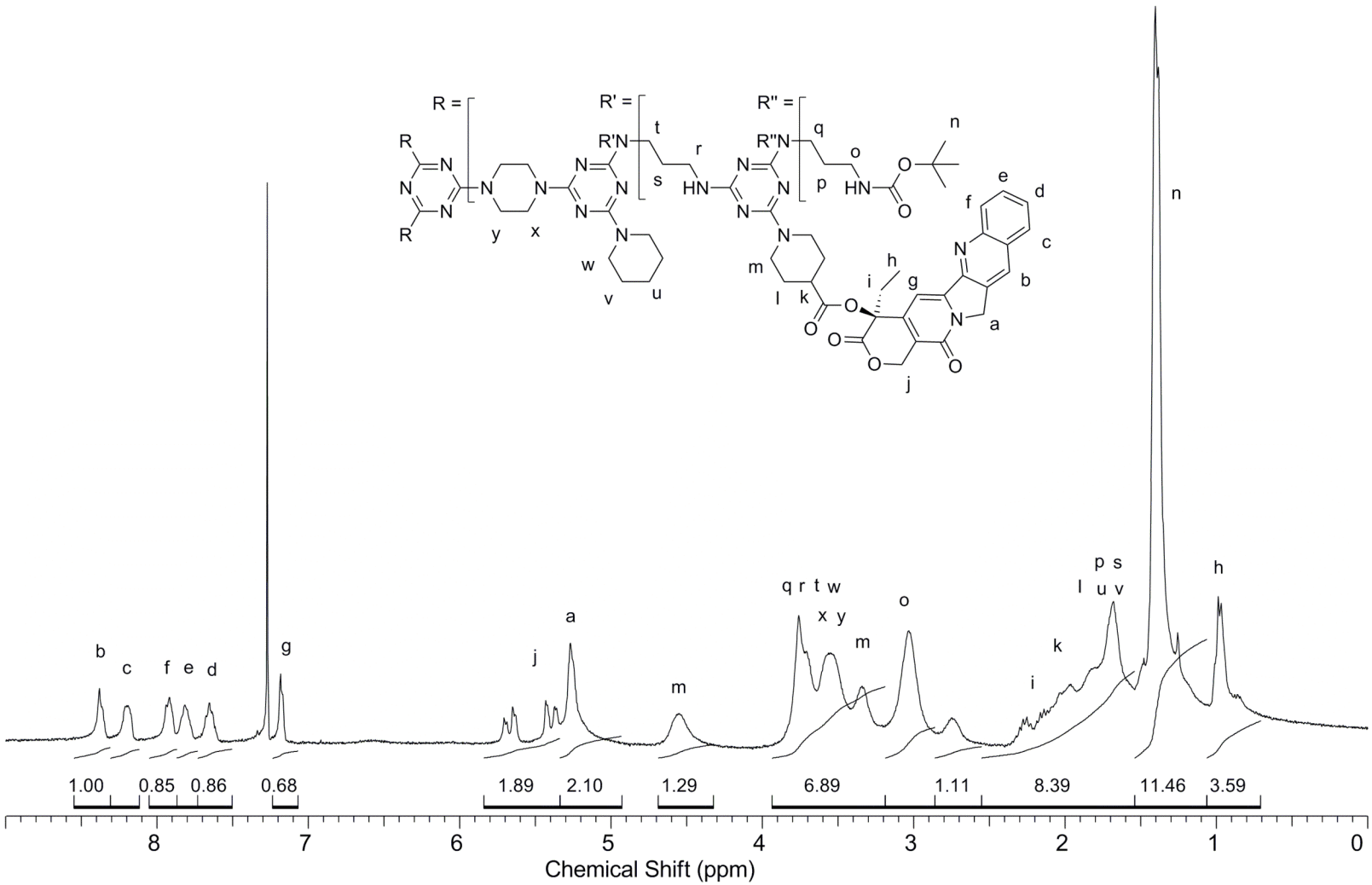
R =
R' =
R'' =
b
c
f e d
g
j
a
m
q r t w
x y
m
o
i
k
l u v
p s
n
h
1.00
0.85
0.86
0.68
1.89
2.10
1.29
6.89
1.11
8.39
11.46
3.59
8
7
6
5
4
3
2
1
0
Chemical Shift (ppm)

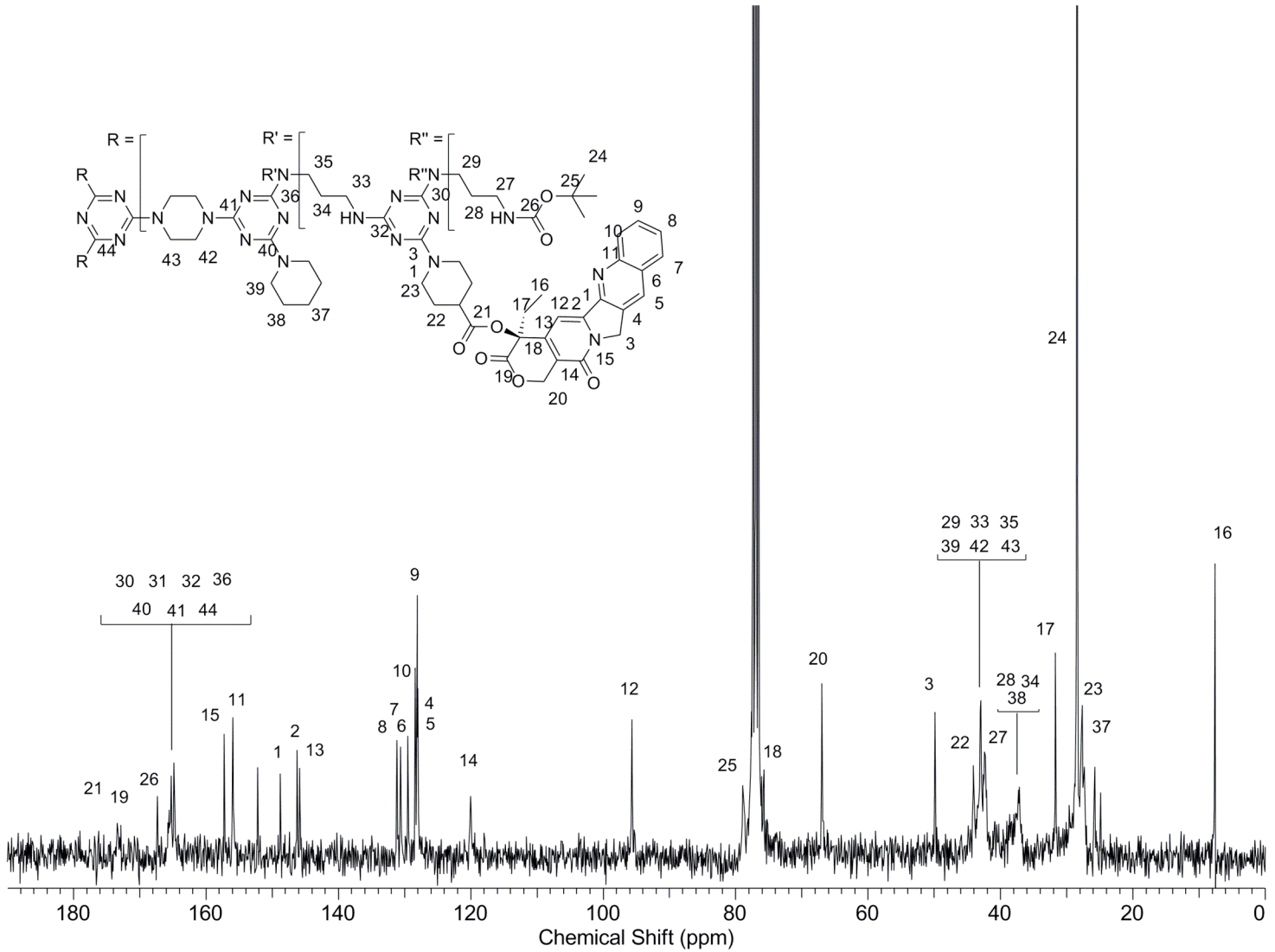
R =
R' =
R'' =
Chemical Shift (ppm)
180
160
140
120
100
80
60
40
20
0

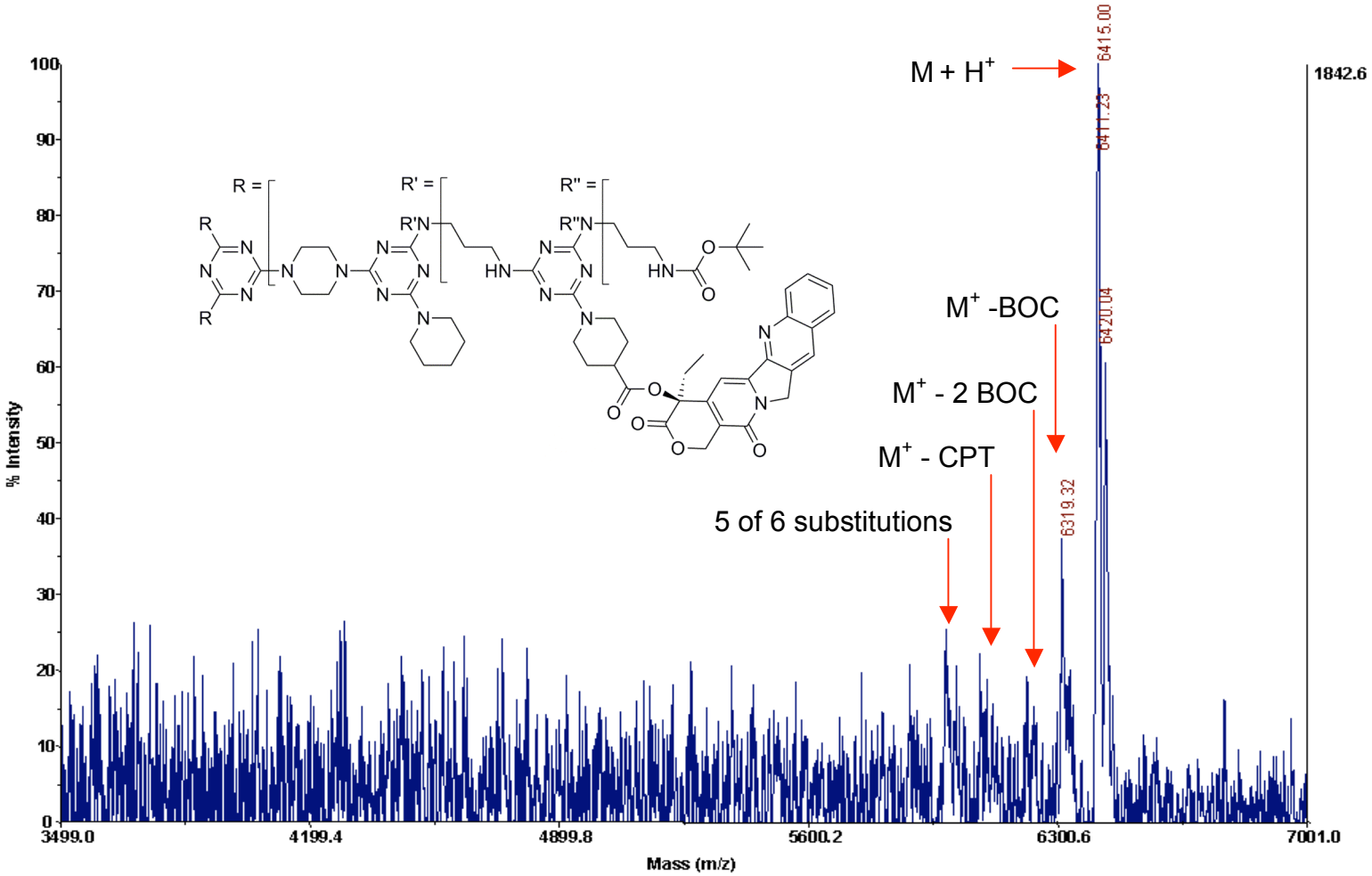
M + H+
M+ -BOC
M+ - 2 BOC
M+ - CPT
5 of 6 substitutions
6415.00
6411.23
6420.04
6319.32
1842.6
% Intensity
Mass (m/z)
3499.0
4199.4
4899.8
5600.2
6300.6
7001.0
R =
R' =
R" =

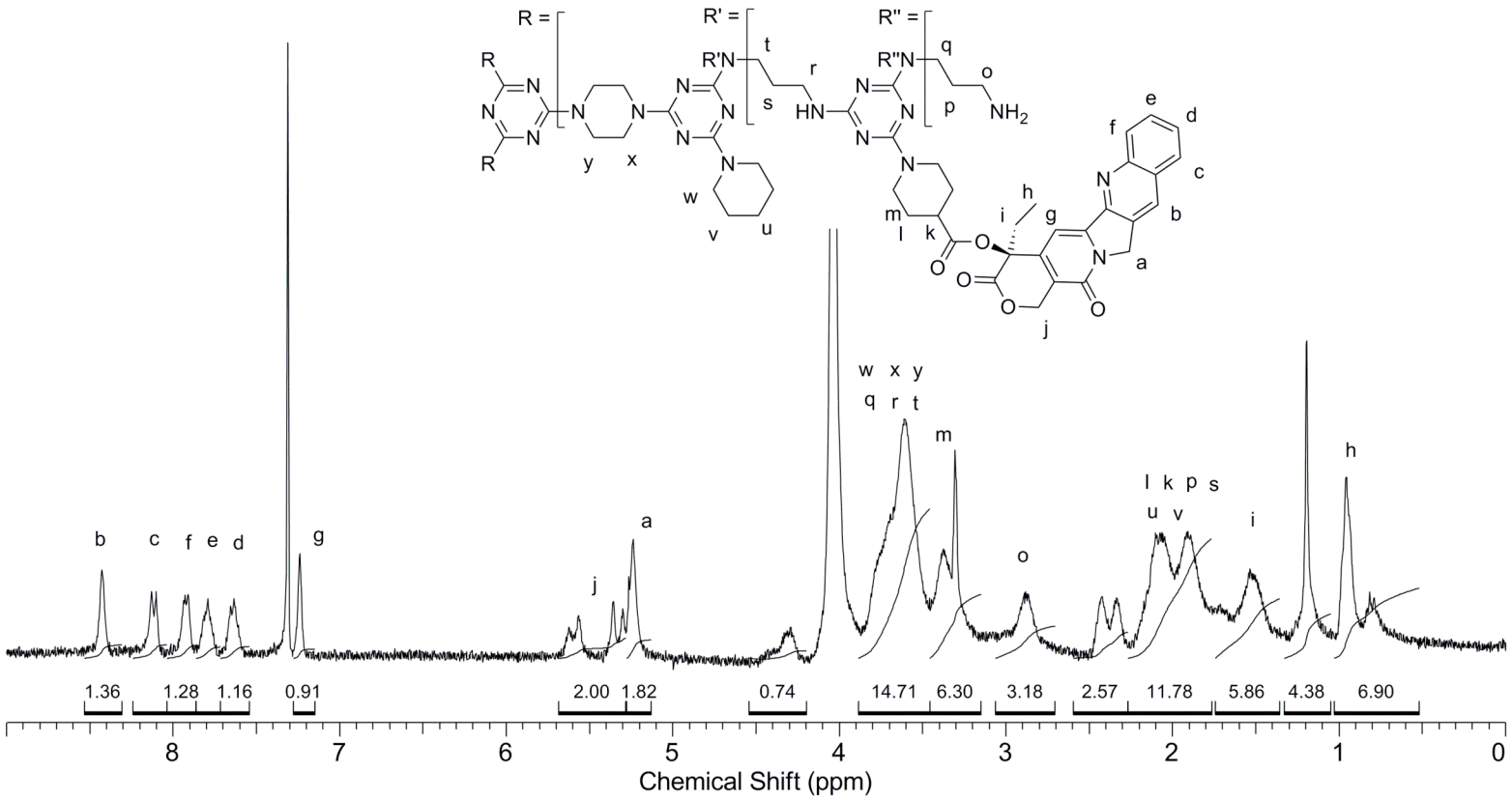
R =
R' =
R'' =
NH2
HN
b c f e d
g
a
j
w x y
q r t
m
o
l k p s
u v
i
h
1.36
1.28
1.16
0.91
2.00
1.82
0.74
14.71
6.30
3.18
2.57
11.78
5.86
4.38
6.90
8
7
6
5
4
3
2
1
0
Chemical Shift (ppm)

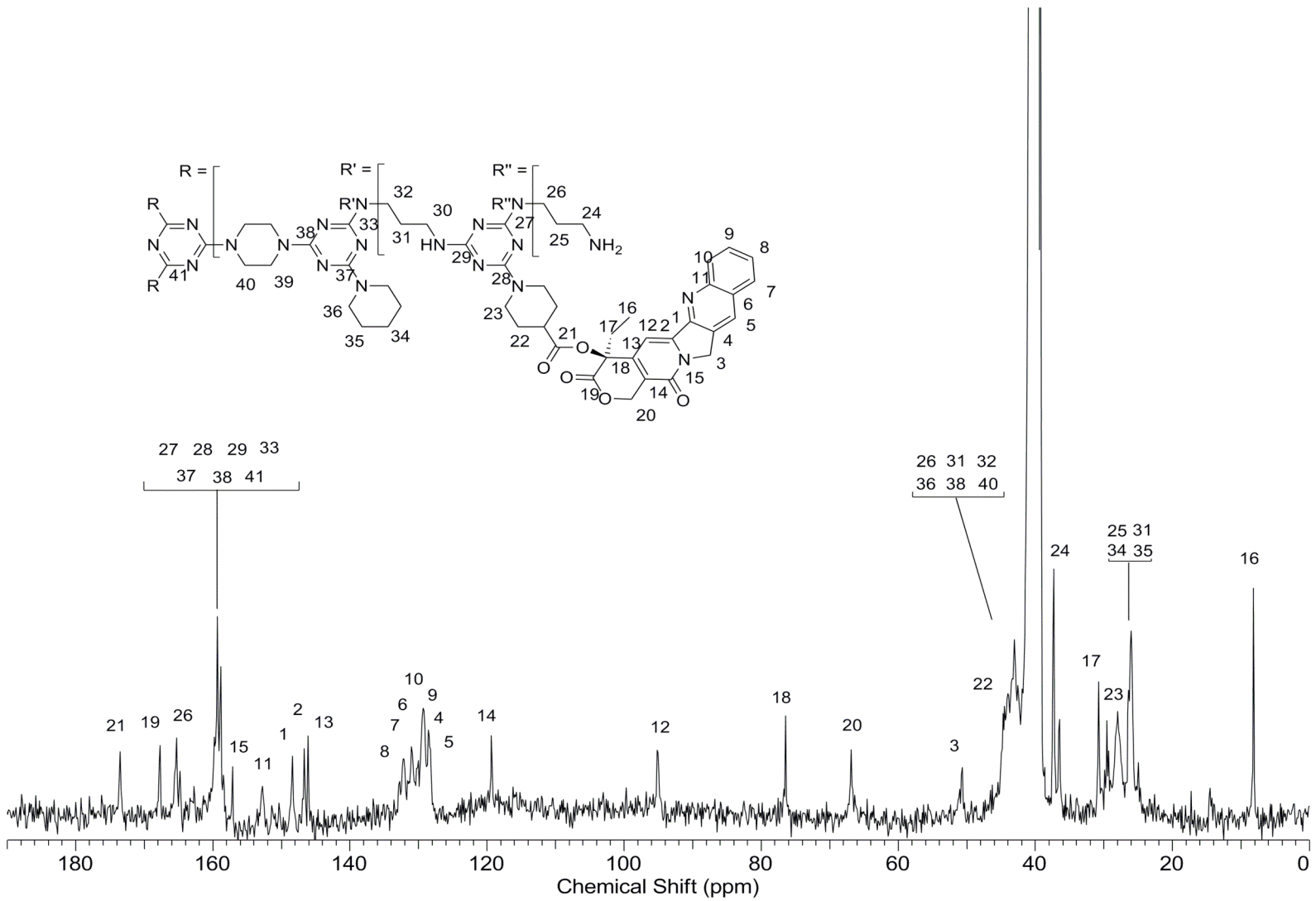
R =
R' =
R'' =
NH2
HN
27 28 29 33
37 38 41
26 31 32
36 38 40
25 31
34 35
Chemical Shift (ppm)
180
160
140
120
100
80
60
40
20
0

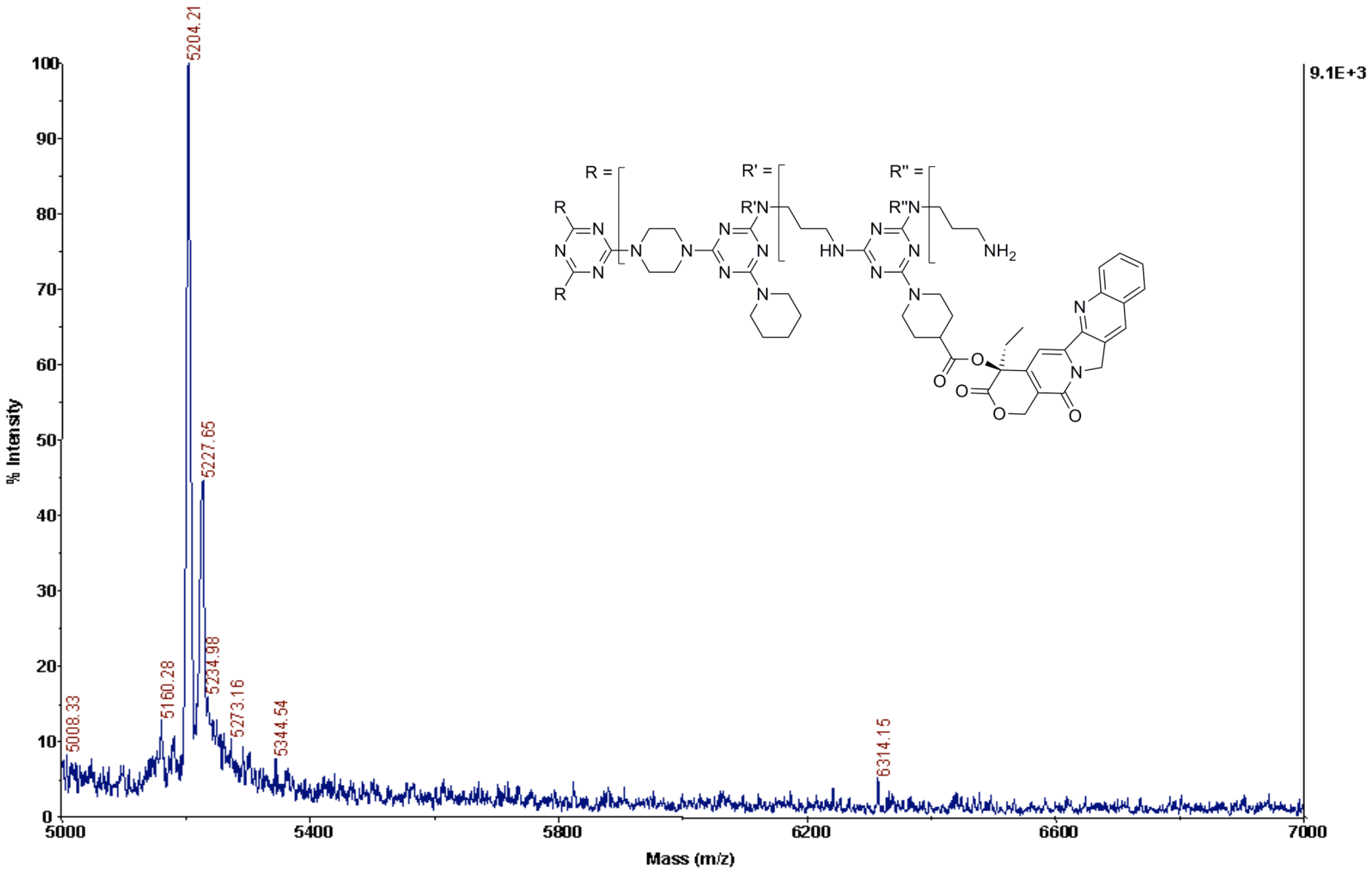
5204.21
5227.65
5234.98
5160.28
5273.16
5344.54
5008.33
6314.15
9.1E+3
% Intensity
Mass (m/z)
100
90
80
70
60
50
40
30
20
10
0
5000
5400
5800
6200
6600
7000
R =
R' =
R'' =
NH2
HN

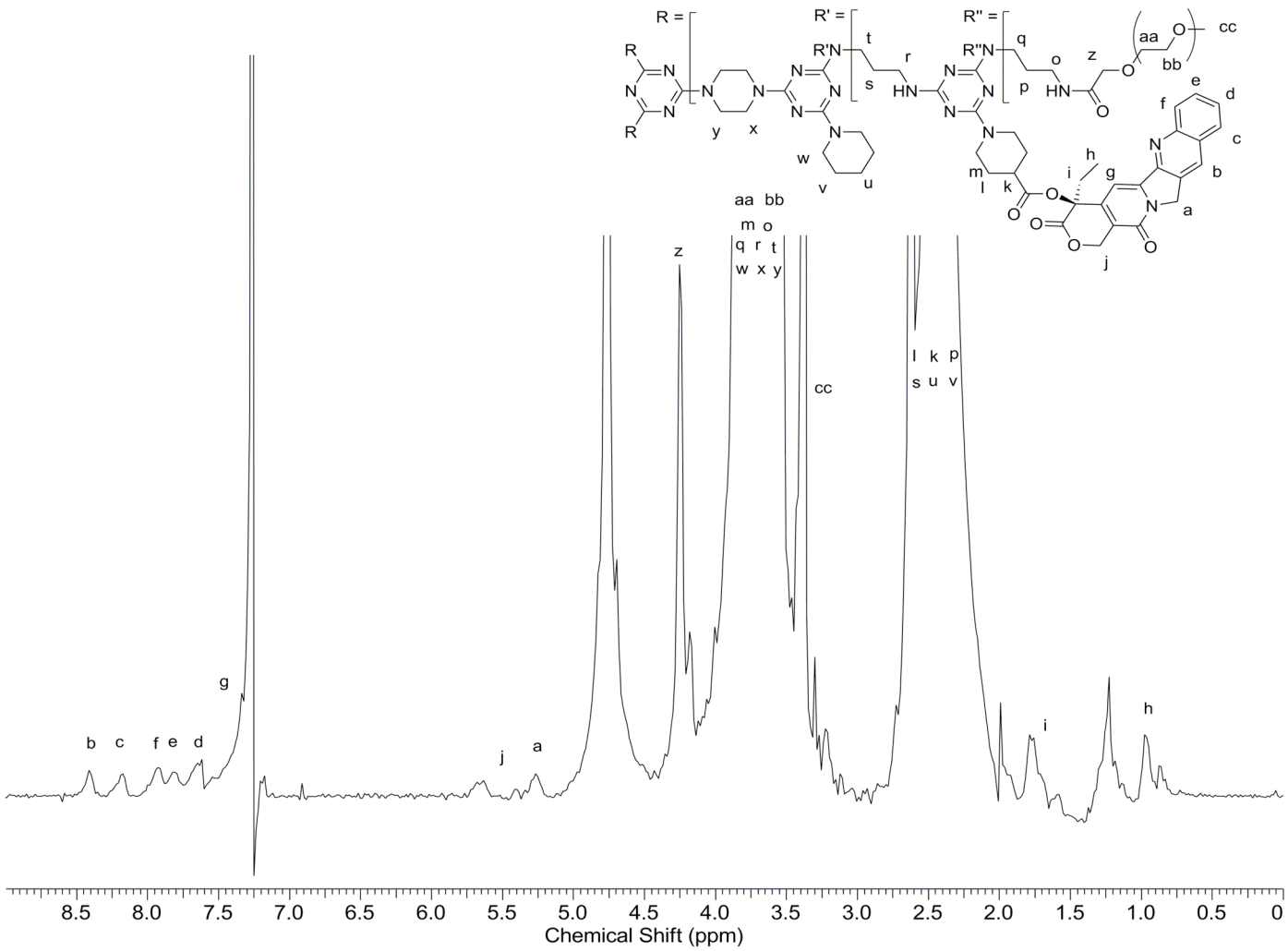
R =
R' =
R'' =
b c f e d
g
j
a
z
aa bb
m o
q r t
w x y
cc
l k p
s u v
i
h
8.5 8.0 7.5 7.0 6.5 6.0 5.5 5.0 4.5 4.0 3.5 3.0 2.5 2.0 1.5 1.0 0.5 0
Chemical Shift (ppm)

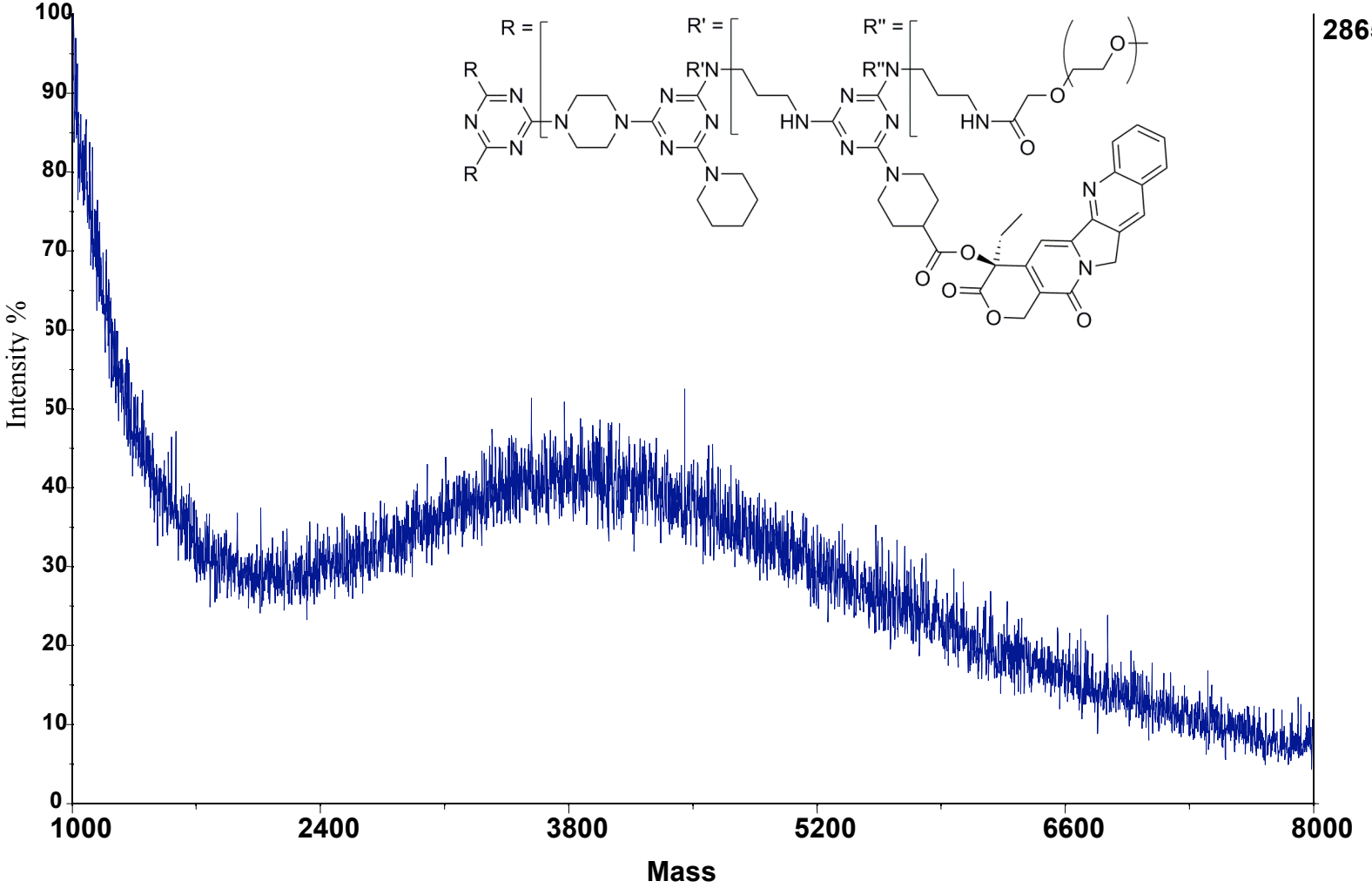
2865.
R =
R' =
R'' =
Intensity %
100
90
80
70
60
50
40
30
20
10
0
1000
2400
3800
5200
6600
8000
Mass

PEG2000-G2-CPT: HPLC (before ultrafiltration)

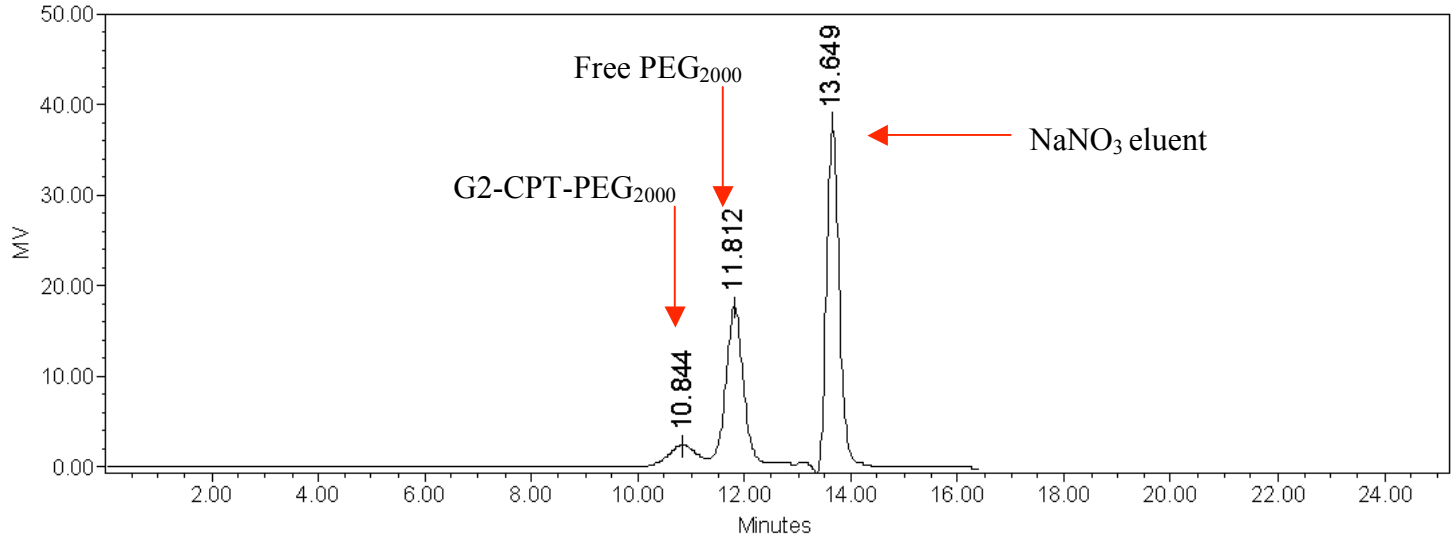

PEG2000-G2-CPT: HPLC (after ultrafiltration)

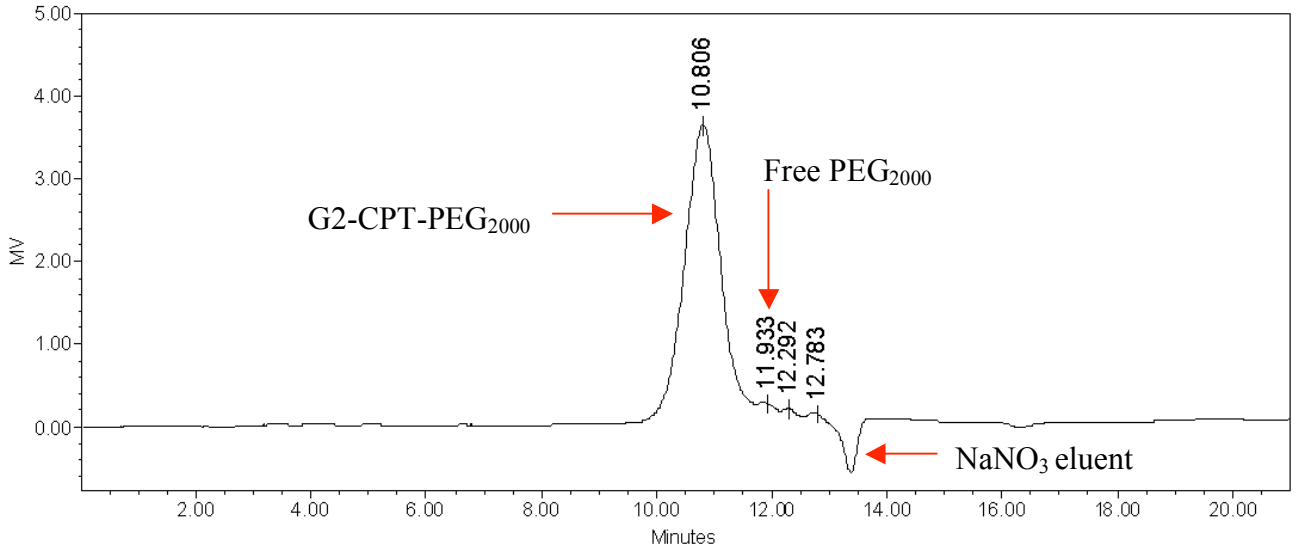

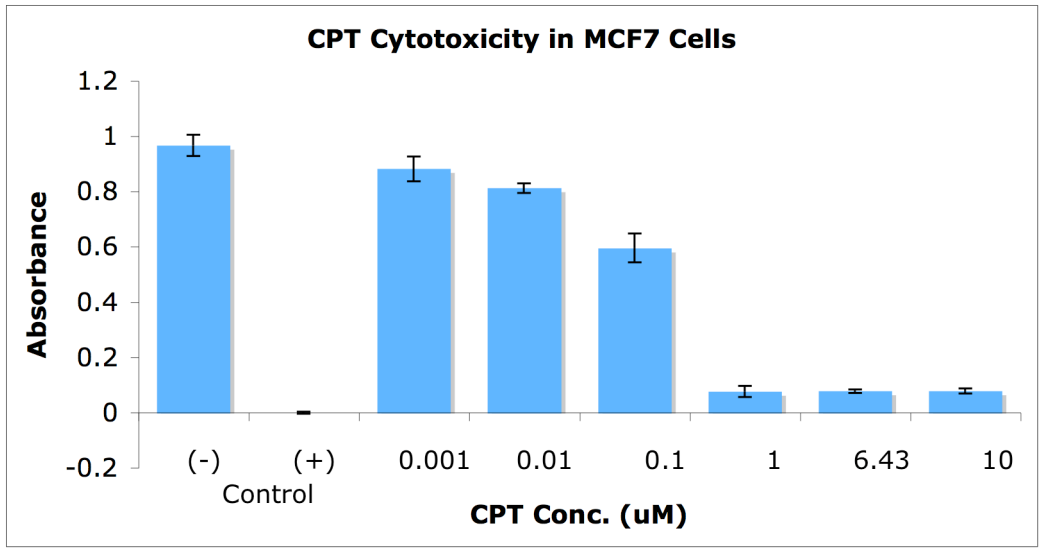
CPT Cytotoxicity in MCF7 Cells
Absorbance
1.2
1
0.8
0.6
0.4
0.2
0
-0.2
(-)
Control
(+)
0.001
0.01
0.1
1
6.43
10
CPT Conc. (uM)

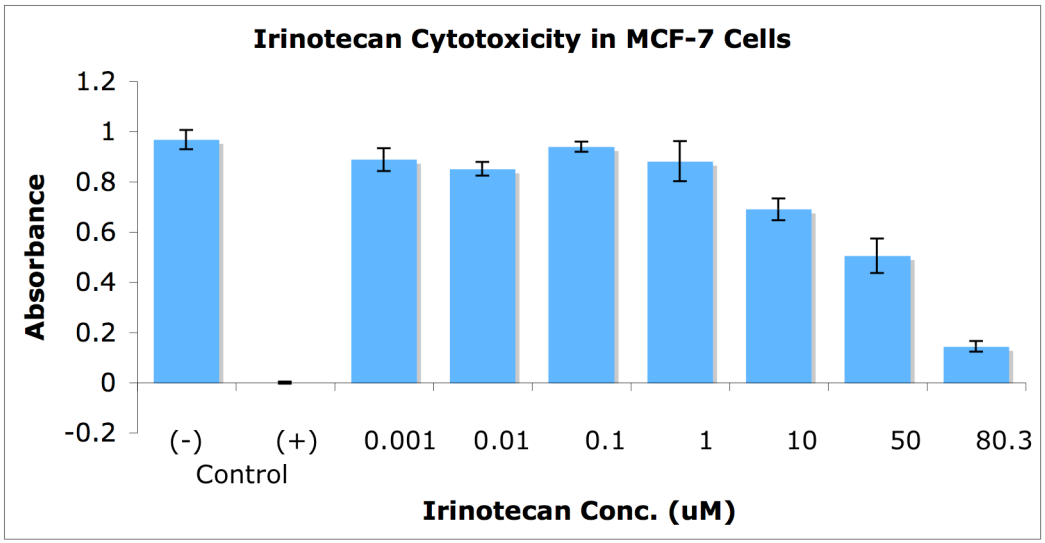
Irinotecan Cytotoxicity in MCF-7 Cells
Absorbance
1.2
1
0.8
0.6
0.4
0.2
0
-0.2
(-)
Control
(+)
0.001
0.01
0.1
1
10
50
80.3
Irinotecan Conc. (uM)

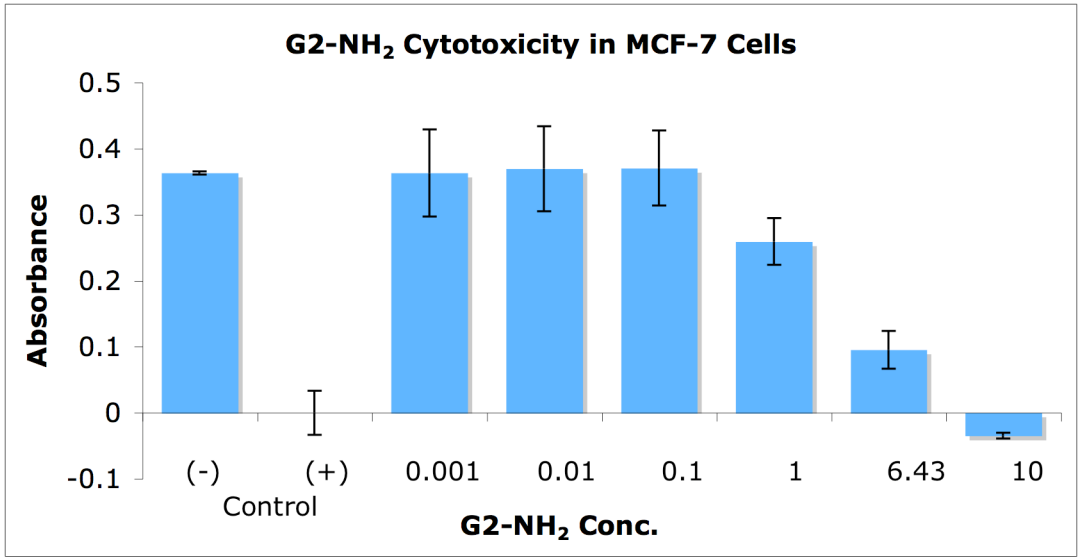
G2-NH2 Cytotoxicity in MCF-7 Cells
Absorbance
0.5
0.4
0.3
0.2
0.1
0
-0.1
(-)
(+)
0.001
0.01
0.1
1
6.43
10
Control
G2-NH2 Conc.

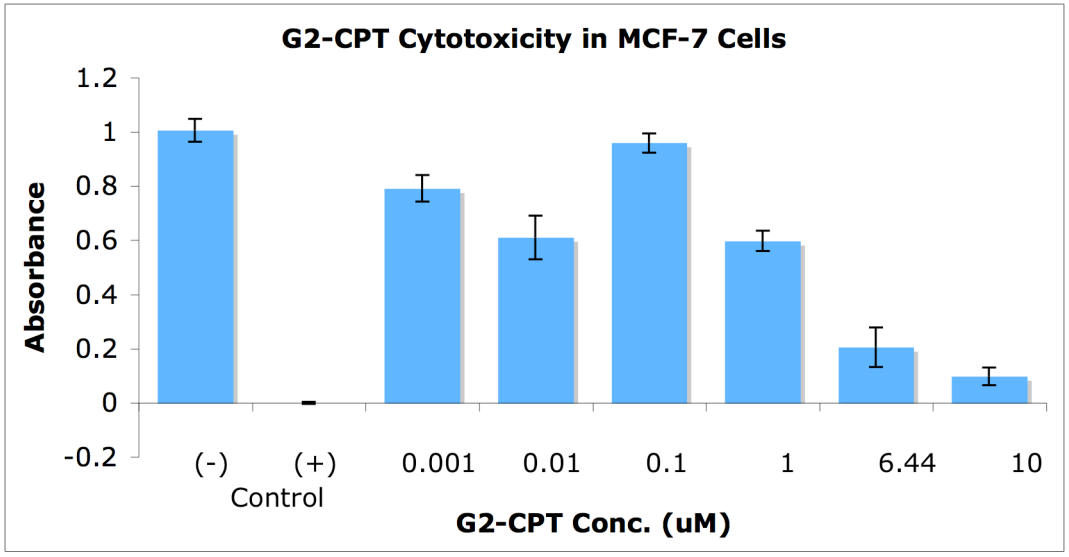
G2-CPT Cytotoxicity in MCF-7 Cells
Absorbance
1.2
1
0.8
0.6
0.4
0.2
0
-0.2
(-)
(+)
0.001
0.01
0.1
1
6.44
10
Control
G2-CPT Conc. (uM)

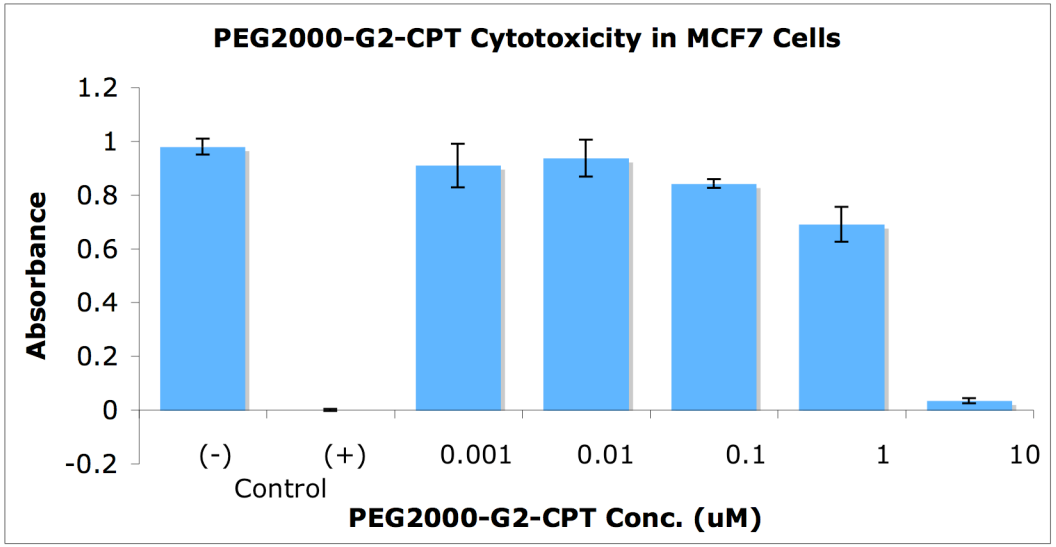
PEG2000-G2-CPT Cytotoxicity in MCF7 Cells
Absorbance
1.2
1
0.8
0.6
0.4
0.2
0
-0.2
(-)
Control
(+)
0.001
0.01
0.1
1
10
PEG2000-G2-CPT Conc. (uM)

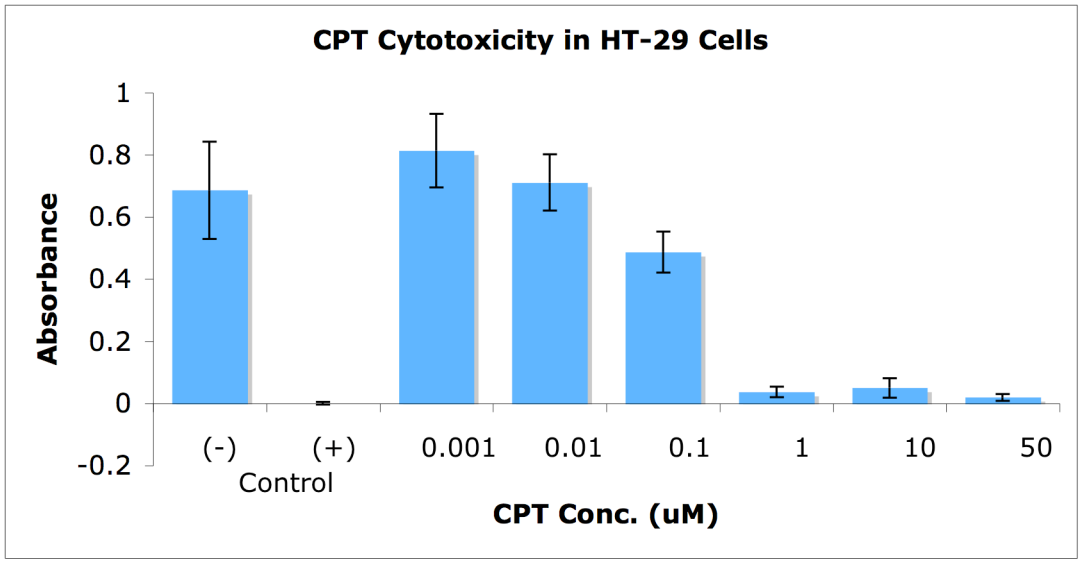
CPT Cytotoxicity in HT-29 Cells
Absorbance
1
0.8
0.6
0.4
0.2
0
-0.2
(-)
Control
(+)
0.001
0.01
0.1
1
10
50
CPT Conc. (uM)

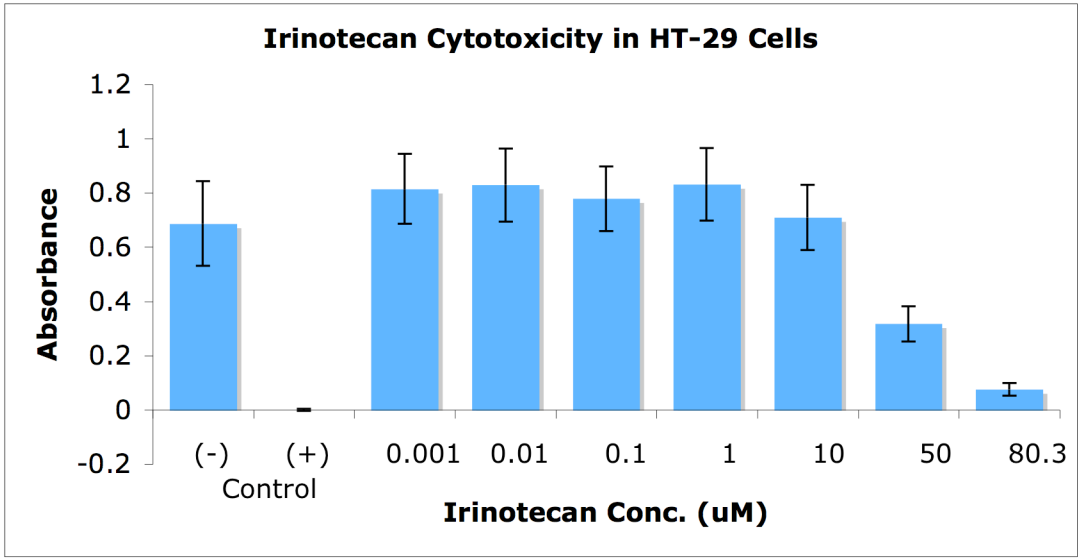
Irinotecan Cytotoxicity in HT-29 Cells
Absorbance
1.2
1
0.8
0.6
0.4
0.2
0
-0.2
(-) Control
(+)
0.001
0.01
0.1
1
10
50
80.3
Irinotecan Conc. (uM)

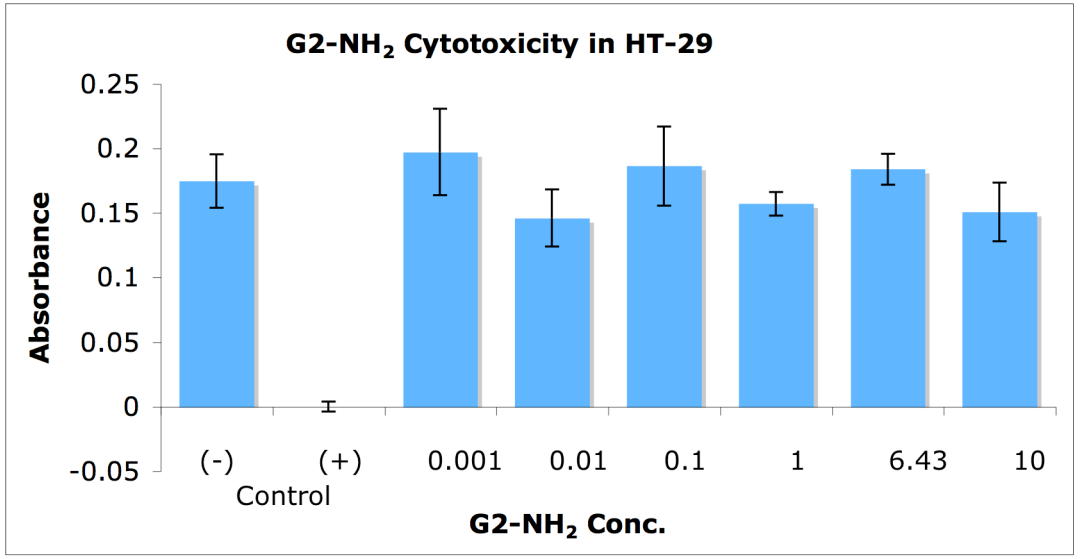
G2-NH2 Cytotoxicity in HT-29
Absorbance
0.25
0.2
0.15
0.1
0.05
0
-0.05
(-) Control
(+)
0.001
0.01
0.1
1
6.43
10
G2-NH2 Conc.

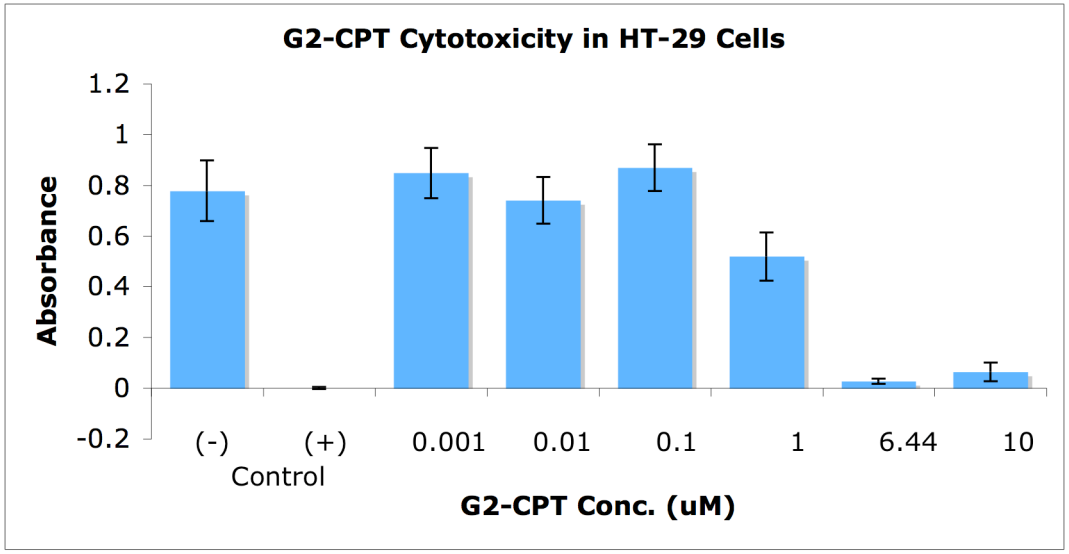
G2-CPT Cytotoxicity in HT-29 Cells
Absorbance
1.2
1
0.8
0.6
0.4
0.2
0
-0.2
(-)
Control
(+)
0.001
0.01
0.1
1
6.44
10
G2-CPT Conc. (uM)

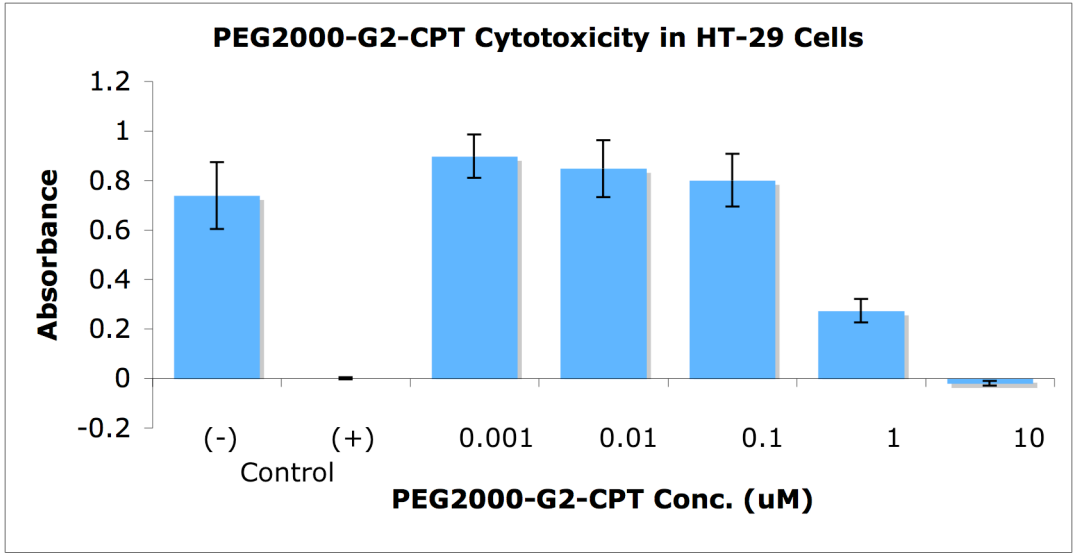
PEG2000-G2-CPT Cytotoxicity in HT-29 Cells
Absorbance
1.2
1
0.8
0.6
0.4
0.2
0
-0.2
(-)
Control
(+)
0.001
0.01
0.1
1
10
PEG2000-G2-CPT Conc. (uM)

VITA

Vincent Joseph Venditto

Education:

Ph.D., Chemistry
Texas A&M University
College Station, TX
December 2009

B.S., Chemistry
Gettysburg College
Gettysburg, PA
May 2003

Permanent Address: Department of Chemistry, MS 3255
College Station, TX 77843

Publications:

Venditto, V.J.; Simanek E.E. Cancer therapies utilizing the camptothecins: a review of in vivo literature. *Molec. Pharmaceut.,* Accepted, **2009**.

Pinnick, V.T.; Venditto, V.J.; Duley, M.; Graham, C.; Everett, C.; Simanek E.E. Lunch with a Scientist: A Cost-Effective Strategy for University and K-12 Partnerships. *School Science and Mathematics,* Submitted, **2009**.

Venditto, V.J.; Allred, K.; Allred, C.; Simanek, E.E. Intercepting triazine dendrimer synthesis for pharmacophore installation as a new efficient route toward drug delivery vehicles. *Chem. Commun.* **2009**, 5541-5542**.**

Simanek, E.E.; Abdou,H.; Lalwani, S.; Lim, J.; Mintzer, M.; Venditto, V.J., Vittur, B. The eight year thicket of triazine dendrimers: strategies, targets and applications. *Proc. Royal Soc*., **2009,** doi: 10.1098/rspa.2009.0108**.**

Lalwani, S.; Venditto, V.J.; Chouai, A.; Shaunak, S.; Simanek, E.E. Electrophoretic behavior of anionic triazine and PAMAM dendrimers: Methods for improving resolution and assessing purity using capillary electrophoresis. *Macromolecules,* **2009**, 42 (8): 3152-3161**.**

Chouai, A.; Venditto, V.J.; Simanek, E.E. Large scale, green synthesis of a generation-1 melamine (triazine) dendrimer. *Org. Syn.* **2009***,* 86: 151-160**.**

Chouai, A.; Venditto, V.J.; Simanek, E.E. Synthesis of 2-[3,3'-di-(tertbutoxycarbonyl)-aminodipropylamine]-4,6-dichloro-1,3,5-triazine as a monomer and 1,3,5-[tris-piperazine]-triazine as a core for the large scale synthesis of melamine (triazine) dendrimers. *Org. Syn.* **2009***,* 86: 141-150**.**